^{40}AR/^{39}AR THERMOCHRONOLOGY AND METAMORPHISM OF AMPHIBOLE FROM THE HUMBOLDT BAY HIGH STRAIN ZONE, WABIGOON SUBPROVINCE, LAKE NIPIGON, ONTARIO

Melanie C. Purves

Submitted in Partial Fulfilment of the Requirements
for the Degree of Bachelor of Science (Honours)
Department of Earth Sciences
Dalhousie University, Halifax, Nova Scotia

April 2002

Dalhousie University

Department of Earth Sciences
Halifax, Nova Scotia
Canada B3H 3J5
(902) 494-2358
FAX (902) 494-6889

DATE April 30th, 2002

AUTHOR Melanie C. Purves

TITLE $^{40}Ar/^{39}Ar$ Thermochronology and Metamorphism of Amphibole from the Humboldt Bay High Strain Zone, Wabigoon Subprovince, Lake Nipigon, Ontario

Degree BSc Honours Convocation May 21st, 2002 Year 2002

$^{40}Ar/^{39}Ar$ Thermochronology and Metamorphism of Amphibole from the Humboldt Bay High Strain Zone, Wabigoon Subprovince, Lake Nipigon, Ontario

Melanie Purves
Dalhousie University

The Humboldt Bay High Strain Zone (HBHSZ) is a shear zone in the Onaman-Tashota Belt, a granite-greenstone belt of the Wabigoon Subprovince of the Archean Superior Province. The HBHSZ represents a boundary within the Onaman-Tashota Belt, separating domains with different tectonic histories. In order to constrain the age of metamorphism and deformation on this boundary, an $^{40}Ar/^{39}Ar$ study using step-heating techniques on 10 samples of hornblende from the HBHSZ is presented. Important relationships seen at both macroscopic and microscopic scales include (1) rocks of the shear zone have undergone polymetamorphism, (2) an earlier phase of actinolitic amphibole (greenschist facies) is replaced in areas by a later phase of hornblendic amphibole (amphibolite facies), (3) peak metamorphism on the HBHSZ is amphibolite facies, and accompanied peak deformation on the shear zone, (4) zones of high strain are inferred to correlate with rocks with a larger amount of hornblende, and (5) zones of lower strain are inferred to correlate with rocks with a larger amount of porphyroclastic actinolite, surrounded by significant amounts of hornblende. $^{40}Ar/^{39}Ar$ spectra from these porphyroclastic samples show disturbed spectra, with step ages ranging from 2598 – 2712 Ma. Samples showing the highest degree of strain and recrystallization yield flat spectra that plateau at an approximate age of 2667 Ma (agreeing within error). This age is taken to represent the age of cooling after the last major deformation along the HBHSZ. The data suggest that late deformation along the HBHSZ was syn-plutonic with respect to the adjacent North Wind Pluton. The age of the North Wind Pluton is thus constrained with a lower limit of 2667 Ma. The relative timing, similar kinematics, and proximity of the HBHSZ to the Wabigoon – Quetico subprovince boundary raises the question of whether peak deformation on the shear zone is related to the subprovince collision, or to a previous event related to the inner-accretion of the eastern Wabigoon. Further work may enable the correlation of the HBHSZ tectonic boundary with boundaries in the western Wabigoon Subprovince.

Keywords: Humboldt Bay High Strain Zone, Wabigoon Subprovince, $^{40}Ar/^{39}Ar$, polymetamorphism, amphibole, Archean, deformation.

TABLE OF CONTENTS

TABLE OF FIGURES

ACKNOWLEDGEMENTS

I would not have been able to complete this project without the help and support of many people. First and foremost, I would like to thank Dr. Nicholas Culshaw, my supervisor and teacher for the past few years. I value the time he spent teaching me, both in the field and in the classroom. His support and encouragement over this time is much appreciated.

I would also like to extend my thanks to Dr. Peter Reynolds for all of his help, especially with the "argon chapter". I am also very grateful to Keith Taylor for his help with the preparation of my samples, for completing the argon analyses, and for helping me present the data. Thanks to Dr. Rebecca Jamieson for her help with the microprobe, photographs, and especially the metamorphic petrology of my samples. Thanks also to Bob MacKay for his expert help with the electron microprobe, and to Gordon Brown for preparing all of the thin sections. I'd also like to acknowledge Sandy Grist for his help and discussions during the separation of my samples. Thanks also to Tom Duffet for all of his technical support. Dr. Marcos Zentilli has been a wealth of good advice this year. Thanks to NSERC for funding student research as well as the project itself. Thank you to Sharon Lee, my "field assistant" and friend. I'd like to thank my parents for their encouragement and support of my education. Finally, I'd like to thank my classmates and close friends, for their help and total support whenever needed throughout the years.

CHAPTER 1

1.1 Introduction and Purpose

The Humboldt Bay High Strain Zone (HBHSZ) is a shear zone within the Onaman-Tashota greenstone belt of the eastern Wabigoon Subprovince, in the Superior Province of Ontario (Fig. 1.1). The purpose of this thesis is to add to the understanding of the geology of the Onaman-Tashota greenstone belt and to investigate the tectonic significance of the HBHSZ. In order to constrain the age of metamorphism and deformation of the shear zone, an $^{40}Ar/^{39}Ar$ study of 10 hornblende samples from across the zone was conducted. A study of this area has particular significance due to the recent seismic work done by Lithoprobe. The HBHSZ is crossed by a seismic reflection corridor from the Western Superior transect, corridor RC3.

The Wabigoon Subprovince is one of 10 generally east-west striking belts, which amalgamated during the Archean to form the Superior Province. The HBHSZ represents a structural boundary within the Wabigoon Subprovince and has potential significance for its tectonic development. The HBHSZ may represent a boundary of accretion within the Wabigoon Subprovince, and/or may be related to the collision of the Wabigoon with the Quetico Subprovince to the south. Its relationship to these tectonic events will be discussed in the final chapter of this thesis.

1.2 Scope and Organization

The main body of this thesis is concerned with argon thermochronology of the HBHSZ. In order to set this data in meaningful context, the metamorphic grade and textures associated with the rocks within the HBHSZ, as well as the field relations are documented. This thesis also presents the argon thermochronology of the area. Topics beyond the scope of this thesis include detailed P-T estimates of the peak grade of metamorphism, detailed mineral chemistry, and detailed structural analysis.

This thesis begins by giving a background to the regional geology of the area, as well as documentation of fieldwork, in Chapter 2. Next, the metamorphic petrology of the rocks in the shear zone is presented in Chapter 3. Argon thermochronology is presented in Chapter 4, as well as interpretations of the spectra obtained. Discussions and conclusions are presented in the final chapter.

1.3 **Methods**

Field work on the study area was carried out in June, 2001. Samples for argon analysis were brought back in both 1999 and 2001, by N. Culshaw and P. Bogutyn, and N. Culshaw and M. Purves, respectively. In both field seasons, transects were completed across the shear zone, during which field relations were documented. Samples were sectioned, and selected samples were probed using the electron microprobe at Dalhousie University, and analyzed for oxide percentages. Back-scatter electron images were also made on the probe. Of the many samples retrieved from the field, only 13 were selected for argon analysis (refer to section 4.2). Using the computer software package, *Minpet* (Richard, 1997), selected microprobe analyses of plagioclase and hornblende were recalculated and classified.

1.4 **Previous Work**

H.R. Williams completed a structural study of the Wabigoon and Quetico Subprovinces in 1987. Along with J.R. Devaney, he developed a cross-section through the Beardmore-Geraldton Belt, which served as the basis for the accretionary model of the area, and was also, the reason for a Lithoprobe reflection line in that location. This model in turn became the prototype for later terrane-accretion models for the development of the Superior Province (Thurston et al., 1991).

The most recent research in the area has been done by G. Stott and others from the Ontario Geological Survey (e.g. Amukun, 1977). Interest in the mineralization of the region prompted a government mapping project. G. Stott and others prepared a comprehensive geological map of the region (Stott, et al., 1996). As a follow-up to this, and in an attempt to coordinate with studies in the western Wabigoon (e.g. Tomlinson et al., 1995), Stott and Davis (1999) undertook more extensive geochronological studies.

Tomlinson (2000) reported findings from several Nd isotope studies, undertaken to map Mesoarchean basement terranes in the Wabigoon Subprovince. Culshaw et al. (2000) used conventional step-heating $^{40}Ar/^{39}Ar$ thermochronology to determine ages of biotite and muscovite samples across the HBHSZ.

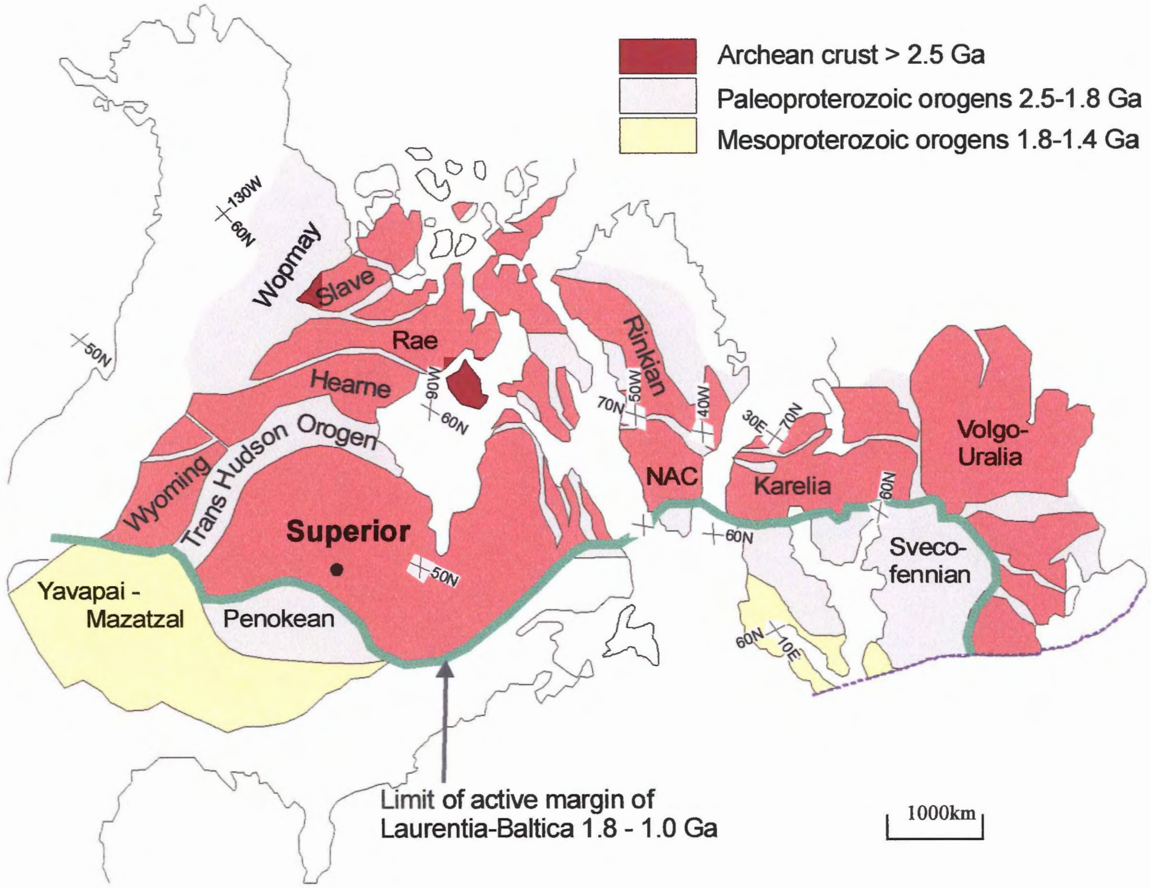

Figure 1.1 – North Atlantic Precambrian patterns. This map shows Archean Provinces, Paleoproterozoic orogens and Mesoproterozoic orogens of North America, shown in their possible orientation with other elements from the North-east European Craton during pre-Grenvillian times. Present day latitudes are also shown. The approximate study area in the Superior Province is indicated with a small circle. (Adapted from Gorbatschev and Bagdanova, 1993).

CHAPTER 2 - REGIONAL GEOLOGY

2.1 Regional Geology

2.1.1 The Superior Province

The Superior Province (Fig. 2.1) is the largest Archean craton in the world, and covers an area of approximately 1 572 000 km^2 (Blackburn et al., 1991). The Superior Province largely consists of a series of subparallel east - northeast - trending belts, which are 100 - 200 km wide. These belts comprise either granite - greenstone assemblages or meta-sedimentary rocks. The boundaries between the belts are faults or shear zones. The belts display different assemblage lithologies, grades, and structures, and are regarded as superterranes (Blackburn et al., 1991). Granite-greenstone belts, or volcano-plutonic belts (terminology of Card, 1990), are characterized by low-grade meta-volcanic and meta-sedimentary sequences with granitic intrusions that range in age from approximately 3.0 - 2.7 Ga. The Wabigoon Subprovince is one of these granite-greenstone belts. Meta-sedimentary belts are characterized by metamorphic turbidite sequences with granitic intrusions that range from 2.7 - 2.6 Ga. The Quetico Subprovince is an example of one of these meta-sedimentary belts. The Wabigoon granite-greenstone belt is just to the north of the Quetico meta-sedimentary belt, and has slightly older zircon ages (Davis, 1998).

There have been changes in thought towards Superior development over the past ~20 years. Original views included the concept of arc accretion. The granite-greenstone belts were originally thought to represent single oceanic island arcs (e.g. Hoffman, 1989). The sediments in the meta-sedimentary belts were thought to have been deposited during periods of volcanism and thus represent accretionary prisms (Hoffman, 1989). The alternating granite-greenstone and meta-sedimentary belts were thought to have accreted to each other before the Superior Province collided with other Archean cratons (Hoffman, 1989; Langford and Morin, 1976).

The next major development in Superior accretionary models regarded each of the alternating belts as superterranes. According to Blackburn et al. (1991), the superterranes consist of different terranes which were amalgamated before their north to south collision with other superterranes during a major period of accretion at 2.7 Ga (Fig. 2.2).

Current views, stemming from recent Lithoprobe-related work in the Western Superior Province, are that the superterranes not only consist of terranes with different assemblages, but also older Archean cratons with rift and drift assemblages (extended abstracts in Harrap and Helmstaedt, 2000). Davis (1998) suggested that subprovinces may represent differential uplift and exposure of a tectonically layered crust.

2.1.2 The Wabigoon Subprovince

The Wabigoon Subprovince is similar in lithology to other granite-greenstone belts in the Superior Province. The Wabigoon is bounded to the south by the meta-sediments of the Quetico Subprovince and to the north by the Winnipeg River and English River Subprovinces. The Wabigoon is divided into 3 lithologic and structural areas. The western Wabigoon is characterized by extensive supracrustal rocks with syn-volcanic batholiths and few gneissic units. The central Wabigoon contains small greenstone belts underlain by gneiss domes and batholiths. The eastern Wabigoon consists of supra-crustal assemblages and syn-volcanic batholiths (Blackburn et al., 1991).

Recent work (e.g. extended abstracts in Harrap and Helmstaedt, 2000) show that the Wabigoon is not a single island arc, but instead is composed of many smaller and distinct terranes, which were amalgamated before the final superterrane collision. Extensive geochronological data show that the basement of the central Wabigoon is 3.0 Ga, and the volcanics are ca. 3.0 Ga. Recent isotopic data from the central Wabigoon suggest that the northern and southern domains are fundamentally different terranes (Tomlinson, 2000). Initial Nd results from the eastern Wabigoon suggest a similar pattern as in the central Wabigoon. Nd model ages in the north-eastern Wabigoon are >3.0 Ga, while model ages in the south-eastern Wabigoon are between 2.81 and 2.85 Ga. Tomlinson (2000) proposed that the basement rocks of the north-eastern Wabigoon contain an older component than the rocks in the south-eastern Wabigoon, and that the boundary between these two areas is found near the HBHSZ. These data show that the central Wabigoon was not amalgamated until the Neoarchean.

2.1.2.1 The Onaman-Tashota greenstone belt

The eastern Wabigoon is divided into two smaller terranes, the Onaman-Tashota greenstone belt and the Beardmore-Geraldton greenstone belt. The Onaman-Tashota greenstone belt (OTGB) dominates the eastern Wabigoon Subprovince (Fig. 2.3). It is a typical greenstone-dominated terrane, with sequences of deformed mafic and felsic volcanics and sedimentary rocks. Volcanic sequences, largely bimodal basalt - dacite flows, dominate, whereas the clastic sedimentary sequences are relatively less common. The volcanic strata in the region are north-dipping, and are assumed to be unconformably overlain by the conglomerate assemblage (Fig. 2.3) (Stott and Morrison, 1995). The conglomerate is polymictic and thought to have been deposited in a synclinal basin during the emplacement of the Onaman and Jackson plutons (Stott and Morrison, 1995).

The Onaman-Tashota greenstone belt was intruded by several large felsic plutons and many syn-volcanic to late-tectonic gabbroic plutons (Tomlinson et al., 2000). The largest of these plutons is the Onaman Pluton, a granite (ss), which has been dated at 2768 Ma (Stott and Davis, 1999). To the south of the HBHSZ is another, smaller, felsic pluton, the North Wind Pluton (NWP). The NWP is foliated and believed to be syn-tectonic with respect to the HBHSZ (Culshaw et al., 2000).

Tectonic assemblages of the OTGB are in the process of being defined. Stott and Davis (1999) divided the Onaman-Tashota greenstone belt into separate domains on the basis of their tectonostratigraphic relationships. The domains from south to north are:

(1) the ca. 2740 Ma Elmhirst-Rickaby basalt-andesite-rhyolite sequence,

(2) the <2707 Ma Conglomerate assemblage which is late-tectonic and characterized as "Timiskiming-type",

(3) the 2769 - 2780 Ma North Onaman volcanic sequence adjacent to the Onaman Pluton,

(4) the </= 2713 Ma Humboldt Bay sequence,

(5) the 2722 Ma Metcalfe-Lake Ste. Marie rhyolitic sequence,

(6) the 3056 Ma Tashota basaltic sequence in the west,

(7) the 2922 Ma Toronto-Willet volcanic sequence, and

(8) the 2739 Ma Marshall assemblage of felsic volcanics.

2.1.2.2 The Beardmore-Geraldton greenstone belt

The Beardmore-Geraldton greenstone belt (BGGB) lies to the south of the Onaman-Tashota terrane (OTT) and is separated from the OTT by the Paint Lake fault (Fig. 2.3). To the south of the BGGB are the meta-sedimentary rocks of the Quetico Subprovince. The Beardmore-Geraldton belt represents the boundary zone between the Wabigoon and the Quetico Subprovinces and underwent significant deformation at the time the two subprovinces were accreted (Williams, 1987). A penetrative, late dextral fabric is seen in the BGGB, which resulted from deformation associated with the Wabigoon – Quetico collision (Williams, 1987).

The BGGB is a group of three supracrustal suites of low grade basalts and gabbros, with three interlayered sedimentary belts. The sediments tend to young and coarsen to the north (Williams, 1987). Devaney and Williams (1989) interpreted the 3 volcanic units as being a coherent unit of oceanic crust with domains representing fan deposits, deltaic sediments, and deep water turbidites. Later work, including a study by Tomlinson et al. (1996), suggested this interpretation does not adequately account for the lithological variations seen in the BGGB.

Tomlinson et al. (1996) used geochemistry and trace element data to distinguish the 3 metavolcanic units and determine their source region. The results suggested that the formation environment for each of the 3 units is different. The northern unit represents back-arc material, the central unit represents an oceanic arc, and the southern unit represents ocean crust. A likely model accounting for these units is one where the fragments were accreted before collision with the Wabigoon arc.

2.1.3 The Humboldt Bay High Strain Zone

The HBHSZ (Fig. 2.3) is a major tectonic boundary within the Onaman-Tashota greenstone belt. It marks an important structural and temporal discontinuity between two terranes of different ages and Nd isotopic characteristics. Stott and Davis (1999) noted that the HBHSZ separates the Elmhirst-Rickaby sequence to the south from the 2769 Ma and > 2920 Ma volcanic packages to the north. They speculate that the HBHSZ comprises a fundamental terrane boundary between these two domains. Tomlinson (2000) indicated that the boundary between the north and south of the eastern Wabigoon lies in the vicinity of the HBHSZ. The basements of these two areas contain different Nd isotopic components.

Culshaw et al. (2000) reported results from a preliminary argon survey along the shoreline of Lake Nipigon from within the North Wind Pluton, to beyond the north side of the HBHSZ. The spectra presented in their report have average muscovite and biotite ages of 2646 Ma and 2626 Ma respectively. These ages are interpreted as cooling ages related to either post-tectonic uplift, or a province-wide heating event, and do not directly constrain the age of the HBHSZ. Currently, the only age constraint available on the HBHSZ comes from a quartz-porphyry that cross-cuts and contains the same foliation as the HBHSZ (Stott, personal comm., 2002). This provides an upper constraint of 2706 Ma on the age of the HBHSZ.

The HBHSZ is a shear zone that consists mainly of mafic volcanic rocks and displays largely greenschist to amphibolite facies metamorphism. The strata young to the north, and there is a strong fabric present in the rocks that dips steeply to the NNW (Stott et al., 1996). The LS fabric is strongly foliated and has a down-dip lineation (Fig. 2.4).

Stott et al. (1996) show the HBHSZ to be generally concordant with D1 and D2 structures reported by Stott and Morrison (1995). D1 of Stott and Morrison (1995) is seen over nearly the entire Onaman-Tashota area as a repeated stacking of strata due to thrust faulting. D2 of Stott and Morrison (1995) is characterized by south-side-up extensional shear zones that formed by reactivation of D1. Using the terminology of Stott and Morrison (1995), the main fabric seen in the Lake Nipigon section of the HBHSZ is herein referred to as S2. Recent field work in the area of the eastern margin of the NWP, showed the pluton cutting the regional fabric of the area (S1 of Stott and Morrison, 1995), while the northern margin of the pluton cross-cut the main fabric of the HBHSZ, S2. S2 formed as a result of a local dextral deformational event, D2 (Culshaw et al., 2000). Recent field work shows that in the Lake Nipigon section, any earlier foliations or bedding, S1 or S0, are completely overprinted by S2. Evidence for some of these structural relationships is presented in the following section.

Subsequent deformations, D3 and D4, produced folds and late cleavage in parts of the HBHSZ (Culshaw et al., 2000). S3 (Fig. 2.4) is defined by axial surfaces of asymmetric, sinistral, west-verging D3 folds. Internal boudinage of S2 and widespread quartz-veins are also D3-related structures (Culshaw et al., 2000). D4-related structures include late cleavage (S4) and asymmetric dextral folds. These structures are less common on the Lake Nipigon section, and are restricted to the south side of the HBHSZ (Culshaw et al., 2000).

The North Wind Pluton lies approximately 1 km south of the HBHSZ (Fig. 2.3). Internally, the pluton contains a penetrative solid-state foliation (Fig. 2.4), which strikes to the north-east and is steeply dipping. In thin section, blocky feldspar crystals are aligned and set in a recrystallized matrix (Culshaw et al., 2000).

2.2 Field Relations

The HBHSZ outcrops on the eastern shores of Lake Nipigon. This shoreline section, along with a few locations inland, comprises the field area of this study. Figure 2.5 shows outcrops visited and locations sampled for this study. The most important field observations are: (1) metamorphic gradient, (2) relationship between granite veins and S2, (3) strong LS fabric, and (4) overprinting of earlier metamorphism. Each of these will be discussed briefly below.

Lithologies present in the HBHSZ are generally meta-basaltic rocks with interlayers of meta-sediments. In the HBHSZ, the rocks display greenschist facies metamorphism, with assemblages of amphibole, chlorite, plagioclase, and epidote. Directly to the south of the HBHSZ, the rocks increase in grade to transitional amphibolite facies assemblages. This increase in grade occurs close to the North Wind Pluton, and is interpreted to be directly linked to its emplacement.

Although the south margin of the HBHSZ, as defined by Stott et al. (1996) does not extend down to the NWP, field work has shown that the high strain zone does continue southwards towards the pluton. The kinematics and the degree of strain are very similar between the rocks of the shear zone (e.g. station 15, Fig. 2.5) and those south of the defined shear zone (e.g. stations 30 and 7, Fig. 2.5). Therefore for this thesis, these units are considered to be continuous, and contain the same fabric. The contact zone of the NWP coincides with the south side of the HBHSZ. There, NWP dykes show two different relationships to the principal fabric (S2). Unfoliated pegmatites, presumably from the NWP, cut the fabric; and foliated granite dykes are boudinaged. This suggests that emplacement of the NWP was syndeformational with respect to D2 (Fig. 2.6).

The main fabric in the HBHSZ is a strong and penetrative LS fabric (Fig. 2.4b). The foliation trends east-west, dipping steeply to the north. It has a down-dip lineation that is defined largely by aligned amphibole grains. Close to the NWP, granite boudins show extension in the vertical direction as well as the horizontal direction (Fig. 2.7). The foliation has a dextral sense of shear, which is seen in the field in the horizontal plane by various types and sizes of kinematic indicators, including rotated epidote 'pods', rotated granite boudins (Fig. 2.8), folded granite and quartz veins, and deformed amphibole porphyroclasts. These different features suggest that there were both compressive and shearing components of strain, thus D2 may have occurred in a transpressional tectonic regime (Tikoff and Fossen, 1993).

Many of the rocks within the HBHSZ contain evidence for an earlier metamorphism. Outcrops visited at stations 15 and 13 (Fig. 2.5) show abundant porphyroclastic rocks. The porphyroclasts are amphibole grains, typically between 1 – 3 mm, that are wrapped by S2. These amphibole porphyroclasts are tentatively assigned to the first metamorphism of the rocks, M1. Presumably, they were subsequently deformed by dextral transpression related to D2. Figure 2.9 shows evidence for the overprinting of this earlier metamorphism by S2. On a centimeter to meter scale, evidence for the formation of S2 is seen in small individual shear bands. This relationship will be further explored in the next chapter.

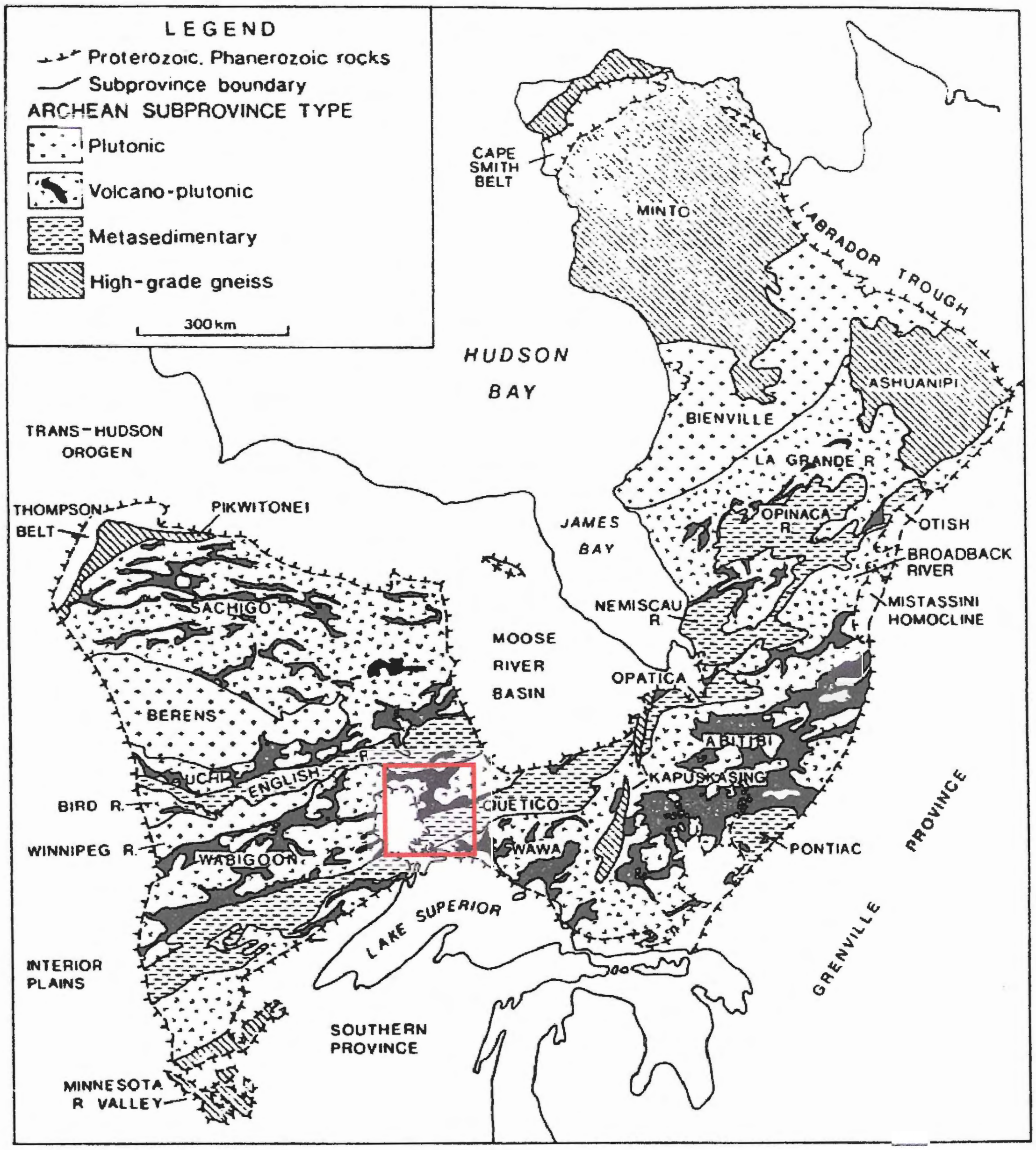

Figure 2.1 – Geological map of the Superior Province of Ontario and Quebec, Canada. The field area and Onaman-Tashota greenstone belt are outlined in red (modified from Card, 1990).

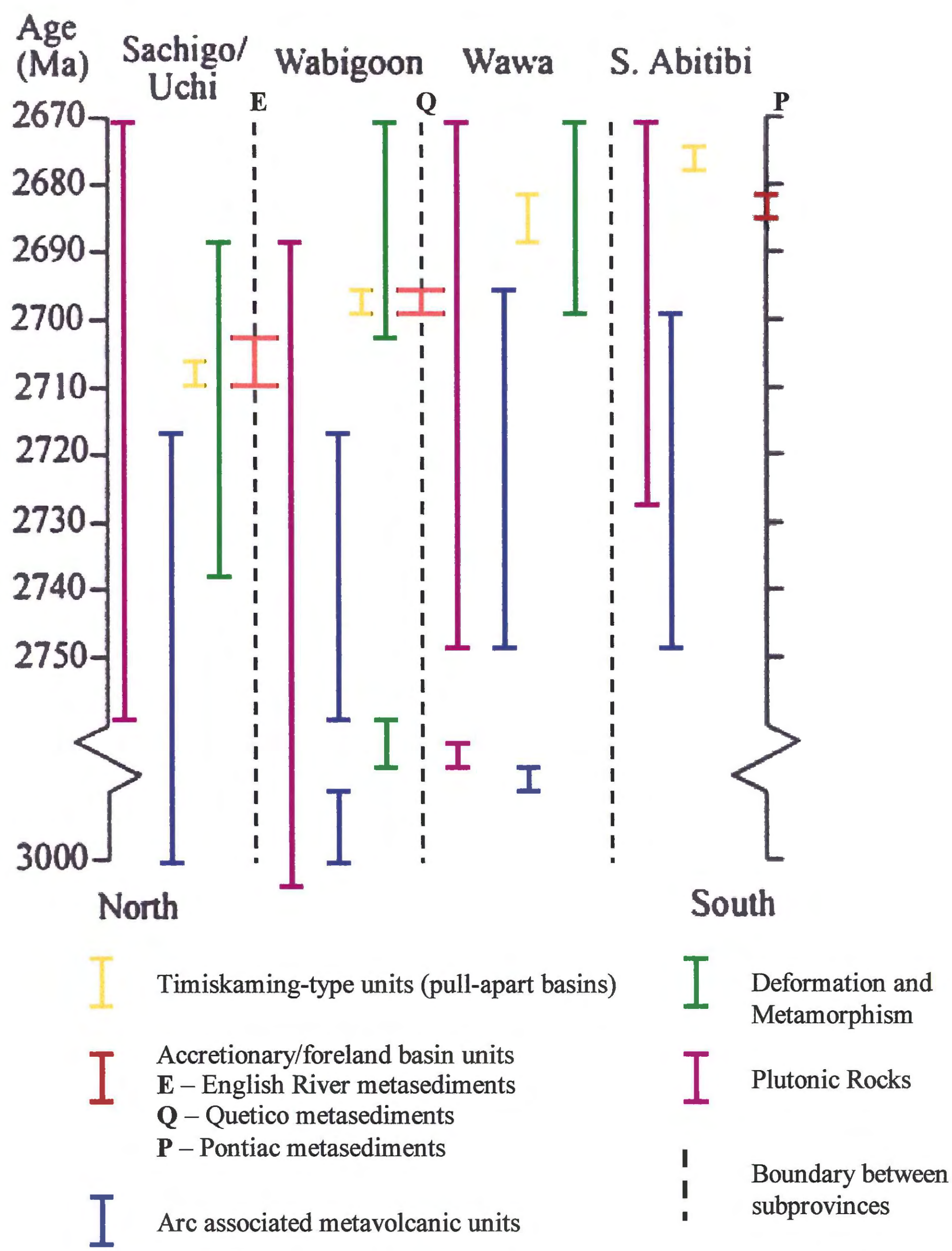

Figure 2.2 – Sequential north-south development of orogenic sedimentary basins, volcanics, and plutons across the Superior Province. Also shown on the diagram are periods of metamorphism and deformation in the subprovinces. (modified from Davis, 1998, and Card, 1990).

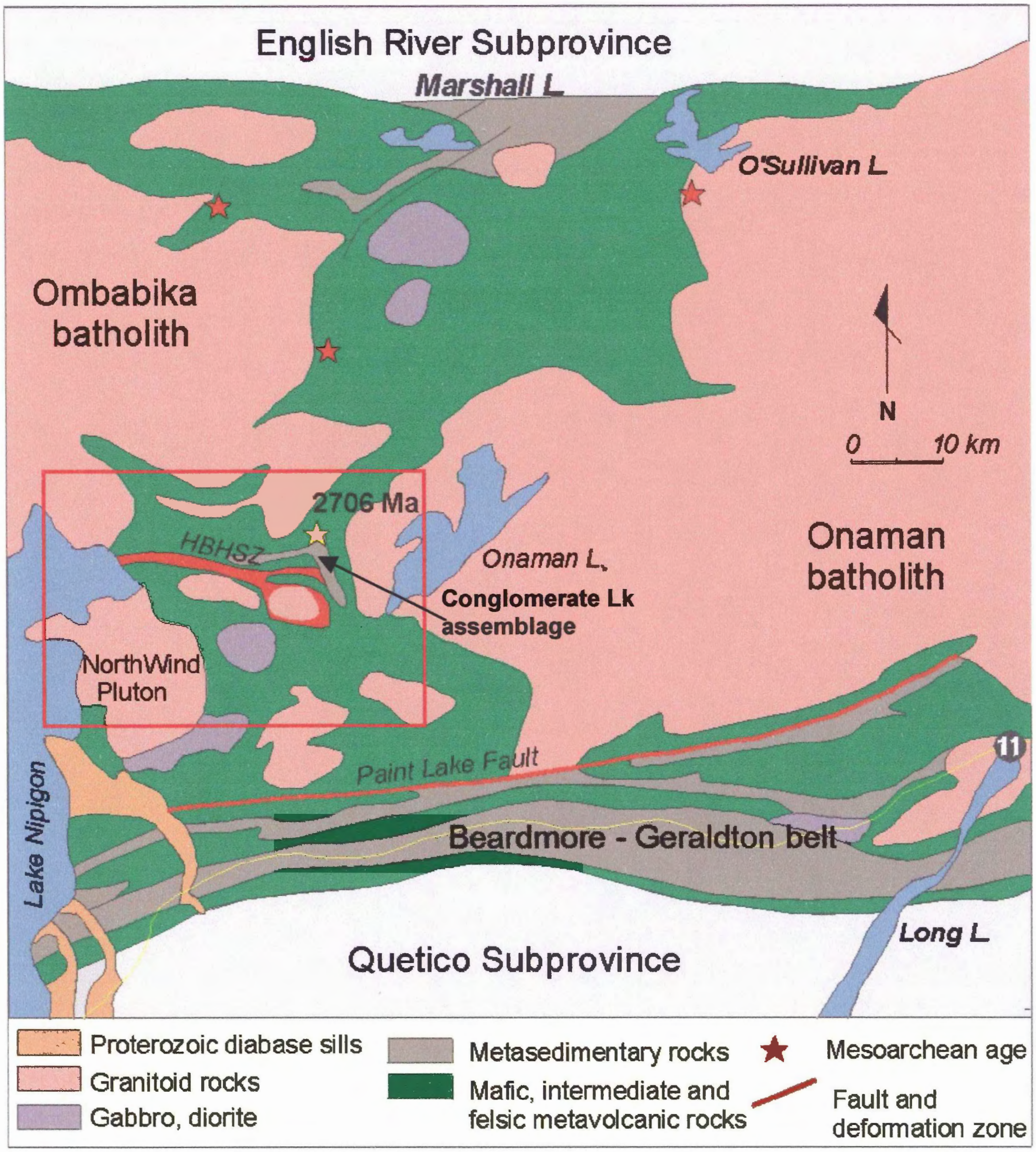

Figure 2.3 – Geology of the Onaman-Tashota greenstone belt of the eastern Wabigoon Subprovince. The Humboldt Bay high strain zone (HBHSZ) is an east-west boundary which outcrops on the eastern shores of Lake Nipigon. The study area is outlined in red. The yellow star shows the location of a constraining U-Pb age of the HBHSZ. Map is based on Stott et al., 1998 (map courtesy of N. Culshaw).

(a)

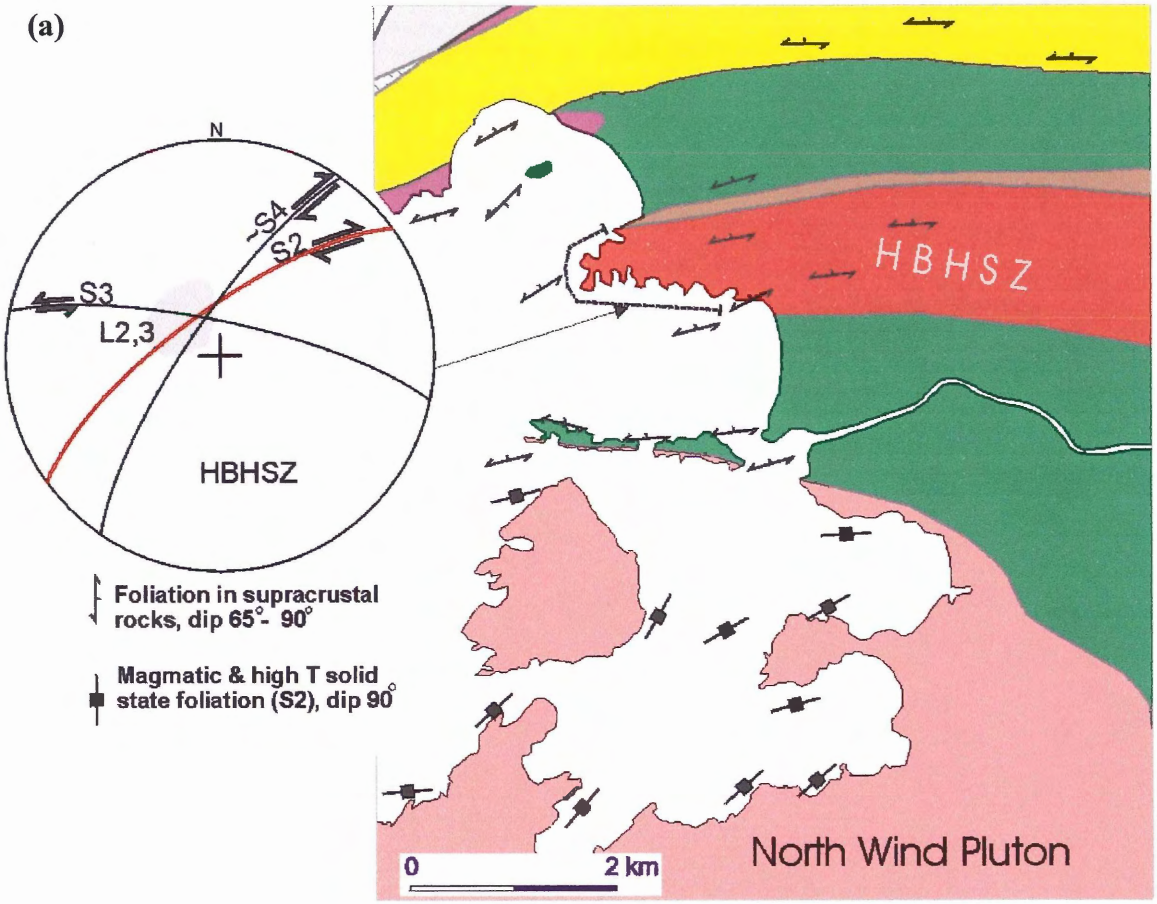

(b)

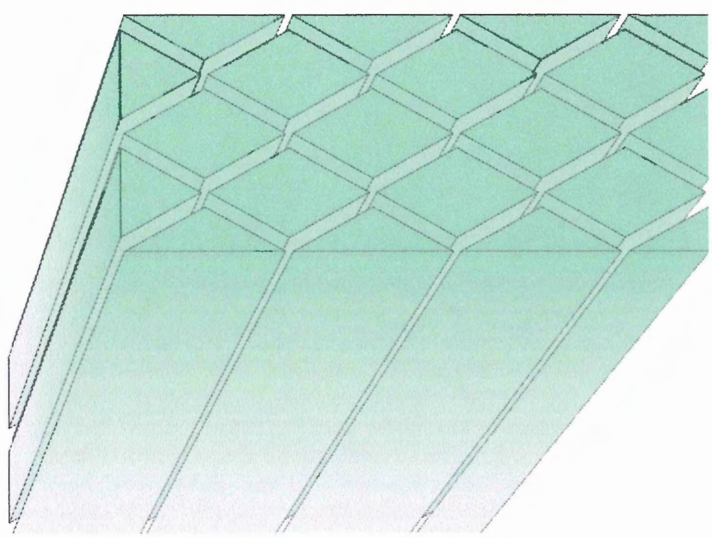

Figure 2.4 –(a) Summary of structures in the HBHSZ area. Foliation and lineation orientations from D2, D3, and D4 are summarized in the stereonet. The age of the thermal deformational event associated with the main foliation of the HBHSZ, S2, is the subject of this argon study. (Legend for map is shown ahead in Figure 2.5.)
(b) 3-dimensional cartoon of the main LS fabric in amphibolitic metabasalts in the HBHSZ (modified from Culshaw et al., 2000).

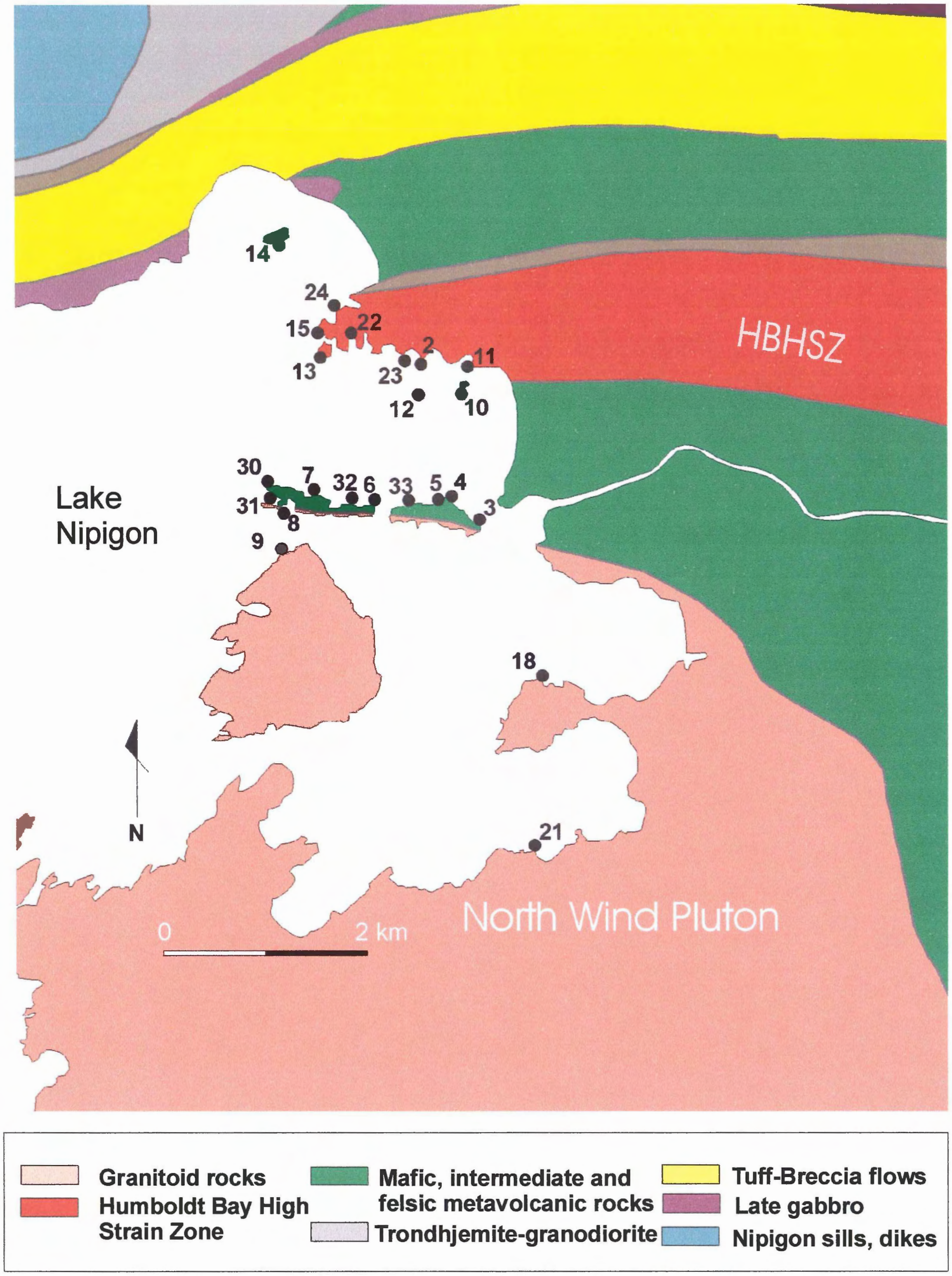

Figure 2.5 – Location map of stations visited on Humboldt Bay. Station numbers include those made in 1999 and 2001. Legend applies to all other similar maps in this thesis. (Source map courtesy of N. Culshaw.)

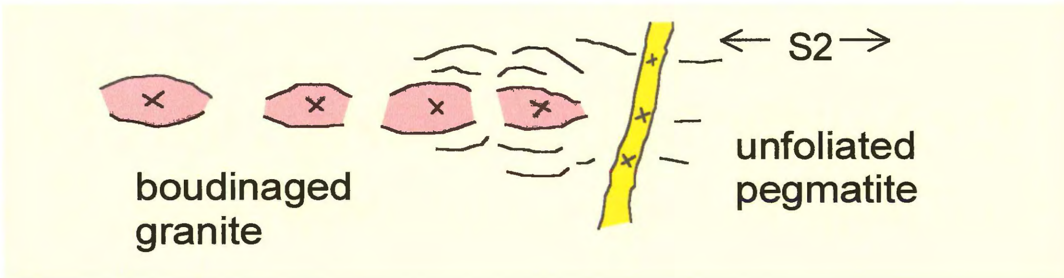

Figure 2.6 - Diagram showing field evidence for syntectonic emplacement of the North Wind Pluton (diagram courtesy of N. Culshaw).

Figure 2.7 – Photograph from station 8 showing steeply dipping foliation. A small granite vein is boudinaged in both the horizontal and vertical direction. This photograph shows the vertical dimension.

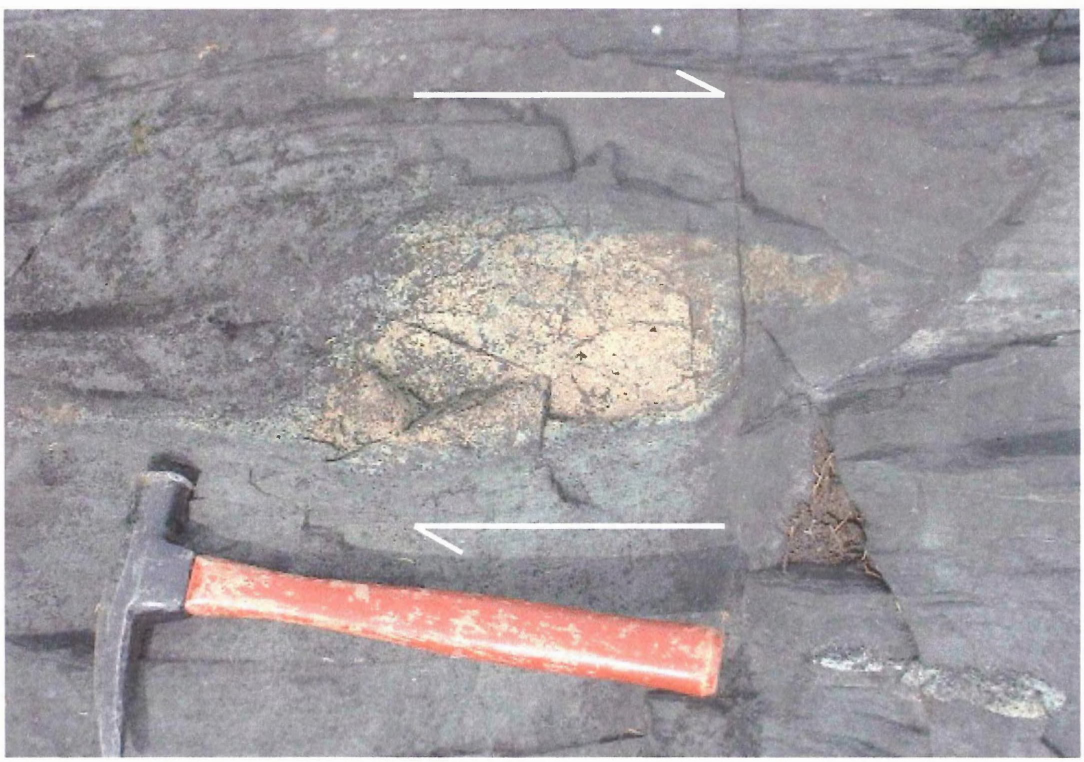

Figure 2.8 – Photographs from stations 30 (top) and 6 (bottom) showing kinematic indicators as evidence for dextral shear. Rock types are metabasalts. Photographs show the horizontal surface

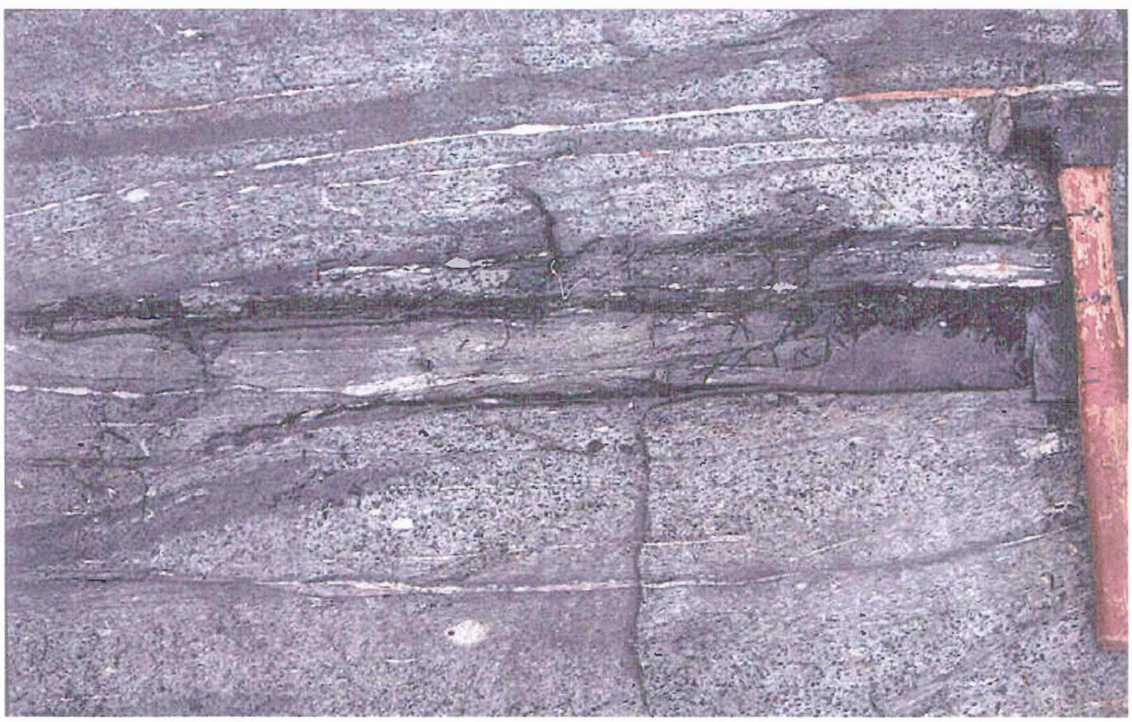

Figure 2.9 – Photographs from station 15 showing the formation of S2 by overprinting an earlier metamorphic fabric. Small dots are amphibole porphyroclasts (Amp 1) formed during M1, which are deformed along internal shear zones. These photographs show deformation in the horizontal plane. The dextral sense of shear is indicated by the arrows.

CHAPTER 3 -METAMORPHISM

3.1 Introduction

As indicated in chapter 2, the dominant lithologies of the HBHSZ are meta-basaltic rocks, which display greenschist facies to transitional amphibolite facies metamorphism. Because the meta-basalts are vastly in the majority, and because the meta-sediments have generally uninformative assemblages, only the metamorphism of the meta-basaltic rocks will be studied in detail. This thesis will concentrate on the polymetamorphic history that is seen in the rocks of the shear zone, but will also briefly discuss the metamorphism of rocks adjacent to the NWP. The mineralogy, textures, and some basic mineral chemistry of the rocks will be presented in this chapter, as well as a brief look at the metamorphic history and P-T conditions.

3.2 Mineral Assemblages and Facies

Detailed petrographic descriptions of the 10 samples that were chosen for argon analysis are presented in Appendix B. A brief summary and discussion of these results are presented here. The increasing metamorphic grade to the south of the HBHSZ is seen in thin section, as well as in the field. Samples 01N030d and 90N007c (refer ahead to Fig. 4.6) come from outcrops to the south of the HBHSZ, and display metamorphic assemblages indicating a slightly higher metamorphic grade than the remainder of the samples from the HBHSZ (i.e. more hornblende rich amphibole, Winter, 2001). These two samples display assemblages consisting largely of hornblende and plagioclase. They appear to be highly recrystallized. The mineralogy of the samples suggests that these rocks were subjected to lower amphibolite facies metamorphism.

Samples from the HBHSZ display more complex assemblages. A second phase of metamorphism (M2) is seen overprinting an earlier phase (M1). Although we see evidence in the field for 3 post-M1 deformational events, the only event that produced significant changes in the mineralogy of the samples was D2. The remainder of the discussion is therefore limited to a description of M1 and its subsequent deformation and metamorphism during D2, and the formation of the S2 fabric.

One of the most significant effects of M2 on the mineralogy of these samples is the formation of a second distinct generation of amphibole. This second generation of amphibole clearly overprints the earlier phase. For the purpose of this thesis, the two phases of amphibole will be referred to as *Amp 1* (associated with M1) and *Amp 2* (associated with M2).

Thin section and microprobe analysis enabled the M1 mineral assemblages to be determined (see Appendix A for abbreviations). In general, the assemblage consists of: act [Amp 1] + plag + qtz + chl + ep +/- ttn +/- ap +/- ilm (Fig. 3.1). This mineral assemblage is typical of greenschist facies metamorphism in meta-basalts (Winter, 2001).

The M2 mineral assemblage is quite similar to that of M1, with the exception that Amp 2 appears to be more hornblende-rich in color and composition than Amp 1. In general: amp [Amp 2] + plag + qtz +/- chl +/- ep +/- ttn +/- ap +/- ilm +/- ksp (Fig. 3.1). Based on mineralogy, the metamorphic grade of M2 is thus interpreted to be transitional greenschist to amphibolite facies (Winter, 2001).

3.3 Textures and Deformation Fabrics

Descriptions and photographs of the textures of each sample are presented in Appendix B. Some important generalizations from the samples will be made here.

Amphibole 1 generally forms large porphyroclasts, deformed and rotated by D2, averaging ~3mm in size. The porphyroclasts are wrapped by S2, have strain shadows, and show some degree of rotation relative to S2. Some of these porphyroclasts contain inclusions of other minerals such as plagioclase and quartz. In some rocks, the plagioclase inclusions are lath-shaped, which most likely represents the original texture of the basalt (Fig. 3.2). In general, it appears that Amp 1 replaced clinopyroxene in the original basalt (sample 90N015d, Appendix B).

Amphibole 2 generally forms on the rims of the large porphyroclasts of Amp 1. It also occurs in the strain shadows of these deformed porphyroclasts, and in the matrix of the samples. Grain size varies significantly; matrix grains are on average <<1mm. Grain shape varies from subidoblastic to xenoblastic blocky grains. The core – rim relationship between Amp 1 and 2 is seen consistently in samples from the HBHSZ. This relationship further supports the conclusion that Amp 1 growth predated Amp 2 growth.

Backscatter electron images (BSEI) are particularly useful for showing the textural relationship between Amp 1 and Amp 2. BSEI images enhance the contrast between amphiboles 1 and 2, and show them as two distinctly different shades of grey. The brightness of the BSEI is related to the mean atomic number (Z) of minerals involved. In the BSEI's, actinolite (Amp 1) is medium grey, while hornblende (Amp 2) is light grey, as it has an overall higher atomic number than actinolite. Low Z minerals such as plagioclase and quartz appear as very dark shades of grey to black, and high Z minerals such as ilmenite and titanite, appear as very bright areas. Figure 3.3 shows a few examples of these images from porphyroclastic samples from the HBHSZ, clearly illustrating the core and rim relationship between the two amphiboles.

Samples from within the HBHSZ contain the penetrative fabric, S2. Presumably, the formation of this fabric caused the porphyroblasts of Amp 1 to be deformed and break down into smaller clasts. In most cases, the dextral sense of shear associated with S2 is indicated by the asymmetric shape of Amp 1 porphyroclasts and their strain shadows (Fig. 3.3). The degree to which the rocks have been deformed by D2 varies from sample to sample. As mentioned in chapter 2.2, within the HBHSZ are both relatively lower and higher strain zones. Transitions between the two zones are clearly seen in the field. In thin section, the mineralogy and textures of these different zones were examined (refer to Appendix B, samples 15-51b & 15-51a). The lower strain zones correspond to the more porphyroclastic samples of the HBHSZ, which are described above. The higher strain zones do not contain any porphyroclasts of Amp 1, presumably as all of the porphyroclasts have broken down and have been completely recrystallized. In samples such as 15-51b, virtually all of the amphibole in the sample is Amp 2 (Fig. 3.4). S2 has thus been determined to have formed concurrently with Amp 2 growth.

In some samples from the HBHSZ, other than those described in Appendix B, there are few grains of Amp 2 (<2%) that have grown across the main fabric, S2. Presumably these grains were not deformed during D2, and finished crystallizing just after S2 formed. The rare occurrence of these grains reinforces the hypothesis that Amp 2 growth is post-S1 and syn to post-S2.

Samples that come from areas south of the HBHSZ, such as 01N030d and 90N007c, contain a very similar fabric to those within the HBHSZ. These samples are highly recrystallized and contain virtually no traces of Amp 1. The higher grade samples are dominated by Amp 2, presumably because of near complete recrystallization due to proximity to the NWP.

3.4 Mineral Chemistry

Extensive microprobe analyses were conducted on many samples from the field area, including analyses of samples not described in Appendix B. Spreadsheets of these analyses are included, in digital format, in the back of this thesis. Microprobe analyses of amphibole and plagioclase grains from samples analyzed for $^{40}Ar/^{39}Ar$ are presented in Appendix D. Recalculation of these analyses and classification of the minerals were completed using geological software, *Minpet* (Richard, 1997). The classification diagrams produced by this program are shown in figures 3.5 and 3.6.

These diagrams clearly show the compositional differences between Amp 1 and Amp 2. Amphibole 1 is classified as actinolite to actinolitic hornblende, while Amp 2 is classified as magnesio-hornblende to tschermakitic hornblende. In Figure 3.5 (b), a rough linear trend can be seen on the plot of Mg/(Mg + Fe2) vs total Si. This linear trend may reinforce the interpretation that Amp 2 is derived from Amp 1 and replaces Amp 1 to different degrees, depending on the grade of the rocks.

The plagioclase classifications (Fig. 3.6) show that most plagioclase is An_{20-40}, and is thus oligoclase to andesine. No samples contain plagioclase compositions between 10 and 20% An; this is consistent with the peristerite gap that exists in plagioclase feldspar compositions between the greenschist and amphibolite facies (Winter, 2001). Generally all of the samples that were judged to be in equilibrium with Amp 2 contain oligoclase to andesine. This is consistent with the classification of these samples as being higher grade, namely amphibolite facies.

3.5 P-T Conditions

Based on the mineralogy of the samples, broad estimates for the P-T conditions of the samples used in this thesis can be obtained. A reasonable estimate for the conditions of greenschist facies M1 would be 350 – 450 °C and 2 – 7 kb (Winter, 2001). The metamorphic grade of M2 appears to be slightly higher than that of M1, and is likely between 500 and 600 °C, and 5 - 10 kb (Winter, 2001) (Fig. 3.1).

More detailed estimates of the P-T conditions were obtained using the hornblende – plagioclase thermometer of Holland and Blundy (1994), and the garnet - biotite thermometer of Ferry and Spear (1978) as reported in Winter (2001). The results are shown in Appendix E, and summarized in Figure 3.7. These calculations yielded temperatures for the samples that were higher than expected, based on mineralogy. The calculations show evidence for a thermal gradient across the study area, ranging from ~700°C near the NWP to ~600°C north of the HBHSZ (for pressures at about 5 kb). Presumably, this gradient is a result of the syn-tectonic emplacement of the NWP. The results in Appendix E also indicate higher temperatures for M2 assemblages (~650°C), when compared to M1 assemblages (~600°C) in the same sample.

The temperatures reached by the rocks, as indicated from thermobarometry, are well within the range for amphibolite facies metamorphism. Despite the fact that only few recrystallized samples actually show amphibolite facies assemblages, the results in Appendix E very convincingly show that all the rocks in the shear zone reached temperatures of over 600 °C. This discrepancy between estimations based on mineralogy and calculations is most likely explained by the fact that many of the samples did not have enough time to re-equilibrate at the high temperatures that were brought about by the short-lived thermal pulse from the NWP. It appears that only those samples that were actively undergoing recrystallization at the time of intrusion of the NWP were able to re-equilibrate to the new temperature conditions.

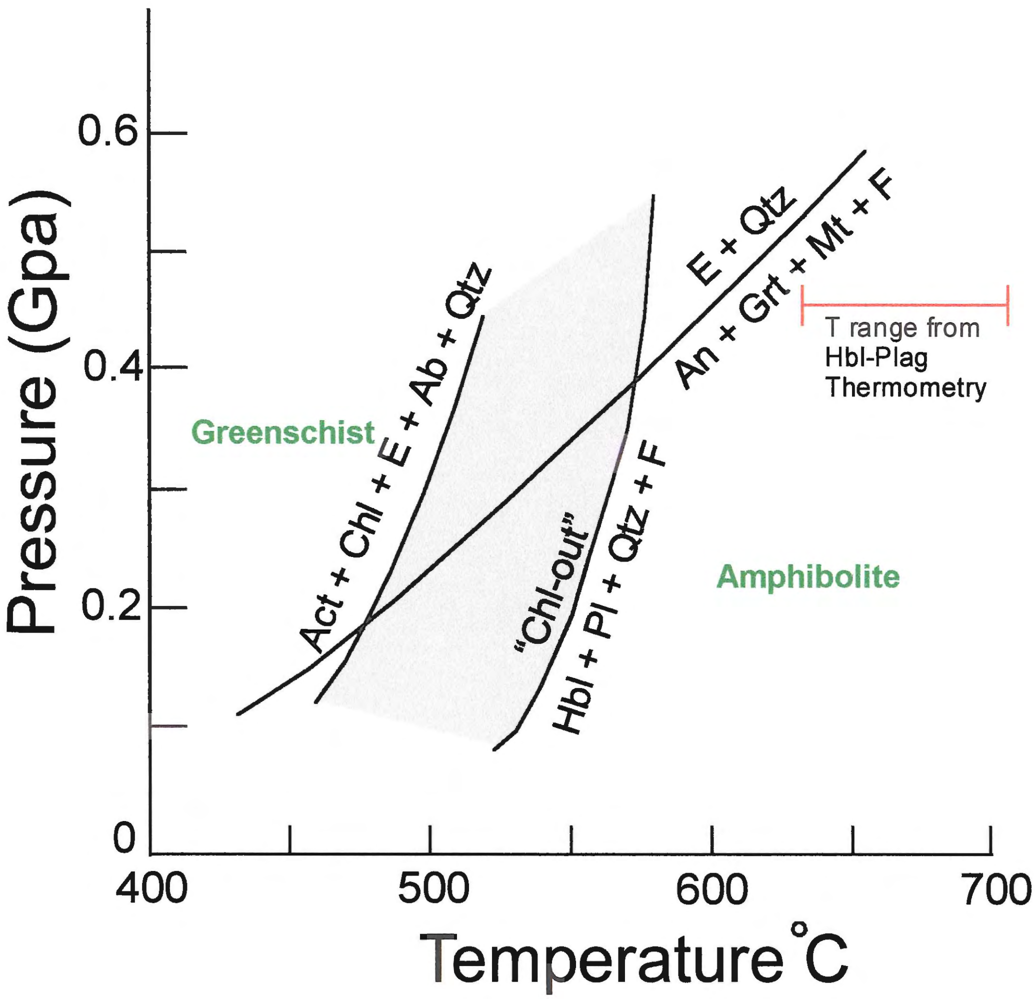

Figure 3.1 - Simplified petrogenetic grid for metamorphosed mafic rocks. Shaded area represents the transitional zone between greenschist and amphibolite facies. Red bar indicates the approximate T range calculated for the samples from this thesis (refer ahead to section 3.5). Mineral abbreviations can be found in Appendix A, as well as: E = an epidote mineral: epidote, zoisite , or clinozoisite, F = fluid, An = anorthite, Ab = albite, Mt = magnetite, Pl = plagioclase. (Adapted from Winter, 2001.)

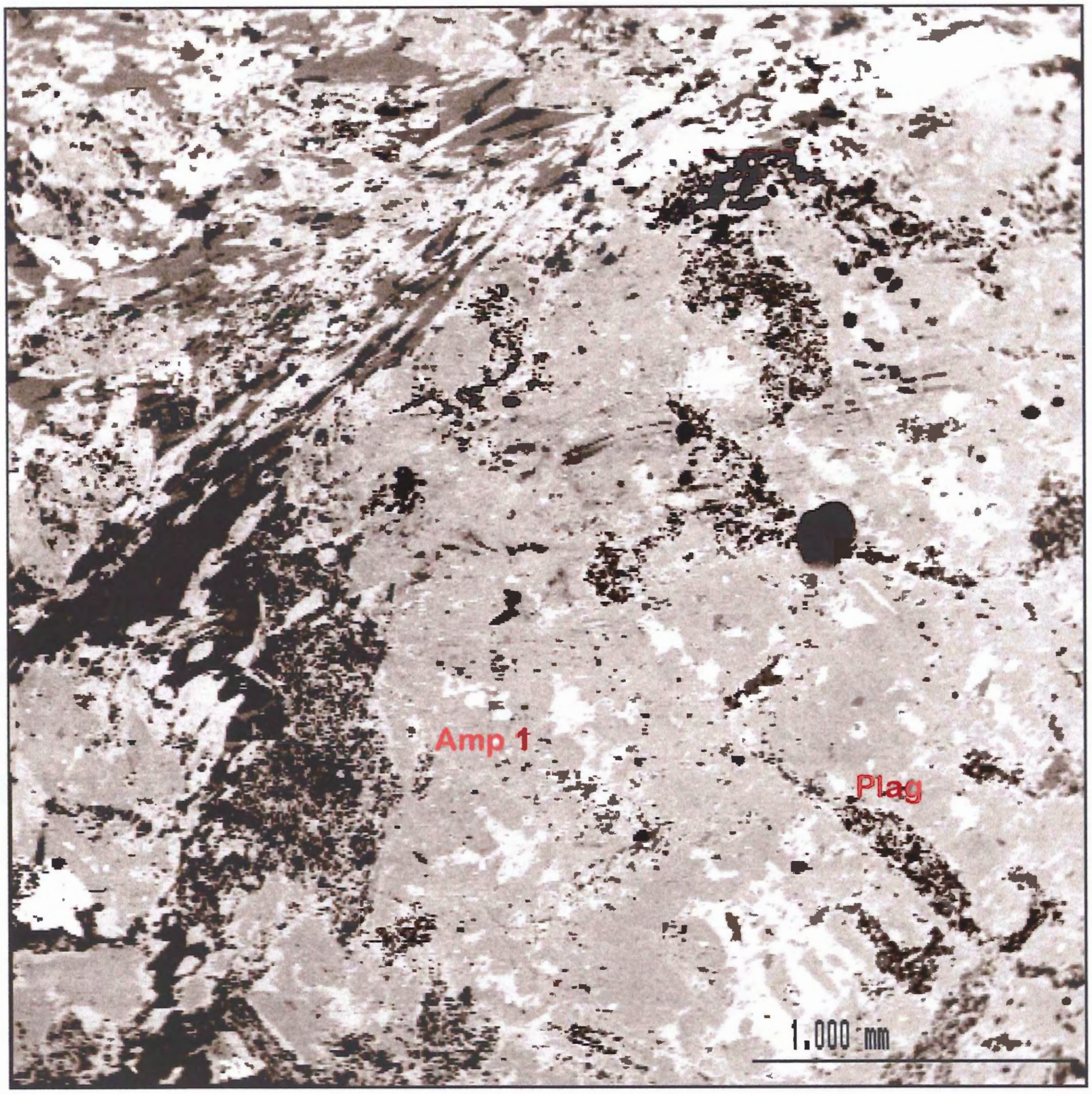

Figure 3.2 – Backscatter electron image of sample 90N002j. The lower and right side of the image is dominated by a large porphyroclast of amphibole. The original texture of the rock preserved in the lath-like shaped plagioclase inclusions.

Figure 3.3 (a) to (c) – Backscatter electron images of porphyroclastic samples from the HBHSZ. The core and rim relationship between Amp 1 and 2 is clearly illustrated in these images. Amp 1 is seen as a medium grey, and Amp 2 as a light grey. Dark shades are plag and qtz, while very bright areas are opaques or other accessory minerals. (Compare with photomicrographs shown in Appendix B.)

(a) Sample 90N013a

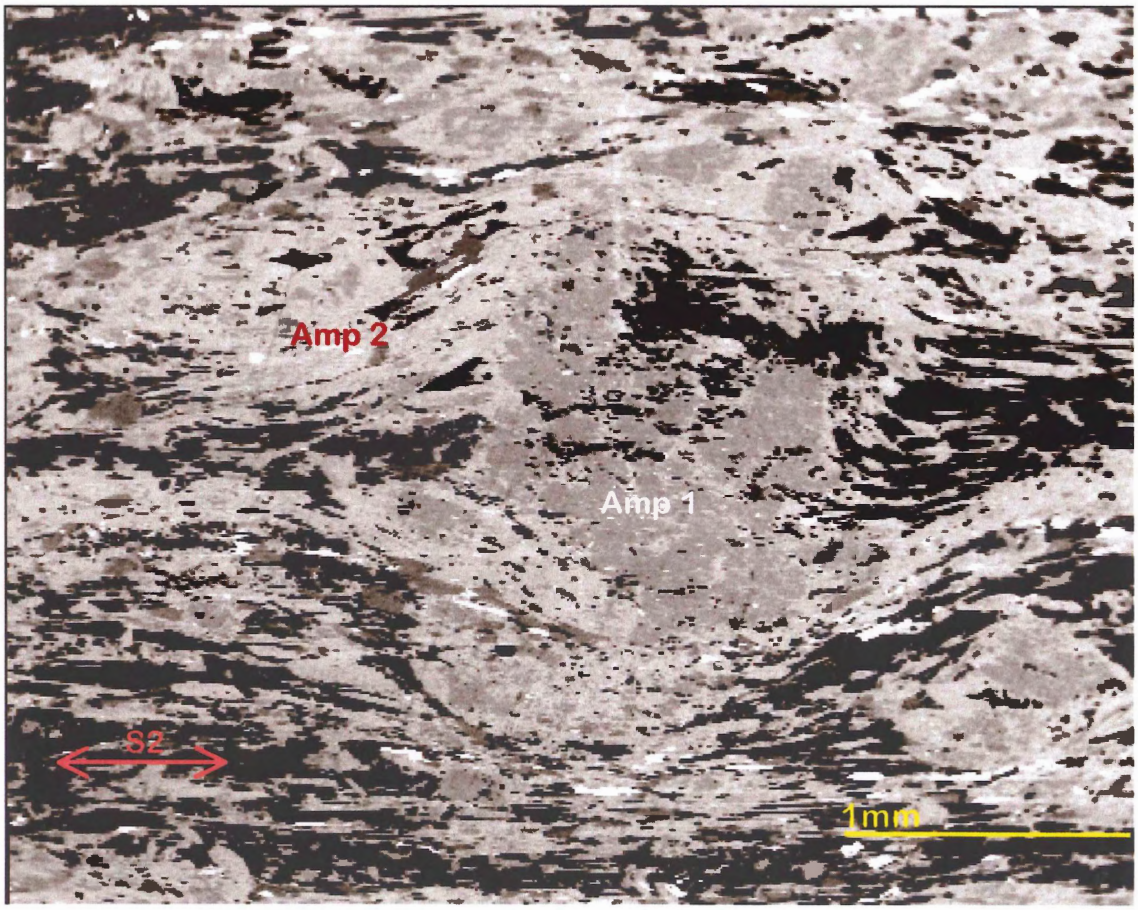

(b) Sample 90N015d

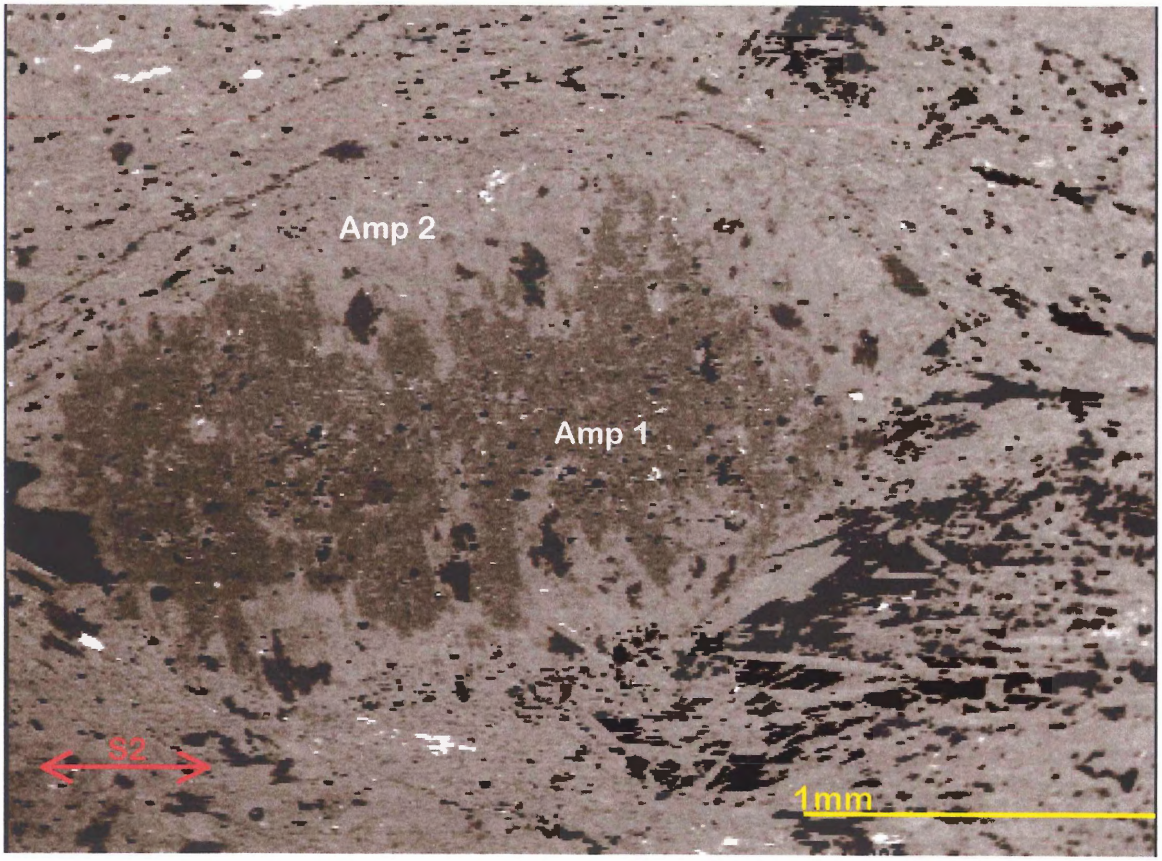

(c) Sample 15

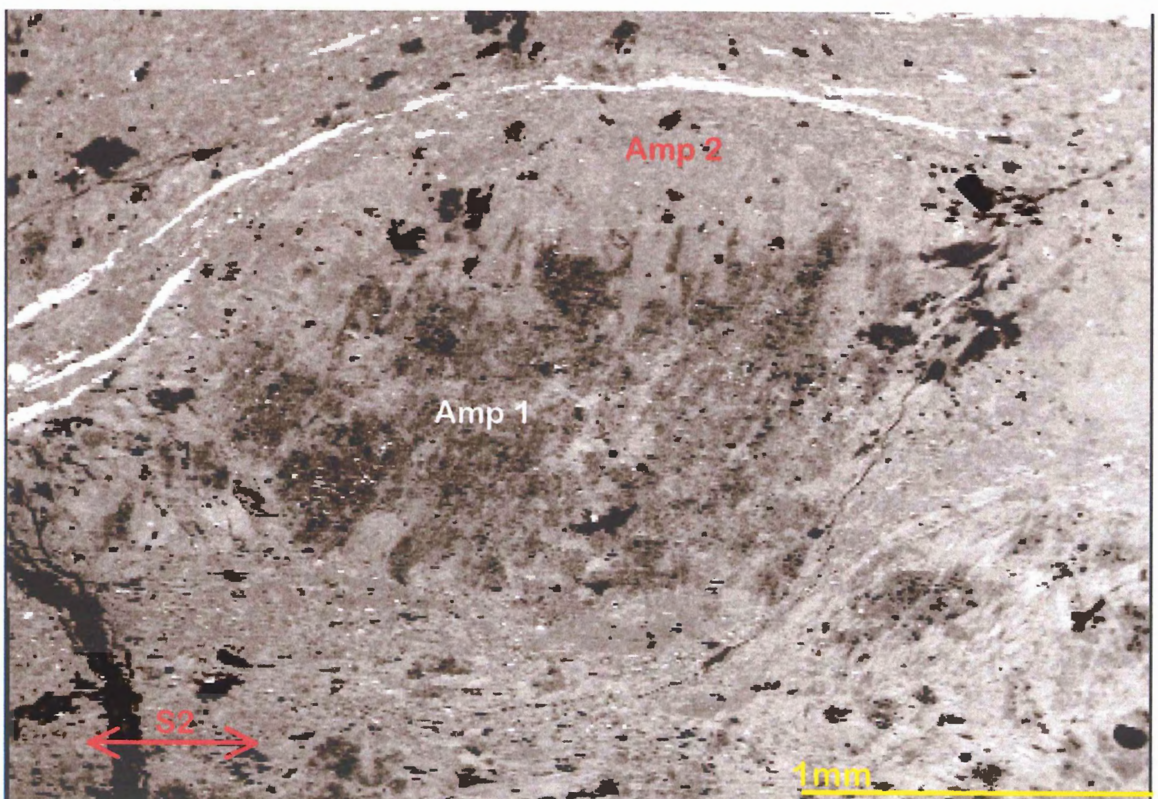

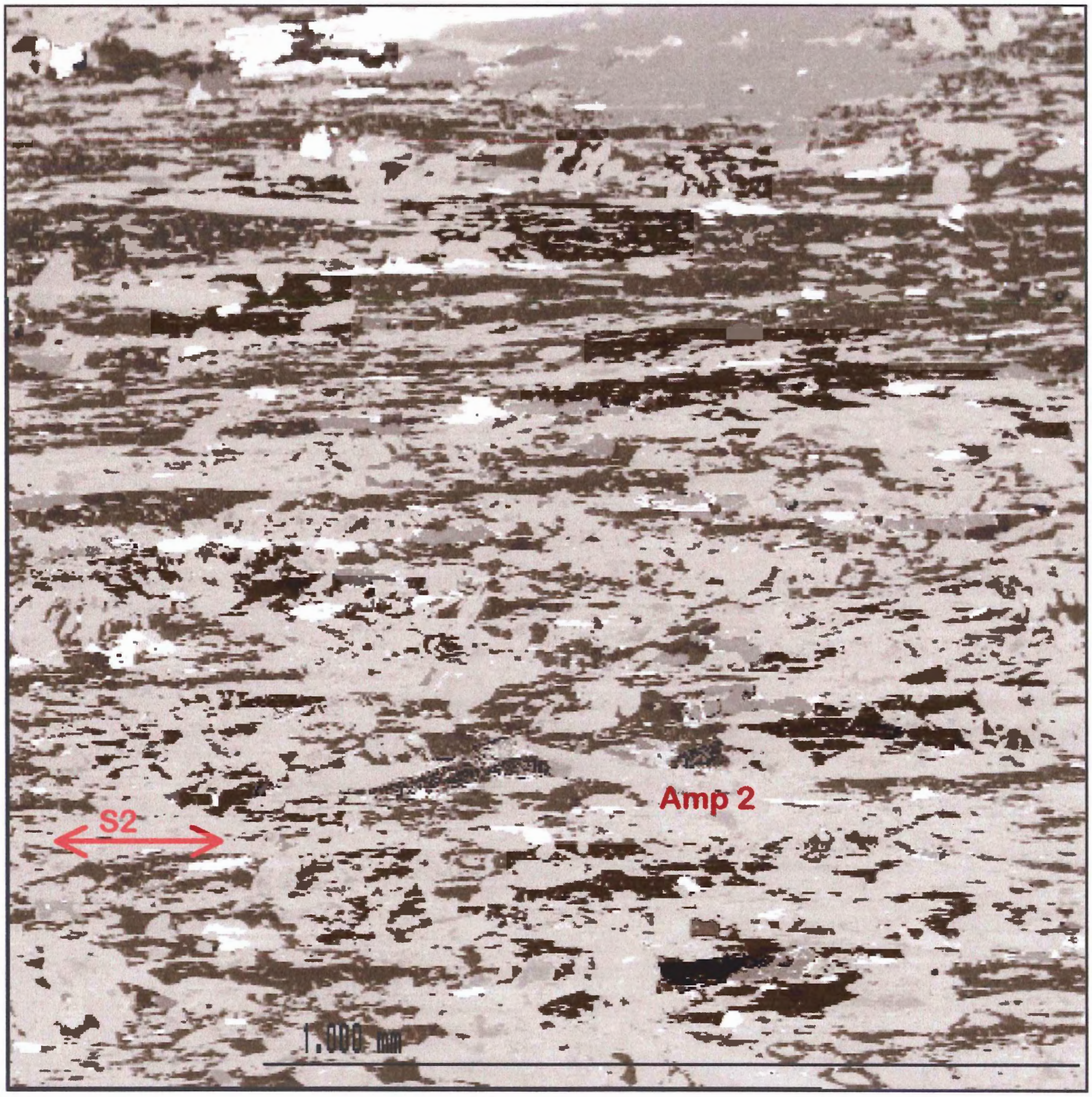

Figure 3.4 – Backscatter electron images of sample 15-51b. This sample is highly strained and very recrystallized. Virtually all of the amphibole in the sample is Amp 2. Dark shades are plag and qtz, while very bright areas are opaques or other minerals with high atomic numbers.

Figure 3.5 (a) to (g)– Classification of all amphibole analysis used for this study. Recalculation of microprobe analyses and classification of these analyses were completed using the geological software *Minpet* (Richard, 1997). The recalculation procedure was based on an anhydrous basis to cations per 23 oxygens, similar to Richard and Clarke, 1990. Classification is according to Hawthorne, 1981.

(a) – All amphibole analyses classified using a plot of the four principal groups

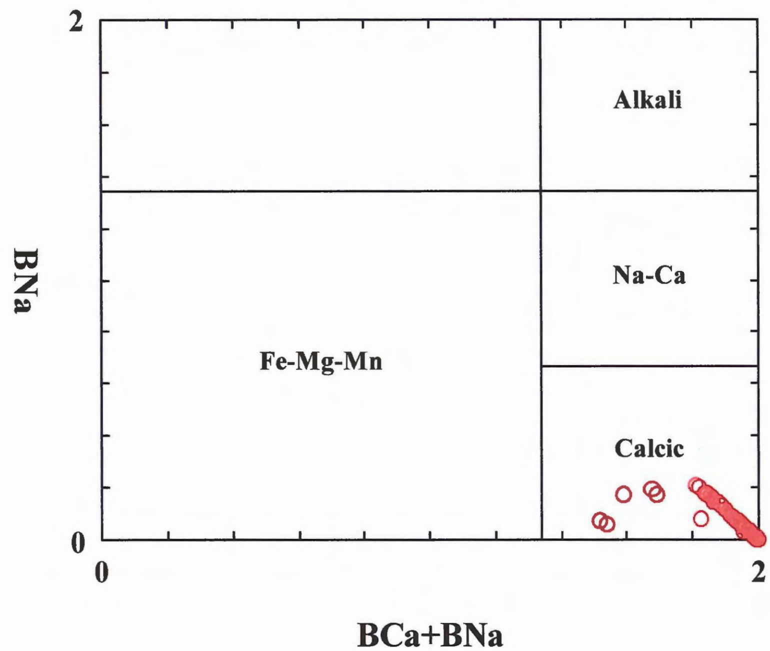

(b) – Classification of all amphibole analyses. Calcic amphiboles, where ANa+AK<0.50 and Ti<0.50.

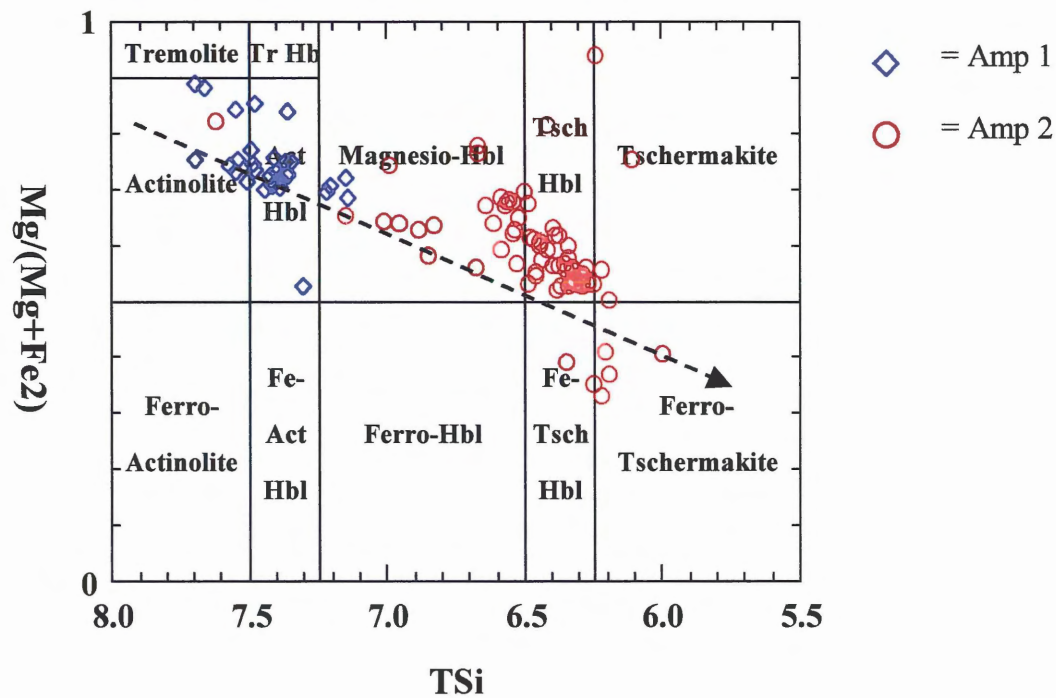

(c) – Classification of amphibole analyses from sample **01N030d**. Calcic amphiboles, where ANa+AK<0.50 and Ti<0.50.

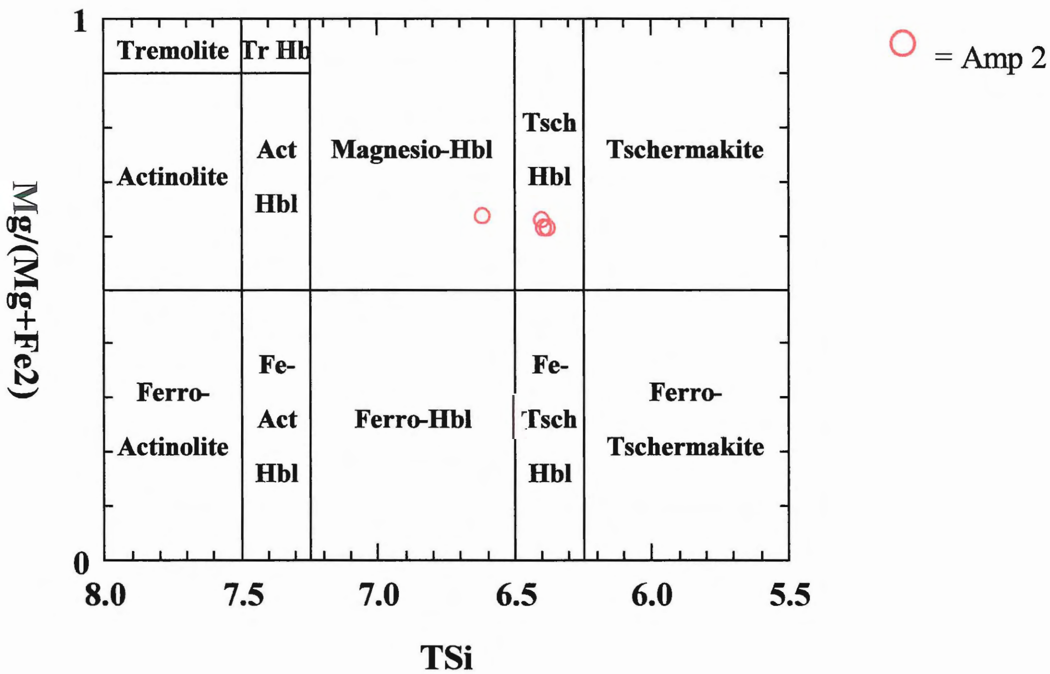

(d) – Classification of amphibole analyses from sample **90N007c**. Calcic amphiboles, where ANa+AK<0.50 and Ti<0.50.

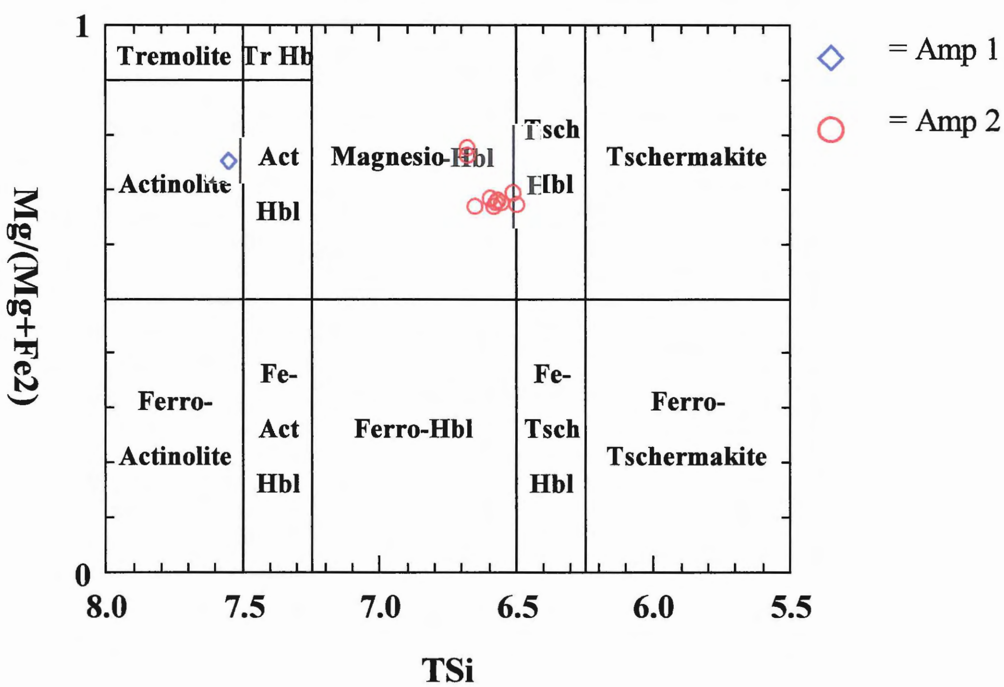

(e) – Classification of amphibole analyses from sample **90N0013a**. Calcic amphiboles, where ANa+AK<0.50 and Ti<0.50.

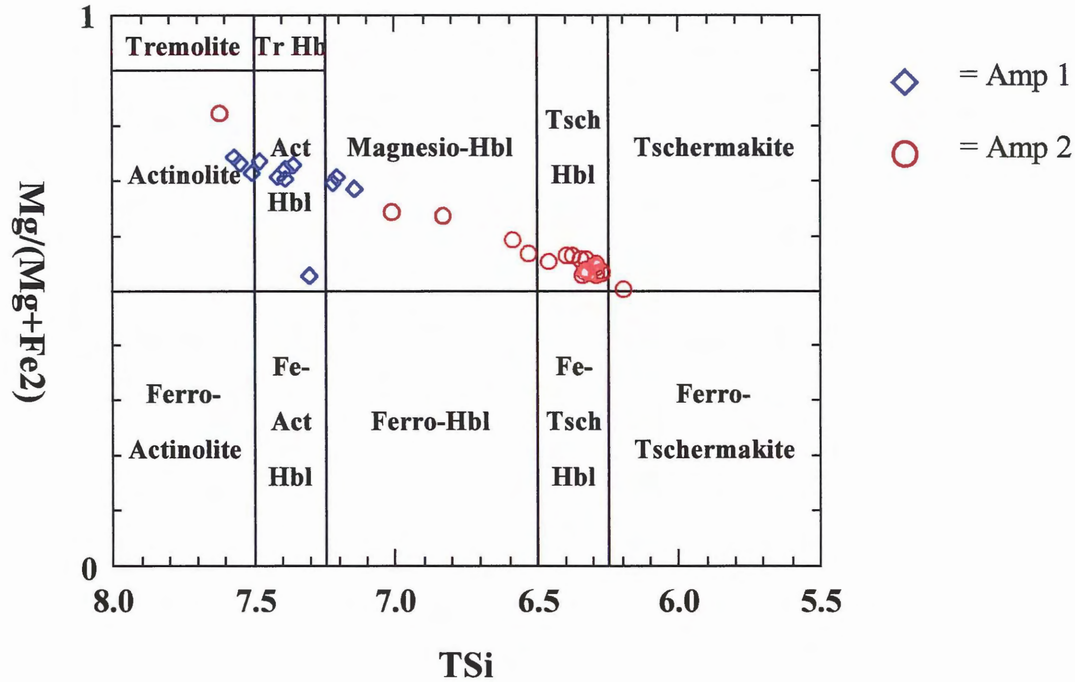

(f) – Classification of amphibole analyses from samples from location 15, in the HBHSZ. Calcic amphiboles, where ANa+AK<0.50 and Ti<0.50.

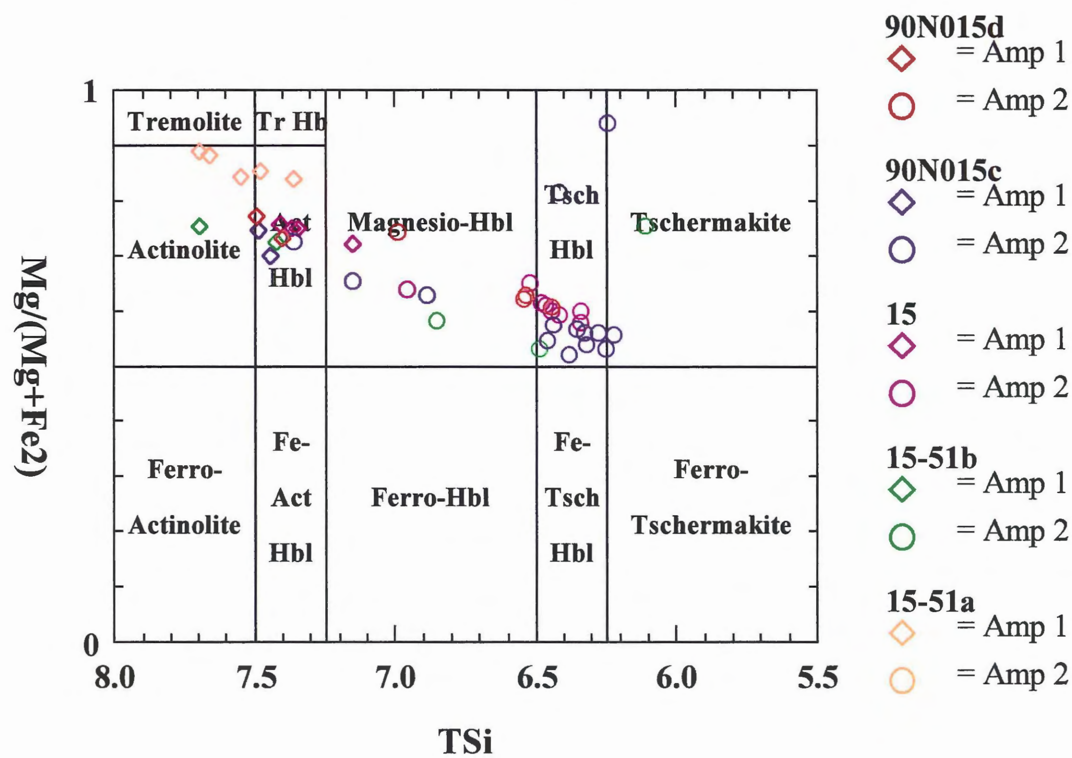

(g) – Classification of amphibole analyses from samples from location 14, north of the HBHSZ. Calcic amphiboles, where ANa+AK<0.50 and Ti<0.50.

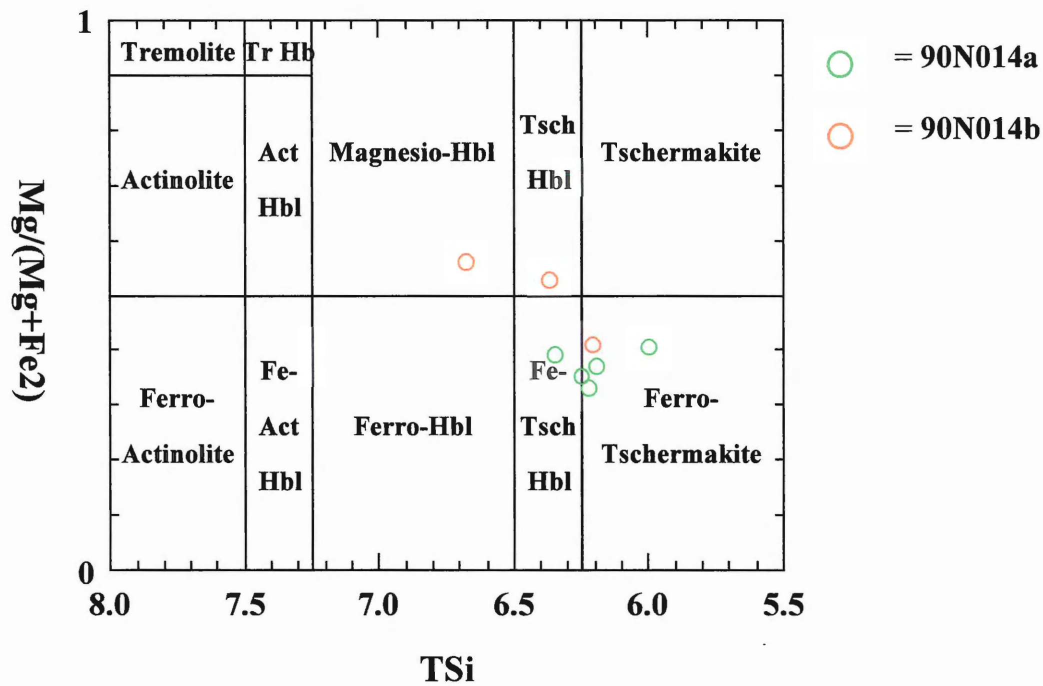

Figure 3.6 (a) to (d)– Classification of plagioclase analyses used in this study. Recalculation of microprobe analyses and classification of these analyses were completed using the geological software *Minpet* (Richard, 1997). The analyses were reclassified on the basis of fixed anions (O + F + Cl). The analyses were classified using the ternary plot Ab-An-Or.

(a) – All plagioclase analyses from samples which are judged to be in equilibrium with Amp 2. Equilibrium was judged optically; criteria include: (1) no reaction textures, (2) phases in physical contact, and (3) textural equilibrium.

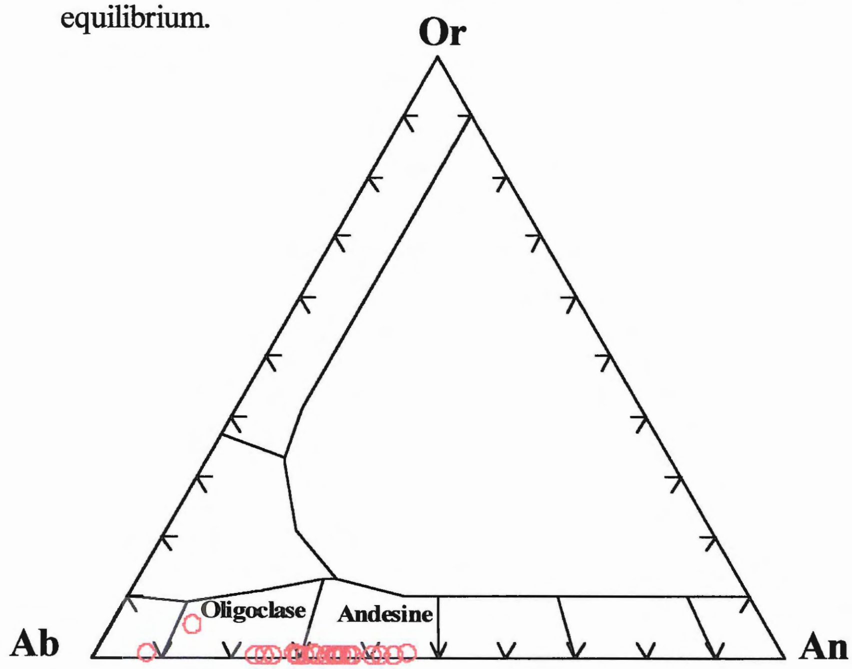

(b) – Sample 01N030d.

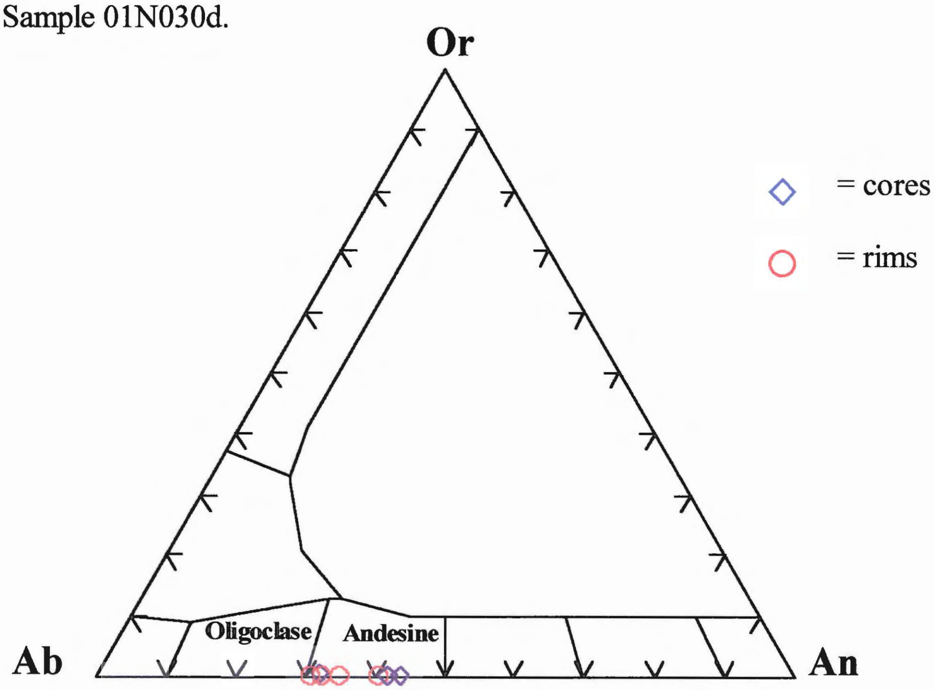

(c) – Sample 90N007c.

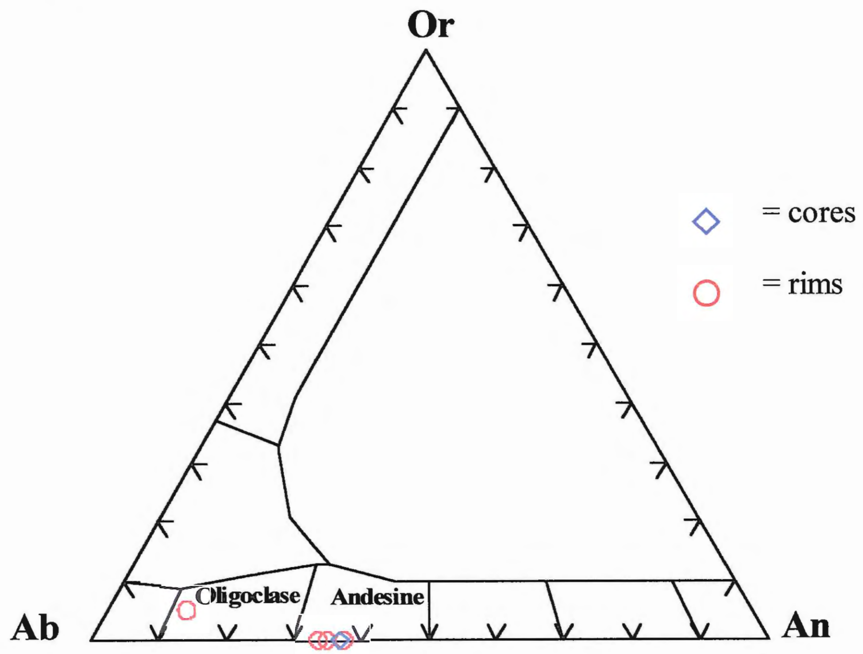

(d) – Sample 15-51b.

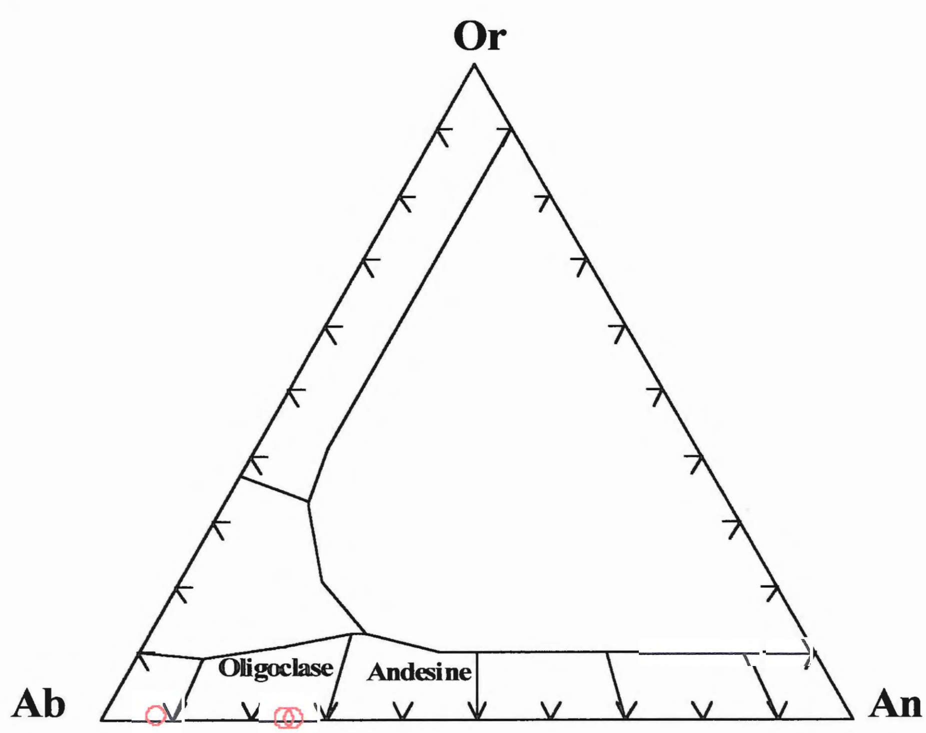

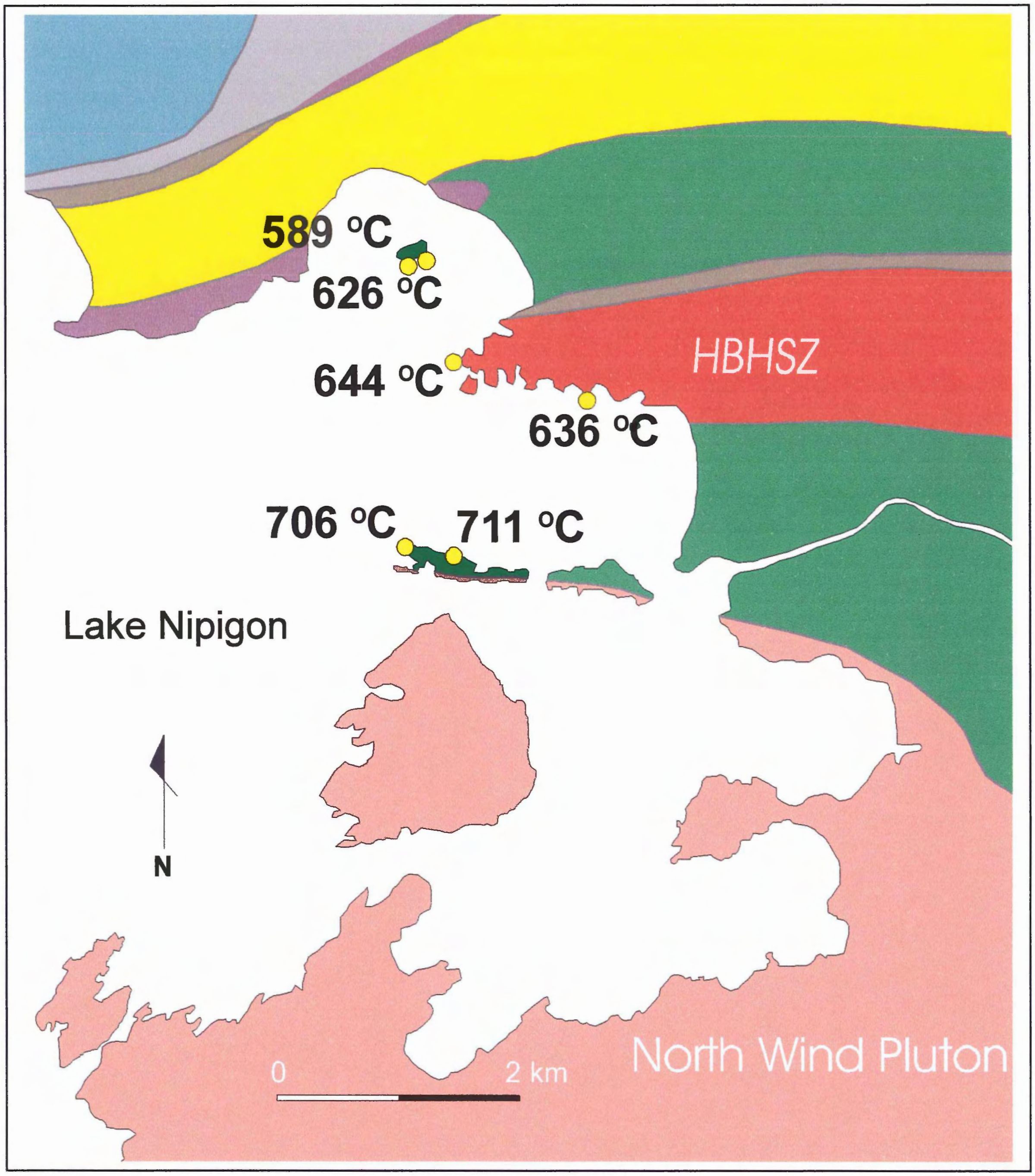

Figure 3.7 – Summary of calculated temperatures of peak metamorphism in the study area. Temperatures in this figure were all calculated by the hornblende-plagioclase thermometer of Holland and Blundy (1994). Some temperatures shown are simple averages of two or more calculations. Refer to Appendix E for details, and to Figure 2.5 for legend. (Map courtesy of N. Culshaw).

CHAPTER 4 - $^{40}Ar/^{39}Ar$ THERMOCHRONOLOGY

4.1 $^{40}Ar/^{39}Ar$ Dating Techniques

4.1.1 Introduction

The detection of the radioactive decay of ^{40}K and the presence of radiogenic ^{40}Ar in the late 1930s, formed the basis of one of the most widely used isotopic dating methods, the potassium - argon (K-Ar) method. Advances of the K-Ar dating method, including the development of the argon - argon ($^{40}Ar/^{39}Ar$) dating method by Merrihue and Turner (1966) and laser heating, have improved the precision and versatility of the method. $^{40}Ar/^{39}Ar$ analysis allows geologists not only to determine the ages of rocks, but also to reconstruct their thermal histories.

4.1.2 Basic Theory

The element potassium (K) is common in potassium feldspars, micas, and hornblende, where it occupies lattice sites in these minerals. Potassium has 18 isotopes, the majority of which are unstable. The isotope ^{40}K is radioactive, and undergoes branched decay to ^{40}Ca and ^{40}Ar by the process illustrated in Figure 4.1. Approximately 11% of ^{40}K atoms decay to ^{40}Ar.

The element argon is a noble gas that becomes "trapped" in minerals. Its presence is easy to detect and measure. This makes the K-Ar method a useful dating tool. The following equation describes the growth of radiogenic argon and calcium:

$$^{40}Ar^{*} + {}^{40}Ca^{*} = {}^{40}K\,(e^{\lambda t} - 1) \qquad (1)$$

where: t = time, $^{40}Ar^{*}$ = radiogenic argon, $^{40}Ca^{*}$ = radiogenic calcium, λ = total decay constant of $^{40}K = 5.543*10^{-10}\ y^{-1}$ (Attendorn and Bowen, 1997). The age equation derived from (1) is:

$$t = \frac{1}{\lambda} \ln\left(\frac{^{40}Ar^{+}}{^{40}K} \left(\frac{\lambda}{\lambda e} \right) + 1 \right) \tag{2}$$

where: λe = the decay of ^{40}K to $^{40}Ar = 0.581 *10^{-10}\ y^{-1}$ (Attendorn and Bowen, 1997). From this, the half-life of ^{40}K has been determined to be 1250 million years. Because this half-life is sufficiently large, there is virtually no limit on the age of rocks used for the K-Ar method.

There are several underlying assumptions on which a reliable date is based:

1) Following closure to Ar retention (see section 4.1.5), no ^{40}Ar has escaped from the crystal by diffusion.
2) No excess argon was present when the mineral formed. (Corrections must be made for the presence of atmospheric argon).
3) The system must have remained closed to K gain or loss throughout its history.
4) There was no unusual isotopic fractionation of K.

These assumptions do not hold true for every case.

Since the half-life has been established, in order to date a rock by the above equation, all that needs to be determined are the concentrations of radiogenic Ar and radioactive K. The earlier K-Ar method and the later $^{40}Ar/^{39}Ar$ method determine these concentrations using different techniques.

4.1.3 $^{40}Ar/^{39}Ar$ Dating

Unlike the conventional K-Ar method, where the sample to be analyzed must be split into two separate fractions to analyze for ^{40}K and ^{40}Ar contents, the $^{40}Ar/^{39}Ar$ method uses only one sample to analyze for both elements. The $^{40}Ar/^{39}Ar$ method measures ^{40}K in the sample via a proxy, i.e. ^{39}Ar produced by neutron irradiation of ^{39}K, the latter being proportional to ^{40}K. The sample is first irradiated in a nuclear reactor to transform a small number of ^{39}K atoms to ^{39}Ar through the high-energy interaction of neutrons. Like the K-Ar method, the sample is then placed in an ultra-high vacuum, where the argon is extracted by high temperature fusion. The relative abundances of all of the Ar isotopes are then measured in a mass spectrometer.

A conversion ratio of ^{39}K to ^{39}Ar is determined indirectly by irradiating a standard of known age. Since the ratio of ^{39}K to ^{40}K is known, a measure of ^{39}Ar will enable the ^{40}K to be determined.

The age equation presented above can thus be re-written as:

$$t = \frac{1}{\lambda} \ln \left(\frac{^{40}Ar^{+}}{^{39}Ar} (J) + 1 \right) \tag{3}$$

where $J = (e^{\lambda tm} - 1) / (^{40}Ar^{+} / {}^{39}Ar)_s$, and where tm is the age of the standard, and $(^{40}Ar^{+}/^{39}Ar)_s$ is the measured standard ratio. The variable J is a dimensionless parameter which, in practice, is determined by irradiating a standard sample of known age along with the samples of unknown age.

Advantages of this method over the K-Ar method include:

(1) Only one sample aliquot needs to be analyzed. Potassium and argon are measured simultaneously by means of a mass spectrometer.

(2) Very small samples can be analyzed.

(3) Step-heating (see section 4.1.4) can provide information on a sample's thermal history.

4.1.4 $^{40}Ar/^{39}Ar$ Step-Heating

This approach to $^{40}Ar/^{39}Ar$ dating involves a step-wise heating of the sample from a few hundred degrees Celsius to complete fusion of the sample. After each increment of temperature increase, the argon gas that is released is analyzed in a mass spectrometer, where the relative abundances of the different isotopes are measured. The $^{40}Ar/^{39}Ar$ ratio and an age are then determined for each increment. Therefore, a single sample of a K-bearing mineral may provide numerous different ages.

The theory behind this technique is that argon diffuses out of the crystal from the edges first. The higher temperature steps are thus sampling argon from inner parts of the crystal. The age given by the inner parts of the crystal should then reflect the original cooling age of the rock, whereas the outer edges (and earlier ages) may be affected by diffusion from later heating and cooling due to metamorphism, and other effects such as irradiation-induced recoil.

The data from this type of analysis are commonly presented as graphical "age spectra". Figure 4.2 illustrates the step-heating method and some typical plots. The $^{40}Ar/^{39}Ar$ step-heating method is one of a very few that may give ages for both the original cooling of the rock and later thermal events (Prothero and Schwab, 1997).

4.1.5 Closure Temperature and Diffusion

Rapidly cooled rocks (e.g. lavas extruded at the earth's surface) that contain K-bearing minerals begin to accumulate Ar as soon as they crystallize. However, metamorphic rocks generally have a long cooling history, and as such, they are not able to retain any Ar until they are cooled below a certain temperature. At this temperature, the loss of Ar by diffusion from the crystal lattice of K-bearing minerals is insignificant when compared to its rate of accumulation. Dodson (1973) named this the closure temperature of the geochronological system. He defined closure temperature as the temperature of a system at the time corresponding to its apparent age. He assumed that diffusion and temperature are related by Arrhenius' Law:

$$D = Do \exp(-E/RT) \tag{4}$$

where E = activation energy, R = gas constant, and Do = pre-exponential constant. The closure temperature (Tc) of a species such as Ar within a particular mineral is given by:

$$Tc = \frac{E/R}{\ln(A) + \ln\left(\frac{Do/a^2 * Tc^2}{E/R * dT/dt}\right)} \tag{5}$$

where Do/a^2 = grain size parameter, a = effective diffusion radius (e.g. grain size), dT/dt = cooling rate, and A = numerical constant depending on geometry and decay constants of the parent (Dodson, 1973). This equation shows that the closing temperature depends on grain size and activation energy, and must be calculated for a specific cooling rate. Higher closure temperatures will be obtained for minerals with a large radius and rapid cooling rates. However, closure temperature depends more on activation energy, and therefore mineralogy, than radius and cooling rate. The closure temperatures of different minerals such as biotite and hornblende are very different (Fig. 4.3). Hornblende is an excellent mineral to date in metamorphic rocks because it is found in many regionally metamorphosed rocks, has a high retention of argon, and thus a high closure temperature. Variations in argon closure temperature as a function of cooling rate and effective diffusion radius for hornblende are shown in Figure 4.4. This figure shows cooling rate on the x-axis as a logarithmic scale, and thus Tc is rather insensitive to cooling rate and also to the effective diffusion radius in this case.

4.1.6 Interpretation of $^{40}Ar/^{39}Ar$ Spectra

$^{40}Ar/^{39}Ar$ spectra have the potential of constraining the thermal history of a region (i.e. of defining a T-t path). A flat spectrum (or plateau) represents an undisturbed system that has remained closed to argon loss (or gain) throughout its history (Fig. 4.5). A generally accepted definition of a 'plateau' is a set of contiguous steps that together contain 50% or more of the total ^{39}Ar released, and for which all apparent ages are indistinguishable. The apparent age of the plateau therefore approximates the time that the sample crystallized or last cooled through its closure temperature after metamorphism.

A spectrum that displays low ages at the lowest extraction temperatures and successively higher ages at higher temperatures represents a disturbed system (Fig. 4.5). Samples that display this type of age spectrum have likely experienced partial argon loss from a later thermal disturbance after their original cooling. The youngest age (at the low end of ^{39}Ar release) provides an upper limit to the time of the thermal event. If the disturbed spectrum does approach a flat plateau, and if the amount of Ar lost is relatively small, this age plateau can be taken to represent the time of original closure.

Disturbed spectra can also indicate very slow cooling of the mineral. The lowest age derived is therefore the time of the final closure of the mineral. A hornblende spectrum that has a high initial spike may represent a sample that contains excess argon. In some cases, highly discordant spectra can represent sheared samples.

4.2 Analytical Methods

4.2.1 Sample Selection and Preparation

Samples for this study were selected on the basis of their field locations, field relationships, mineralogy, and texture. Samples were taken from different locations across the width of the HBHSZ in order to obtain a representative transect. Samples 01N030d and 90N007c were taken close to the edge of the North Wind Pluton, while samples 90N013a, 15, 15-51a, 15-51b, 90N015d, 90N015c, 90N014a, and 90N014b were taken from areas successively farther north of the pluton (Fig. 4.6).

These locations were sampled carefully in the field, from units that were laterally continuous and geologically significant. For example, samples 15-51a and 15-51b were sampled within meters of each other, but sample b is from a high strain zone, and sample a is from a lower strain 'pod' within that high strain zone (section 2.3).

Samples 90N013a, 90N015c and 90N015d were sampled from rocks similar to 15-51a. They contain abundant porphyroclastic amphiboles. Samples 01N030d and 90N007c, on the other hand, do not contain any porphyroclasts, and in the field appear to be highly recrystallized. These two samples were obtained from an island close to the NWP. Samples 90N014a and 90N014b were taken from an island to the north of the HBHSZ.

The samples were also chosen for their mineralogy in order to avoid other K-bearing phases. Samples that contained abundant hornblende, little biotite, and little sericite were chosen, as well as samples which appeared to be the least weathered. Finally, the samples were assessed for adequate K content. Samples that contain amphiboles with K_2O >/= 0.1% were preferred.

The 10 chosen samples were crushed using a jawcrusher and rotary mill, and sieved using sieve size ranges of 0.841-0.3 mm and 0.3-0.15 mm. The "cleaner" fraction of the two, i.e. the fraction which contained fewer polymineralic grains, was then magnetically separated using the Frantz magnetic separator. The samples were then examined under a binocular microscope, and single amphibole grains were hand-picked using a small brush. Approximately 30 - 40 mg of amphibole was picked from each sample.

Because some of the samples from the shear zone contain two phases of amphibole growth, the following technique was used in order to distinguish between the two phases in samples 90N015c and 90N015d. A ~50 mm slab was placed on top of a light source and selected grains were cut out with a scalpel. This technique maximized recovery of the desired amphibole (i.e. hornblende).

4.2.2 $^{40}Ar/^{39}Ar$ Analytical Techniques

Each of the 13 separates were tightly wrapped in aluminum foil and stacked in an irradiation canister by K. Taylor, Dalhousie University. Interspersed with the samples were aliquots of the standard sample, MMHb-1. The canister was then sent for irradiation in the McMaster University reactor in Hamilton, Ontario. After irradiation and several weeks of 'cooling', the samples and standards were then loaded into the fully automated analytical system in the Argon Isotope Research Lab at Dalhousie University. Each sample was heated in temperature increments from 650 to 1450 °C. After each temperature increment, the released gas was transferred from the furnace to a mass spectrometer. In the mass spectrometer, the relative concentrations of ^{36}Ar, ^{37}Ar, ^{39}Ar, and ^{40}Ar were repeatedly measured and recorded using an automated data acquisition system. The J values for each standard were calculated by the computer, and plotted against vertical distance in the canister. Figure 4.7 shows the linear relationship between the J values and distance. This graph was then used to interpolate J values for individual samples. The software first accounted for any interfering isotopes (i.e. argon isotopes produced during the irradiation other than the ^{39}Ar produced from ^{39}K), and for the presence of atmospheric argon, then calculated the apparent age for each temperature step.

4.3 Results and Interpretation of Spectra

Argon summary sheets for each of the 10 analyses are presented in Appendix C. A summary map and plot for preferred ages of hornblende are shown in figures 4.8 and 4.9. Step-heating age spectra and corresponding $^{37}Ar/^{39}Ar$ ratio spectra for each of the analyses are presented together in Figure 4.10. Also shown on the $^{37}Ar/^{39}Ar$ spectra are the calculated $^{37}Ar/^{39}Ar$ ranges for hornblendes. These ranges were calculated from microprobe data (Appendix D) on Ca and K abundances (Fig. 4.11), in order to confirm that the argon gas from each sample was indeed released from hornblende. Corresponding plateaus that overlie calculated ranges indicate that the gas is all derived from hornblende and that the age given is a reliable age for hornblende. Calculation of this ratio was based on the following relationship:

$$\{(Ca^{2+} / K^{+})_M * (Ca^{2+} / K^{+})\}/1.9 = {}^{37}Ar/{}^{39}Ar \qquad (6)$$

Where: $(Ca^{2+} / K^{+})_M$ is the atomic ratio from CaO and K_2O oxide percents, and (Ca^{2+} / K^{+}) is the ratio of atomic weights.

The numerical ages presented on the spectra in Figure 4.10 are mean ages, calculated over a specified range of temperature steps. These mean ages are determined using a weighted-average calculation, based on the percentage of argon released at each step. Calculation of a mean age for each hornblende sample was based largely on interpretation of the age spectra, and is therefore somewhat subjective. Two main criteria were adopted in order to establish the range over which the mean age was calculated. The first criterion was that the steps employed must be ones for which calculated $^{37}Ar/^{39}Ar$ ratios are in accordance with observed ones. Secondly, steps were chosen where there was no (or very minimal) age gradient, and where the steps approximated a plateau. In the present study, these criteria were not followed rigorously, and some exceptions were made. Therefore, some of the calculated age 'plateaus' are only 'pseudo-plateaus'. Each analysis presented in Figure 4.10 is discussed briefly below. For additional information on each sample location, mineralogy, and texture, refer to Appendix B.

General observations

The spectra presented in Figure 4.10 generally show age gradients with varying degrees of noise. In cases where the spectra are quite disturbed, one can speculate that the crystal structure of the amphibole dated was simply not as 'strong', and the material was more poorly recrystallized, when compared to the other cases. In general, the first 10 – 20 % of gas released is from material that has lower observed $^{37}Ar/^{39}Ar$ ratios than the rest of the spectrum. Because the ratio of $^{37}Ar/^{39}Ar$ is a measure of Ca/K, a lower $^{37}Ar/^{39}Ar$ ratio indicates the presence of an unknown high K or low Ca impurity. This phase would likely be a fine-grained white mica, as there was usually some degree of sericitic alteration of plagioclase in the samples. In practice, micas outgas at lower temperatures and have younger ages than amphibole.

(a) 01N030d – This analysis comes from a highly recrystallized sample on the margins of the NWP. There is good agreement between the measured and calculated $^{37}Ar/^{39}Ar$ ratios over the latter ~90% of gas release; thus the sample analyzed is predominantly hornblende, with a very narrow compositional range. The age spectrum yields a good plateau that covers more than 50% of the argon released. The plateau age is determined to be 2662 +/- 18 Ma.

(b) 90N007c – This sample is similar in mineralogy and texture to sample 01N030d. It also yields a flat spectrum, with a reliable age plateau at 2675 +/- 18 Ma.

(c) 90N013a – This sample from the HBHSZ is texturally complex, with both actinolite porphyroclasts [Amp 1] and hornblende grains [Amp 2] present. The spectrum from this analysis is quite disturbed, having no reliable age plateau. The best age that can be determined from this spectrum is 2630 +/- 23 Ma, using the above criteria. However, because it is the average of only 2 steps, constituting only 8% of gas released, it is not very reliable. Although the calculated and observed $^{37}Ar/^{39}Ar$ ratios for Amp 2 agree over the latter 75% if gas release, there is a wide range of values. The calculated $^{37}Ar/^{39}Ar$ range for Amp 1 is 36 – 73; this range is consistently higher than that of Amp 2. Because the observed $^{37}Ar/^{39}Ar$ ratios generally agree with the calculated range for Amp 2, we can conclude that the majority of gas released in the sample comes from Amp 2 as opposed to Amp 1. The discordant spectrum cannot be conclusively linked to the textural complexity of the sample. Perhaps the disturbed spectra can be attributed to the internal crystal structure of Amp 2, or from disturbance by a later event (D3).

(d) 90N015d – This sample, also from the HBHSZ, is texturally complex, with both Amp 1 and Amp 2 present. This spectrum resembles the disturbed one in the previous sample. Again, no reliable age can be determined from this spectrum. The best age estimate, 2598 +/- 22 Ma, is from the 3 small steps near the end of the spectrum that have no apparent gradient. The calculated ratio for $^{37}Ar/^{39}Ar$ was constrained within a very small range. The three chosen steps do not lie within the calculated range of $^{37}Ar/^{39}Ar$ for this sample; an exception to the stated criteria was made in this case.

Speculations as to why the spectrum in this sample is so disturbed include: (1) the unique method of separation of amphibole grains from the rock did not yield the desired results, and (2) the higher percentage of porphyroclastic amphibole [Amp 1] in the sample when compared to other samples (Appendix B), may have influenced the argon released. The $^{37}Ar/^{39}Ar$ spectra indicates that the final ~50% of the gas released may be a mixture of both Amp 1 and 2.

(e) 90N015c – This sample is also texturally complex, with grains of both Amp 1 and Amp 2. This sample also yielded a disturbed spectrum. The best age that can be calculated from the spectrum is 2683 +/- 23 Ma. This age is calculated from two of the final steps in the spectrum, which make up approximately 16% of the gas from the sample, not an insignificant amount, but still well below the generally accepted 50% mark. The $^{37}Ar/^{39}Ar$ ratios generally agree, and presumably the gas released is therefore principally from Amp 2, rather than Amp 1. The disturbed nature of the spectrum for this sample may be also be attributed to the unique method of separation employed. Alternatively, textural and structural features of the Amp 2 grains in the sample maybe responsible for the disturbed spectrum.

(f) 15 – This sample, also from the HBHSZ, displays the same textural relationships as the previous sample. The spectrum is also disturbed to some extent; however, it also shows some interesting features. The calculated ranges of $^{37}Ar/^{39}Ar$ for Amp 1 and Amp 2 in the sample both plot on the scale of the graph. The ranges are fairly close, and both overlap with portions of the measured $^{37}Ar/^{39}Ar$ spectrum. Using the stated criteria, two ages can be calculated for sample 15. (1) The higher age, 2688 +/- 19 Ma, an average over the last 30% of the ^{39}Ar released, is a best value for hornblende [Amp 2] in the sample. These last 8 steps lie closely within the calculated range of $^{37}Ar/^{39}Ar$ for amphibole 2, and have no age gradient; therefore the above age can be regarded as being somewhat reliable. (2) The lower age, 2538 +/- 9 Ma, is obtained from one step in the analysis that contained approximately 17% of the gas released. The age from this step is quoted because its corresponding $^{37}Ar/^{39}Ar$ ratio falls within the calculated $^{37}Ar/^{39}Ar$ range for Amp 1, but because it is only one step, it may or may not be significant.

It is very difficult to determine exactly what effect the presence of both amphiboles would have had in the furnace during the diffusion process. If this first large step indeed represents gas from an earlier phase of actinolitic amphibole, then this would mean than the earlier phase of amphibole outgassed at a lower temperature than the later phase of hornblende, which is contrary to what one would expect with the given core and rim relationship between the two phases. It also suggests that the actinolite is younger than the hornblende, which is contrary to evidence seen in the field and in thin section. If this first large step is not ignored, one must attempt to explain these apparent contradictions. It is possible that the lower grade amphibole, actinolite, would be likely to outgas before the higher-grade amphibole, hornblende, if actinolite is less retentive to argon than hornblende. It is also possible that the actinolitic porphyroclasts in the sample contain more fractures or diffusion pathways than the fresher hornblende grains. This might enhance argon diffusion in actinolite relative to that in hornblende. This might also explain the presence of a younger age for Amp 1, as the actinolite crystals might have lost argon during a subsequent deformation. The age, 2538 Ma, thus would not represent the original cooling age for Amp 1, but may be affected by later shearing events after D2 (i.e. D3).

(g) 15-51b – This sample is one from the HBHSZ that is highly sheared, and contains a large proportion of recrystallized hornblende [Amp 2]. The spectrum is relatively flat. A reliable plateau age of 2664 +/- 17 Ma can be derived from the 14 steps that lie within the calculated range for $^{37}Ar/^{39}Ar$ and represent the final ~70% of the age spectrum.

(h) 15-51a – This sample comes from a low-strain zone adjacent to sample 15-51b. It contains a higher proportion of Amp 1 porphyroclasts and low proportions of Amp 2 (refer to Appendix B). However, the age spectrum is not as as texturally similar samples 90N015c, 90N015d, and 90N013a. This may be due to a number of factors, including a 'cleaner' separation, or differences in the crystal structure of the amphiboles. Also, it is possible that the age spectrum is less disturbed because the sample was less affected by subsequent deformation events. Evidence supporting this is that the surrounding rock (i.e. 15-51b) is not significantly affected by D3. Another likely explanation is that the average K_2O content of the amphibole 1 (actinolite) in this sample (~0.09 wt.%), is quite a bit lower than the K_2O content of actinolite in the other samples (~0.15%) (Appendix D). Thus the influence of actinolite on the spectrum would have been minimal. The calculated age for this sample is 2712 +/- 19 Ma. The steps used in the calculation of this mean age cover approximately the last 30% of ^{39}Ar released, but lie just above the range calculated for $^{37}Ar/^{39}Ar$ in Amp 2.

(i) 90N014a – This sample comes from an island immediately north of the HBHSZ. It does not contain any actinolitic porphyroclasts and overgrowths of hornblende, which are present in the samples from the HBHSZ, but instead contains a homogeneous growth of hornblende. The resulting spectrum is quite disturbed, and the hornblende age, 2654 +/- 22 Ma, is poorly defined. This age is calculated from two relatively large adjacent steps in the spectrum that are similar in age. The steps near the high T end of the spectrum are quite variable in age and have large associated errors, and were therefore not included in the mean age calculation. There is a good match between calculated and observed $^{37}Ar/^{39}Ar$ ratios.

(j) 90N014b – The location of this sample is similar to the one above, but the texture of the amphibole consists of both porphyroblasts and 'feathery' amphibole. This sample also has a very disturbed spectrum. The best age that can be quoted, 2685 +/- 27 Ma, comes from a single step that covers approximately 18% of the argon spectrum towards the high T end. The measured range of $^{37}Ar/^{39}Ar$ for this sample lies below the calculated range, without overlap. This indicates a higher K content in the analyzed sample. The most plausible explanation for the excess K is the presence sericite, as some of the plagioclase in the sample is most certainly altered to a small degree. The step that was quoted, 2685 +/- 27 Ma, can only be taken as a lower limit for the amphibole age of this sample.

Summary

The results in Figure 4.10 show that texturally complex samples from the HBHSZ yield disturbed spectra, while the highly recrystallized samples yield relatively flat spectra, from which reliable ages can be calculated. There is a clear correlation between the texturally complex samples and the discordant ages; however, the precise reason for this relationship is unclear. As discussed above, the presence of actinolite in the samples does not likely contribute any significant proportion of K to the analyses. The reason for the disturbed spectra may then be attributed to: (1) the presence of sericitised plagioclase, (2) to the crystal structure of the amphibole 2 in those particular samples, (3) disturbance from later deformational events (D3?), or (4) to some other unknown factor.

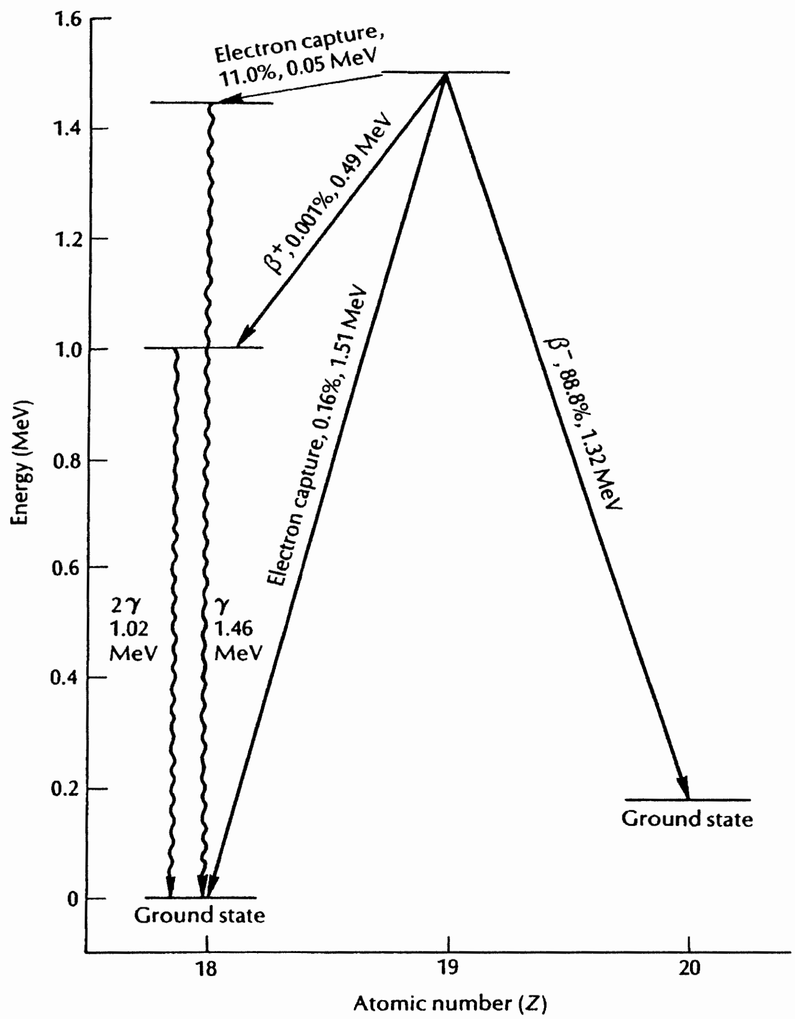

Figure 4.1 - Decay scheme diagram for the branched decay of ^{40}K to ^{40}Ar by electron capture and by positron (β^+) emission, and to ^{40}Ca by emission of negative beta particles (β^-). The percentage of the parent material in each decay path and the energy changes are also shown. (From Prothero & Schwab, 1996.)

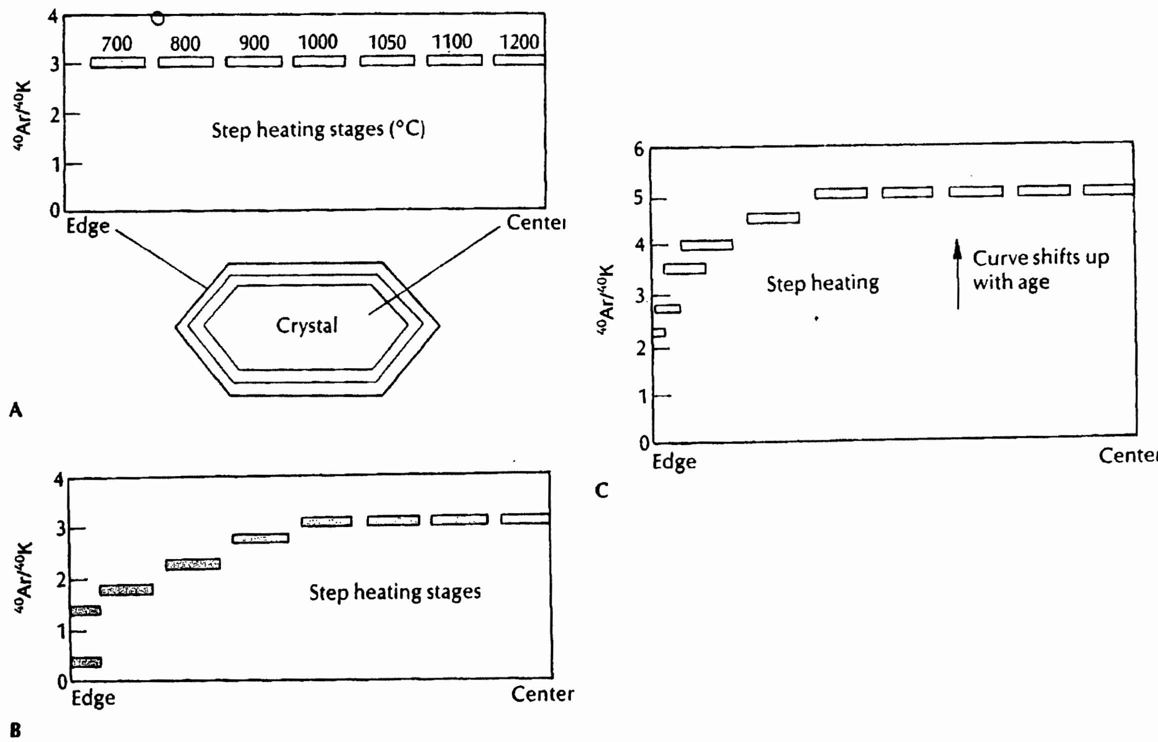

Figure 4.2 - The argon/argon dating method. (A) Plot of the $^{40}Ar/^{40}K$ ratio with step heating of an unaltered crystal. If there has been no leakage, the outer rim of the crystal will release the same amount of material at low temperatures as the center releases at high temperatures. (B) An altered crystal, however, will show lower ratios at the lower temperatures due to leakage of argon from the edge. The plateau at the higher temperatures should give the true age of the unaltered center of the crystal. (C) As time passes and the crystal gets older, the entire curve shifts upward, but the plateau remains as long as no further alteration takes place. (From Prothero & Schwab, 1996.)

Estimated Argon Closure Temperatures (for moderate cooling rates)	
Hornblende	500 +/- 50 °C
Muscovite	ca. 350 +/- 50 °C
Biotite	300 +/- 50 °C
K-Feldspar	350 to 125 °C *

Figure 4.3 - * Strongly dependent on composition and microstructure. References: Foland, 1974; Harrison, 1981; Harrison and McDougall, 1982; Harison et al., 1985; Lovera et al., 1989; Purdy and Jager, 1976. (Adapted from Hanes, 1991).

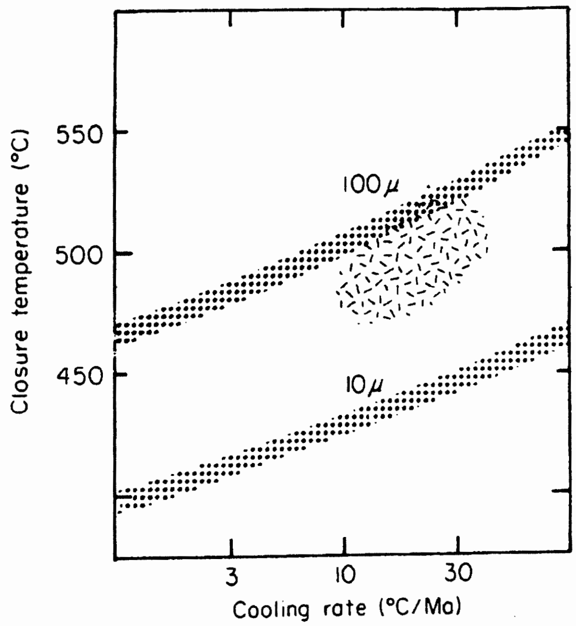

Figure 4.4 - Variations in closure temperature for argon diffusion in hornblende using data from Harrison (1981). Closure temperatures for two grain-sizes are shown as a function of cooling rate; the width of the stippled bands corresponds to the uncertainty in activation energy for diffusion. The oval jackstraw area delimits the range of effective grain radius suggested by Harrison & McDougall (1980b) and typical post-orogenic cooling rates. (From Cliff, 1985.)

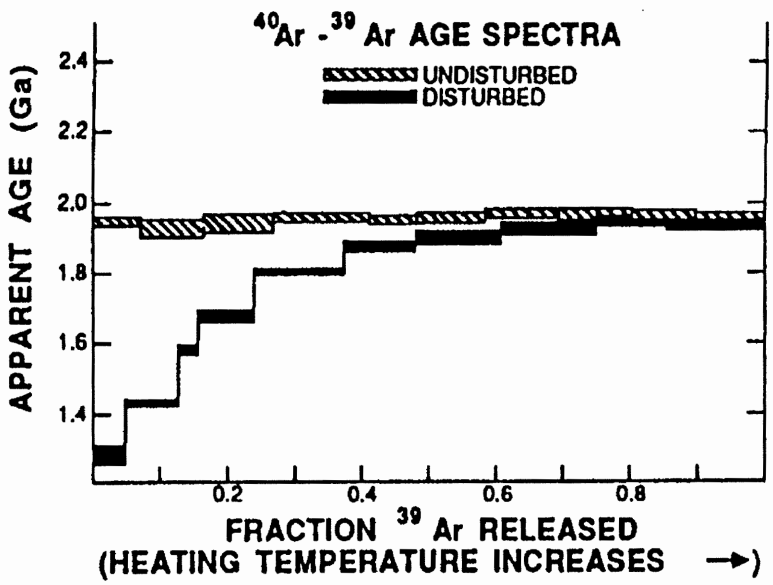

Figure 4.5 - Idealized $^{40}Ar/^{39}Ar$ age spectra. "Undisturbed" spectrum is a flat "plateau". Each box represents a single step-heating fraction, with the vertical width of the box being a measure of the analytical error. (From Hanes, 1991).

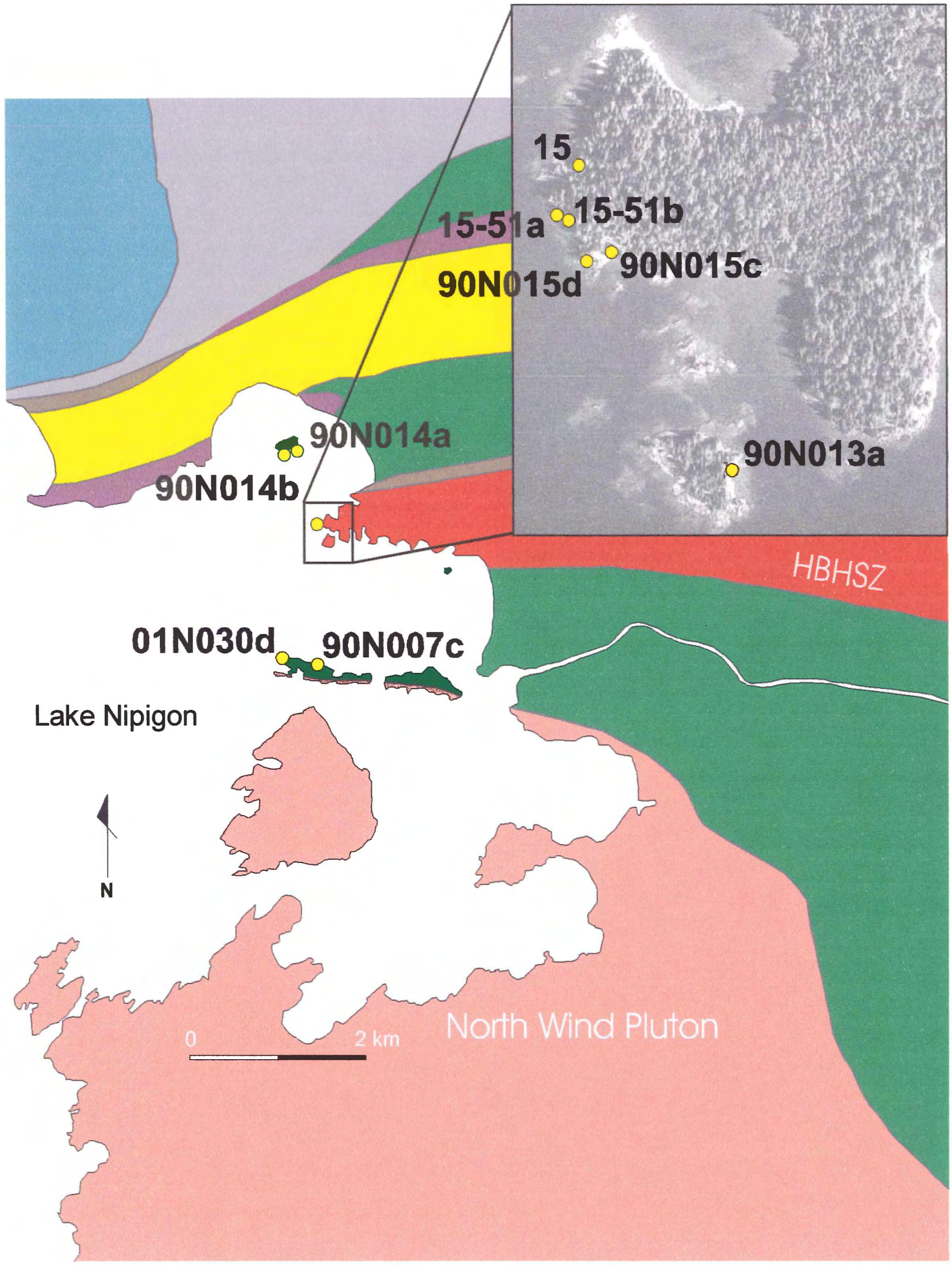

Figure 4.6 – Sample location map for dated phases used in this study. Refer to Figure 2.5 for legend. (Source map courtesy of N. Culshaw)

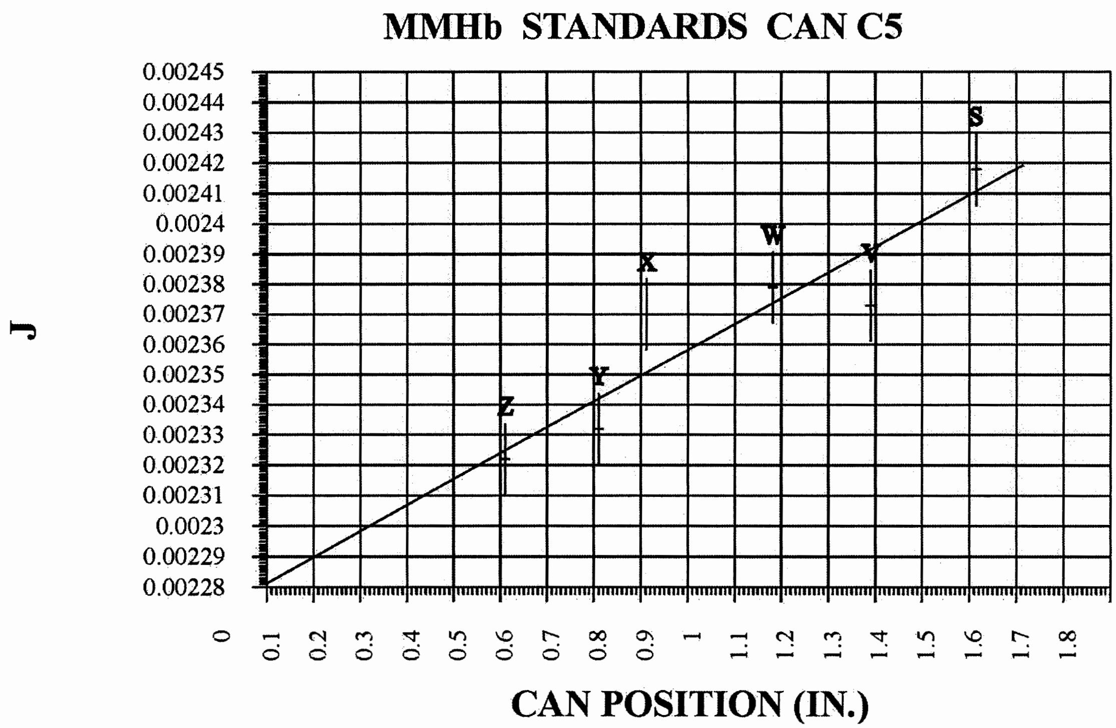

Figure 4.7 – Graphical relationship between the J values and distance in canister for irradiated standards.

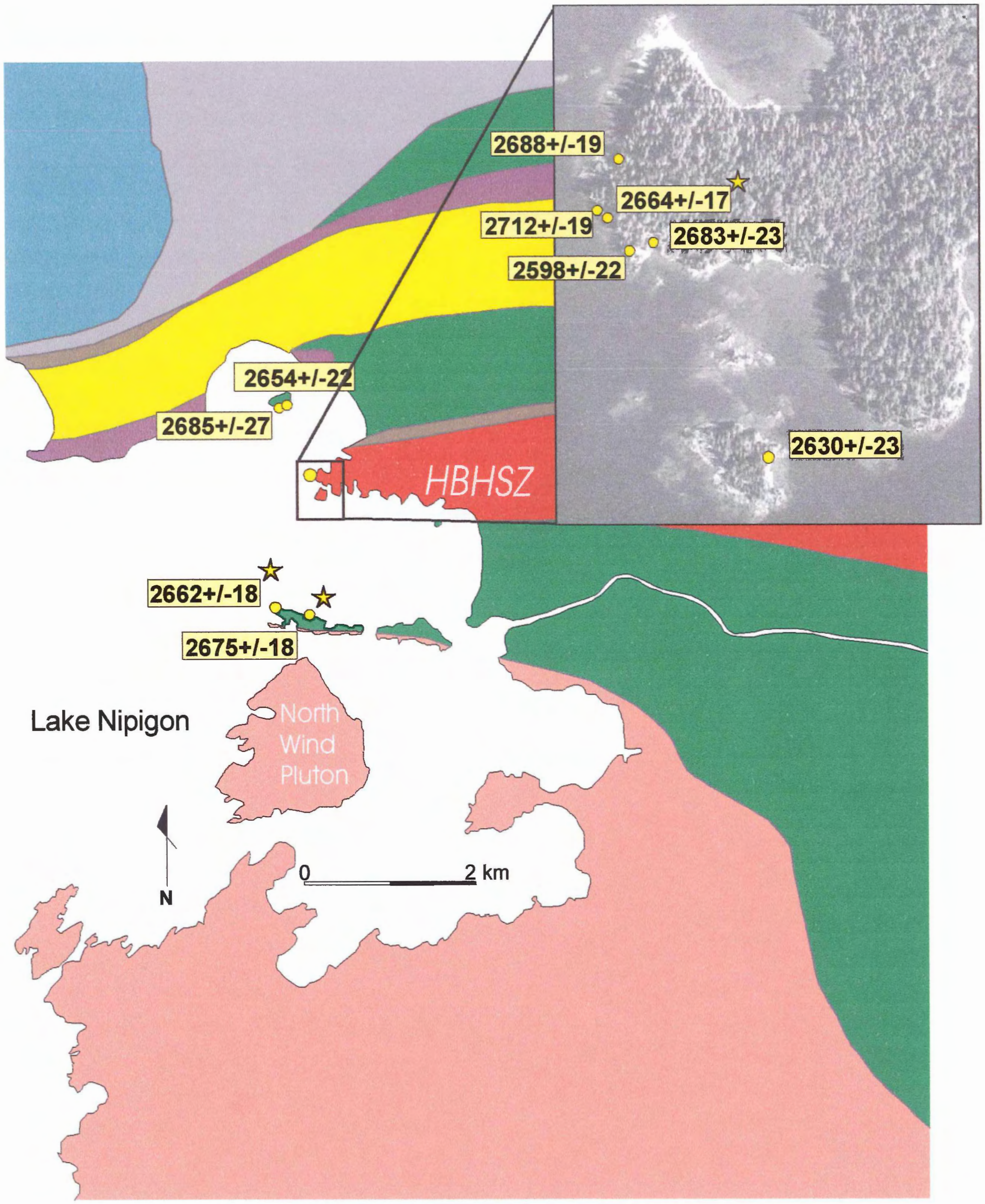

Figure 4.8 – Summary map of hornblende ages from $^{40}Ar/^{39}Ar$ analysis in this study. Stars represent the most reliable age plateaus. Refer to Figure 2.5 for legend (map courtesy of N. Culshaw).

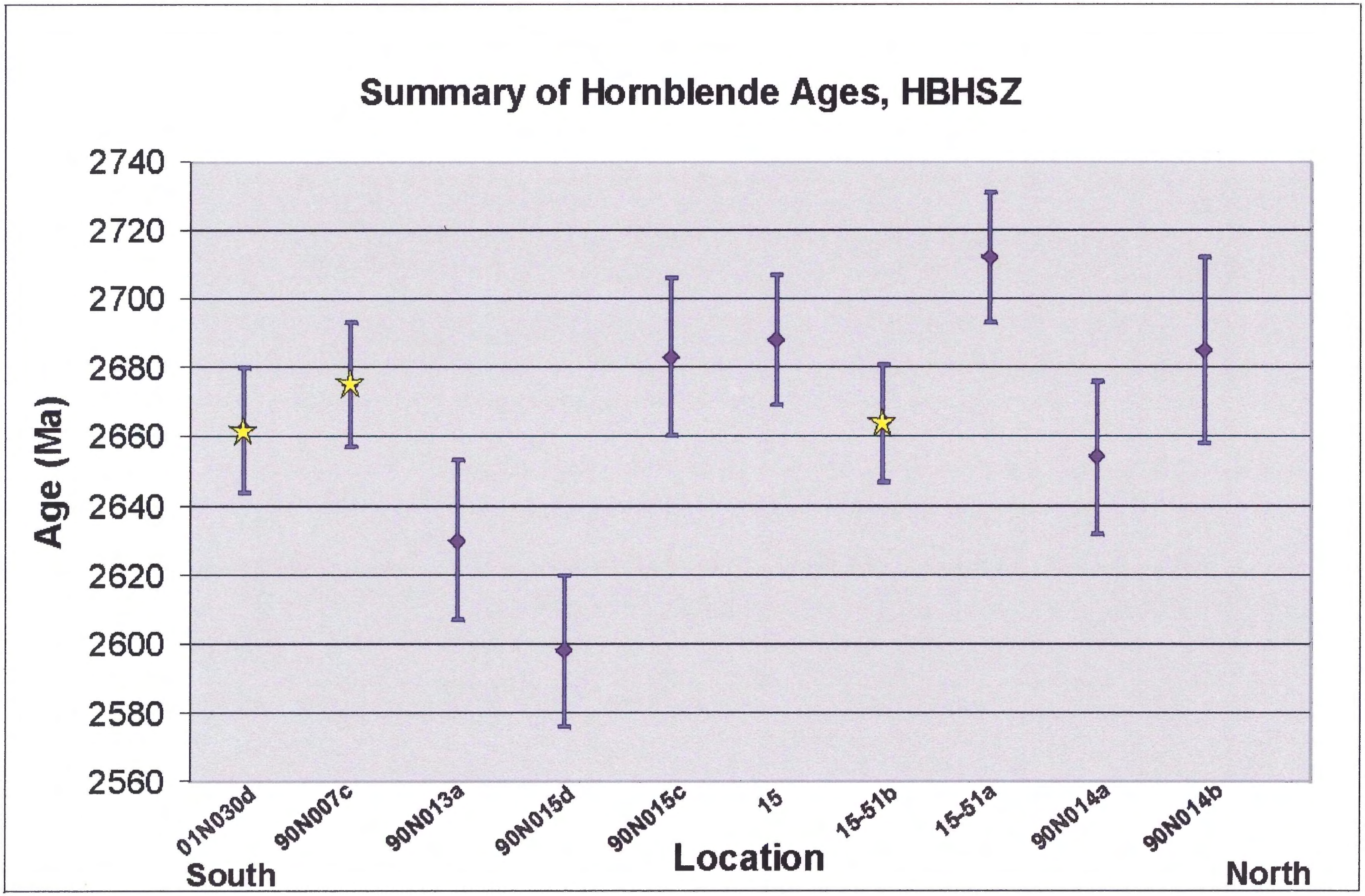

Figure 4.9 - Summary of hornblende ages from this study. Stars represent the most reliable age plateaus. Horizontal dimension represents an overall ~2 km transect from south of the HBHSZ to north of the HBHSZ. Samples are spaced equally for clarity.

Figure 4.10 (a) through (j) - $^{40}Ar/^{39}Ar$ age spectra and corresponding $^{37}Ar/^{39}Ar$ ratio spectra for each hornblende analysis in this study. Spectra are presented in general geographic location from south to north. Also shown on the $^{37}Ar/^{39}Ar$ spectra, in grey boxes, are the calculated $^{37}Ar/^{39}Ar$ ranges for hornblendes [Amp 2]. In some cases, the calculated $^{37}Ar/^{39}Ar$ ranges for actinolite [Amp 1] are also indicated with arrows.

a)

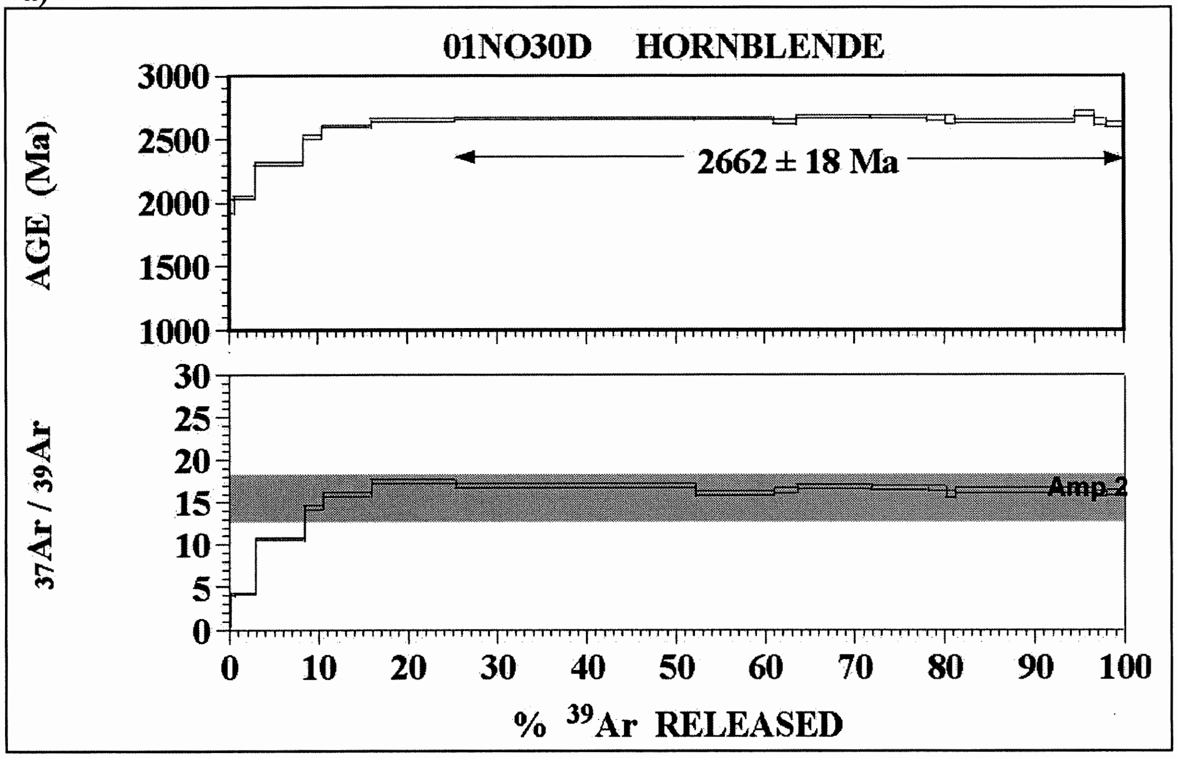

b)

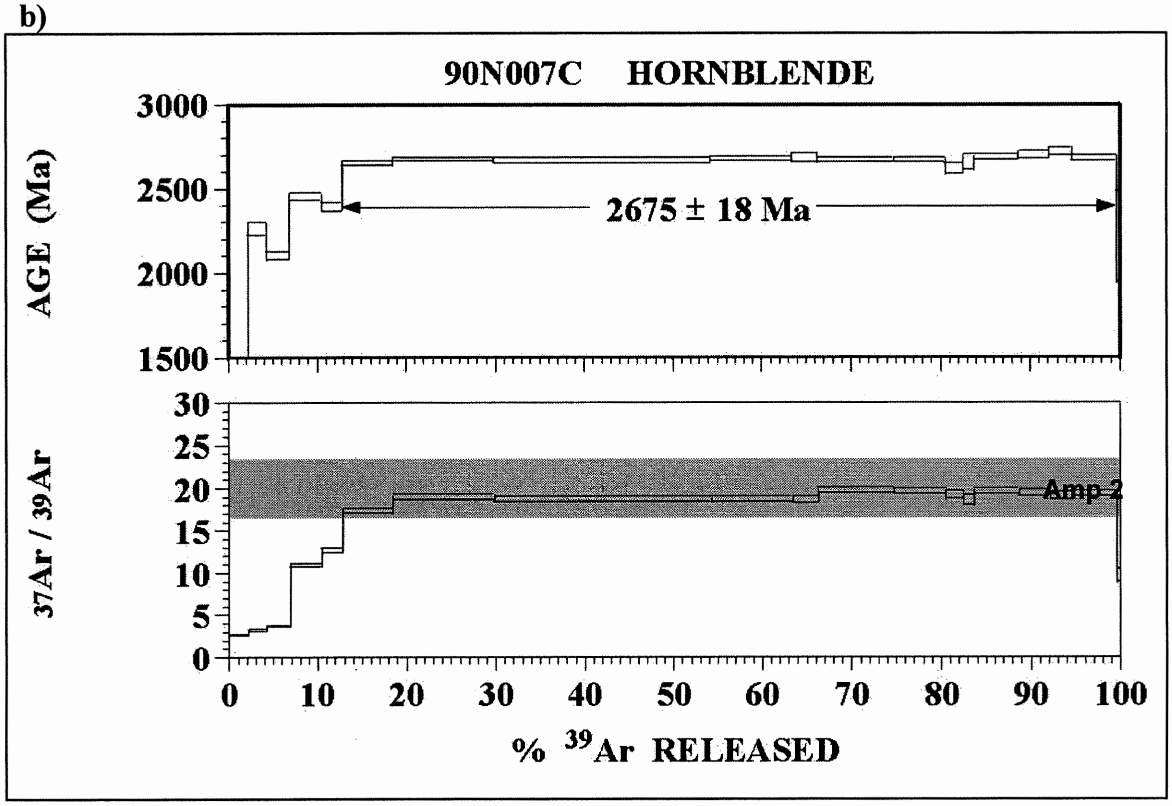

c)

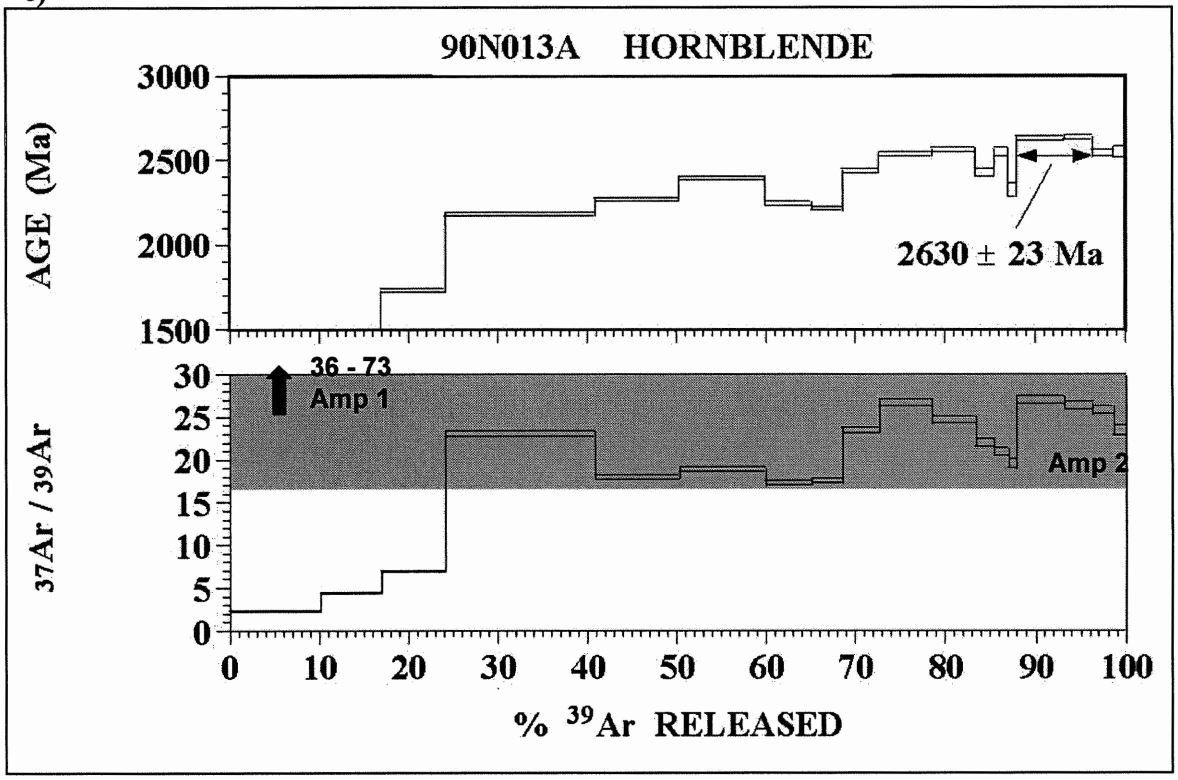
90N013A HORNBLENDE
AGE (Ma)
3000
2500
2000
1500
2630 ± 23 Ma
37Ar / 39Ar
30
25
20
15
10
5
0
36 - 73
Amp 1
Amp 2
0
10
20
30
40
50
60
70
80
90
100
% 39Ar RELEASED

d)

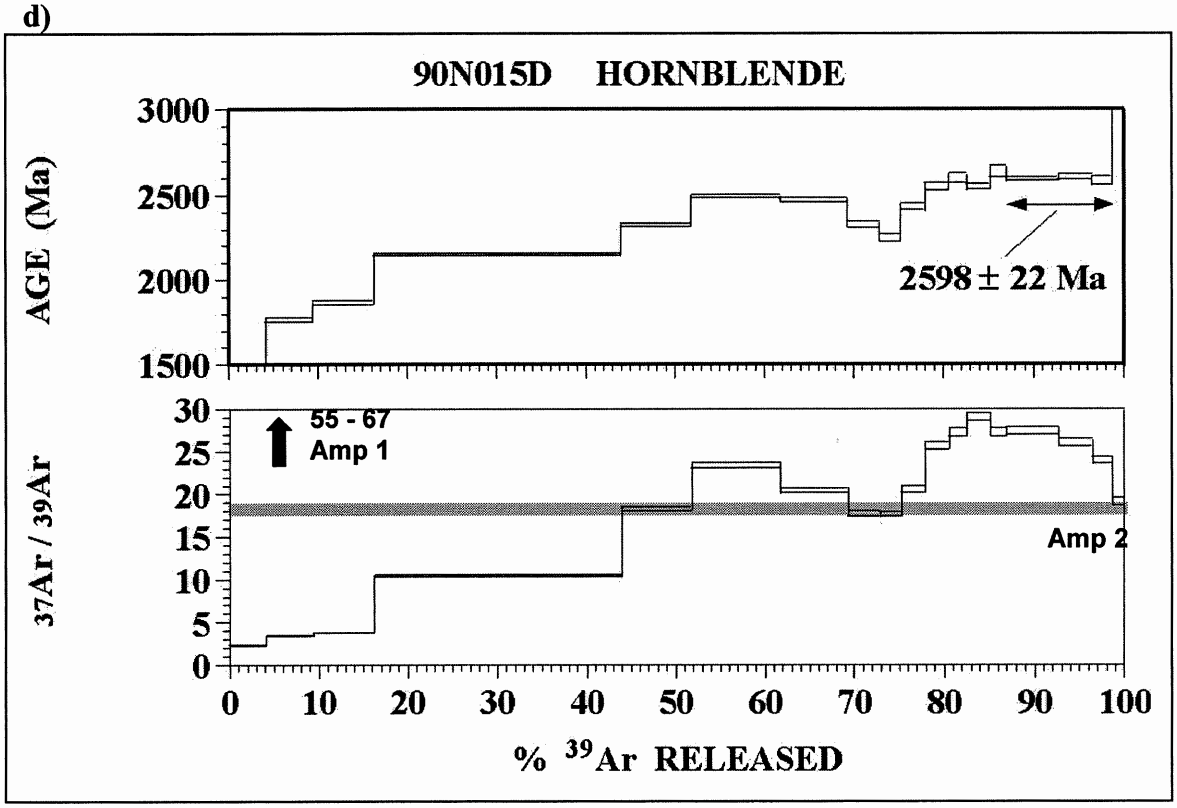
90N015D HORNBLENDE
AGE (Ma)
3000
2500
2000
1500
2598 ± 22 Ma
37Ar / 39Ar
30
25
20
15
10
5
0
55 - 67
Amp 1
Amp 2
0
10
20
30
40
50
60
70
80
90
100
% 39Ar RELEASED

e)

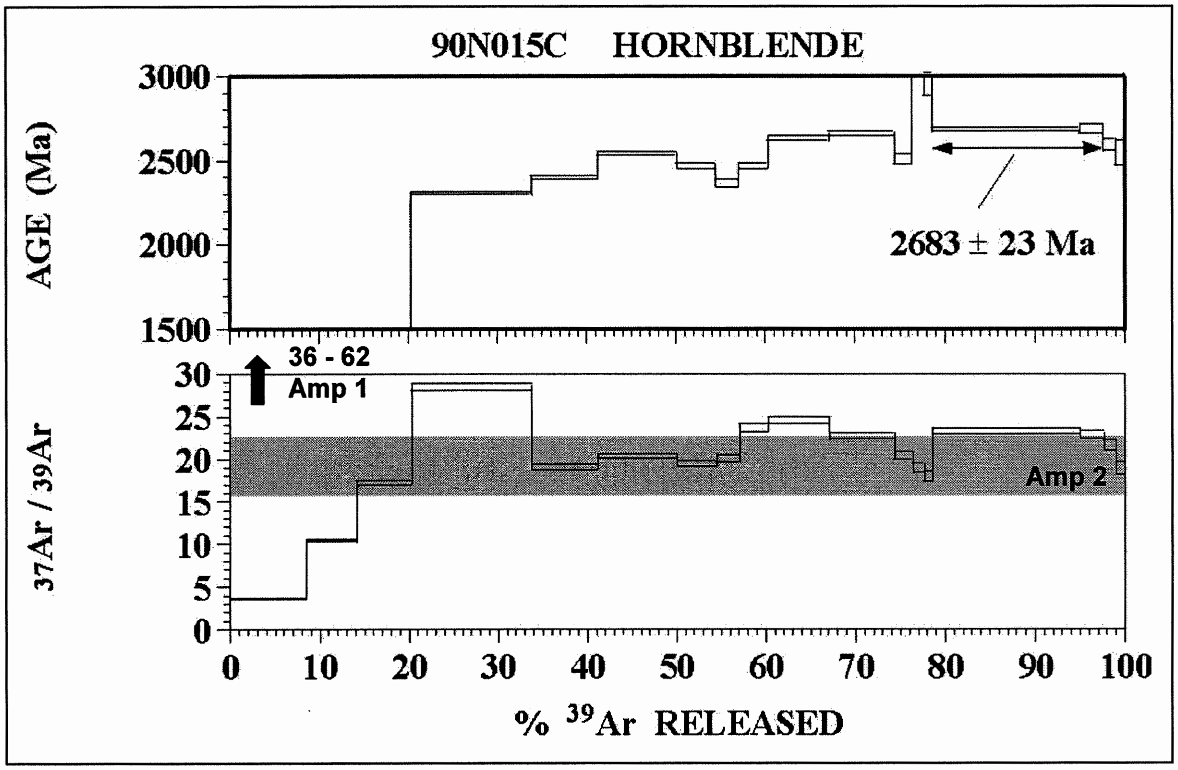
90N015C HORNBLENDE
AGE (Ma)
3000
2500
2000
1500
2683 ± 23 Ma
36 - 62
Amp 1
Amp 2
37Ar / 39Ar
30
25
20
15
10
5
0
0 10 20 30 40 50 60 70 80 90 100
% 39Ar RELEASED

f)

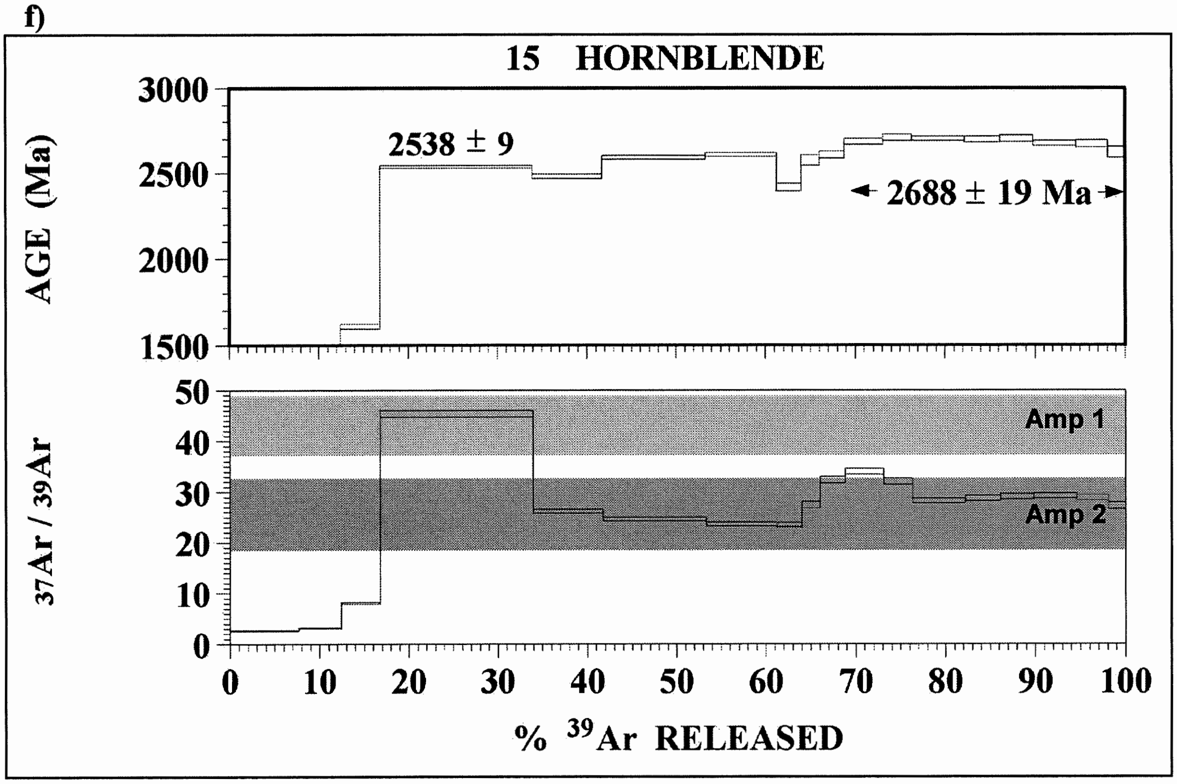
15 HORNBLENDE
AGE (Ma)
3000
2500
2000
1500
2538 ± 9
2688 ± 19 Ma
Amp 1
Amp 2
37Ar / 39Ar
50
40
30
20
10
0
0 10 20 30 40 50 60 70 80 90 100
% 39Ar RELEASED

g)

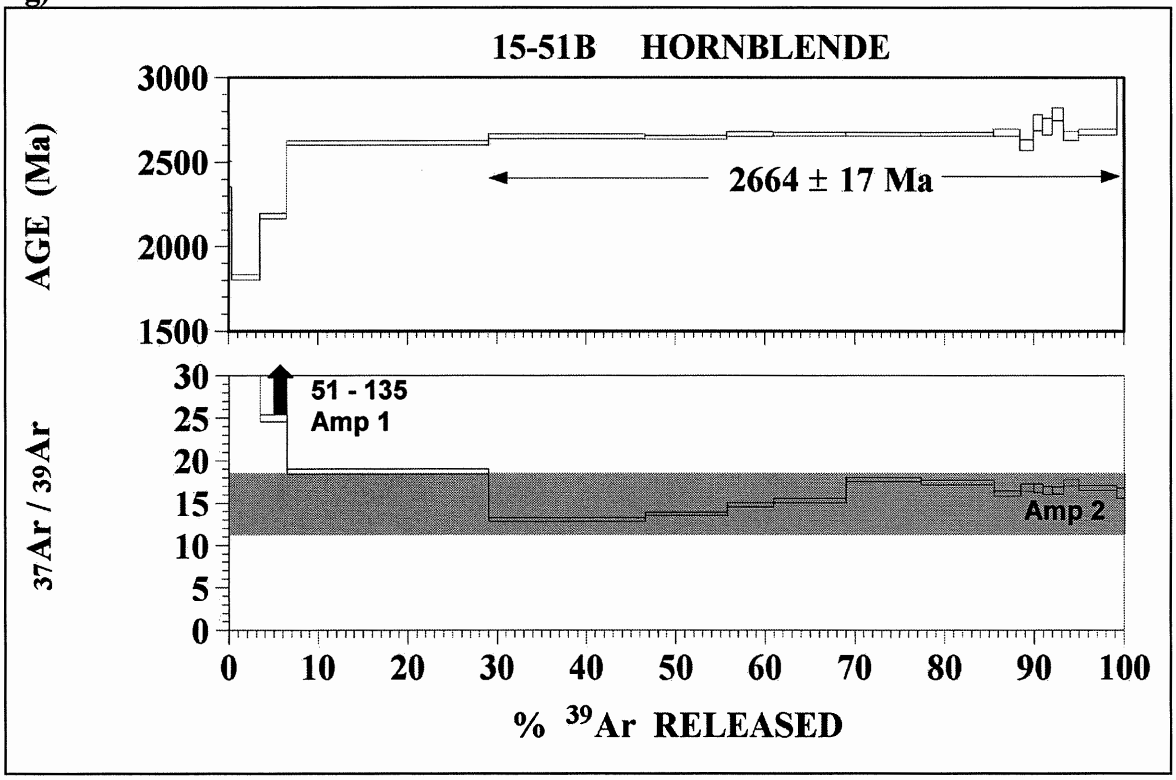
15-51B HORNBLENDE
3000
2500
2000
1500
AGE (Ma)
2664 ± 17 Ma
30
25
20
15
10
5
0
37Ar / 39Ar
51 - 135
Amp 1
Amp 2
0 10 20 30 40 50 60 70 80 90 100
% 39Ar RELEASED

h)

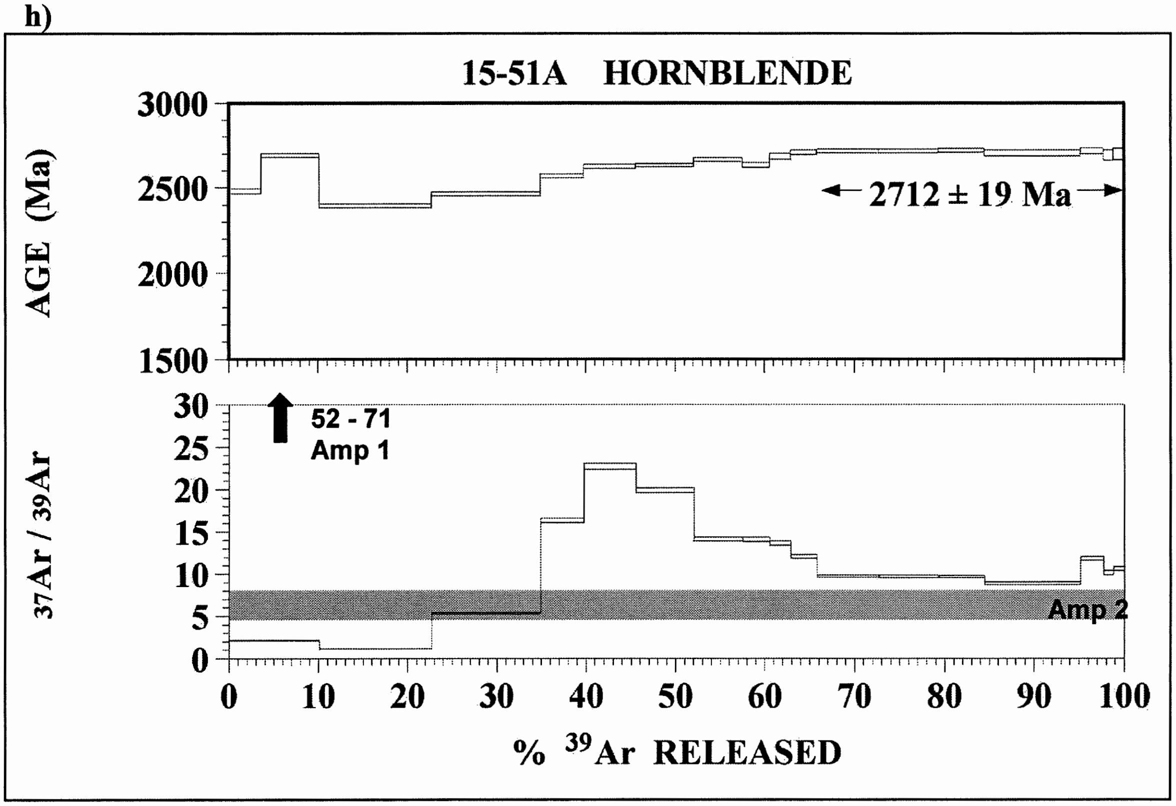
15-51A HORNBLENDE
3000
2500
2000
1500
AGE (Ma)
2712 ± 19 Ma
30
25
20
15
10
5
0
37Ar / 39Ar
52 - 71
Amp 1
Amp 2
0 10 20 30 40 50 60 70 80 90 100
% 39Ar RELEASED

i)

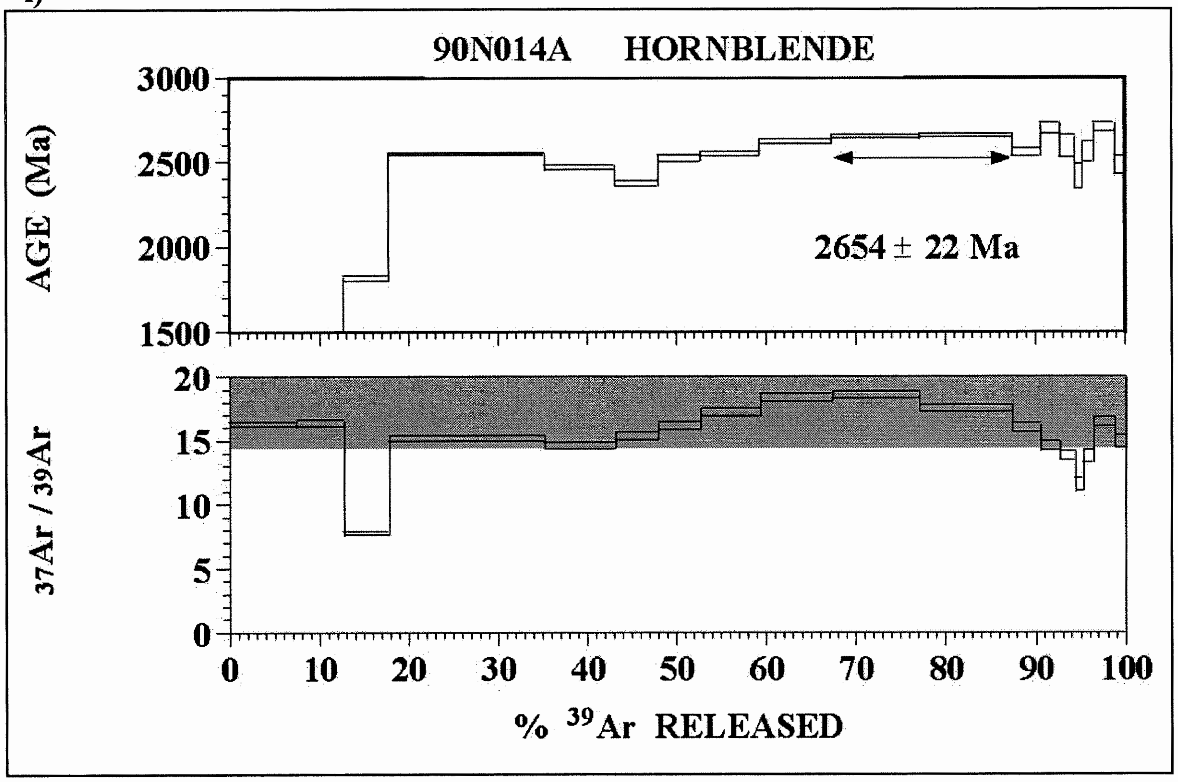

90N014A HORNBLENDE
AGE (Ma)
3000
2500
2000
1500
2654 ± 22 Ma
37Ar / 39Ar
20
15
10
5
0
0 10 20 30 40 50 60 70 80 90 100
% 39Ar RELEASED

j)

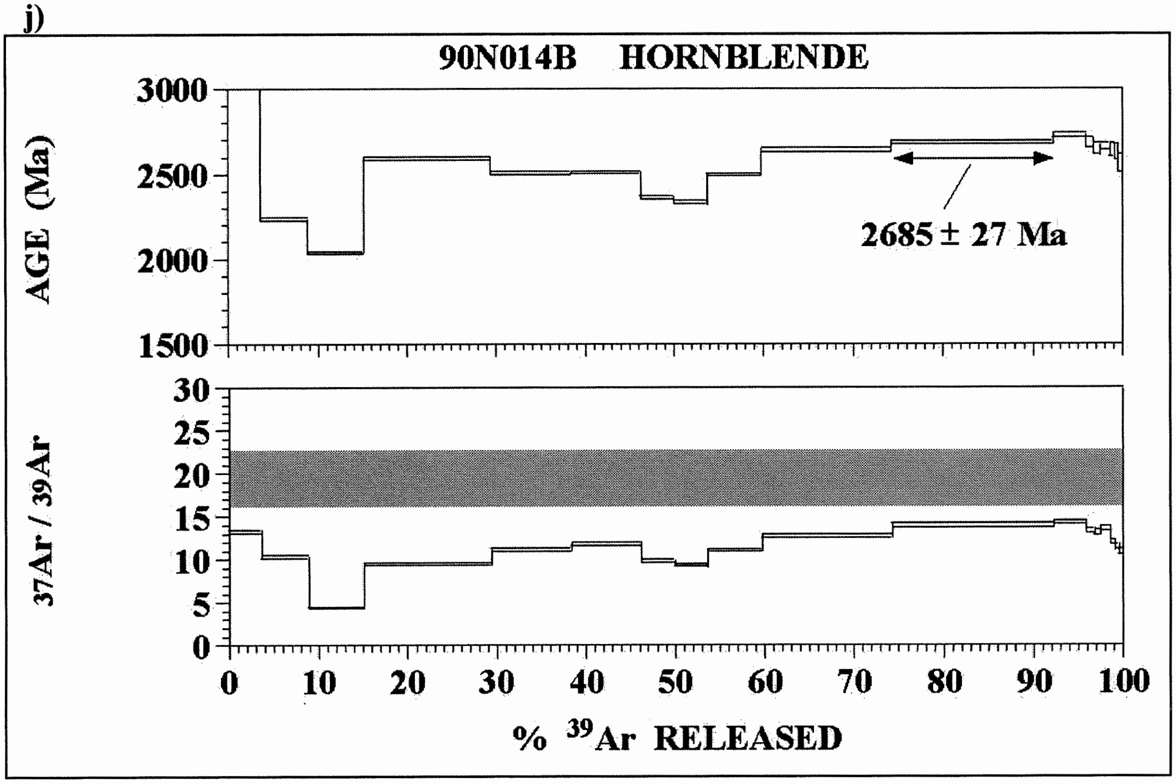

90N014B HORNBLENDE
AGE (Ma)
3000
2500
2000
1500
2685 ± 27 Ma
37Ar / 39Ar
30
25
20
15
10
5
0
0 10 20 30 40 50 60 70 80 90 100
% 39Ar RELEASED

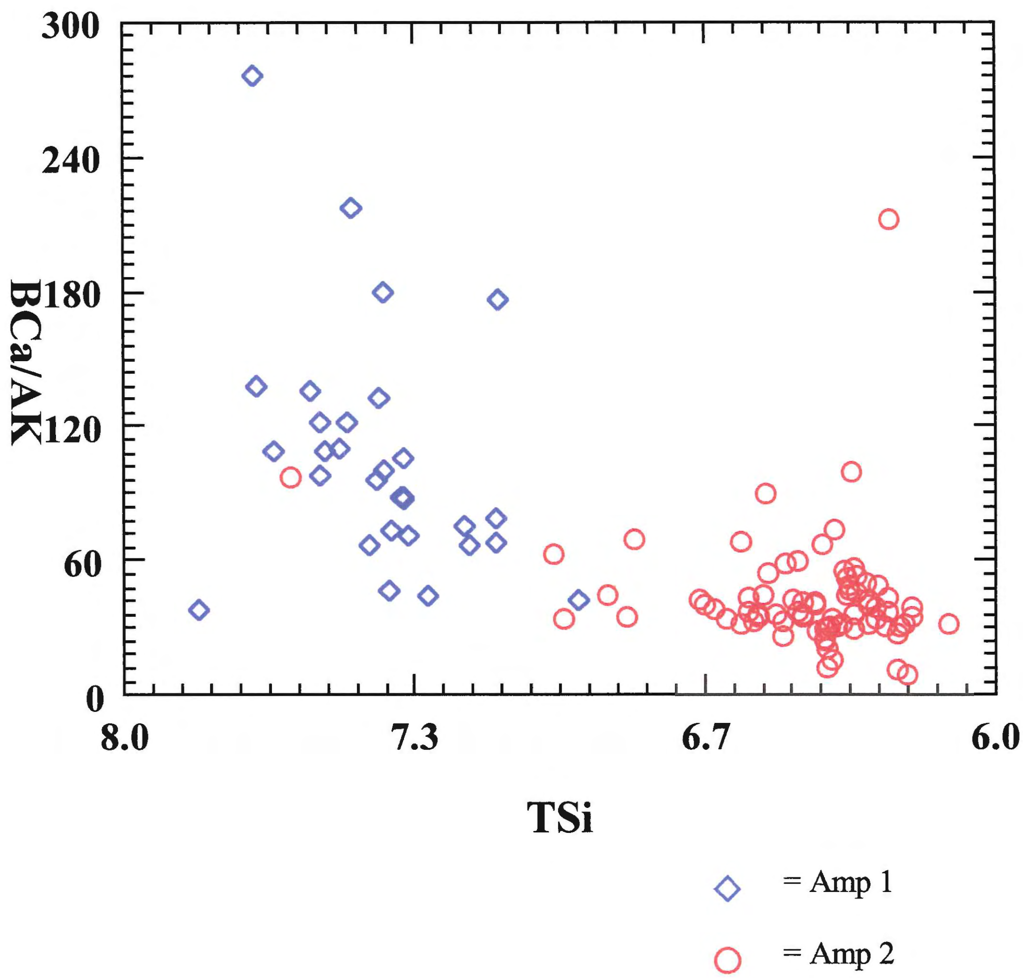

Figure 4.11 – Binary plot of Ca/K vs total Si, for amphibole analyses from the HBHSZ. This plot was completed using the geological software *Minpet* (Richard, 1997).

CHAPTER 5 - DISCUSSION & CONCLUSIONS

5.1 Discussion

The results and interpretations presented in chapters 3 and 4 are discussed here in terms of their significance to the metamorphic, tectonic, and temporal history of the HBHSZ.

Petrographic evidence suggests that the protoliths of many of the rocks from the HBHSZ are mafic basaltic rocks. Initial metamorphism in the rocks of the HBHSZ is indicated by the greenschist facies M1 metamorphic assemblage, which includes actinolite (Amp 1) that likely replaced clinopyroxene in the original rocks. Petrographic and chemical evidence suggests that a subsequent phase of transitional greenschist to amphibolite facies metamorphism affected the same rocks. This metamorphic assemblage, M2, is characterized by hornblendes, which are largely aligned with the main foliation of the shear zone (S2). Transpressional deformation, forming S2, is thought to have occurred during growth of Amp 2. Subsequent deformations, including sinistral shear associated with D3, and dextral shear associated with D4, are not recorded as new metamorphic assemblages in the samples used for this study. Therefore, only a very general T-t path can be determined from the metamorphism and deformation seen in the rocks (Fig. 5.1).

Because Amp 2 is thought to have formed during D2, concurrently with S2, and because hornblende has a high closure temperature (~500°C), the age given by Amp 2 is most likely quite close to the age of peak metamorphism and deformation of the HBHSZ. It is important to note that the temperatures calculated for the samples (Appendix E) are above the closure temperature for hornblende. Therefore, the ages obtained in this study are most likely cooling ages, as opposed to growth ages. The actual age calculated then, would be slightly lower than the peak age of metamorphism and deformation on the shear zone. Since plutons normally cool quite rapidly, it is probable that cooling of the rocks in the HBHSZ through 500°C was not much later than the thermal peak of the shear zone, and that the cooling ages given by this study are likely close to, although not coincident with, the age of S2.

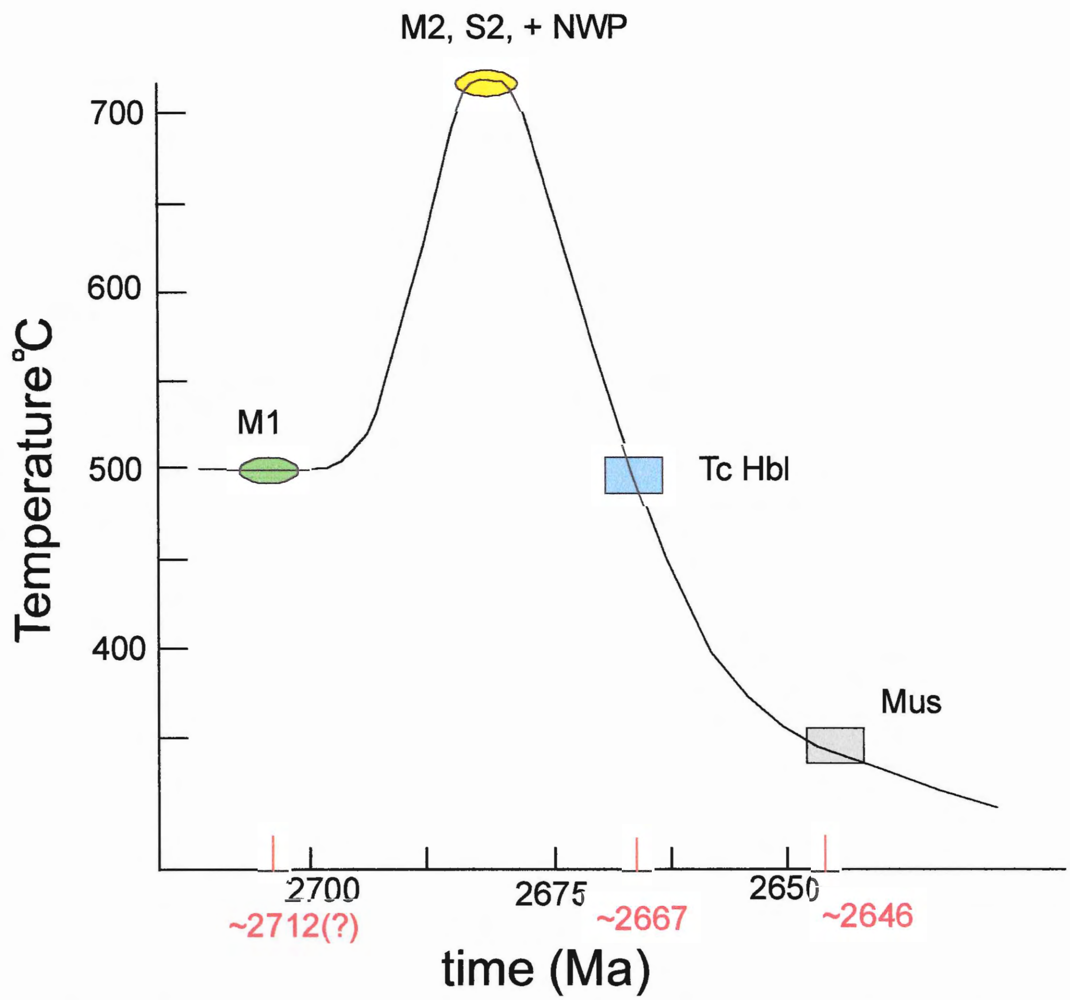

Figure 5.1 - Diagrammatic sketch of most likely T-t path of rocks from the HBHSZ. Curve and size of shaded areas are arbitrary. Muscovite ages are included from Culshaw et al. (2000).

Reliable hornblende ages of 2662 +/- 18 Ma, 2675 +/- 18 Ma, and 2664 +/- 17 Ma have been obtained from highly recrystallized samples in the HBHSZ. The average of these three ages is ~ 2667 Ma. Because this age is a cooling age from Amp 2 in the rocks, it can be taken as a lower limit on the age of peak deformation of the HBHSZ. An upper limit for peak deformation on the shear zone has already been established at 2706 Ma (Stott, personal comm., 2002). Therefore, the age of peak deformation on the HBHSZ is constrained between 2706 and ~ 2667 Ma. Field evidence suggests that the North Wind Pluton is syn-deformational with respect to the HBHSZ. Therefore, the age given by Amp 2 of the shear zone, ~2667 Ma, also provides a lower limit to the age of the emplacement of the NWP.

The only age constraint in this study for the earlier phase of metamorphism in the HBHSZ comes from sample 15-51a. The age given by the spectrum, 2712 +/- 19 Ma, is slightly older than the rest of the ages obtained from this study. Because this sample does not contain the S2 fabric that is associated with the main phase of deformation of the shear zone, this older age may represent an earlier age of metamorphism that is preserved within small low strain zones of the HBHSZ. However, it is possible that the slightly older age from this sample is simply due to the presence of a small amount of excess argon.

Although there is good evidence in the field for later deformation on the shear zone, there are only very limited geochronological data from this study to support this. The age given by sample 15, 2538 Ma, is the only possible geochronological evidence for D3, as it may represent a resetting event for Amp 1. The muscovite and biotite ages given by Culshaw et al. (2000), 2646 Ma and 2626 Ma respectively, indicate uplift and cooling of the HBHSZ, or a province-wide thermal event affecting the rocks of the HBHSZ, subsequent to the events described above.

Now that the age of shearing of the HBHSZ has been constrained, the tectonic significance of this event must be examined. At least four possible scenarios exist, explaining D2 deformation on the HBHSZ. They are: (1) oblique convergence during amalgamation of sub-terranes within the Wabigoon Subprovince, prior to collision with the Quetico Subprovince, and (2) oblique convergence associated with subduction just prior to the accretion of the BGGB and the Quetico to the Wabigoon, (3) oblique convergence associated with the amalgamation of the Wabigoon and Quetico subprovinces, and (4) post-collisional shearing related to activity in the lower crust. There is evidence to support these different theories theories, however, the latter two seem to be more compatible with current knowledge, as explained below.

The HBHSZ separates domains with different basement model ages (Tomlinson, 2000), suggesting that it may be related to the amalgamation of different domains within the Wabigoon Subprovince. However, field work has shown that the North Wind Pluton post-dated S1, and is coeval with S2. Stott and Morrison (1995) suggested that the regional fabric in the Onaman-Tashota greenstone belt, S1, is related to thrusting. If D1 were related to intra-Wabigoon accretion, then this would effectively rule out D2 as originating during this time. It is quite possible however, that D2 on the HBHSZ formed as a result of reactivation of a D1 boundary.

Alternatively, S2 on the HBHSZ may have formed during the accretionary events between the Wabigoon and Quetico subprovinces, but prior to the actual accretion of the BGGB and the Quetico to the Wabigoon. Oblique convergence during this Andean arc stage could possibly account for transpression on the HBHSZ, and the syn-tectonic emplacement of the NWP. In this case, the NWP and other local plutons would be part of a related calk-alkaline suite. These relationships have not currently been documented.

The HBHSZ is rather close to the BGGB, the site of deformation associated with the amalgamation of the Wabigoon and Quetico subprovinces. The HBHSZ and the BGGB are similar in both strike direction (E-W) and sense of shear (dextral). These facts combined, seem to suggest that peak deformation on the HBHSZ is related to accretion between the Wabigoon and Quetico subprovinces. Also, the age determined by this study, 2706 - 2667 Ma, approximately agrees with the period of amalgamation of the subprovinces, which is poorly constrained at about 2.7 Ga (Card, 1990). Therefore, according to current evidence, it is most likely that peak deformation on the HBHSZ was associated with the collision of the Wabigoon and Quetico subprovinces. In this case, the NWP would be post-collisional, and emplaced after the amalgamation of the Wabigoon and Quetico subprovinces.

The ages given by this study and by Culshaw et al. (2000), may be compared with U – Pb ages from other areas of the Superior Province, given by Krogh (1993). Krogh (1993) indicated that there was widespread tectonic underplating and granulitization under much of the Superior Province, after main periods of volcanism and batholith formation ceased around 2700 and 2680 Ma, respectively. Granulite formation in the Kapuskasing structural zone of the Superior Province occurred between 2660 and 2640 Ma, while ductile deformation continued until 2585 Ma. These events in the lower crust were synchronous with deformation in fault zones and hydrothermal emplacement of gold deposits in the upper crust, with ages between 2670 and 2585 Ma (Krogh, 1993).

Hajnal et al. (1996) suggested a similar scenario for the Trans-Hudson Orogen, in which low-angle detachments in the lower crust can be traced to high-angle faults in the upper crust. The muscovite ages given by Culshaw et al. (2000), and the hornblende ages given by this study, roughly correlate with the ages given by Krogh (1993). It is plausible that deformation on the HBHSZ was related to post-collisional activity in the lower crust of the Superior Province, between about 2660 and 2585 Ma.

5.2 Conclusions

(1) Rocks from the HBHSZ have a polymetamorphic history, with greenschist to transitional amphibolite facies M1 assemblages, and amphibolite facies M2 assemblages.

(2) Hornblende ages from M1 assemblages in low strain zones suggest an age of 2712 Ma for M1.

(3) Peak metamorphism, M2, accompanied main deformation (D2) and development of S2 on the HBHSZ.

(4) The age of D2, and the age of the syn-tectonic North Wind Pluton are constrained between 2706 and ~2667 (range of reliable ages is 2662 – 2675) Ma.

(5) Post – D2 events on the HBHSZ have approximate ages of 2646 to 2538 Ma, and may be related to activity in the lower crust.

(6) D2 was most likely related to the accretion of the Quetico and Wabigoon subprovinces at about 2700 Ma.

5.3 Recommendations

An U-Pb study of the area would be useful in constraining the age of the NWP, as well as other plutons and geological units in the area. A geochemical study of all the plutons in the area would be useful in determining whether or not the NWP is part of a large calk-alkaline suite. More extensive Nd isotopic work in the area may enable the correlation of the HBHSZ tectonic boundary with boundaries in the western Wabigoon. Finally, a synthesis of the data presented in this study with the results from the Lithoprobe Western Superior transects is recommended.

References

Amukun, S.E. 1977. Geology of the Conglomerate Lake Area, District of Thunder Bay; Ontario Geological Survey Report **197**, 101p. Accompanied by Map 2429, scale 1:31 680.

Attendorn, H.G., & Bowen, R.N.C. 1997. Radioactive and Stable Isotope Geology. Chapman & Hall, pp. 193-225.

Blackburn, C.E., Johns, G.W., Ayer, J., and Davis, D.W. 1991. Wabigoon Subprovince. *In* Geology of Ontario. *Edited by* Thurston, P.C., Williams, H.R., Sutcliffe, R.H., and Stott, G.M. Ontario Geological Survey, Special Volume 4, part 1. Ministry of Northern Development and Mines, Ontario, pp. 303–382.

Card, K.D. 1990. A review of the Superior Province of the Canadian Shield, a product of Archean accretion. Precambrian Research, **48:** 99-156.

Cliff, R.A. (1985) Isotopic dating in metamorphic belts. Journal of the Geological Society of London, **142**: 97-110.

Culshaw, N.G., Reynolds, P., and Bogutyn, P. 2000. The Humboldt Bay high strain zone, Onaman-Tashota greenstone belt, Wabigoon Subprovince: a preliminary report. *In* 2000 Western Superior Transect Sixth Annual Workshop. *Edited by* Harrap, R.M., and Helmstaedt, H.H. Lithoprobe Report # 77, Lithoprobe Secretariat, University of British Columbia, pp. 29–36.

Dalrymple, G.B., & Lanphere, M.A. 1969. Potassium-Argon Dating: Principles, Techniques and Applications to Geochronology. W.H. Freeman and Company.

Davis, D.W. 1998. Speculations on the formation and crustal structure of the Superior province from U-Pb geochronology. *In* 2000 Western Superior Transect 1998 Annual Meeting. *Edited by* Harrap, R.M., and Helmstaedt, H.H. Lithoprobe Report # 65, Lithoprobe Secretariat, University of British Columbia, pp. 21-28.

Deer, W.A., Howie, R.A., and Zussman, J. 1966. An introduction to rock forming minerals. Longmans, Group Ltd, London, England, pp. 528.

Devaney, J.R., and Williams, H.R. 1989. Evolution of an Archean subprovince boundary: a sedimentological and structural study of part of the Wabigoon – Quetico boundary in northern Ontario. Canadian Journal of Earth Sciences, **26:** 1013 – 1026.

Dodson, M.H. 1973. Closure Temperature in Cooling Geochronological and Petrological Systems. Contributions to Mineralogy and Petrology, **40**: 259-274.

Ferry, T.M., and Spear, F.S. 1978. Experimental calibration of the partitioning of Fe and Mg between biotite and garnet. Contributions to Mineralogy and Petrology, **66:** 113-117.

Gorbatschev, R., and Bagdanova, S. 1993. Frontiers in the Baltic Shield. Precambrian Research, **64:** 3-21.

Hajnal, Z., Lucas, S., White, D., Lewry, J., Bezdan, S., Stauffer, M.R., and Thomas, M.D. 1996. Seismic reflection images of high-angle faults and liked detachments in the Trans-Hudson Orogen. Tectonics, **15:** 427-439.

Hanes, J.A. 1991. K-Ar and $^{40}Ar/^{39}Ar$ geochronology: methods and applications. *In* Short course handbook on application of radiogenic isotope systems to problems in geology. *Edited by* L. Heaman and J.N. Ludden. Mineralogical Association of Canada, Short Course Handbook, **19**: 27-57.

Harrison, T.M. 1981. Diffusion of ^{40}Ar in hornblende. Contributions to Mineralogy and Petrology, **78:** 324-331.

Hawthorne, F.C. 1981. Crystal chemistry of the amphiboles. *In* Amphiboles and other hydros pyriboles; mineralogy. *Edited by* Veblen D.R. Reviews in Mineralogy, Mineralogical Society of America, Washington, DC, US.

Harrap, R.M., and Helmstaedt, H.H. 2000 Western Superior Transect Sixth Annual Workshop. Lithoprobe Report # 77, Lithoprobe Secretariat, University of British Columbia.

Hoffman, P.F. 1989. Precambrian geology and tectonic history of North America. *In*: The Geology of North - An Overview. *Edited by:* Bally, A.W., and Palmer, A.R. The Geology of North America, A. Geological Society of America, pp. 447-512.

Holland, T., and Blundy, J. 1994. Non-ideal interactions in calcic amphiboles and their bearing on amphibole-plagioclase thermometry. Contributions to Mineralogy and Petrology, **116:** 443 - 447.

Ketz, R. 1983. Symbols for rock-forming minerals. American Mineralogist, **68**: 277-279.

Krough, T.E. 1993. High precision U-Pb ages for granulite metamorphism and deformation in the Archean Kapuskasing structural zone, Ontario: implications for structure and development of the lower crust. Earth and Planetary Science Letters, **119:** 1-18.

Langford, F.F., and Morin, J.A. 1976. The development of the Superior Province of northwestern Ontario by merging island arcs. American Journal of Science, **276:** 1023-1034.

McDougall, I., & Harrison, T.M. 1988. Geochronology and Thermochronology by the $^{40}Ar/^{39}Ar$ Method. Oxford Monographs on Geology and Geophysics, No. 9, Oxford University Press.

Merrihue, C., and Turner, G. 1966. Potassium-argon dating by activation with fast neutrons. Journal of Geophysical Research, **71:** 2852-2859.

Prothero, D.R, & Schwab, F. 1996. Sedimentary Geology. W.H. Freeman and Company, pp.428-436.

Richard, L.R. 1997. Minpet for Windows, Version 2.02, Reference Manual. Minpet Geological Software, Quebec, Canada.

Richard L.R., and Clarke, D.B. 1990. AMPHIBOL; a program for calculating structural formulae and for classifying and plotting chemical analyses of amphiboles. American Mineralogist, **75:** 421-423.

Stott, G.M., Davis, D.W., and Morrison, D. 1998. Observations on the tectonic framework of the eastern Wabigoon Subprovince. *In* 1998 Western Superior Transect Fourth Annual Workshop, March 23-24, 1998. *Edited by* R.M. Harrap, H.H. Helmstaedt. Lithoprobe Report # 65, Lithoprobe Secretariat, University of British Columbia, pp. 74-76.

Stott, G.M., and Davis, D.W., 1999. Contributions to the tectonostratigraphic analysis of the Onaman-Tashota greenstone belt, eastern Wabigoon Subprovince. *In* 1999 Western Superior Transect Fifth Annual Workshop. *Edited by* Harrap, R.M., and Helmstaedt, H.H. Lithoprobe Report # 70, Lithoprobe Secretariat, University of British Columbia, pp. 122-123.

Stott, G.M., and Morrison, D. 1995. The geology and tectonic sequence of events in the south-central Onaman-Tashota greenstone belt, east Wabigooon Subprovince. In Summary of Field Work and Other Activities 1995, Ontario Geological Survey Miscellaneous Paper **164**: 41-44.

Stott, G.M., Morrison, D., Gale, V., and Wachowiak, N. 1996. Precambrian Geology of South-Central Onaman-Tashota Greenstone Belt; Ontario Geological Survey, Preliminary Map P.3352, scale 1:50 000.

Thurston, P.C., Williams, H.R., Sutcliffe, R.H., and Stott, G.M. 1991. Geology of Ontario. Ontario Geological Survey, Spec. Vol. 4, Part 1, Ministry of Northern Development and Mines, Ontario.

Tikoff, B., and Fossen, H. 1993. The deformation matrix for simultaneous simple shearing, pure shearing and volume change, and its application to transpression-transtension tectonics. Journal of Structural Geology, **15:** 413-422.

Tomlinson, K.Y., Hall, R.P., Hughes, D.J., and Thurston, P.C. 1996. Geochemistry and assemblage accretion of metavolcanic rocks in the Beardmore-Geraldton greenstone belt, Superior Province. Canadian Journal of Earth Sciences, **33**: 1520-1533.

Tomlinson, K.Y., and Stott, G.M. 2000. Nd isotopes in the eastern Wabigoon Subprovince: implications for crustal recycling and correlations within the central Wabigoon. *In* 2000 Western Superior Transect Sixth Annual Workshop. *Edited by* Harrap, R.M., and Helmstaedt, H.H. Lithoprobe Report # 77, Lithoprobe Secretariat, University of British Columbia, pp. 119-126.

Tomlinson, K.Y., Thurston, P.C., Hughes, D.J., and Keays, R.R. 1995. The Central Wabigoon Region: Petrogenesis of Mafic-Ultramafic Rocks in the Steep Rock, Lumby Lake and Obonga Lake Greenstone Belts (Continental Rifting and Drifting in the Archean). *In* 1995 Western Superior Transect Sixth Annual Workshop. *Edited by* Harrap, R.M., and Helmstaedt, H.H. Lithoprobe Report # 77, Lithoprobe Secretariat, University of British Columbia, pp. 65-73.

Williams, H.R. 1987. Ontario Geoscience Research Program, Grant No. 242; Structural Studies in the Wabigoon and Quetico Subprovinces; Ontario Geological Survey, Open File Report 5668, 163p., and 83 figures.

Winter, J.D. 2001. An Introduction to Igneous and Metamorphic Petrology. Prentice Hall, New Jersey, pp. 496-586.

APPENDIX A

Abbreviations used in this thesis

Mineral Abbreviations (generally according to Kretz, 1983)

Act	Actinolite
Amp	Amphibole
Ap	Apatite
Bt	Biotite
Cal	Calcite
Chl	Chlorite
Cpx	Clinopyroxene
Ep	Epidote
Fsp	Feldspar
Grt	Garnet
Hbl	Hornblende
Ilm	Ilmenite
Ksp	K - Feldspar
Ms	Muscovite
Plag	Plagioclase
Qtz	Quartz
Rt	Rutile
Ttn	Titanite

Other Abbreviations

ss	Strain shadow
Ppl	Plane polarized light
Xn	Crossed nichols
Amp 1	Refers to earlier phase of amphibole seen in cores of porphyroclasts in rocks from the shear zone. They are chemically classified as actinolite
Amp 2	Refers to later phase of amphibole, which grows over Amp 1, and is seen on rims of porphyroclasts in strain shadows and matrix. Amp 2 is seen extensively in higher grade samples adjacent to the North Wind Pluton
HBHSZ	Humboldt Bay High Strain Zone
NWP	North Wind Pluton
BGGB	Beardmore-Geraldton greenstone belt
OTGB	Onaman-Tashota greenstone belt
OTT	Onaman-Tashota terrane

APPENDIX B

Petrographic Descriptions

The sample descriptions are organized in general geographic location from south (next to the NWP) to north (above the HBHSZ). For exact locations, refer back to figure 4.6. $^{40}Ar/^{39}Ar$ data for these samples are shown in figure 4.8 and Appendix C.

01N030d

Outcrop: Station 30 (Fig. 2.5). The outcrop consists largely of interlayered granites and foliated amphibolites. This sample has a very strong foliation and down-dip lineation, and is very dark.

Thin Section: fine-grained (~0.5mm) amphibolite. Recrystallized hbl [presumably Amp 2] (85%) + plag (7%) + qtz (7%) + opaque oxides (1%) + minor Ksp + minor rt + minor ap + minor ep + minor ttn +/- bt (?). Strong foliation is defined by sub-idioblastic amphibole grains. Amphibole grains display crystallographic alignment.

Photographs:

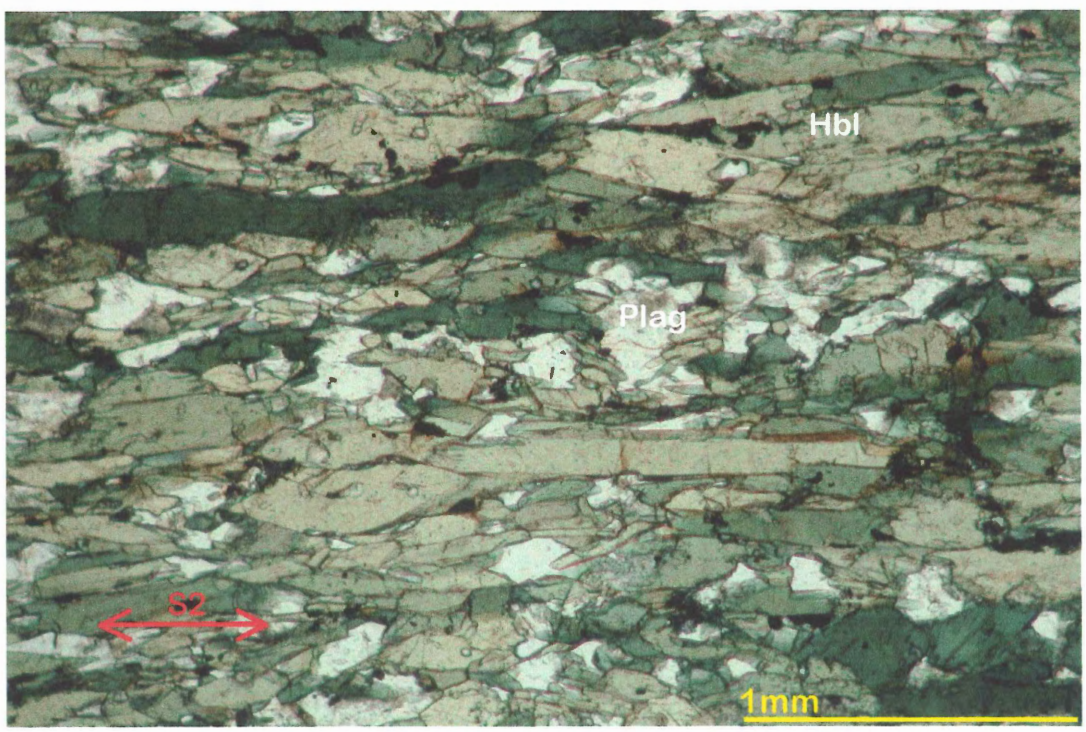

ppl, polished thin section, section cut perpendicular to S2 and parallel to L

01N030d continued:

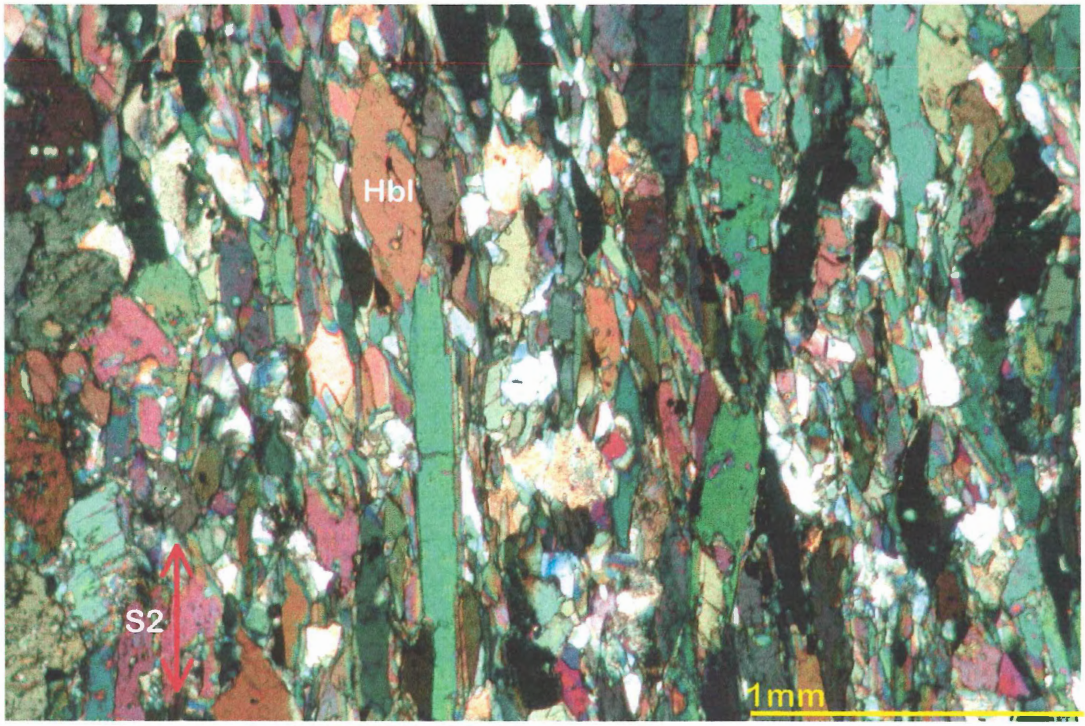

xn, polished thin section, rotation of stage is 90 ° to first photograph, section cut perpendicular to S2 and parallel to L

90N007c

Outcrop Station 7 (Fig. 2.5). Sample collected by N. Culshaw in 1999. The sample is taken from an island adjacent to the NWP. It displays characteristics typical of amphibolites close to the NWP: a good LS fabric, good foliation, and is very dark.

Thin Section: fine grained (~0.5mm) amphibolite. Recrystallized hbl [Amp 2] (~60%) + plag (40%) + minor ttn + minor Ksp + minor ep + very minor chl. Grain boundaries of amphibole and plagioclase are somewhat sutured. Grain shapes are subidioblastic. Plagioclase is highly altered to sericite in certain patches. Amphibole grains define the foliation, and display crystallographic preferred orientation.

Photographs:

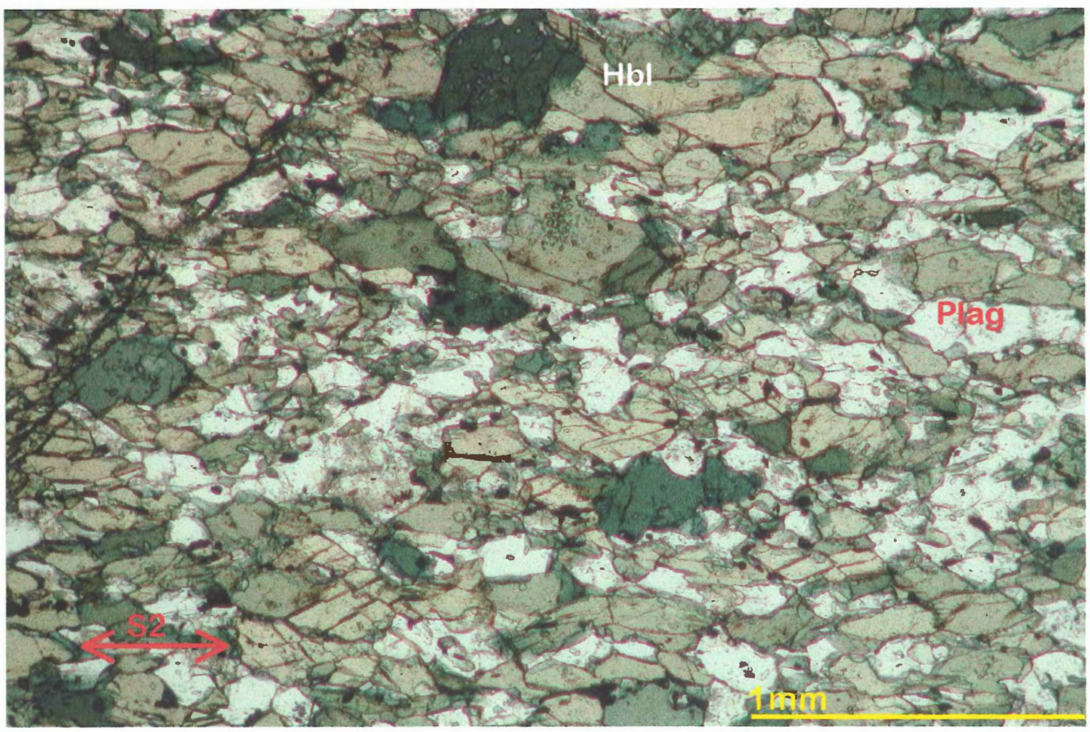

ppl, polished thin section, section cut perpendicular to S2 and parallel to L

90N007c continued:

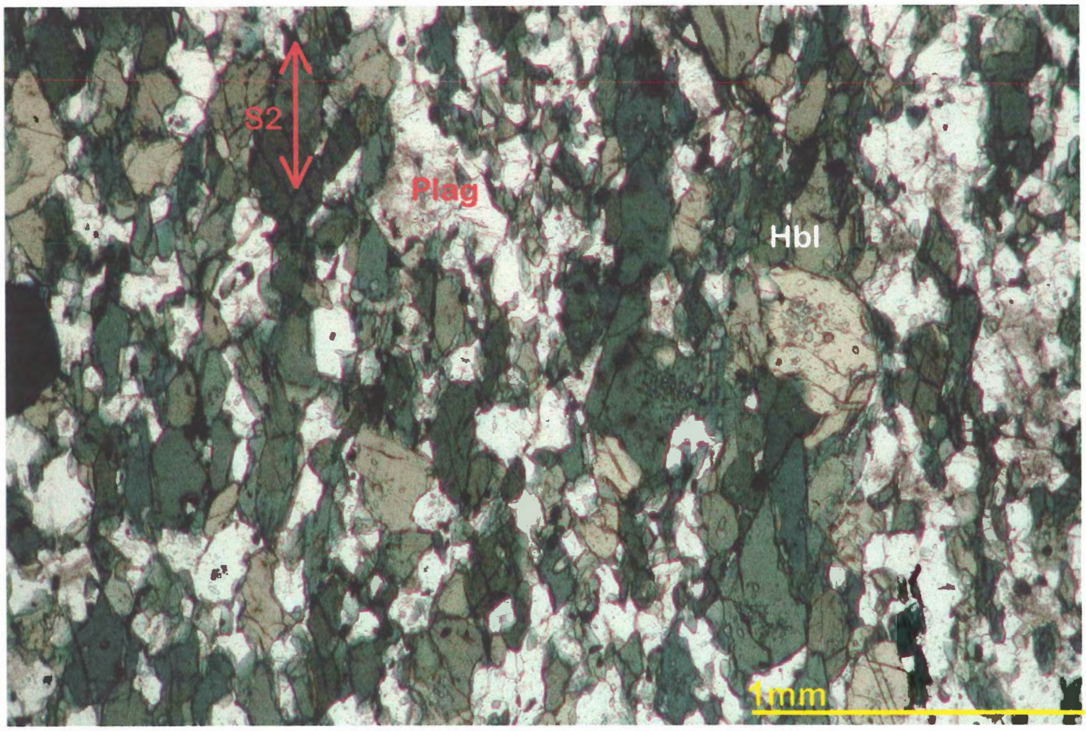

rotation of stage is 90° to first photograph, ppl, polished thin section, section cut perpendicular to S2 and parallel to L

90N013a

Outcrop: Station 13 (Fig. 2.5). Sample 90N013a, collected in 1999, comes from a large outcrop that displays S2 and contains Amp 1 porphyroclasts. Other locations in this island show very intense folding and evidence for D3.

Thin Section: Strongly foliated, medium grained to fine grained porphyroclastic amphibolite.

Porphyroclasts - amp ~ 1mm in size [Amp 1] (30%), contain minor inclusions of plag + qtz + ttn + ap

Matrix - amp [Amp 2] (60%) + plag (10%) + qtz + minor chl, Ksp, ep, ap, ilm, ttn.

Some amphibole porphyroclasts exhibit undulose extinction. Amphibole porphyroclasts in this sample pre-date the main fabric in the rock [S2]. The porphyroclasts are deformed and have been rotated. The porphyroclasts have well developed strain shadows, which indicate dextral shear in this sample. Less altered amphibole grains [Amp 2] occur largely in the strain shadows and matrix of the sample. Some grains of Amp 2 grow over the Amp 1 porphyroclasts as rims.

Photograph:

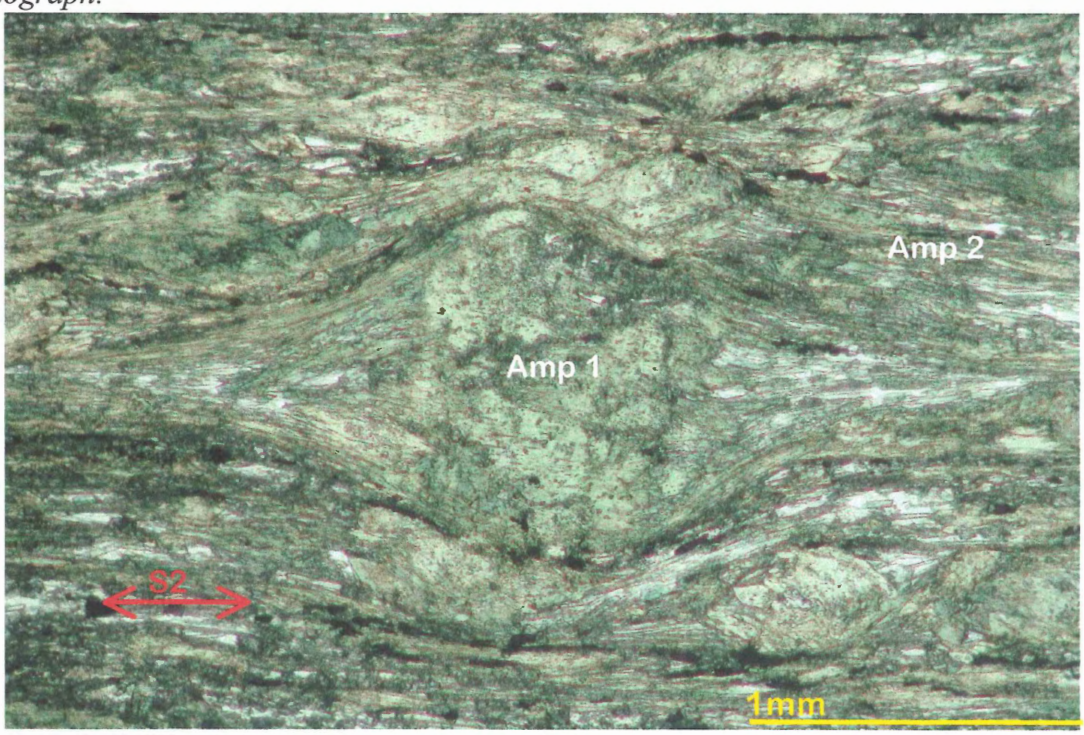

ppl, polished thin section, section cut perpendicular to S2 and parallel to L

90N015c

Outcrop: Station 15 (Fig. 2.5). This sample was collected in 1999 from an outcrop of "spotty" amphibole rich rocks. The rocks in this particular location less recrystallized when compared to other rocks in the shear zone (e.g. sample 15-51b). Despite the fact that this sample is from a 'lower strain' zone, it still has a penetrative LS fabric and is well foliated.

Thin Section: Strongly foliated, medium-grained porphyroclastic amphibolite.

<u>Porphyroclasts</u>: amp ~ 1-2mm in size [Amp 1] (40%), with minor inclusions of plag +/- ilm.

<u>Matrix</u>: amp [Amp 2] (40%) + plag (10%) + qtz (10%) + chl + ep + minor ilm, Ksp.

As in sample 90N013a, the amphibole porphyroclasts in this sample predate the main foliation [S2]. A second amphibole [Amp 2] occurs in the matrix, strain shadows, and rims of porphyroclasts. The foliation is largely defined by these amphiboles and the other matrix minerals such as plagioclase. However, in a few places, some Amp 2 grains overgrow the foliation. Therefore, in this sample, it appears that D2 occurred during growth of amp and stopped just before growth of Amp 2 ceased.

Photograph:

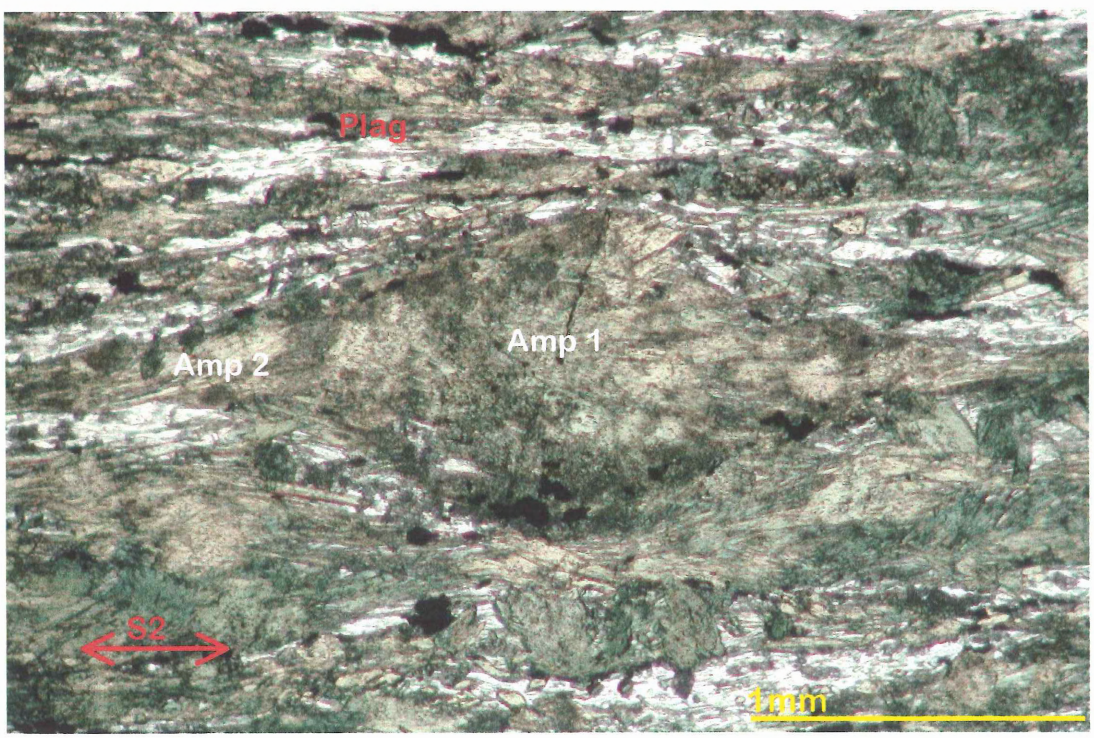

ppl, polished thin section, section cut perpendicular to S2 and parallel to L

90N015d

Outcrop: Station 15 (Fig. 2.5). This sample was taken from a similar outcrop as 90N015c, further north along the shore from the previous location. The outcrop is also similar in that it is a relatively less recrystallized rock.

Thin Section: Well-foliated, coarse-grained porphyroclastic amphibolite.

Porphyroclasts: Amp ~ 3-5mm [Amp 1] (40%), with visible inclusions of plag + ttn.

Matrix: amp [Amp 2] (50%) + plag (10%) + qtz + chl + minor Ksp, ttn

As in other samples from the shear zone, the amphibole porphyroclasts predate the main foliation [S2]. Amp 2 occurs in the matrix, strain shadows, and rims of Amp 1 porphyroclasts. Both amphiboles appear to be deformed by the foliation [S2]. Several porphyroclasts of Amp 1 exhibit simple twinning. The porphyroclasts are large and blocky. They often contain in their cores, a heterogeneous intergrowth of amphibole, as well as plag inclusions. The inclusions are interpreted to represent the original texture of the rock, and the intergrowth is interpreted to be a product of Amp 1 replacing primary igneous cpx. This would be consistent with an interpretation of a basaltic protolith.

Photographs:

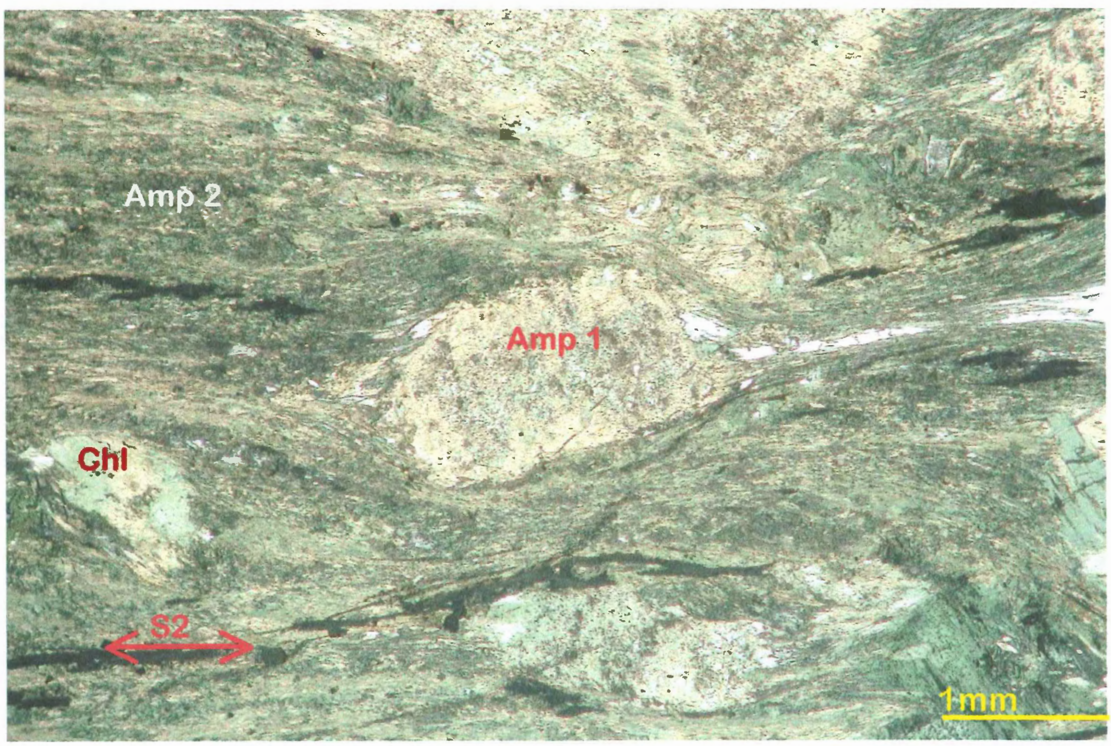

ppl, polished thin section, section cut perpendicular to S2 and parallel to L

90N015d continued:

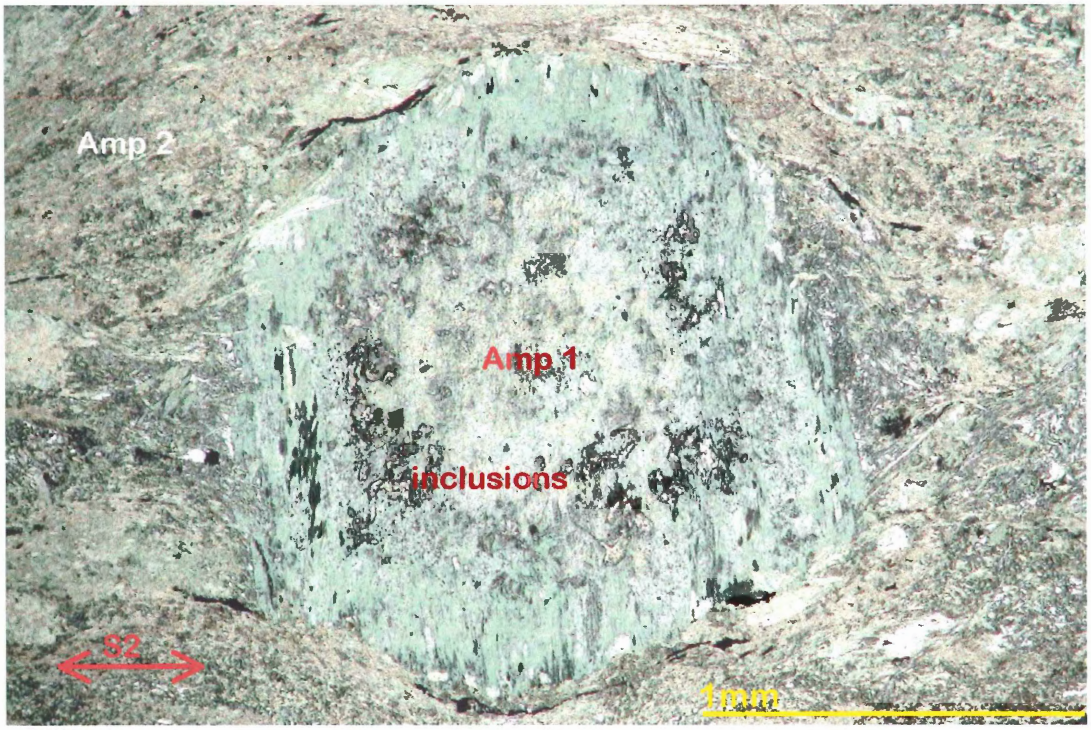

ppl, normal thin section, section cut perpendicular to S2 and parallel to L

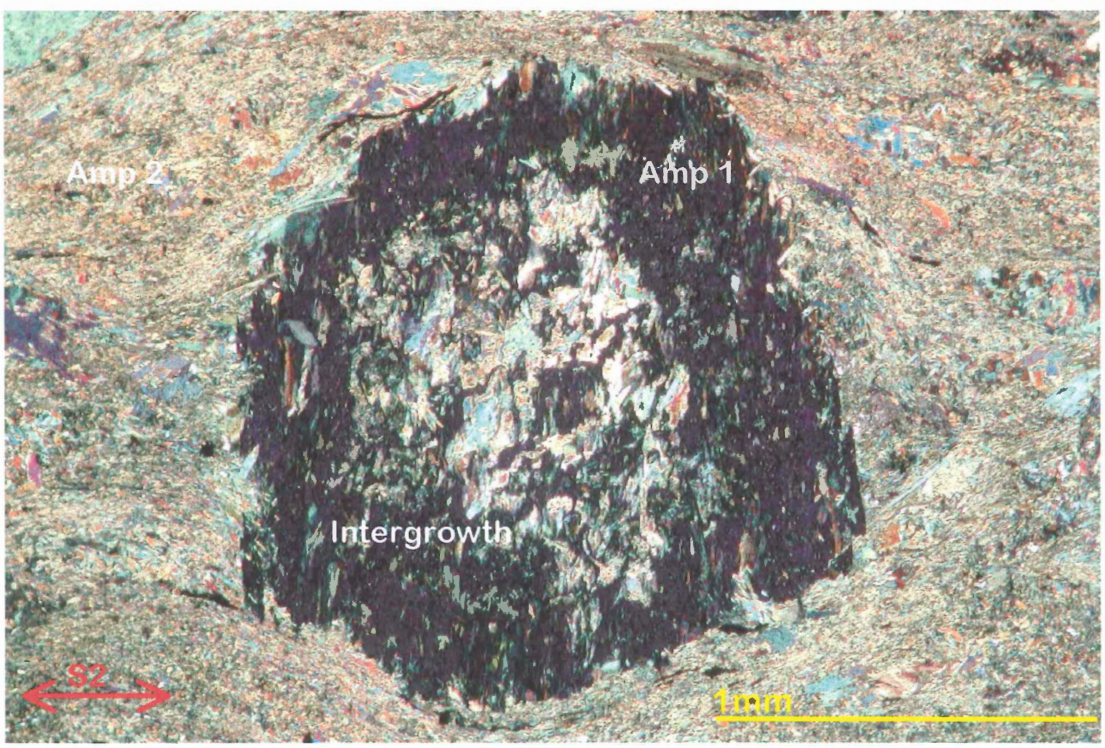

xn, normal thin section, section cut perpendicular to S2 and parallel to L

15-51b

Outcrop: Station 15 (Fig. 2.5). The sample is taken from a section of rock that is highly strained and highly recrystallized. The rocks have a strong LS fabric with a down-dip lineation that is defined by amphibole. The section of rock appears to be largely unaffected by any subsequent deformation (i.e. no D3 structures are seen).

Thin Section: Fine-grained, strongly foliated amphibolite. Recrystallized amp [Amp 2] (70%) + plag (10%) + qtz (5%) + chl (5%) + ep + ilm. The foliation is defined by Amp 2 and plag layers. Plagioclase is altered to sericite in places. There are few chlorite porphyroclasts that are deformed by S2, and fewer Amp 2 porphyroblasts overgrowing S2.

Photograph:

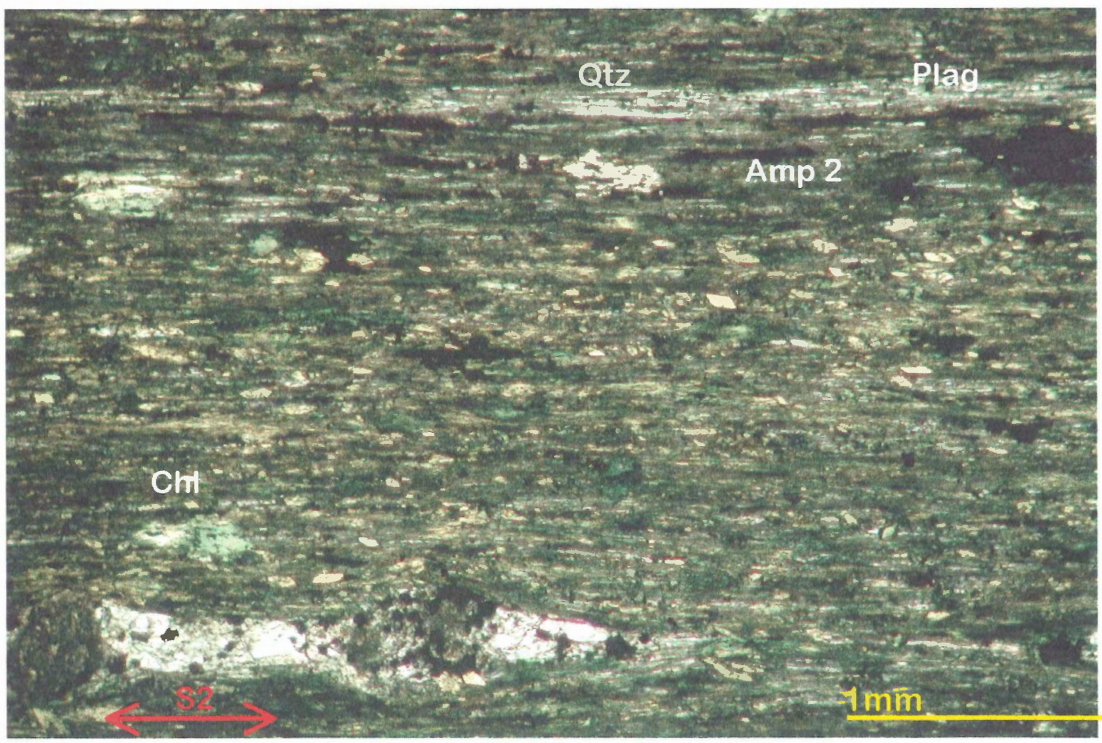

ppl, polished thin section, section cut perpendicular to S2 and parallel to L

15-51a

Outcrop: Station 15 (Fig. 2.5). This sample comes from a small, low-strain pod-shaped zone within the highly strained rocks of sample 15-51b. In the field, this sample is interpreted to represent the less sheared equivalent of 15-51b.

Thin Section: Unfoliated porphyroblastic amphibolite.
<u>Porphyroblasts</u> - amp ~0.2 mm [Amp 1] (80%)
<u>Matrix</u> - plag (10%) + qtz (10%) + chl + ep + minor ilm
Amp grains are generally subidioblastic, approximately 5% of amp occurs as larger porphyroblasts ~1-2 mm in size. Chlorite occurs in small veins.

Photograph:

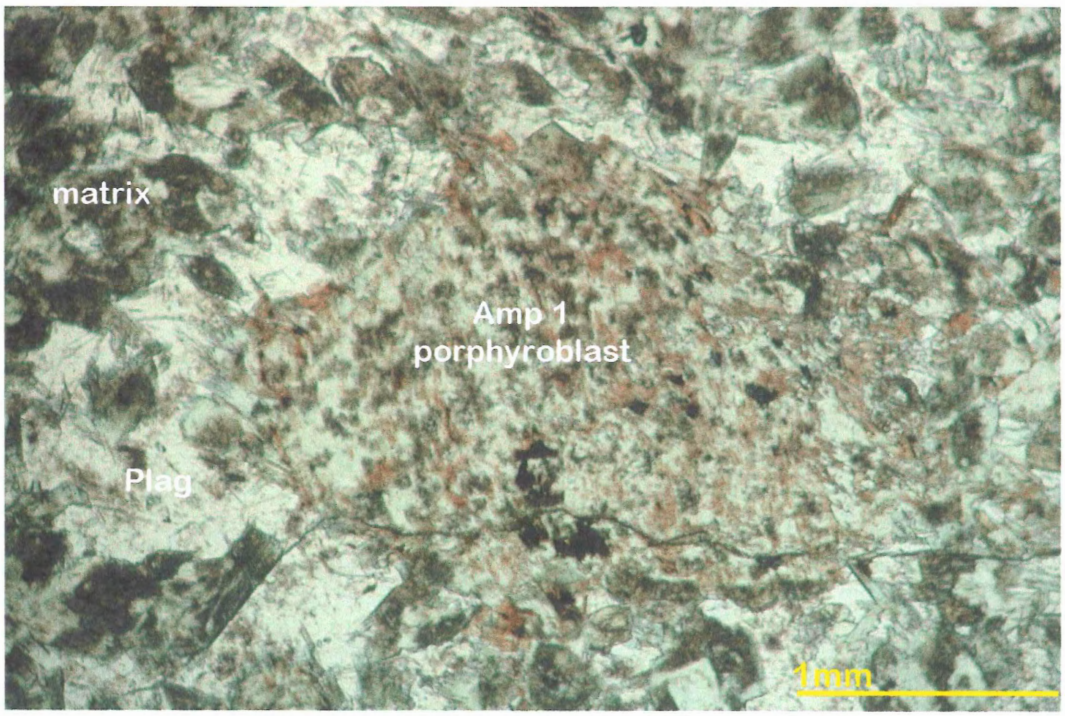

ppl, polished thin section

15-51a continued:

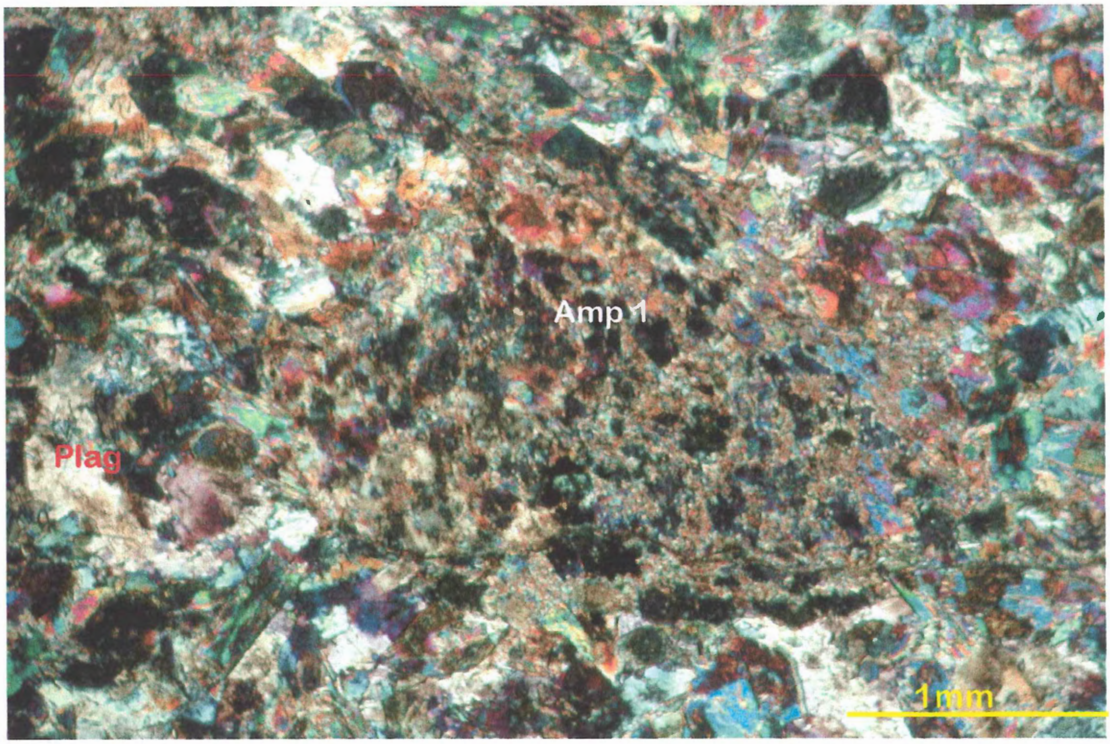

xn, polished thin section

15

Outcrop: Station 15 (Fig. 2.5). This particular outcrop contains a largely "spotty" porphyroclastic rocks, but contains many small high strain east-west shear zones (as in Fig. 2.9) throughout the rock. The small shear zones occur every 15 cm or so, and may be several cm thick. This outcrop clearly shows the main fabric [S2] forming at the expense of an earlier, porphyroblastic amphibole. This particular thin section comes from the gradational boundary between one of the higher strain zones and the lower strain zones.

Thin Section: Foliated porphyroclastic amphibolite.

<u>Porphyroclasts</u>: amp 2-3 mm [Amp 1] (39%) + chl (1%)

<u>Matrix</u>: amp [Amp 2] (35%) + plag (10%) + qtz (5%) + ep (5%) + chl (5%) + minor ttn, ilm

This sample shows the main fabric [S2] overprinting and deforming the earlier porphyroclastic amphiboles [Amp 1]. It also shows Amp 2 replacing Amp 1 and defining the foliation. The pleochroism of amp porphyroclasts differs from core to rim, indicating that Amp 2 replaced Amp 1. Gradationally alternating layers of amp and plag are seen.

Photograph:

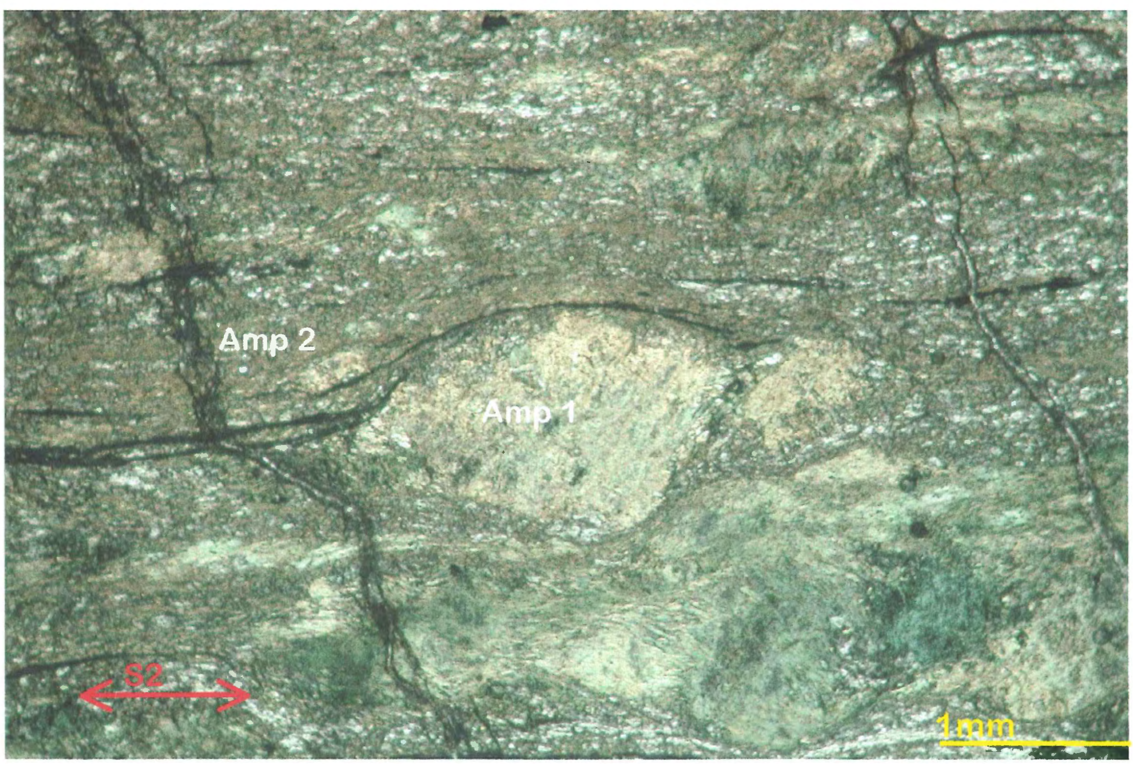

ppl, polished thin section, section cut perpendicular to S2 and parallel to L

15 continued:

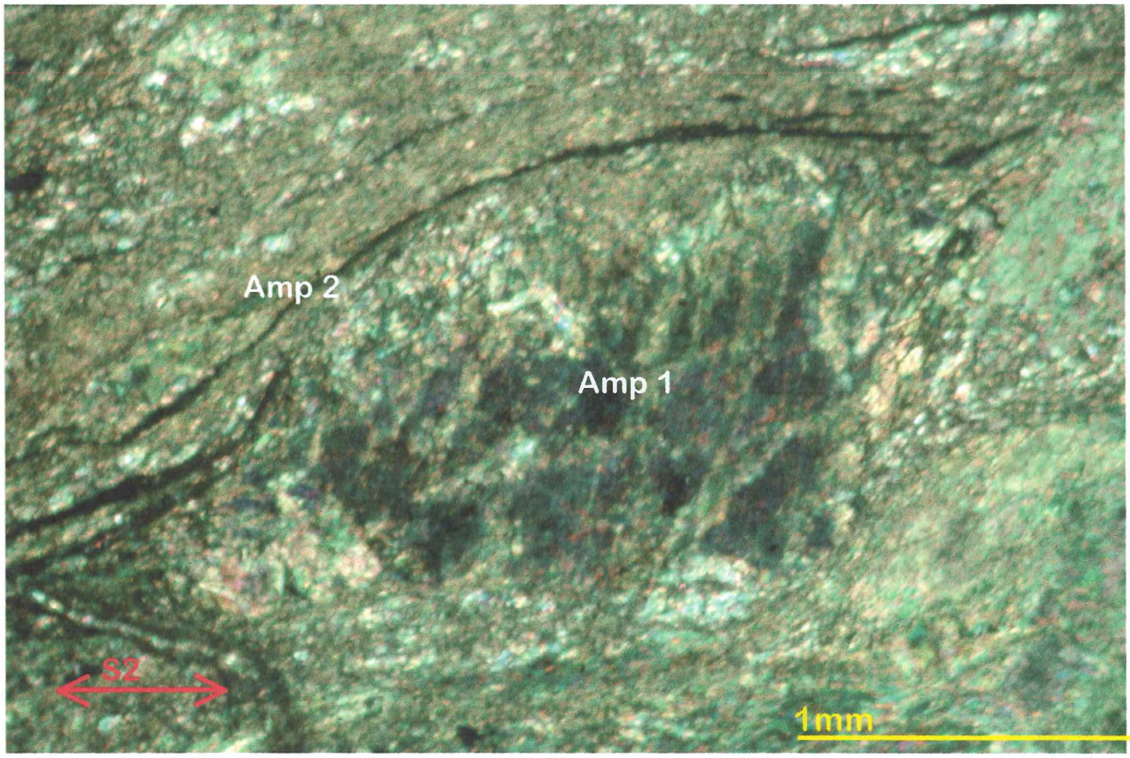

xn, polished thin section, section cut perpendicular to S2 and parallel to L

90N014a

Outcrop: Station 14 (Fig. 2.5). Sample collected by N. Culshaw in 1999. The outcrop consists of a homogeneous amphibolite with zones of finer grained 'feathery' amphibolite. This sample was taken from the homogeneous amphibolite. These rocks are very texturally different form those in the HBHSZ. Therfore, the amp camnot be compared in terms of Amp 1 vs. Amp 2.

Thin Section: Medium grained, foliated amphibolite, weak lineation. Amp ~0.5mm (70%) + plag (15%) + qtz (10%) + opaque oxides (5%) + chl. Elongate amp grains define foliation. Plag grains are xenoblastic, and form aggregates of many small grains. Opaque oxides are very fine grained and occur throughout the entire section, as inclusions in all other minerals.

Photograph:

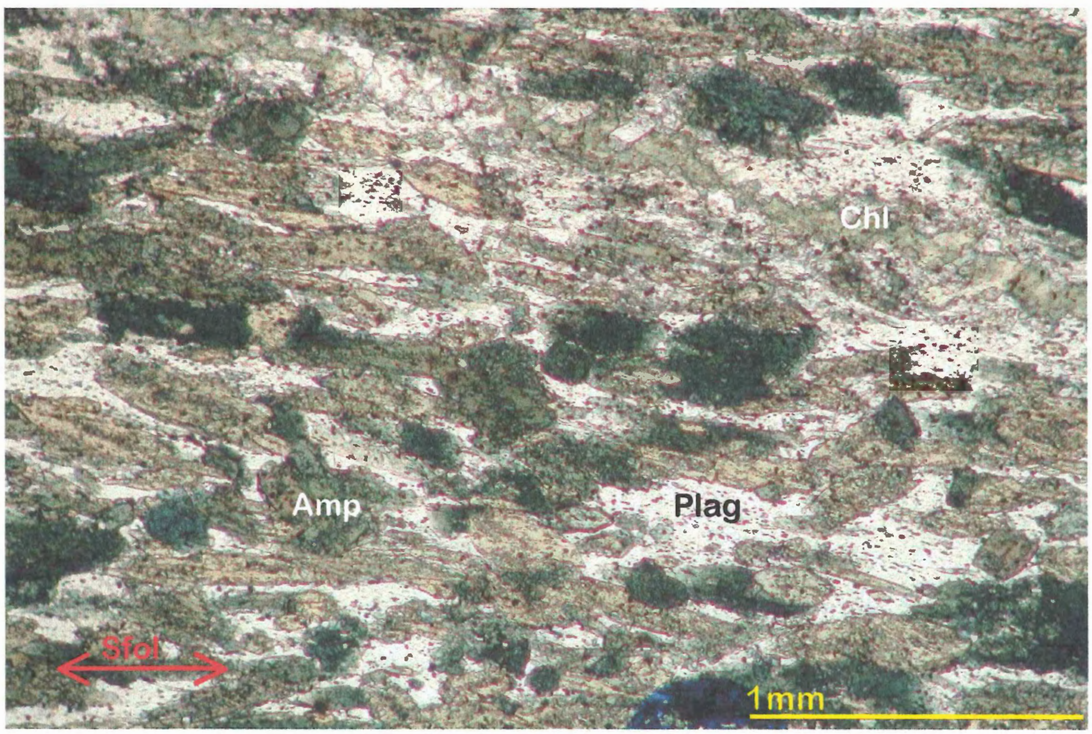

ppl, polished thin section, section cut perpendicular to S2 and parallel to L

90N014b

Outcrop: Station 14 (Fig. 2.5). This sample was taken from one of the 'feather amphibolite' zones.

Thin Section: Weakly foliated feathery amphibolite.

Porphyroblasts - amp (30%)

Matrix - amp (10%) + plag (30%) + qtz (20%) + chl (5%) + bt + ep + ttn

Cores of amp porphryoblasts contain staight inclusion trails of mainly plagioclase, and therefore overgrow an earlier fabric [S1?]. The rims of the amp porphyroblasts consists of fine-grained acicular and radiating amp grains. These "feathery" amphiboles post date the cores of the porphyroblasts, however, it is not clear whether this is a completely different phase of growth or not. The composition appears to be similar. Matrix plag and qtz occur as fine grained recrystallized patches. Carbonate bands occur throughout the sample.

Photographs:

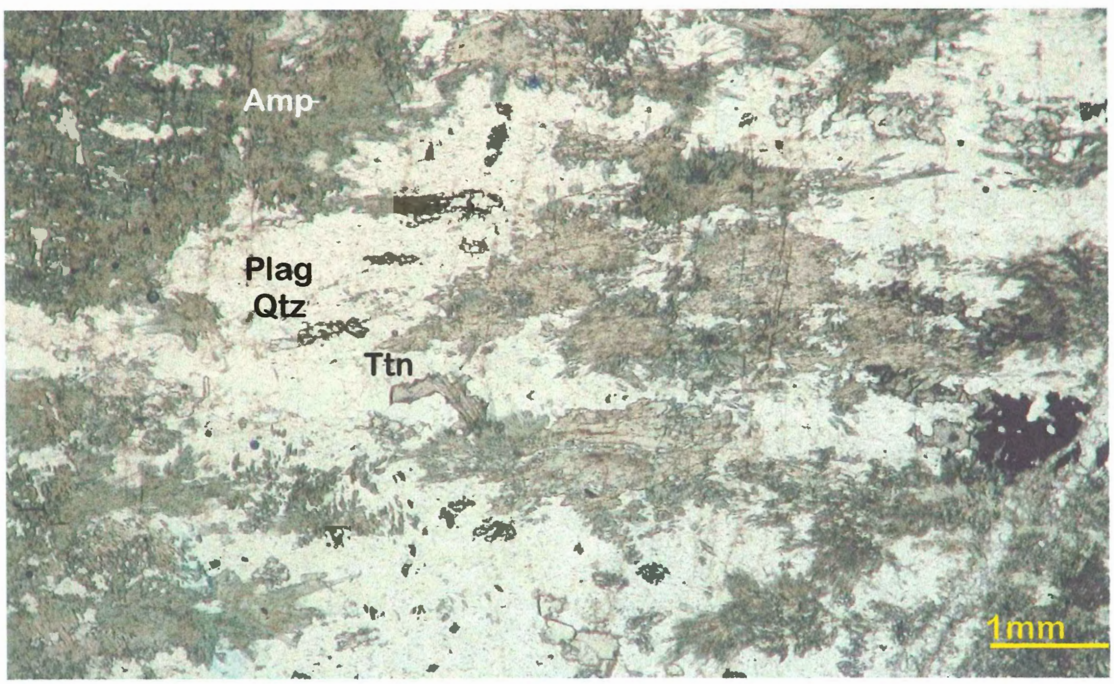

ppl, polished thin section

90N014b continued:

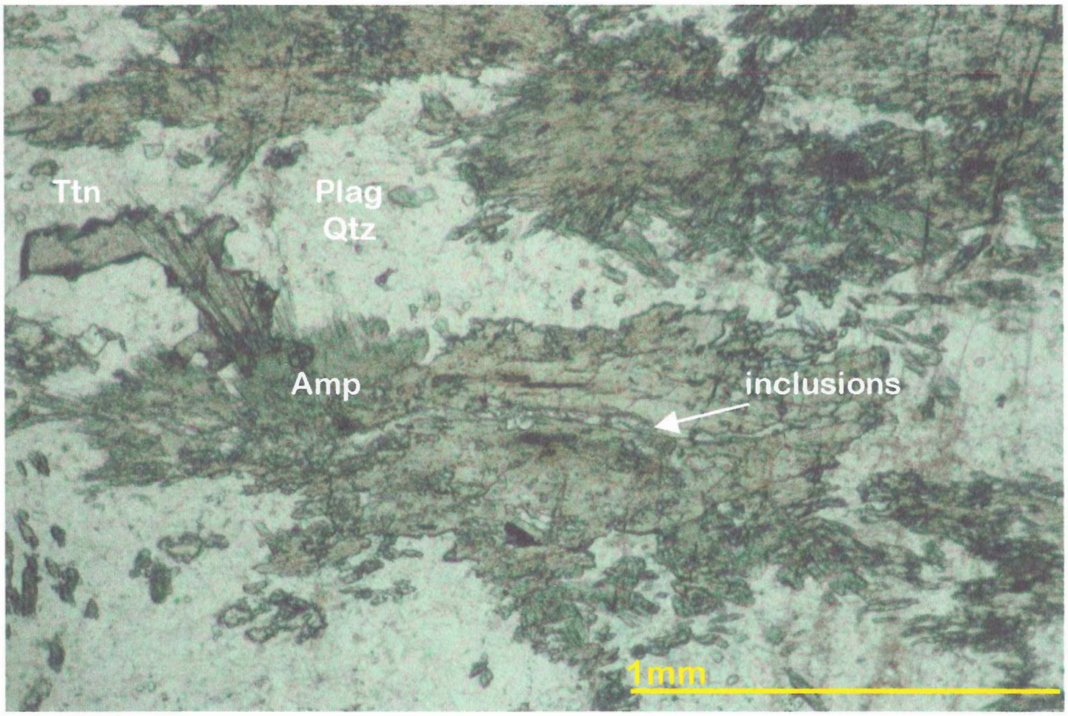

ppl, polished thin section

APPENDIX C

Argon summary sheets

Analysis are presented roughly in geographic location from south to north, and in the same order as the corresponding spectra presented in figure 4.8.

01N030D HORNBLENDE ARGON SUMMARY

T°C	mV 39	39%	AGE (Ma)±1σ	% ATM	37/39	36/40	39/40	% IIC
650	0.4	0	1152.8 ± 321	2.5	0.59	0.000088	0.002595	0.05
750	3.9	0.5	1975.4 ± 54.4	9.2	4.15	0.000312	0.001084	0.3
850	15.4	2.2	2043.7 ± 15	3.3	4.21	0.000114	0.00109	0.31
950	37.4	5.4	2311 ± 9.6	3.4	10.67	0.000118	0.000881	0.76
975	13.8	2	2516 ± 16.9	0.8	14.42	0.000031	0.000776	1.02
1000	37.3	5.4	2605 ± 11	0.6	15.99	0.000022	0.000728	1.12
1025	63.8	9.3	2650.7 ± 9.8	0.5	17.43	0.000017	0.000706	1.22
1050	183.2	26.8	2664.3 ± 11.4	0.3	16.99	0.000011	0.0007	1.19
1075	60.3	8.8	2665.4 ± 10	0.2	16.04	0.00001	0.0007	1.12
1100	17.6	2.5	2636.5 ± 15.7	0.8	16.35	0.000028	0.000711	1.15
1125	56	8.2	2679.1 ± 11.6	0.5	16.83	0.000017	0.000691	1.18
1150	42.8	6.2	2674 ± 12.3	0.5	16.68	0.000018	0.000694	1.17
1175	14	2	2666.9 ± 21.2	1.2	16.58	0.000041	0.000693	1.16
1200	7	1	2657.8 ± 34.3	2.3	15.92	0.00008	0.000689	1.12
1250	90.3	13.2	2643.9 ± 16	0.8	16.37	0.000029	0.000707	1.15
1300	15.3	2.2	2701.6 ± 19.2	1.6	16.4	0.000057	0.000672	1.15
1350	8.7	1.2	2638.5 ± 29.3	4.9	16.01	0.000168	0.00068	1.12
1450	13.5	1.9	2619.1 ± 23.5	9.9	16.08	0.000337	0.000653	1.13

MEAN AGE(1050°C-1450°C)= 2661.8 ± 17.8 Ma (2σ UNCERTAINTY,INCLUDING ERROR IN J)

J = .002376 ± .0000238 (1 %)

37/39,36/40 AND 39/40 Ar RATIOS ARE CORRECTED FOR MASS SPECTROMETER DISCRIMINATION,INTERFERING ISOTOPES AND SYSTEM BLANKS

% IIC - INTERFERING ISOTOPES CORRECTION

90N007C HORNBLENDE ARGON SUMMARY

T°C	mV 39	39%	AGE (Ma)±1σ	% ATM	37/39	36/40	39/40	% IIC
650	8.4	2.1	1416.9 ± 27.8	5.6	2.69	0.000191	0.001874	0.21
750	8.3	2.1	2264.3 ± 40.4	4.8	3.23	0.000163	0.000899	0.23
850	10.2	2.6	2103.7 ± 24.9	2.3	3.69	0.00008	0.001047	0.26
950	14	3.5	2456.3 ± 20.4	1.7	11	0.000059	0.000802	0.78
975	9.2	2.3	2393.9 ± 26.1	1.2	12.75	0.000042	0.000845	0.91
1000	22	5.6	2654 ± 15.6	0.6	17.37	0.000023	0.000701	1.22
1025	44.2	11.3	2676.8 ± 10.8	0.4	19.03	0.000015	0.000692	1.33
1050	95.3	24.3	2670.5 ± 14	0.2	18.76	0.00001	0.000696	1.31
1075	35.9	9.2	2679.3 ± 11.2	0.2	18.77	0.00001	0.000691	1.32
1100	10.9	2.7	2687.4 ± 27.6	0.7	18.74	0.000025	0.000685	1.31
1125	33.3	8.5	2671.4 ± 11.6	0.4	19.78	0.000015	0.000694	1.39
1150	22.6	5.7	2673.8 ± 14.2	0.4	19.61	0.000015	0.000693	1.37
1175	7.6	1.9	2620.5 ± 32.1	0.8	19.28	0.000031	0.000717	1.36
1200	4.7	1.2	2657.4 ± 45.4	1.5	18.64	0.000054	0.000694	1.31
1250	19.2	4.9	2687.4 ± 15.4	0.8	19.65	0.000028	0.000684	1.38
1300	13.4	3.4	2703.3 ± 21.8	1.3	19.47	0.000044	0.000673	1.36
1350	9.8	2.5	2723.2 ± 22.5	2.6	19.14	0.00009	0.000654	1.34
1450	19.7	5	2683 ± 16.3	3.5	19.42	0.00012	0.000667	1.36
1500	1.2	0.3	2213.6 ± 270	47.6	9.73	0.001613	0.000515	0.7

MEAN AGE(1000°C-1450°C)= 2675.3 ± 17.5 Ma (2σ UNCERTAINTY,INCLUDING ERROR IN J)

J = .002371 ± .000024 (1 %)

37/39,36/40 AND 39/40 Ar RATIOS ARE CORRECTED FOR MASS SPECTROMETER DISCRIMINATION,INTERFERING ISOTOPES AND SYSTEM BLANKS

% IIC - INTERFERING ISOTOPES CORRECTION

90N013A HORNBLENDE ARGON SUMMARY

T°C	mV 39	39%	AGE (Ma)±1σ	% ATM	37/39	36/40	39/40	% IIC
650	64.9	10.1	835.5 ± 5.9	5.9	2.25	0.000202	0.003805	0.21
750	43.2	6.7	1433.7 ± 8.6	3.4	4.41	0.000116	0.001896	0.35
850	45.8	7.1	1729.4 ± 9.1	1.4	6.92	0.000048	0.001461	0.52
950	106.6	16.7	2180.9 ± 7.4	0.8	23.12	0.00003	0.001005	1.68
975	60.6	9.4	2265.8 ± 8.8	0.5	17.99	0.000017	0.000944	1.29
1000	61.1	9.5	2393.4 ± 9.8	0.3	18.85	0.000014	0.000857	1.34
1025	33	5.1	2245.2 ± 11.8	0.5	17.27	0.000019	0.000959	1.24
1050	22.2	3.4	2213.5 ± 11.8	0.7	17.57	0.000025	0.000981	1.27
1075	26	4	2435.3 ± 12	0.5	23.47	0.000019	0.000829	1.67
1100	37.9	5.9	2535.3 ± 10.9	0.4	26.75	0.000016	0.000771	1.89
1125	30.8	4.8	2563.1 ± 11.4	0.5	24.72	0.000018	0.000755	1.75
1150	13.2	2	2427.2 ± 21.9	0.8	22.02	0.000028	0.000832	1.57
1175	9.6	1.5	2547.9 ± 26.4	1	20.91	0.000036	0.000759	1.48
1200	5.9	0.9	2322.5 ± 38.4	1.4	19.56	0.000052	0.000895	1.4
1250	33.4	5.2	2628 ± 12	0.5	27.03	0.000018	0.00072	1.9
1300	19.9	3.1	2632.8 ± 14.3	0.8	26.37	0.000029	0.000715	1.85
1350	14.9	2.3	2541 ± 20	1.4	25.83	0.00005	0.00076	1.83
1450	8.5	1.3	2548.3 ± 33.1	4	23.46	0.000138	0.000736	1.66

MEAN AGE(1250°C-1300°C)= 2629.8 ± 23 Ma (2σ UNCERTAINTY,INCLUDING ERROR IN J)

J = .002385 ± .0000238 (.9 %)

37/39,36/40 AND 39/40 Ar RATIOS ARE CORRECTED FOR MASS SPECTROMETER DISCRIMINATION,INTERFERING ISOTOPES AND SYSTEM BLANKS

% IIC - INTERFERING ISOTOPES CORRECTION

90N015D HORNBLENDE ARGON SUMMARY

T°C	mV 39	39%	AGE (Ma)±1σ	% ATM	37/39	36/40	39/40	% IIC
650	16.1	4	1474.5 ± 16.2	18.1	2.32	0.000615	0.001558	0.18
750	21	5.3	1766 ± 11.3	8.7	3.45	0.000295	0.001322	0.26
850	27.1	6.8	1868.3 ± 10.4	2	3.77	0.000068	0.001298	0.28
950	109.6	27.6	2153.2 ± 6.6	0.6	10.43	0.000022	0.00104	0.76
975	31.2	7.8	2323.8 ± 9.6	0.4	18.32	0.000018	0.000911	1.31
1000	39.4	9.9	2493.2 ± 9.7	0.4	23.36	0.000015	0.000803	1.66
1025	29.8	7.5	2473.7 ± 11.3	0.3	20.42	0.000012	0.000815	1.45
1050	14.1	3.5	2329.3 ± 17.9	0.5	17.74	0.00002	0.000907	1.27
1075	9.5	2.4	2249.7 ± 20.9	0.8	17.68	0.00003	0.000962	1.28
1100	10.5	2.6	2433.9 ± 19.5	0.9	20.54	0.000034	0.000835	1.46
1125	10.5	2.6	2555 ± 21.9	1.7	25.65	0.000062	0.000757	1.81
1150	7.6	1.9	2600.9 ± 28.5	3.1	27.29	0.000108	0.000722	1.92
1175	10.4	2.6	2552.1 ± 17.9	2.7	29.07	0.000094	0.000751	2.06
1200	7.1	1.8	2637.7 ± 35.1	3.7	27.24	0.000126	0.000699	1.92
1250	22.6	5.7	2595.6 ± 11.5	2.1	27.39	0.000071	0.000732	1.93
1300	14.9	3.7	2609.2 ± 13.8	3.6	26.04	0.000123	0.000714	1.84
1350	8.6	2.1	2585.1 ± 24.1	7.4	23.98	0.000253	0.000698	1.69
1450	5.2	1.3	3900.1 ± 92.7	10.3	19.12	0.000351	0.00028	1.28

MEAN AGE(1250°C-1350°C)= 2598.1 ± 21.8 Ma (2σ UNCERTAINTY,INCLUDING ERROR IN J)

J = .002408 ± .000024 (.9 %)

37/39,36/40 AND 39/40 Ar RATIOS ARE CORRECTED FOR MASS SPECTROMETER DISCRIMINATION,INTERFERING ISOTOPES AND SYSTEM BLANKS

% IIC - INTERFERING ISOTOPES CORRECTION

90N015C HORNBLENDE ARGON SUMMARY

T°C	mV 39	39%	AGE (Ma)±1σ	% ATM	37/39	36/40	39/40	% IIC
650	34.7	8.5	570.2 ± 7.5	18.6	3.58	0.00063	0.005258	0.4
750	22.7	5.5	1180.2 ± 9.3	9.5	10.45	0.000324	0.002352	0.88
850	24.9	6.1	1470.5 ± 9.1	2.7	17.25	0.000095	0.001854	1.37
950	54.8	13.5	2308.1 ± 8.3	0.8	28.47	0.000029	0.000918	2.05
975	30	7.3	2400.4 ± 11.8	0.4	19.04	0.000017	0.000858	1.36
1000	36	8.8	2543.4 ± 10.4	0.3	20.32	0.000013	0.000773	1.44
1025	18	4.4	2466.5 ± 14.9	0.6	19.48	0.000023	0.000816	1.38
1050	10.3	2.5	2364.9 ± 23.2	0.9	20.11	0.000034	0.000878	1.44
1075	13.1	3.2	2469.6 ± 17.4	0.6	23.7	0.000023	0.000814	1.68
1100	27.5	6.7	2631.4 ± 12.7	0.3	24.57	0.000012	0.000725	1.73
1125	29.6	7.2	2659.5 ± 11.6	0.3	22.74	0.000014	0.00071	1.6
1150	8.1	1.9	2509.1 ± 30.2	1.1	20.47	0.00004	0.000786	1.45
1175	5.3	1.3	3654 ± 69.5	0.9	18.95	0.000032	0.000361	1.28
1200	3.7	0.9	2951.3 ± 66.8	2.3	17.99	0.00008	0.000567	1.24
1250	66.6	16.4	2682.2 ± 9.6	0.4	23.3	0.000017	0.000698	1.63
1300	10.5	2.6	2688.6 ± 26.7	2.1	22.79	0.000074	0.000683	1.6
1350	5.6	1.3	2593.2 ± 35.7	6.7	21.68	0.000229	0.000698	1.53
1450	3.9	0.9	2547.7 ± 73.9	22.4	18.94	0.000758	0.0006	1.34

MEAN AGE(1250°C-1300°C)= 2683.1 ± 22.9 Ma (2σ UNCERTAINTY,INCLUDING ERROR IN J)

J = .002403 ± .000024 (.9 %)

37/39,36/40 AND 39/40 Ar RATIOS ARE CORRECTED FOR MASS SPECTROMETER DISCRIMINATION,INTERFERING ISOTOPES AND SYSTEM BLANKS

% IIC - INTERFERING ISOTOPES CORRECTION

15 HORNBLENDE ARGON SUMMARY

T°C	mV 39	39%	AGE (Ma)±1σ	% ATM	37/39	36/40	39/40	% IIC
650	34.7	7.6	904.4 ± 11.6	21.5	2.59	0.00073	0.002883	0.24
750	21.4	4.7	1411.7 ± 13.5	11.1	3.12	0.000375	0.001792	0.25
850	19.7	4.3	1608.8 ± 14.1	5.3	8.09	0.00018	0.001574	0.62
950	77.4	17.1	2537.5 ± 8.7	0.9	45.35	0.00003	0.000769	3.21
975	35	7.7	2481 ± 11.9	0.5	26.23	0.000019	0.000805	1.86
1000	52.4	11.6	2591.6 ± 10	0.4	24.58	0.000015	0.000743	1.73
1025	35.5	7.8	2609 ± 11.2	0.4	23.59	0.000014	0.000733	1.66
1050	12.3	2.7	2417.2 ± 22.3	0.7	23.48	0.000025	0.000843	1.67
1075	9.3	2	2574.6 ± 30.1	0.7	27.46	0.000027	0.00075	1.94
1100	12.6	2.8	2608.2 ± 19.8	0.6	32.36	0.000022	0.000733	2.28
1125	19.2	4.2	2684.2 ± 18	0.5	33.99	0.000021	0.000694	2.39
1150	14.5	3.2	2709.3 ± 19.1	0.6	32.02	0.000022	0.000681	2.24
1175	26.6	5.8	2703 ± 11.7	0.4	28.24	0.000016	0.000685	1.98
1200	17.7	3.9	2698.4 ± 17.8	0.5	28.71	0.000021	0.000687	2.01
1250	16.5	3.6	2703 ± 18.4	0.7	29.06	0.000026	0.000683	2.04
1300	21.6	4.8	2675.3 ± 14.7	0.7	29.16	0.000026	0.000697	2.05
1350	15.8	3.5	2671.2 ± 20.2	1.1	28.87	0.000039	0.000696	2.03
1450	8.5	1.8	2623.5 ± 32.5	3.7	27.2	0.000128	0.000702	1.91

MEAN AGE(1125°C-1450°C)= 2687.9 ± 18.7 Ma (2σ UNCERTAINTY,INCLUDING ERROR IN J)

J = .002394 ± .000024 (1 %)

37/39,36/40 AND 39/40 Ar RATIOS ARE CORRECTED FOR MASS SPECTROMETER DISCRIMINATION,INTERFERING ISOTOPES AND SYSTEM BLANKS

% IIC - INTERFERING ISOTOPES CORRECTION

15-51B HORNBLENDE ARGON SUMMARY

T°C	mV 39	39%	AGE (Ma)±1σ	% ATM	37/39	36/40	39/40	% IIC
650	1.7	0.3	2097.9 ± 256	56.5	52.46	0.001915	0.000472	3.84
750	15.1	3	1817.9 ± 16.1	7.6	93.55	0.00026	0.001263	7.04
850	15	3	2181.1 ± 16.2	1.4	24.98	0.00005	0.000996	1.81
950	110.5	22.5	2614.2 ± 12.9	0.2	18.72	0.000009	0.000727	1.32
975	85.9	17.5	2653.4 ± 13.9	0.1	13.06	0.000005	0.000707	0.91
1000	44.8	9.1	2647.6 ± 10.7	0.1	13.72	0.000006	0.00071	0.96
1025	25.7	5.2	2666.1 ± 13.4	0.2	14.79	0.000008	0.0007	1.04
1050	39.4	8	2666.1 ± 11.7	0.1	15.3	0.000006	0.0007	1.07
1075	41	8.3	2665.5 ± 11.7	0.2	17.75	0.000008	0.0007	1.24
1100	39.9	8.1	2666.2 ± 10.7	0.1	17.42	0.000006	0.0007	1.22
1125	14.7	3	2674.4 ± 20.7	0.2	16.12	0.000008	0.000696	1.13
1150	6.9	1.4	2600.9 ± 32.3	0.3	16.8	0.000013	0.000733	1.18
1175	5	1	2733.5 ± 47.2	0.3	16.74	0.000013	0.000667	1.17
1200	5.1	1	2709.8 ± 47.4	0.3	16.45	0.000015	0.000678	1.15
1250	6.1	1.2	2783.9 ± 38.8	0.5	16.47	0.000021	0.000642	1.15
1300	8.2	1.6	2656.2 ± 27.5	0.9	17.39	0.000032	0.0007	1.22
1350	20.7	4.2	2677.9 ± 17.7	0.6	16.76	0.000024	0.000691	1.17
1450	3.9	0.8	3216.9 ± 57.8	6.1	16.16	0.000209	0.00045	1.11

MEAN AGE(975°C-1350°C)= 2663.9 ± 17.1 Ma (2σ UNCERTAINTY,INCLUDING ERROR IN J)

J = .002377 ± .0000238 (1 %)

37/39,36/40 AND 39/40 Ar RATIOS ARE CORRECTED FOR MASS SPECTROMETER DISCRIMINATION,INTERFERING ISOTOPES AND SYSTEM BLANKS

% IIC - INTERFERING ISOTOPES CORRECTION

15-51A HORNBLENDE ARGON SUMMARY

T°C	mV 39	39%	AGE (Ma)±1σ	% ATM	37/39	36/40	39/40	% IIC
650	30.2	3.5	2479.5 ± 13.9	13.6	2.15	0.000461	0.000701	0.15
750	56	6.5	2690.1 ± 11.1	6.5	2.12	0.00022	0.000651	0.14
850	106.8	12.5	2393.8 ± 12.1	1.4	1.15	0.000049	0.000853	0.08
950	104	12.2	2464.3 ± 11.9	1.2	5.35	0.000041	0.000811	0.38
975	41.3	4.8	2570.2 ± 11.1	1.2	16.36	0.000041	0.00075	1.15
1000	49.4	5.8	2625.9 ± 11.7	0.9	22.73	0.000031	0.000722	1.6
1025	55	6.4	2632 ± 10.4	0.7	19.89	0.000024	0.000721	1.4
1050	46.4	5.4	2666.3 ± 11.1	0.6	14.09	0.000021	0.000704	0.99
1075	26.2	3	2634.8 ± 14.2	0.7	14.08	0.000024	0.000719	0.99
1100	19.8	2.3	2684.5 ± 18.8	0.7	13.63	0.000024	0.000694	0.95
1125	24.7	2.9	2709.7 ± 12.9	0.7	12.08	0.000025	0.000681	0.84
1150	58.4	6.8	2716.5 ± 10.9	0.8	9.73	0.000028	0.000678	0.68
1175	56.9	6.6	2716.7 ± 10.5	0.8	9.69	0.000029	0.000677	0.68
1200	43.4	5.1	2720.3 ± 12.3	0.8	9.66	0.000028	0.000676	0.67
1250	91	10.6	2704.2 ± 16.9	0.8	8.88	0.000027	0.000684	0.62
1300	21.9	2.5	2716.8 ± 16.8	1	11.8	0.000036	0.000676	0.82
1350	9	1	2691.6 ± 30.1	2.5	10.13	0.000085	0.000678	0.71
1450	10.3	1.2	2698.3 ± 33.6	4.5	10.61	0.000154	0.000661	0.74

MEAN AGE(1150°C-1450°C)= 2711.9 ± 19.3 Ma (2σ UNCERTAINTY,INCLUDING ERROR IN J)

J = .002399 ± .000024 (1 %)

37/39,36/40 AND 39/40 Ar RATIOS ARE CORRECTED FOR MASS SPECTROMETER DISCRIMINATION,INTERFERING ISOTOPES AND SYSTEM BLANKS

% IIC - INTERFERING ISOTOPES CORRECTION

90N014A HORNBLENDE ARGON SUMMARY

T°C	mV 39	39%	AGE (Ma)±1σ	% ATM	37/39	36/40	39/40	% IIC
650	28.6	7.3	958.9 ± 12.1	13	7.93	0.00044	0.00295	0.71
750	20.7	5.3	1339.8 ± 13.5	7.5	16.37	0.000255	0.001997	1.33
850	19.9	5.1	1816.2 ± 13.9	2.1	7.78	0.000072	0.001341	0.58
950	67.7	17.3	2547.7 ± 9.1	0.4	15.21	0.000016	0.000762	1.07
975	30.9	7.9	2468.1 ± 12.4	0.3	14.62	0.000012	0.000809	1.04
1000	18.7	4.8	2374.6 ± 15.4	0.4	15.38	0.000016	0.000867	1.1
1025	18.5	4.7	2522.4 ± 18.2	0.4	16.16	0.000015	0.000777	1.14
1050	25.5	6.5	2550.9 ± 13.7	0.3	17.24	0.000013	0.000761	1.22
1075	31	7.9	2622.9 ± 12.7	0.3	18.37	0.000013	0.000722	1.29
1100	38.3	9.8	2651.5 ± 11.9	0.3	18.59	0.000012	0.000708	1.3
1125	40.2	10.3	2657 ± 11.7	0.2	17.55	0.000009	0.000705	1.23
1150	11.9	3	2558.9 ± 22.7	0.5	16.03	0.000019	0.000755	1.13
1175	8.4	2.1	2700.7 ± 32.8	0.6	14.62	0.000024	0.000681	1.02
1200	6.5	1.6	2594.1 ± 64.5	0.8	13.82	0.000029	0.000734	0.97
1250	3.3	0.8	2415.7 ± 70.4	1.7	11.55	0.000059	0.00083	0.82
1300	4.5	1.1	2563.3 ± 59.7	1.6	13.79	0.000055	0.000745	0.97
1350	9.3	2.4	2705.9 ± 26.4	1.1	16.49	0.000039	0.000675	1.15
1450	4.5	1.1	2483.2 ± 52.7	5.9	14.9	0.000203	0.000755	1.06

MEAN AGE(1100°C-1125°C)= 2654.3 ± 21.7 Ma (2σ UNCERTAINTY,INCLUDING ERROR IN J)

J = .00238 ± .0000238 (1 %)

37/39,36/40 AND 39/40 Ar RATIOS ARE CORRECTED FOR MASS SPECTROMETER DISCRIMINATION,INTERFERING ISOTOPES AND SYSTEM BLANKS

% IIC - INTERFERING ISOTOPES CORRECTION

90N014B HORNBLENDE ARGON SUMMARY

T°C	mV 39	39%	AGE (Ma)±1σ	% ATM	37/39	36/40	39/40	% IIC
650	32.8	3.5	3157.4 ± 13.6	5.7	13.28	0.000194	0.000468	0.91
750	47.5	5.2	2236.5 ± 8.2	2.9	10.37	0.000098	0.000934	0.75
850	57.3	6.2	2039.3 ± 7.2	1.1	4.45	0.00004	0.001113	0.32
950	130.5	14.2	2596 ± 9.9	0.6	9.53	0.000021	0.000729	0.67
975	81.8	8.9	2507.8 ± 7.8	0.3	11.14	0.000013	0.00078	0.79
1000	71.7	7.8	2509.9 ± 8.3	0.2	11.85	0.00001	0.000779	0.84
1025	34.7	3.8	2363.7 ± 9.4	0.3	9.83	0.000011	0.000869	0.7
1050	33.6	3.6	2335.6 ± 9.6	0.4	9.35	0.000014	0.000887	0.67
1075	54.8	6	2499.2 ± 8.2	0.3	11.11	0.000013	0.000785	0.78
1100	133.1	14.5	2644 ± 11	0.3	12.78	0.000011	0.000706	0.9
1125	163.9	17.9	2684.9 ± 11.4	0.2	13.98	0.00001	0.000686	0.98
1150	33.1	3.6	2729.4 ± 10.9	0.4	14.29	0.000014	0.000664	1
1175	8.3	0.9	2686 ± 28.3	1	13.35	0.000034	0.000681	0.93
1200	5.9	0.6	2648.9 ± 33.3	1.5	13.14	0.000054	0.000695	0.92
1250	10.2	1.1	2660.6 ± 19.8	1.4	13.65	0.000049	0.00069	0.96
1300	4.6	0.5	2643.4 ± 42.2	4.3	12.01	0.000146	0.000679	0.84
1350	4.1	0.4	2632.1 ± 45.4	7.5	11.49	0.000255	0.000661	0.8
1450	4	0.4	2564.4 ± 49.6	15.8	10.92	0.000537	0.000632	0.77

MEAN AGE(1125°C)= 2684.9 ± 26.8 Ma (2σ UNCERTAINTY,INCLUDING ERROR IN J)

J = .002363 ± .0000236 (.9 %)

37/39,36/40 AND 39/40 Ar RATIOS ARE CORRECTED FOR MASS SPECTROMETER DISCRIMINATION,INTERFERING ISOTOPES AND SYSTEM BLANKS

% IIC - INTERFERING ISOTOPES CORRECTION

APPENDIX D

Microprobe Analysis

Table D.1 - Amphibole compositions used for thermochronology, classification, and thermobarometry. Formulae calculated on the basis of 23 oxygens, averaging the results (after site distribution) of both the 15-NK and 13-CNK methods.

Sample	01N030d	01N030d	01N030d	01N030d	01N030d	01N030d
Analysis	30d-1	30d-2	30d-3	30d-4	30d-5	30d-6
Location	core	rim	core	rim	core	rim
Mineral	amp	amp	amp	amp	amp	amp
SiO2	44.13	42.93	42.63	42.81	43.01	43.01
TiO2	0.64	0.62	0.47	0.33	0.56	0.58
Al2O3	11.5	13.45	13.63	13.6	13.35	13.01
FeO	13.89	14.28	14.49	14.53	14.83	15.03
Cr2O3	0.14	0.11	0.22	0.09	0.14	0.12
MnO	0.35	0.27	0.29	0.21	0.28	0.25
MgO	11.48	10.88	10.61	10.47	10.76	10.93
CaO	11.41	11.75	11.65	11.95	11.82	11.61
Na2O	1.47	1.77	1.63	1.74	1.61	1.54
K2O	0.28	0.4	0.29	0.36	0.34	0.33
Total	95.16	96.35	95.69	96	96.58	96.29
TSi	6.612	6.391	6.372	6.41	6.385	6.393
TAl	1.388	1.609	1.628	1.59	1.615	1.607
TFe3	0	0	0	0	0	0
CAl	0.641	0.75	0.771	0.808	0.719	0.67
CCr	0.017	0.013	0.026	0.011	0.016	0.014
CFe3	0.285	0.255	0.34	0.212	0.354	0.448
CTi	0.072	0.069	0.053	0.037	0.063	0.065
CMg	2.564	2.415	2.364	2.337	2.381	2.422
CFe2	1.399	1.482	1.427	1.582	1.449	1.365
CMn	0.022	0.017	0.018	0.013	0.018	0.016
BFe2	0.056	0.042	0.044	0.025	0.038	0.055
BMn	0.022	0.017	0.018	0.013	0.018	0.016
BCa	1.832	1.874	1.866	1.917	1.88	1.849
BNa	0.09	0.067	0.072	0.044	0.064	0.081
ANa	0.337	0.444	0.401	0.461	0.399	0.363
AK	0.054	0.076	0.055	0.069	0.064	0.063
Sum_cat	15.391	15.52	15.456	15.53	15.464	15.426

Sample	90n007c	90n007c	90n007c	90n007c	90n007c	90n007c	90n007c
Analysis	1	7c	7r	8	9	2c	2r
Location		core	rim			core	rim
Mineral	amp	amp	amp	amp	amp	amp	amp
SiO2	44.74	46.29	45.39	44.69	44.96	43.69	53.39
TiO2	0.8	0.94	0.87	0.8	0.48	0.66	0.1
Al2O3	11.89	9.51	11.47	11.75	12.12	11.8	4.02
FeO	13.91	15.56	13.47	14.87	14.45	13.52	10.66
Cr2O3	0	0	0	0.05	0.08	0.13	0.26
MnO	0.19	0.37	0.17	0.22	0.3	0.29	0.05
MgO	12.27	13.72	12.48	12.53	12.26	12.01	16.67
CaO	11.02	9.61	11.36	10.68	11.01	10.53	12.98
Na2O	1.87	1.4	1.7	1.77	1.7	1.85	0.49
K2O	0.25	0.2	0.25	0.25	0.26	0.27	0.1
Total	96.97	97.65	97.16	97.58	97.57	94.62	98.46
TSi	6.566	6.666	6.64	6.5	6.541	6.553	7.537
TAl	1.434	1.334	1.36	1.5	1.459	1.447	0.463
TFe3	0	0	0	0	0	0	0
CAl	0.621	0.279	0.616	0.512	0.617	0.637	0.205
CCr	0	0	0	0.006	0.009	0.015	0.029
CFe3	0.388	0.969	0.308	0.618	0.501	0.442	0.095
CTi	0.088	0.102	0.096	0.088	0.053	0.074	0.011
CMg	2.685	2.945	2.722	2.717	2.659	2.685	3.508
CFe2	1.206	0.683	1.248	1.047	1.143	1.127	1.149
CMn	0.012	0.022	0.01	0.013	0.018	0.018	0.003
BFe2	0.113	0.222	0.092	0.144	0.115	0.126	0.014
BMn	0.012	0.023	0.011	0.014	0.019	0.019	0.003
BCa	1.733	1.483	1.781	1.664	1.716	1.692	1.963
BNa	0.142	0.192	0.117	0.178	0.151	0.163	0.02
ANa	0.39	0.199	0.366	0.321	0.329	0.375	0.114
AK	0.047	0.037	0.047	0.046	0.048	0.052	0.018
Sum_cat	15.437	15.155	15.412	15.368	15.377	15.426	15.132

Sample	90n007c	90n007c	90n007c
Analysis	3r	c	r
Location	rim	core	rim
Mineral	amp	amp	amp
SiO2	45.54	46.81	45.53
TiO2	0.64	0.62	0.77
Al2O3	11.5	9.38	11.76
FeO	14.73	16.1	14.26
Cr2O3	0.19	0.12	0.42
MnO	0.23	0.39	0.17
MgO	12.62	14.08	12.56
CaO	10.81	9.32	11.15
Na2O	1.77	1.26	1.79
K2O	0.29	0.2	0.22
Total	98.13	98.16	98.21
TSi	6.58	6.667	6.563
TAl	1.42	1.333	1.437
TFe3	0	0	0
CAl	0.536	0.24	0.56
CCr	0.022	0.013	0.048
CFe3	0.526	1.061	0.434
CTi	0.07	0.066	0.083
CMg	2.718	2.989	2.699
CFe2	1.115	0.607	1.165
CMn	0.014	0.023	0.01
BFe2	0.139	0.25	0.12
BMn	0.014	0.024	0.01
BCa	1.673	1.422	1.722
BNa	0.173	0.17	0.147
ANa	0.323	0.178	0.353
AK	0.053	0.036	0.04
Sum_cat	15.376	15.081	15.393

Sample	90n013a	90N013a	90N013a	90N013a	90N013a	90N013a	90N013a
Analysis	1	13a1	13a11	13a16	13a2	13a20	13a21
Location	matrix	rim		matrix	core	matrix	matrix
Mineral	amp	amp	amp	amp	amp	amp	amp
SiO2	42.42	42.67	42.42	50.25	50.93	43.01	47.81
TiO2	0.42	0.39	0.38	0.29	0.21	0.42	0.31
Al2O3	16.06	15.5	15.67	13.01	4.95	14.72	8.76
FeO	15.29	15.64	15.85	13.85	12.04	15.63	13.68
Cr2O3	0.12	0	0.04	0.12	0.31	0	0
MnO	0.16	0.24	0.27	0.29	0.12	0.35	0.24
MgO	9.12	9.12	8.97	8.68	15.36	9.43	12.54
CaO	11.98	12	11.83	10.41	12.39	11.94	12.65
Na2O	1.72	1.75	1.66	1.58	0.72	1.24	0.84
K2O	0.3	0.19	0.25	0.2	0.12	0.14	0.17
Total	97.47	97.5	97.31	98.56	96.84	96.88	97.04
TSi	6.271	6.318	6.29	7.305	7.359	6.371	7.01
TAl	1.729	1.682	1.71	0.695	0.641	1.629	0.99
TFe3	0	0	0	0	0	0	0
CAl	1.067	1.021	1.027	1.532	0.202	0.939	0.523
CCr	0.014	0	0.005	0.014	0.035	0	0
CFe3	0.141	0.148	0.198	0	0.222	0.325	0.141
CTi	0.047	0.043	0.042	0.032	0.023	0.047	0.034
CMg	2.01	2.013	1.983	1.881	3.309	2.083	2.741
CFe2	1.711	1.759	1.729	1.524	1.202	1.584	1.537
CMn	0.01	0.015	0.017	0.018	0.007	0.022	0.024
BFe2	0.038	0.03	0.039	0.16	0.031	0.027	0
BMn	0.01	0.015	0.017	0.018	0.007	0.022	0.006
BCa	1.897	1.904	1.88	1.621	1.918	1.895	1.987
BNa	0.055	0.051	0.064	0.2	0.044	0.056	0.007
ANa	0.438	0.451	0.413	0.245	0.158	0.3	0.232
AK	0.057	0.036	0.047	0.037	0.022	0.026	0.032
Sum_cat	15.495	15.487	15.46	15.282	15.18	15.327	15.264

Sample	90N013a	90N013a	90N013a	90N013a	90N013a	90N013a	90N013a
Analysis	13a24	13a26	13a3	13a30	13a31	13a33	13a34
Location			rim	matrix	matrix	matrix	core
Mineral	amp	amp	amp	amp	amp	amp	amp
SiO2	42.02	47.15	45.05	42	42.25	42.19	49.65
TiO2	0.44	0.22	0.31	0.45	0.32	0.39	0.26
Al2O3	16.27	10.24	13	15.45	15.72	15.5	6.1
FeO	15.32	14.31	14.88	14.87	14.77	15.45	12.62
Cr2O3	0.02	0.22	0	0.02	0.08	0.11	0.31
MnO	0.3	0.16	0.24	0.28	0.33	0.32	0.32
MgO	8.85	12.27	10.81	9.25	9.02	9.02	14.42
CaO	11.91	12.52	12.09	12	11.88	12.04	12.54
Na2O	1.76	1.27	1.53	1.53	1.58	1.7	1.02
K2O	0.27	0.15	0.15	0.32	0.28	0.25	0.14
Total	97.14	98.29	98.06	96.16	96.17	96.86	97.1
TSi	6.246	6.829	6.58	6.292	6.324	6.288	7.216
TAl	1.754	1.171	1.42	1.708	1.676	1.712	0.784
TFe3	0	0	0	0	0	0	0
CAl	1.094	0.575	0.816	1.017	1.095	1.009	0.26
CCr	0.002	0.025	0	0.002	0.009	0.013	0.036
CFe3	0.141	0.2	0.191	0.161	0.122	0.146	0.168
CTi	0.049	0.024	0.034	0.051	0.036	0.044	0.028
CMg	1.961	2.649	2.354	2.066	2.013	2.004	3.124
CFe2	1.734	1.517	1.591	1.685	1.704	1.764	1.363
CMn	0.019	0.01	0.015	0.018	0.021	0.02	0.02
BFe2	0.029	0.017	0.036	0.017	0.023	0.016	0.002
BMn	0.019	0.01	0.015	0.018	0.021	0.02	0.02
BCa	1.897	1.943	1.892	1.926	1.905	1.923	1.953
BNa	0.055	0.031	0.058	0.04	0.051	0.041	0.025
ANa	0.452	0.326	0.376	0.405	0.408	0.45	0.262
AK	0.051	0.028	0.028	0.061	0.053	0.048	0.026
Sum_cat	15.503	15.354	15.404	15.466	15.461	15.498	15.288

Sample	90N013a	90N013a	90N013a	90N013a	90N013a	90N013a	90N013a
Analysis	13a35	13a4	13a5	2d	2dd	2l	2ll
Location	rim	core	rim	p/c	p/c	p/c	rim
Mineral	amp	amp	amp	amp	amp	amp	amp
SiO2	42.97	51.97	42.74	51.7	53.69	47.69	44.22
TiO2	0.25	0.15	0.29	0.25	0.24	0.14	0.38
Al2O3	15.25	4.81	15.22	5.45	3.49	3.54	14.4
FeO	15.68	12.35	15.11	12.3	11.6	8.13	15.67
Cr2O3	0	0.34	0.12	0.27	0.13	0.14	0.04
MnO	0.25	0.17	0.26	0.31	0.33	0.17	0.23
MgO	9.51	15.54	9.51	14.94	16.4	15.5	9.83
CaO	12.16	12.68	11.74	12.37	12.61	10.2	12.03
Na2O	1.6	0.68	1.71	0.88	0.5	0.54	1.55
K2O	0.18	0.23	0.19	0.14	0.08	0.09	0.17
Total	97.85	98.6	96.77	98.49	98.95	86	98.49
TSi	6.322	7.389	6.343	7.386	7.57	7.618	6.454
TAl	1.678	0.611	1.657	0.614	0.43	0.382	1.546
TFe3	0	0	0	0	0	0	0
CAl	0.965	0.195	1.003	0.303	0.15	0.284	0.929
CCr	0	0.038	0.014	0.03	0.014	0.018	0.005
CFe3	0.256	0.19	0.203	0.123	0.165	0.274	0.19
CTi	0.028	0.016	0.032	0.027	0.025	0.017	0.042
CMg	2.086	3.294	2.104	3.182	3.447	3.691	2.139
CFe2	1.65	1.257	1.627	1.316	1.178	0.705	1.682
CMn	0.016	0.01	0.016	0.019	0.02	0.011	0.014
BFe2	0.023	0.022	0.046	0.031	0.024	0.108	0.041
BMn	0.016	0.01	0.016	0.019	0.02	0.012	0.014
BCa	1.917	1.932	1.867	1.894	1.905	1.746	1.881
BNa	0.044	0.037	0.071	0.057	0.051	0.083	0.063
ANa	0.412	0.151	0.421	0.187	0.086	0.084	0.375
AK	0.034	0.042	0.036	0.026	0.014	0.018	0.032
Sum_cat	15.446	15.193	15.457	15.212	15.1	15.051	15.407

Sample	90N013a	90N013a	90N013a	90N013a	90N013a	90N013a	90N013a
Analysis	3d	3l	4d	4l	5d	5l	6d
Location	core	light	dark	light			dark
Mineral	amp	amp	amp	amp	amp	amp	amp
SiO2	53.32	42.99	52.16	43	52.97	44.52	49.85
TiO2	0.13	0.29	0.23	0.4	0.21	0.33	0.46
Al2O3	3.85	15.6	4.79	15.45	4.04	13.93	7.3
FeO	11.51	15.78	12.76	15.81	11.88	15	12.78
Cr2O3	0.09	0	0.14	0.06	0.22	0.17	0.33
MnO	0.25	0.32	0.12	0.26	0.3	0.27	0.36
MgO	16.17	9.06	15.18	9.17	16.13	10.06	14.02
CaO	12.87	11.96	13.03	11.94	12.76	12.02	12.64
Na2O	0.55	1.68	0.42	1.63	0.71	1.52	0.93
K2O	0.09	0.21	0.08	0.1	0.02	0.11	0.06
Total	98.74	97.91	98.77	97.79	99.02	97.8	98.42
TSi	7.55	6.336	7.416	6.332	7.48	6.524	7.141
TAl	0.45	1.664	0.584	1.668	0.52	1.476	0.859
TFe3	0	0	0	0	0	0	0
CAl	0.192	1.044	0.218	1.011	0.151	0.927	0.372
CCr	0.01	0	0.016	0.007	0.025	0.02	0.037
CFe3	0.104	0.168	0.188	0.202	0.176	0.155	0.145
CTi	0.014	0.032	0.025	0.044	0.022	0.036	0.05
CMg	3.413	1.991	3.217	2.013	3.395	2.198	2.994
CFe2	1.252	1.745	1.33	1.707	1.212	1.647	1.38
CMn	0.015	0.02	0.007	0.016	0.018	0.017	0.022
BFe2	0.007	0.032	0	0.038	0.014	0.036	0.006
BMn	0.015	0.02	0.007	0.016	0.018	0.017	0.022
BCa	1.953	1.889	1.985	1.884	1.93	1.887	1.94
BNa	0.025	0.059	0.008	0.062	0.037	0.06	0.032
ANa	0.126	0.421	0.108	0.403	0.157	0.372	0.226
AK	0.016	0.039	0.015	0.019	0.004	0.021	0.011
Sum_cat	15.142	15.46	15.122	15.422	15.161	15.392	15.237

Sample	90N013a	90N013a	90N013a	90N013a	90N013a	90N013a	90N013a
Analysis	6dd	6l	6ll	m1	m3	m5c	m5d
Location	dark	light	light	matrix	matrix	core	core
Mineral	amp	amp	amp	amp	amp	amp	amp
SiO2	50.69	43.04	42.86	42.64	41.88	43.82	53.23
TiO2	0.22	0.27	0.37	0.3	0.42	0.33	0.04
Al2O3	6.58	16.29	15.83	16.21	17.6	14.81	3.93
FeO	12.86	15.64	15.63	15.98	15.3	15.94	12.79
Cr2O3	0.14	0.03	0.02	0.01	0.02	0	0.05
MnO	0.3	0.3	0.18	0.24	0.2	0.31	0.31
MgO	14.72	9.12	9.34	8.85	8.24	9.67	15.68
CaO	12.64	11.81	11.99	12.12	12.17	11.9	13.09
Na2O	0.87	1.51	1.72	1.39	1.47	1.38	0.52
K2O	0.16	0.2	0.24	0.21	0.26	0.15	0.1
Total	99.06	98.23	98.16	97.95	97.54	98.33	99.69
TSi	7.208	6.294	6.29	6.268	6.19	6.395	7.506
TAl	0.792	1.706	1.71	1.732	1.81	1.605	0.494
TFe3	0	0	0	0	0	0	0
CAl	0.31	1.099	1.026	1.074	1.253	0.941	0.159
CCr	0.016	0.003	0.002	0.001	0.002	0	0.006
CFe3	0.23	0.242	0.188	0.252	0.094	0.321	0.184
CTi	0.024	0.03	0.041	0.033	0.047	0.036	0.004
CMg	3.12	1.988	2.043	1.939	1.816	2.104	3.296
CFe2	1.282	1.62	1.688	1.685	1.776	1.579	1.324
CMn	0.018	0.018	0.011	0.015	0.012	0.019	0.027
BFe2	0.016	0.051	0.042	0.027	0.021	0.046	0
BMn	0.018	0.019	0.011	0.015	0.013	0.019	0.01
BCa	1.926	1.85	1.885	1.909	1.927	1.861	1.978
BNa	0.04	0.08	0.061	0.049	0.039	0.074	0.012
ANa	0.2	0.348	0.428	0.348	0.382	0.316	0.13
AK	0.029	0.037	0.045	0.039	0.049	0.028	0.018
Sum_cat	15.229	15.386	15.473	15.387	15.431	15.344	15.148

Sample	90N015d	90N015d	90N015d	90N015d	90N015d	90N015d
Analysis	15d11	15d14	15d15	15d2	15d3	15d6
Location	matrix	matrix	matrix	core	rim	matrix
Mineral	amp	amp	amp	amp	amp	amp
SiO2	51.35	44.69	31.74	52.19	44.07	44.6
TiO2	0	0.51	0.21	0.15	0.36	0.38
Al2O3	5.05	13.4	9.77	3.65	14.11	13.41
FeO	11.47	13.57	5.1	10.7	14.3	13.81
Cr2O3	0.01	0	0	0.31	0	0.05
MnO	0.18	0.3	0.12	0.2	0.34	0.35
MgO	15.48	11.27	8.14	16.64	10.71	10.97
CaO	13.07	12.16	6.8	12.67	12.35	12.14
Na2O	0.51	1.35	1.05	0.54	1.37	1.17
K2O	0.11	0.23	0.17	0.09	0.3	0.3
Total	97.22	97.48	63.1	96.86	97.91	97.14
TSi	7.402	6.531	6.987	7.489	6.44	6.542
TAl	0.598	1.469	1.013	0.511	1.56	1.458
TFe3	0	0	0	0	0	0
CAl	0.259	0.838	1.52	0.105	0.868	0.859
CCr	0.001	0	0	0.035	0	0.006
CFe3	0.155	0.196	0.004	0.228	0.239	0.219
CTi	0	0.056	0.035	0.016	0.04	0.042
CMg	3.326	2.455	2.671	3.559	2.333	2.399
CFe2	1.227	1.436	0.76	1.044	1.499	1.454
CMn	0.022	0.019	0.011	0.012	0.021	0.022
BFe2	0	0.026	0.175	0.012	0.01	0.021
BMn	0	0.019	0.011	0.012	0.021	0.022
BCa	2	1.904	1.604	1.948	1.934	1.908
BNa	0	0.051	0.209	0.028	0.035	0.049
ANa	0.143	0.331	0.239	0.122	0.353	0.284
AK	0.02	0.043	0.048	0.016	0.056	0.056
Sum_cat	15.173	15.374	15.286	15.139	15.409	15.34

Sample	90N015c	90N015c	90N015c	90N015c	90N015c	90N015c	90N015c
Analysis	15c1	15c10	15c12	15c13	15c14	15c18	15c2
Location	core	matrix	matrix	core	rim	matrix	rim
Mineral	amp	amp	amp	amp	amp	amp	amp
SiO2	52.9	41.91	42.08	51.02	42.87	46.92	42.57
TiO2	0.15	0.41	0.42	0.12	0.3	0.41	0.34
Al2O3	3.83	15.81	15.82	4.44	13.43	9.73	14.62
FeO	11.47	15.67	15.82	12.36	15.76	14.1	15.94
Cr2O3	0.48	0	0	0.15	0.19	0.06	0.05
MnO	0.22	0.4	0.48	0.21	0.15	0.18	0.25
MgO	16.35	8.86	9.17	14.87	9.5	12.17	9.54
CaO	12.87	11.91	11.93	12.85	12.01	12.23	11.9
Na2O	0.64	1.58	1.54	0.57	1.49	1.21	1.59
K2O	0.09	0.33	0.33	0.16	0.27	0.23	0.34
Total	98.52	96.88	97.59	96.6	95.83	97.21	97.09
TSi	7.484	6.249	6.218	7.439	6.455	6.886	6.324
TAl	0.516	1.751	1.782	0.561	1.545	1.114	1.676
TFe3	0	0	0	0	0	0	0
CAl	0.122	1.025	0.97	0.201	0.836	0.568	0.881
CCr	0.054	0	0	0.017	0.023	0.007	0.006
CFe3	0.17	0.218	0.334	0.118	0.198	0.143	0.304
CTi	0.016	0.046	0.047	0.013	0.034	0.045	0.038
CMg	3.448	1.969	2.02	3.232	2.132	2.663	2.113
CFe2	1.177	1.716	1.599	1.389	1.767	1.563	1.643
CMn	0.013	0.025	0.03	0.026	0.01	0.011	0.016
BFe2	0.01	0.02	0.022	0	0.019	0.025	0.034
BMn	0.013	0.025	0.03	0	0.01	0.011	0.016
BCa	1.951	1.903	1.889	2	1.938	1.923	1.894
BNa	0.026	0.052	0.059	0	0.033	0.041	0.057
ANa	0.149	0.405	0.382	0.161	0.402	0.303	0.401
AK	0.016	0.063	0.062	0.03	0.052	0.043	0.064
Sum_cat	15.165	15.468	15.444	15.195	15.453	15.346	15.466

Sample	90N015c	90N015c	90N015c	90N015c	90N015c	90N015c	90N015c
Analysis	15c25	15c26	15c27	15c28	15c3	15c31	15c33
Location	core	core	rim	matrix	rim	matrix	matrix
Mineral	amp	amp	amp	amp	amp	amp	amp
SiO2	42.74	51.19	42.24	41.76	43.25	48.05	42.73
TiO2	0.32	0.13	0.37	0.53	0.42	0.14	0.11
Al2O3	15.63	5.13	14.49	14.62	14.04	7.03	9.64
FeO	15.45	12.18	14.94	15.91	14.75	13.9	15.33
Cr2O3	0	0.11	0.03	0.15	0.04	0	0
MnO	0.42	0.41	0.2	0.28	0.29	0.35	0.3
MgO	9.54	15.21	9.69	8.86	10	12.84	15.75
CaO	12.12	12.57	11.92	11.67	11.94	12.33	9.49
Na2O	1.74	0.7	1.57	1.34	1.53	0.83	0.41
K2O	0.26	0.12	0.32	0.22	0.24	0.13	0.04
Total	98.23	97.67	95.75	95.24	96.46	95.6	93.8
TSi	6.272	7.36	6.351	6.319	6.439	7.148	6.238
TAl	1.728	0.64	1.649	1.681	1.561	0.852	1.637
TFe3	0	0	0	0	0	0	0.125
CAl	0.973	0.229	0.916	0.924	0.9	0.38	0.021
CCr	0	0.012	0.004	0.018	0.005	0	0
CFe3	0.241	0.222	0.212	0.298	0.177	0.214	1.521
CTi	0.035	0.014	0.042	0.06	0.047	0.016	0.012
CMg	2.087	3.26	2.172	1.999	2.219	2.848	3.428
CFe2	1.637	1.238	1.642	1.683	1.634	1.515	0
CMn	0.026	0.025	0.013	0.018	0.018	0.028	0.018
BFe2	0.018	0.005	0.024	0.032	0.026	0	0.225
BMn	0.026	0.025	0.013	0.018	0.018	0.016	0.019
BCa	1.906	1.936	1.92	1.892	1.905	1.965	1.484
BNa	0.05	0.034	0.043	0.058	0.051	0.019	0.057
ANa	0.445	0.161	0.415	0.336	0.391	0.221	0.059
AK	0.049	0.022	0.061	0.042	0.046	0.025	0.007
Sum_cat	15.493	15.183	15.476	15.378	15.436	15.245	14.852

Sample	90N015c	90N015c
Analysis	15c5	15c7
Location	rim	matrix
Mineral	amp	amp
SiO2	43.87	42.48
TiO2	0.12	0.52
Al2O3	9.85	14.4
FeO	18.34	15.83
Cr2O3	0	0.09
MnO	0.32	0.19
MgO	13.1	9.02
CaO	9.23	12
Na2O	0.54	1.56
K2O	0.19	0.33
Total	95.61	96.33
TSi	6.415	6.382
TAl	1.56	1.618
TFe3	0.025	0
CAl	0.136	0.929
CCr	0	0.011
CFe3	1.558	0.116
CTi	0.013	0.059
CMg	2.856	2.02
CFe2	0.418	1.853
CMn	0.019	0.012
BFe2	0.242	0.02
BMn	0.02	0.012
BCa	1.446	1.932
BNa	0.075	0.037
ANa	0.078	0.418
AK	0.035	0.063
Sum_cat	14.897	15.481

Sample	15	15	15	15	15	15	15
Analysis	15-1	15-10	15-12	15-13	15-2	15-3	15-5
Location	core	matrix	matrix	matrix	core	core	rim
Mineral	amp	amp	amp	amp	amp	amp	amp
SiO2	50.6	45.27	43.6	44.61	52.19	52.22	44.04
TiO2	0.23	0.44	0.34	0.36	0.18	0.14	0.28
Al2O3	7.51	13.61	16.02	14.47	5.73	5.21	15.03
FeO	11.67	13.37	14.41	13.95	10.96	10.52	14.63
Cr2O3	0.51	0.07	0.11	0.05	0.4	0.22	0.03
MnO	0.2	0.34	0.24	0.08	0.24	0.23	0.3
MgO	14.91	11.7	9.84	10.87	16.01	16.19	10.12
CaO	12.92	12.26	12.13	12.05	12.75	13.02	12.26
Na2O	0.76	1.34	1.28	1.38	0.58	0.51	1.11
K2O	0.16	0.19	0.23	0.17	0.15	0.06	0.26
Total	98.96	98.52	98.1	97.94	98.79	98.1	98.06
TSi	7.148	6.521	6.341	6.48	7.345	7.404	6.413
TAl	0.852	1.479	1.659	1.52	0.655	0.596	1.587
TFe3	0	0	0	0	0	0	0
CAl	0.397	0.83	1.085	0.955	0.295	0.274	0.991
CCr	0.057	0.008	0.013	0.006	0.044	0.025	0.003
CFe3	0.16	0.251	0.2	0.199	0.175	0.141	0.263
CTi	0.024	0.048	0.037	0.039	0.019	0.015	0.031
CMg	3.14	2.513	2.134	2.354	3.359	3.422	2.197
CFe2	1.21	1.33	1.517	1.442	1.093	1.107	1.497
CMn	0.012	0.021	0.015	0.005	0.014	0.017	0.018
BFe2	0.009	0.029	0.036	0.053	0.022	0	0.022
BMn	0.012	0.021	0.015	0.005	0.014	0.01	0.019
BCa	1.955	1.892	1.89	1.875	1.923	1.978	1.913
BNa	0.024	0.058	0.059	0.067	0.041	0.012	0.047
ANa	0.184	0.317	0.302	0.322	0.117	0.128	0.267
AK	0.029	0.035	0.043	0.032	0.027	0.011	0.048
Sum_cat	15.213	15.352	15.345	15.354	15.144	15.139	15.315

Sample	15	15	15	15	15
Analysis	15-6	15-7	15-8	15-9	3
Location	rim	rim	core	rim	rim
Mineral	amp	amp	amp	amp	amp
SiO2	44.87	44.49	52.24	48.42	43.32
TiO2	0.48	0.47	0.21	0.17	0.88
Al2O3	15.18	14.37	5.81	9.56	15.33
FeO	14.17	13.79	10.53	14.02	13.84
Cr2O3	0	0.09	0.47	0.33	0.01
MnO	0.32	0.28	0.31	0.39	0.3
MgO	10.55	10.83	15.93	12.48	10.31
CaO	12.19	12.34	12.85	12.57	12.04
Na2O	1.33	1.3	0.53	0.93	1.43
K2O	0.29	0.25	0.12	0.25	0.22
Total	99.38	98.12	98.53	98.81	97.67
TSi	6.442	6.462	7.363	6.954	6.336
TAl	1.558	1.538	0.637	1.046	1.664
TFe3	0	0	0	0	0
CAl	1.008	0.921	0.328	0.571	0.977
CCr	0	0.01	0.052	0.037	0.001
CFe3	0.18	0.176	0.11	0.166	0.176
CTi	0.052	0.051	0.022	0.018	0.097
CMg	2.258	2.345	3.347	2.672	2.248
CFe2	1.482	1.479	1.123	1.511	1.483
CMn	0.019	0.017	0.018	0.024	0.019
BFe2	0.039	0.02	0.009	0.007	0.034
BMn	0.02	0.017	0.019	0.024	0.019
BCa	1.875	1.92	1.941	1.934	1.887
BNa	0.067	0.042	0.032	0.035	0.06
ANa	0.304	0.324	0.113	0.224	0.345
AK	0.053	0.046	0.022	0.046	0.041
Sum_cat	15.357	15.37	15.135	15.27	15.386

Sample	15-51b	15-51b	15-51b	15-51b	15-51b	15-51b	15-51b
Analysis	51b-10	51b-11	51b-12	51b-19	51b-7	51b-8	51b-9
Location	core	rim	rim			core	rim
Mineral	amp	amp	amp	amp	amp	amp	amp
SiO2	52.41	42.33	42.24	46.06	40.73	53.97	43.04
TiO2	0.19	0.35	0.55	0.28	0.33	0.04	0.38
Al2O3	4.31	13.57	13.69	9.77	12.84	1.95	13.04
FeO	13.27	16.68	16.62	15.46	18.65	11.8	16.16
Cr2O3	0.12	0	0.09	0.1	0.16	0.07	0.14
MnO	0.11	0.23	0.16	0.24	0.14	0.17	0.23
MgO	15.55	9.21	8.98	11.08	10.92	16.77	9.39
CaO	12.6	11.7	11.84	12.51	9.46	12.66	11.86
Na2O	0.52	1.76	1.59	1.13	1.2	0.36	1.58
K2O	0.11	0.41	0.48	0.3	0.25	0.04	0.39
Total	99.07	96.24	96.22	96.83	94.52	97.76	96.07
TSi	7.421	6.39	6.384	6.845	6.107	7.697	6.488
TAl	0.579	1.61	1.616	1.155	1.893	0.303	1.512
TFe3	0	0	0	0	0	0	0
CAl	0.14	0.803	0.821	0.555	0.374	0.025	0.803
CCr	0.013	0	0.011	0.012	0.019	0.008	0.017
CFe3	0.316	0.249	0.189	0.153	1.535	0.225	0.16
CTi	0.02	0.04	0.063	0.031	0.037	0.004	0.043
CMg	3.283	2.073	2.023	2.455	2.441	3.566	2.11
CFe2	1.221	1.822	1.883	1.769	0.585	1.163	1.853
CMn	0.007	0.015	0.01	0.026	0.009	0.01	0.015
BFe2	0.035	0.035	0.028	0	0.218	0.02	0.025
BMn	0.007	0.015	0.01	0.004	0.009	0.01	0.015
BCa	1.912	1.892	1.917	1.992	1.52	1.935	1.916
BNa	0.047	0.057	0.044	0.004	0.171	0.035	0.045
ANa	0.096	0.458	0.422	0.321	0.177	0.065	0.417
AK	0.02	0.079	0.093	0.057	0.048	0.007	0.075
Sum_cat	15.115	15.537	15.514	15.378	15.143	15.072	15.492

Sample	15-51a	15-51a	15-51a	15-51a	15-51a	15-51a	15-51a
Analysis	51a-1	51a-11	51a-12	51a-13	51a-14	51a-3	51a-4
Location	core	rim	core	core	rim	core	rim
Mineral	amp	amp	amp	amp	amp	amp	amp
SiO2	52.58	43.89	53.63	53.15	41.98	55.72	43.91
TiO2	0.2	0.76	0.09	0.13	0.5	0.11	1.48
Al2O3	5.24	13.43	3.05	4.2	16.08	1.86	12.46
FeO	8.22	11.53	7.96	7.28	11.68	6.68	10.33
Cr2O3	0.15	0.12	0.62	0.15	0.15	0.4	0.03
MnO	0.27	0.14	0.15	0.06	0.26	0.18	0.28
MgO	18.22	13.28	18.73	18.86	11.5	20.35	14.22
CaO	12.61	12	13.03	12.96	11.67	13.03	12.01
Na2O	0.85	1.66	0.47	0.6	1.84	0.22	1.68
K2O	0.1	0.68	0.11	0.05	1.09	0.08	0.84
Total	98.31	97.4	97.26	97.29	96.61	98.23	97.21
TSi	7.356	6.375	7.548	7.477	6.198	7.694	6.386
TAl	0.644	1.625	0.452	0.523	1.802	0.294	1.614
TFe3	0	0	0	0	0	0.012	0
CAl	0.22	0.672	0.053	0.173	0.993	0.009	0.52
CCr	0.017	0.014	0.069	0.017	0.017	0.044	0.003
CFe3	0.234	0.321	0.2	0.184	0.183	0.235	0.273
CTi	0.021	0.083	0.01	0.014	0.056	0.011	0.162
CMg	3.8	2.875	3.93	3.955	2.531	4.189	3.083
CFe2	0.693	1.026	0.729	0.655	1.204	0.502	0.94
CMn	0.016	0.009	0.009	0.004	0.016	0.01	0.017
BFe2	0.035	0.053	0.007	0.018	0.056	0.023	0.043
BMn	0.016	0.009	0.009	0.004	0.016	0.011	0.017
BCa	1.89	1.867	1.965	1.953	1.846	1.928	1.872
BNa	0.059	0.071	0.019	0.025	0.082	0.029	0.069
ANa	0.172	0.397	0.109	0.139	0.445	0.03	0.405
AK	0.018	0.126	0.02	0.009	0.205	0.014	0.156
Sum_cat	15.19	15.523	15.129	15.148	15.65	15.034	15.561

Sample	15-51a	15-51a
Analysis	51a-8	51a-9
Location	core	rim
Mineral	amp	amp
SiO2	55.5	42.92
TiO2	0	0.89
Al2O3	2.37	12.85
FeO	6.49	12.41
Cr2O3	0.33	0.05
MnO	0.2	0.12
MgO	20.28	13.88
CaO	13.22	12.35
Na2O	0.42	2.19
K2O	0.1	0.94
Total	98.62	98.56
TSi	7.657	6.222
TAl	0.343	1.778
TFe3	0	0
CAl	0.042	0.416
CCr	0.036	0.006
CFe3	0.184	0.46
CTi	0	0.097
CMg	4.171	3
CFe2	0.555	1.014
CMn	0.012	0.007
BFe2	0.01	0.031
BMn	0.012	0.007
BCa	1.954	1.918
BNa	0.025	0.044
ANa	0.088	0.572
AK	0.018	0.174
Sum_cat	15.105	15.746

Sample	90N014a	90N014a	90N014a	90N014a	90N014a
Analysis	1	14a-2	14a-3	14a-4	14a-8
Location	core	core	core	core	matrix
Mineral	amp	amp	amp	amp	amp
SiO2	38.45	41.13	41.26	41.16	42.07
TiO2	1.08	0.34	0.4	0.22	0.26
Al2O3	15.79	16.59	16.77	16.76	16.03
FeO	20.9	21.15	19.85	20.42	19.55
Cr2O3	0.09	0.03	0.08	0.18	0.07
MnO	0.48	0.41	0.3	0.51	0.53
MgO	5.79	5.18	5.52	5.73	6.09
CaO	9.92	10.84	11.22	10.83	10.58
Na2O	1.31	1.75	1.57	1.72	1.74
K2O	0.34	0.34	0.22	0.26	0.16
Total	94.1	97.73	97.11	97.63	97.02
TSi	5.993	6.221	6.244	6.189	6.347
TAl	2.007	1.779	1.756	1.811	1.653
TFe3	0	0	0	0	0
CAl	0.891	1.176	1.233	1.156	1.194
CCr	0.011	0.004	0.01	0.021	0.008
CFe3	0.752	0.3	0.204	0.36	0.317
CTi	0.127	0.039	0.046	0.025	0.03
CMg	1.345	1.168	1.245	1.284	1.37
CFe2	1.842	2.288	2.244	2.12	2.047
CMn	0.031	0.026	0.019	0.032	0.034
BFe2	0.129	0.088	0.065	0.087	0.102
BMn	0.032	0.026	0.019	0.033	0.034
BCa	1.657	1.757	1.819	1.745	1.71
BNa	0.182	0.129	0.096	0.136	0.154
ANa	0.214	0.384	0.365	0.366	0.355
AK	0.068	0.066	0.042	0.05	0.031
Sum_cat	15.282	15.45	15.407	15.416	15.386

Sample	90N014b	90N014b	90N014b	90N014b
Analysis	14b-1	14b-3	14b-4	14b-6
Location	core	core	core	rim
Mineral	amp	amp	amp	amp
SiO2	41.34	51.71	45.13	43.08
TiO2	0.31	1.2	0.56	0.72
Al2O3	17.67	12.24	12.2	15.2
FeO	17.81	10.68	15.57	15.31
Cr2O3	0.07	0.12	0.07	0.28
MnO	0.34	0.25	0.3	0.46
MgO	6.37	6.69	10.07	8.94
CaO	11.39	11.57	11.86	12.07
Na2O	1.41	1.81	1.1	1.32
K2O	0.31	0.26	0.24	0.33
Total	96.98	96.45	97.03	97.43
TSi	6.206	7.829	6.676	6.365
TAl	1.794	0.171	1.324	1.635
TFe3	0	0	0	0
CAl	1.33	2.012	0.801	1.01
CCr	0.008	0.014	0.008	0.033
CFe3	0.185	0	0.177	0.116
CTi	0.035	0.137	0.062	0.08
CMg	1.426	1.51	2.221	1.969
CFe2	1.994	1.311	1.712	1.763
CMn	0.021	0.016	0.019	0.029
BFe2	0.057	0.041	0.037	0.013
BMn	0.022	0.016	0.019	0.029
BCa	1.832	1.877	1.88	1.911
BNa	0.089	0.066	0.064	0.048
ANa	0.321	0.466	0.251	0.331
AK	0.059	0.05	0.045	0.062
Sum_cat	15.38	15.516	15.297	15.393

Table D.2 - Plagioclase compositions used for classification and thermobarometry. Formulae calculated on the basis of 32 oxygens after the method of Deer et al., 1966.

Sample	01N030d	01N030d	01N030d	01N030d	01N030d	01N030d	01N030d
Analysis	30d-13	30d-16	30d-17	30d-18	30d-19	30d-7	30d-8
location		core	rim	core	rim	rim	core
Mineral	plag	plag	plag	plag	plag	plag	plag
SiO2	57.87	60.92	60.44	57.79	60.82	60.14	57.64
TiO2	0	0	0	0.09	0	0	0.09
Al2O3	25.63	24.78	24.27	26.55	24.49	25.08	26.56
Fe2O3	0	0	0	0	0	0	0
FeO	0.06	0.16	0.35	0.19	0.1	0.1	0.27
MnO	0.03	0.01	0	0	0	0	0.02
MgO	0.01	0.04	0.04	0.11	0	0.07	0
BaO	0	0	0	0	0	0	0
CaO	8.32	6.4	6.33	9.02	6.32	7.23	9.25
Na2O	6.74	7.56	7.38	6.99	7.95	7.52	6.66
K2O	0.03	0.09	0.04	0.08	0.06	0.05	0.05
Total	98.69	99.96	98.85	100.82	99.74	100.19	100.54
Si	10.485	10.824	10.859	10.304	10.84	10.698	10.303
Al	5.469	5.185	5.135	5.575	5.14	5.254	5.591
Fe3	0	0	0	0	0	0	0
Ti	0	0	0	0.012	0	0	0.012
Fe2	0.009	0.024	0.053	0.028	0.015	0.015	0.04
Mn	0.005	0.002	0	0	0	0	0.003
Mg	0.003	0.011	0.011	0.029	0	0.019	0
Ba	0	0	0	0	0	0	0
Ca	1.615	1.218	1.219	1.723	1.207	1.378	1.772
Na	2.368	2.605	2.571	2.417	2.747	2.594	2.308
K	0.007	0.02	0.009	0.018	0.014	0.011	0.011
Cations	19.961	19.889	19.857	20.106	19.963	19.969	20.04
X	15.954	16.009	15.994	15.891	15.98	15.952	15.906
Z	4.007	3.88	3.863	4.215	3.983	4.017	4.134
Ab	59.3	67.8	67.7	58.1	69.2	65.1	56.4
An	40.5	31.7	32.1	41.4	30.4	34.6	43.3
Or	0.2	0.5	0.2	0.4	0.4	0.3	0.3

Sample	90n007c	90n007c	90n007c	90n007c	90n007c
Analysis	2	3	3r	4c	4r
location			rim	core	rim
Mineral	plag	plag	plag	plag	plag
SiO2	65.36	58.6	59.16	58.67	59.89
TiO2	0.03	0.01	0	0	0.01
Al2O3	22.22	25.91	25.31	25.95	25.22
Fe2O3	0	0	0	0	0
FeO	0.14	0.11	0.18	0.11	0.11
MnO	0.01	0.09	0	0	0
MgO	0.08	0.09	0	0.06	0.03
BaO	0.08	0	0.17	0.21	0.17
CaO	1.95	7.91	7.33	7.78	7.06
Na2O	7.62	7.29	7.51	7.36	7.63
K2O	0.75	0.04	0.02	0.03	0.01
Total	98.24	100.05	99.68	100.17	100.13
Si	11.601	10.482	10.609	10.49	10.673
Al	4.645	5.458	5.345	5.464	5.293
Fe3	0	0	0	0	0
Ti	0.004	0.001	0	0	0.001
Fe2	0.021	0.016	0.027	0.016	0.016
Mn	0.002	0.014	0	0	0
Mg	0.021	0.024	0	0.016	0.008
Ba	0.006	0	0.012	0.015	0.012
Ca	0.371	1.516	1.408	1.49	1.348
Na	2.623	2.528	2.611	2.552	2.637
K	0.17	0.009	0.005	0.007	0.002
Cations	19.47	20.048	20.029	20.065	20.002
X	16.25	15.941	15.954	15.954	15.967
Z	3.214	4.107	4.063	4.096	4.023
Ab	82.9	62.4	64.9	63	66.1
An	11.7	37.4	35	36.8	33.8
Or	5.4	0.2	0.1	0.2	0.1

Sample	15-51b	15-51b	15-51b
Analysis	51b-13	51b-16	51b-5
location			
Mineral	plag	plag	plag
SiO2	62.21	62.17	67.46
TiO2	0.05	0.06	0
Al2O3	23.79	23.72	20.5
Fe2O3	0	0	0
FeO	0.36	0.35	0.29
MnO	0	0	0
MgO	0.09	0.02	0.06
BaO	0	0	0
CaO	5.4	5.05	1.43
Na2O	8.48	8.42	9.56
K2O	0.01	0.04	0.09
Total	100.39	99.83	99.39
Si	10.998	11.034	11.838
Al	4.953	4.958	4.236
Fe3	0	0	0
Ti	0.007	0.008	0
Fe2	0.053	0.052	0.043
Mn	0	0	0
Mg	0.024	0.005	0.016
Ba	0	0	0
Ca	1.023	0.96	0.269
Na	2.907	2.898	3.253
K	0.002	0.009	0.02
Cations	19.967	19.924	19.675
X	15.958	16	16.074
Z	4.009	3.924	3.601
Ab	73.9	74.9	91.8
An	26	24.8	7.6
Or	0.1	0.2	0.6

Sample	90N015c	90N015c	90N015c	90N015c	90N015c	90N015c
Analysis	15c11	15c22	15c23	15c24	15c29	15c35
Location	matrix	ss	ss	ss	matrix	matrix
Mineral	plag	plag	plag	plag	plag	plag
SiO2	62.02	51.93	60.24	59.35	59.45	60
TiO2	0	0	0	0.04	0	0.04
Al2O3	23.72	30.05	24.62	25.01	24.52	24.82
Fe2O3	0	0	0	0	0	0
FeO	0.14	0.47	0.26	0.21	0.45	0.25
MnO	0	0	0	0.01	0.07	0
MgO	0.16	0.14	0	0.14	0.03	0.09
BaO	0	0	0	0	0	0
CaO	5.36	12.99	6.56	6.93	6.55	6.75
Na2O	8.8	4.43	7.55	7.89	7.91	7.28
K2O	0	0.05	0.08	0.05	0.03	0.05
Total	100.2	100.06	99.31	99.63	99.01	99.28
Si	10.988	9.45	10.791	10.641	10.721	10.749
Al	4.949	6.44	5.194	5.281	5.208	5.237
Fe3	0	0	0	0	0	0
Ti	0	0	0	0.005	0	0.005
Fe2	0.021	0.072	0.039	0.031	0.068	0.037
Mn	0	0	0	0.002	0.011	0
Mg	0.042	0.038	0	0.037	0.008	0.024
Ba	0	0	0	0	0	0
Ca	1.017	2.533	1.259	1.331	1.266	1.296
Na	3.023	1.563	2.623	2.743	2.766	2.529
K	0	0.012	0.018	0.011	0.007	0.011
Cations	20.04	20.108	19.924	20.082	20.055	19.888
X	15.937	15.89	15.985	15.927	15.929	15.991
Z	4.103	4.218	3.939	4.155	4.126	3.897
Ab	74.8	38	67.3	67.1	68.5	65.9
An	25.2	61.7	32.3	32.6	31.3	33.8
Or	0	0.3	0.5	0.3	0.2	0.3

Sample	90N014b	90N014b	90N014b	90N014a	90N014a
Analysis	14b-10	14b-11	14b-12	14a-5	14a-6
location	matrix	matrix	matrix	matrix	matrix
Mineral	plag	plag	plag	plag	plag
SiO2	60.62	57.11	60.21	63.48	68.23
TiO2	0	0	0	0.08	0
Al2O3	26.18	27.68	26.15	24.03	21.61
Fe2O3	0	0	0	0	0
FeO	0.08	0.11	0.03	0.23	0.31
MnO	0	0.02	0.04	0.01	0.06
MgO	0.07	0.03	0.04	0.04	0
BaO	0	0.15	0	0.01	0
CaO	7.19	9.09	7.38	5.79	4.33
Na2O	7.27	5.99	7.26	7.7	7.8
K2O	0.06	0.1	0.05	0.04	0.01
Total	101.47	100.28	101.16	101.41	102.35
Si	10.63	10.21	10.601	11.068	11.664
Al	5.406	5.828	5.422	4.934	4.351
Fe3	0	0	0	0	0
Ti	0	0	0	0.01	0
Fe2	0.012	0.016	0.004	0.034	0.044
Mn	0	0.003	0.006	0.001	0.009
Mg	0.018	0.008	0.01	0.01	0
Ba	0	0.011	0	0.001	0
Ca	1.351	1.741	1.392	1.082	0.793
Na	2.472	2.077	2.478	2.603	2.585
K	0.013	0.023	0.011	0.009	0.002
Cations	19.902	19.928	19.924	19.753	19.448
X	16.036	16.038	16.023	16.012	16.015
Z	3.866	3.879	3.901	3.74	3.433
Ab	64.4	54.1	63.8	70.5	76.5
An	35.2	45.3	35.9	29.3	23.5
Or	0.3	0.6	0.3	0.2	0.1

Table D.3 - Garnet and biotite compositions used for thermobarometry. Formulae calculated using the geological software, *Minpet* (Richard, 1997).

Sample	90N015I
Analysis	15I2
Location	rim
Mineral	garnet
SiO2	36.3
TiO2	0.02
Al2O3	20.5
Cr2O3	0.04
FeO	31.32
Fe2O3	0
MnO	6.83
MgO	0.37
CaO	4.41
Cl	0.05
Total	99.8
O_F_Cl	0.01
CTotal	99.79
TSi	2.971
TAl	0.029
Sum_T	3
AlVI	1.947
Fe3	0
Ti	0.001
Cr	0.003
Sum_A	1.951
Fe2	2.144
Mg	0.045
Mn	0.473
Ca	0.387
Na	0
Sum_B	3.049
Sum_cat	8
O	12
CF	0
CCl	0.007
Alm	70.308
And	0
Gross	12.55
Pyrope	1.481
Spess	15.529
Uvaro	0.133
XCagnt	0.127
XFegnt	0.703
XMggnt	0.015
Fe_Mggnt	47.644

Sample	90N015I
Analysis	15I10
Location	matrix
Mineral	biotite
SiO2	46.89
TiO2	0.09
Al2O3	34.52
Cr2O3	0.04
FeO	3.04
Fe2O3	0
MnO	0.07
MgO	0.6
BaO	0.64
CaO	0.05
Na2O	0.52
K2O	9.29
F	0
Cl	0
Total	96.16
O_F_Cl	0
Si	6.527
AlIV	1.473
AlVI	4.186
Ti	0.009
Fe3	0
Fe2	0.354
Cr	0.004
Mn	0.008
Mg	0.125
Ba	0.035
Ca	0.007
Na	0.14
K	1.65
Cations	14.518
CF	0
CCl	0
OH	0
O	24
Fe_FeMg	0.74
Mg_FeMg	0.26

APPENDIX E

Thermobarometry

Table E.1 - Pressure-temperature calculations for select samples from the study area. Calculations were performed according to the hornblende-plagioclase thermometer of Holland and Blundy (1994), using the data shown in Appendix D. Specific analysis numbers are shown in brackets. Ranges of pressures are shown for comparison, however, a pressure estimate of ~5 kbar is likely appropriate for the samples. Samples are organized generally from south to north. Each sample's approximate location is indicated (note that NWP = North Wind Pluton). For specific station locations, refer back to figure 2.6. Specific analyses were chosen in an attempt to represent conditions from each phase of metamorphism. Where possible, the phase of metamorphism believed to be associated with the calculation is indicated as either M1 or M2.

90N030d - (# 30d-6 & 30d-7) - M2 - adjacent to NWP

Pressure (kbar)	**0**	**5**	**10**	**15**
Temp. (degC) (ed-tr)	692	706	720	734

90N007c - (ave of amp analyses & #3r) - M2 - adjacent to NWP

Pressure (kbar)	**0**	**5**	**10**	**15**
Temp. (degC) (ed-tr)	711	711	711	711

90N015d - (# 15d6 & 15d7) - M2 - HBHSZ

Pressure (kbar)	**0**	**5**	**10**	**15**
Temp. (degC) (ed-tr)	595	631	667	703

90N015c - (# 15c3 & 15c24) - M2 - HBHSZ

Pressure (kbar)	**0**	**5**	**10**	**15**
Temp. (degC) (ed-tr)	673	688	703	718

15-51b - (# 51b-11 & 51b-16) - M2 - HBHSZ

Pressure (kbar)	**0**	**5**	**10**	**15**
Temp. (degC) (ed-tr)	613	646	678	711

15-51a - (# 51a-4 & 51a-5) - M2 - HBHSZ

Pressure (kbar)	0	5	10	15
Temp. (degC) (ed-tr)	718	710	702	694

15-51a - (# 51a-8 & 51a-7) - M1 (?) - HBHSZ

Pressure (kbar)	0	5	10	15
Temp. (degC) (ed-tr)	589	545	502	458

90N002j - (# 32 & 41) - M1 - HBHSZ

Pressure (kbar)	0	5	10	15
Temp. (degC) (ed-tr)	673	613	554	494

90N002j - (# 53 & 68) - M2 - HBHSZ

Pressure (kbar)	0	5	10	15
Temp. (degC) (ed-tr)	580	633	686	739

90N002f - (#2f3 & 2f5) - M2 - HBHSZ

Pressure (kbar)	0	5	10	15
Temp. (degC) (ed-tr)	685	689	693	697

90N002f - (# 2f11 & 2f16) - M1 - HBHSZ

Pressure (kbar)	0	5	10	15
Temp. (degC) (ed-tr)	657	610	563	516

90N014b - (#14b-6 & 14b-10) - North of HBHSZ

Pressure (kbar)	0	5	10	15
Temp. (degC) (ed-tr)	567	626	686	746

90N014a - (# 14a-8 & 14a-5) - North of HBHSZ

Pressure (kbar)	0	5	10	15
Temp. (degC) (ed-tr)	511	589	667	745

Table E.2 - Temperature calculations for sample 90N015l. Temperatures were calculated using the garnet-biotite thermometer of Ferry and Spear (1978), as presented by Winter (2001), based on the data shown in Appendix D.

90N015I - (# 15I2 & 15I10) - HBHSZ

Pressure (kbar)	**0**	**5**	**10**	**15**
Temp. (degC)	656	679	701	723

22

Sample	Analysis	Location	Mineral	SiO2	TiO2	Al2O3	FeO	MnO	MgO	CaO	Na2O	K2O	Cr2O3	NiO	P2O5	Cl	BaO	SrO	ZrO2	La2O3	Total
kkcontrol	1.00	1	amphibole	39.97	4.81	14.28	10.58	0.01	12.75	10.16	2.46	2.19	0.02	0.12	0.00	0.05	0.27	0.00	0.03	0.23	97.94
15	2.00	?	titanite	30.73	38.91	1.02	0.40	0.00	0.13	29.34	0.06	0.00	0.03	0.24	0.02	0.00	0.47	0.00	0.00	0.28	101.64
15	3.00	rim	amphibole	43.32	0.88	15.33	13.84	0.30	10.31	12.04	1.43	0.22	0.01	0.01	0.00	0.00	0.00	0.00	0.00	0.00	97.68
15	15-1	core	amphibole	50.60	0.23	7.51	11.67	0.20	14.91	12.92	0.76	0.16	0.51	0.02	0.00	0.00	0.00	0.00	0.01	0.00	99.50
15	15-2	core	amphibole	52.19	0.18	5.73	10.96	0.24	16.01	12.75	0.58	0.15	0.40	0.00	0.00	0.00	0.00	0.00	0.06	0.05	99.30
15	15-3	core	amphibole	52.22	0.14	5.21	10.52	0.23	16.19	13.02	0.51	0.06	0.22	0.00	0.00	0.00	0.00	0.00	0.08	0.00	98.40
15	15-4	core	epidote	38.91	0.19	29.27	6.01	0.09	0.00	24.80	0.08	0.01	0.01	0.00	0.00	0.00	0.00	0.00	0.00	0.04	99.44
15	15-5	rim	amphibole	44.04	0.28	15.03	14.63	0.30	10.12	12.26	1.11	0.26	0.03	0.00	0.00	0.03	0.04	0.00	0.00	0.01	98.15
15	15-6	rim	amphibole	44.87	0.48	15.18	14.17	0.32	10.55	12.19	1.33	0.29	0.00	0.00	0.00	0.00	0.00	0.00	0.16	0.00	99.54
15	15-7	rim	amphibole	44.49	0.47	14.37	13.79	0.28	10.83	12.34	1.30	0.25	0.09	0.07	0.00	0.00	0.05	0.00	0.00	0.03	98.36
15	15-8	core	amphibole	52.24	0.21	5.81	10.53	0.31	15.93	12.85	0.53	0.12	0.47	0.04	0.00	0.00	0.00	0.00	0.00	0.00	99.06
15	15-9	rim??	amphibole	48.42	0.17	9.56	14.02	0.39	12.48	12.57	0.93	0.25	0.33	0.00	0.00	0.02	0.11	0.00	0.00	0.12	99.36
15	15-10	matrix	amphibole	45.27	0.44	13.61	13.37	0.34	11.70	12.26	1.34	0.19	0.07	0.16	0.00	0.00	0.00	0.00	0.08	0.00	98.85
15	15-11	matrix	epidote	38.97	0.33	29.46	5.63	0.12	0.11	24.80	0.00	0.00	0.00	0.01	0.00	0.00	0.00	0.00	0.00	0.00	99.41
15	15-12	matrix	amphibole	43.60	0.34	16.02	14.41	0.24	9.84	12.13	1.28	0.23	0.11	0.00	0.00	0.01	0.15	0.00	0.00	0.05	98.41
15	15-13	matrix	amphibole	44.61	0.36	14.47	13.95	0.08	10.87	12.05	1.38	0.17	0.05	0.08	0.00	0.00	0.00	0.00	0.00	0.00	98.08
15	15-14	matrix	titanite	30.98	39.09	0.97	0.34	0.03	0.02	29.39	0.02	0.00	0.09	0.00	0.00	0.01	0.90	0.00	0.00	0.27	102.12
15	15-15	matrix	chlorite	26.10	0.01	21.49	21.11	0.24	18.42	0.05	0.03	0.00	0.00	0.02	0.00	0.00	0.12	0.00	0.00	0.11	87.69
15	15-16	matrix	chlorite	26.04	0.10	21.37	19.52	0.27	18.69	0.14	0.09	0.01	0.05	0.06	0.00	0.03	0.00	0.00	0.12	0.00	86.48
15	15-17	matrix	chlorite	26.15	0.01	21.88	20.43	0.45	18.43	0.00	0.09	0.07	0.00	0.10	0.00	0.00	0.00	0.00	0.06	0.00	87.69
15	15-18	matrix	chlorite	26.26	0.02	21.49	20.34	0.17	18.89	0.09	0.00	0.00	0.01	0.00	0.00	0.00	0.07	0.00	0.01	0.04	87.37
90N014a	1	core	amphibole	38.45	1.08	15.79	20.90	0.48	5.79	9.92	1.31	0.34	0.09	0.00	0.00	0.04	0.00	0.00	0.00	0.03	94.21
90N014a	14a-2	core	amphibole	41.13	0.34	16.59	21.15	0.41	5.18	10.84	1.75	0.34	0.03	0.00	0.00	0.00	0.01	0.00	0.11	0.12	98.00
90N014a	14a-3	core	amphibole	41.26	0.40	16.77	19.85	0.30	5.52	11.22	1.57	0.22	0.08	0.08	0.00	0.00	0.00	0.00	0.00	0.10	97.36
90N014a	14a-4	core	amphibole	41.16	0.22	16.76	20.42	0.51	5.73	10.83	1.72	0.26	0.18	0.04	0.00	0.02	0.01	0.00	0.17	0.00	98.04
90N014a	14a-5	matrix	plag	63.48	0.08	24.03	0.23	0.01	0.04	5.79	7.70	0.04	0.00	0.00	0.00	0.00	0.01	0.00	0.00	0.01	101.41
90N014a	14a-6	matrix	plag	68.23	0.00	21.61	0.31	0.06	0.00	4.33	7.80	0.01	0.00	0.00	0.00	0.00	0.00	0.00	0.02	0.02	102.39
90N014a	14a-7	matrix	quartz	97.73	0.05	1.59	0.14	0.00	0.02	0.05	1.01	0.00	0.04	0.08	0.00	0.00	0.01	0.00	0.07	0.00	100.79
90N014a	14a-8	matrix	amphibole	42.07	0.26	16.03	19.55	0.53	6.09	10.58	1.74	0.16	0.07	0.00	0.00	0.01	0.09	0.00	0.00	0.05	97.23
90N014a	14a-9	vein	chlorite	24.28	0.00	20.42	31.89	0.69	9.83	0.04	0.09	0.04	0.12	0.00	0.00	0.00	0.00	0.00	0.03	0.00	87.45
90N014a	14a-10	vein	calcite	0.14	0.00	0.00	1.10	1.07	0.15	58.21	0.01	0.02	0.00	0.00	0.10	0.03	0.00	0.10	0.01	0.00	60.94
90N014a	14a-11	vein	calcite	0.12	0.09	0.00	0.00	0.14	0.02	60.91	0.11	0.00	0.01	0.03	0.07	0.00	0.00	0.09	0.00	0.00	61.59
90N014a	14a-12	vein	chlorite	24.23	0.12	21.09	31.56	0.48	9.91	0.12	0.00	0.01	0.06	0.00	0.00	0.03	0.00	0.00	0.00	0.05	87.64
90N014b	14b-1	core	amphibole	41.34	0.31	17.67	17.81	0.34	6.37	11.39	1.41	0.31	0.07	0.00	0.00	0.03	0.00	0.00	0.08	0.06	97.18
90N014b	14b-2	vein	chlorite	25.63	0.13	20.65	22.91	0.15	16.03	0.11	0.11	0.07	0.12	0.01	0.00	0.00	0.00	0.00	0.05	0.00	85.97
90N014b	14b-3	core	amphibole	51.71	1.20	12.24	10.68	0.25	6.69	11.57	1.81	0.26	0.12	0.00	0.00	0.04	0.00	0.00	0.17	0.07	96.81
90N014b	14b-4	core	amphibole	45.13	0.56	12.20	15.57	0.30	10.07	11.86	1.10	0.24	0.07	0.00	0.00	0.00	0.00	0.00	0.00	0.05	97.14
90N014b	14b-5	core	chlorite	26.24	0.14	19.02	23.64	0.33	15.82	0.16	0.21	0.02	0.03	0.15	0.00	0.03	0.00	0.00	0.08	0.10	85.97
90N014b	14b-6	fresh	amphibole	43.08	0.72	15.20	15.31	0.46	8.94	12.07	1.32	0.33	0.28	0.13	0.00	0.00	0.00	0.00	0.00	0.00	97.82
90N014b	14b-7	core	epidote	38.84	0.24	29.46	5.40	0.26	0.08	24.46	0.00	0.02	0.10	0.04	0.00	0.01	0.00	0.00	0.00	0.00	98.91
90N014b	14b-8	core	epidote	38.79	0.28	28.89	5.81	0.30	0.07	24.23	0.00	0.00	0.48	0.08	0.00	0.00	0.00	0.00	0.10	0.00	99.02
90N014b	14b-9	core	titanite	30.36	37.06	2.19	0.09	0.10	0.00	29.32	0.10	0.02	0.06	0.03	0.00	0.00	0.50	0.00	0.00	0.13	99.96
90N014b	14b-10	matrix	plag	60.62	0.00	26.18	0.08	0.00	0.07	7.19	7.27	0.06	0.03	0.00	0.00	0.00	0.00	0.00	0.00	0.00	101.51
90N014b	14b-11	matrix	plag	57.11	0.00	27.68	0.11	0.02	0.03	9.09	5.99	0.10	0.06	0.00	0.00	0.01	0.15	0.00	0.12	0.01	100.48
90N014b	14b-12	matrix	plag	60.21	0.00	26.15	0.03	0.04	0.04	7.38	7.26	0.05	0.00	0.02	0.00	0.00	0.00	0.00	0.00	0.02	101.21
01N041	41-1	grotty	amphibole	36.71	2.16	16.60	17.13	0.00	12.52	0.04	0.14	9.85	0.27	0.01	0.00	0.00	0.27	0.00	0.00	0.02	95.73
01N041	41-2	fresher	amphibole	36.13	1.97	16.45	17.62	0.01	12.24	0.00	0.19	9.08	0.19	0.06	0.00	0.01	0.34	0.00	0.03	0.07	94.39
01N041	41-3	fresher	amphibole	43.89	0.45	12.02	17.76	0.24	9.98	12.13	1.24	0.34	0.10	0.16	0.00	0.00	0.00	0.00	0.00	0.00	98.31
01N041	41-4	fresher	amphibole	43.72	0.32	12.33	18.64	0.26	9.47	11.98	1.35	0.37	0.00	0.01	0.00	0.00	0.02	0.00	0.05	0.04	98.56
01N041	41-5	matrix	plag	67.99	0.00	21.85	0.14	0.00	0.10	2.02	10.25	0.00	0.09	0.00	0.00	0.00	0.08	0.00	0.00	0.00	102.53
01N041	41-6	matrix	plag	68.09	0.05	21.02	0.29	0.00	0.35	0.96	9.88	0.00	0.00	0.08	0.00	0.00	0.00	0.00	0.00	0.00	100.71
01N041	41-7	matrix	plag	46.29	0.55	9.52	16.36	0.39	11.41	12.08	1.10	0.14	0.08	0.09	0.00	0.00	0.00	0.00	0.30	0.00	98.29

22

Sample	Analysis	Location	Mineral	SiO2	TiO2	Al2O3	FeO	MnO	MgO	CaO	Na2O	K2O	Cr2O3	NiO	P2O5	Cl	SrO	ZrO2	La2O3	BaO	Total
90N002j	1	c	amphibole	50.97	0.02	6.04	11.49	0.15	15.50	12.85	0.69	0.14	0.06	0.05	0.00	0.03	0.00	0.04	0.21	0.24	98.48
90N002j	2	c	apatite	0.08	0.09	0.09	0.14	0.02	0.06	57.90	0.11	0.00	0.00	0.17	43.23	0.65	0.00	0.00	0.10	0.08	102.72
90N002j	3	c	amphibole	43.77	0.41	14.49	15.08	0.26	10.41	12.35	1.30	0.31	0.00	0.00	0.00	0.00	0.00	0.00	0.02	0.02	98.41
90N002j	4	dark core	amphibole	49.56	0.35	7.47	11.70	0.25	14.76	12.43	0.98	0.18	0.16	0.00	0.00	0.00	0.00	0.00	0.00	0.00	97.83
90N002j	5	light core	epidote	39.13	0.02	25.47	8.10	0.19	1.84	22.38	0.36	0.10	0.00	0.00	0.00	0.01	0.00	0.13	0.01	0.11	97.85
90N002j	6	c	amphibole	44.02	0.45	13.22	13.99	0.22	11.03	12.14	1.45	0.32	0.00	0.05	0.00	0.00	0.00	0.00	0.05	0.00	96.94
90N002j	7	c	chlorite	26.05	0.08	21.49	18.49	0.19	19.94	0.19	0.06	0.00	0.02	0.10	0.00	0.00	0.00	0.03	0.09	0.00	86.72
90N002j	8	c	chlorite	25.85	0.05	21.71	18.45	0.18	20.31	0.01	0.15	0.01	0.08	0.08	0.00	0.00	0.00	0.00	0.00	0.09	86.98
90N002j	9	c	chlorite	26.14	0.00	21.23	18.68	0.23	19.62	0.00	0.00	0.03	0.05	0.11	0.00	0.00	0.00	0.00	0.00	0.05	86.15
90N002j	10	c	apatite	4.77	4.73	0.17	0.12	0.00	0.17	52.49	0.06	0.00	0.06	0.00	35.42	0.29	0.00	0.00	0.00	0.20	98.47
90N002j	11	c	?	30.03	39.19	0.90	0.38	0.00	0.00	29.13	0.09	0.00	0.06	0.18	0.00	0.00	0.00	0.09	0.33	0.58	100.96
90N002j	12	dark core	amphibole	48.04	0.38	8.71	12.45	0.23	13.74	12.24	1.05	0.16	0.09	0.11	0.00	0.02	0.00	0.05	0.00	0.00	97.26
90N002j	13	c	plag	57.36	0.19	26.05	0.45	0.00	0.10	8.18	6.62	0.10	0.03	0.00	0.00	0.00	0.00	0.06	0.00	0.00	99.13
90N002j	14	c	plag	57.84	0.08	26.23	0.30	0.08	0.00	8.45	6.90	0.08	0.00	0.00	0.00	0.02	0.00	0.05	0.00	0.00	100.03
90N002j	15	c	plag	61.05	0.03	24.36	0.17	0.02	0.05	5.89	8.37	0.06	0.00	0.00	0.01	0.00	0.00	0.07	0.01	0.00	100.09
90N002j	16	c	qz	97.36	0.00	0.00	0.05	0.00	0.07	0.00	0.00	0.00	0.00	0.05	0.00	0.00	0.00	0.00	0.00	0.00	97.53
90N002j	17	c	amphibole	46.09	0.35	11.91	13.81	0.28	11.76	12.31	1.28	0.27	0.05	0.07	0.00	0.00	0.00	0.00	0.00	0.00	98.19
90N002j	18	c	biotite	37.02	1.88	16.89	15.50	0.10	13.65	0.01	0.18	9.34	0.04	0.00	0.00	0.01	0.00	0.08	0.00	0.35	95.05
90N002j	19	m	plag	62.78	0.00	23.18	0.12	0.08	0.04	4.18	8.58	0.10	0.02	0.00	0.00	0.02	0.00	0.00	0.04	0.00	99.13
90N002j	20	m	plag	60.11	0.03	24.79	0.12	0.00	0.00	6.76	7.46	0.06	0.00	0.00	0.00	0.01	0.00	0.00	0.02	0.00	99.36
90N002j	21	m	chlorite	26.80	0.05	22.03	17.49	0.15	20.30	0.21	0.37	0.01	0.07	0.13	0.00	0.01	0.00	0.18	0.01	0.04	87.83
90N002j	22	m	amphibole	38.27	0.03	27.15	7.23	0.05	0.04	24.46	0.26	0.07	0.04	0.13	0.00	0.00	0.00	0.00	0.07	0.06	97.87
90N002j	23	m core	amphibole	38.81	0.00	31.72	1.95	0.00	0.10	25.13	0.00	0.01	0.00	0.09	0.00	0.00	0.00	0.00	0.01	0.00	97.82
90N002j	24	m rim	amphibole	38.32	0.00	29.55	3.38	0.16	0.48	24.53	0.02	0.00	0.11	0.07	0.00	0.02	0.00	0.00	0.04	0.14	96.80
90N002j	25	m	plag	60.68	0.03	24.07	0.01	0.00	0.06	5.97	8.04	0.00	0.02	0.00	0.00	0.00	0.00	0.00	0.00	0.00	98.88
90N002j	26	m	plag	61.19	0.00	24.53	0.18	0.00	0.04	6.30	8.05	0.03	0.12	0.00	0.00	0.00	0.00	0.00	0.17	0.23	100.85
90N002j	27	light core	amphibole	43.14	0.34	14.50	15.03	0.23	9.74	12.11	1.53	0.40	0.61	0.13	0.00	0.01	0.00	0.06	0.00	0.07	97.89
90N002j	28	dark core	amphibole	52.57	0.11	3.25	10.44	0.13	16.47	12.99	0.36	0.11	0.63	0.00	0.00	0.00	0.00	0.00	0.00	0.00	97.05
90N002j	29	light core	amphibole	42.45	0.28	13.64	15.23	0.34	9.44	12.14	1.26	0.35	1.01	0.01	0.00	0.02	0.00	0.00	0.04	0.08	96.30
90N002j	30	dark core	amphibole	53.12	0.12	2.59	10.04	0.16	17.28	13.05	0.20	0.03	0.82	0.06	0.00	0.00	0.00	0.02	0.00	0.00	97.50
90N002j	31	light core	amphibole	42.13	0.54	14.23	14.77	0.31	9.32	12.08	1.38	0.33	0.82	0.05	0.00	0.00	0.00	0.10	0.00	0.00	96.08
90N002j	32	dark core	amphibole	52.96	0.11	3.48	10.19	0.22	17.27	12.72	0.50	0.04	0.71	0.02	0.00	0.00	0.00	0.00	0.00	0.00	98.21
90N002j	33	in amp p/b	chlorite	26.20	0.18	19.43	18.83	0.32	19.66	0.13	0.14	0.05	1.10	0.12	0.00	0.00	0.00	0.00	0.03	0.00	86.20
90N002j	34	in amp p/b	chlorite	25.78	0.03	21.40	17.70	0.24	20.36	0.10	0.04	0.00	0.21	0.00	0.00	0.00	0.00	0.14	0.03	0.00	86.04
90N002j	35	in amp p/b	titanite	30.58	37.96	1.58	0.59	0.15	0.06	29.30	0.05	0.00	0.23	0.08	0.00	0.00	0.00	0.02	0.28	0.38	101.27
90N002j	36	in altered plag	plag	61.83	0.00	23.52	0.22	0.00	0.00	5.10	9.06	0.10	0.00	0.07	0.00	0.01	0.00	0.00	0.08	0.04	100.03
90N002j	37	in altered plag	chlorite	26.90	0.07	20.39	17.22	0.21	20.86	0.20	0.06	0.06	0.08	0.00	0.00	0.00	0.00	0.08	0.03	0.13	86.27
90N002j	38	in altered plag	epidote	39.16	0.08	27.56	6.54	0.10	0.03	23.74	0.28	0.01	0.05	0.00	0.00	0.00	0.00	0.03	0.00	0.07	97.66
90N002j	39	in altered plag	amphibole	42.66	0.29	15.51	14.86	0.21	9.54	12.35	1.42	0.41	0.14	0.00	0.00	0.02	0.00	0.00	0.00	0.00	97.42
90N002j	40	in altered plag	epidote	38.50	0.15	28.22	6.20	0.12	0.00	25.21	0.00	0.00	0.04	0.00	0.00	0.02	0.00	0.01	0.15	0.23	98.84
90N002j	41	in altered plag	plag	59.01	0.26	25.48	0.21	0.08	0.05	7.60	7.34	0.08	0.00	0.00	0.00	0.18	0.00	0.00	0.00	0.00	100.27
90N002j	42	in altered plag	epidote	38.00	0.00	27.92	6.36	0.06	0.09	24.53	0.00	0.00	0.07	0.09	0.00	0.02	0.00	0.00	0.05	0.30	97.49
90N002j	43	in altered plag	epidote	38.38	0.06	28.23	5.90	0.00	0.00	24.78	0.00	0.01	0.11	0.00	0.00	0.01	0.00	0.08	0.00	0.00	97.55
90N002j	44	in altered plag	epidote	37.87	0.00	27.56	6.51	0.12	0.04	24.39	0.09	0.00	0.06	0.00	0.00	0.04	0.00	0.00	0.04	0.07	96.78
90N002j	45	in altered plag	plag	59.38	0.00	25.77	0.20	0.00	0.10	7.65	7.26	0.06	0.10	0.08	0.00	0.00	0.00	0.00	0.05	0.00	100.67
90N002j	46	in altered plag	epidote	38.46	0.00	30.72	3.07	0.02	0.09	24.84	0.14	0.02	0.05	0.00	0.00	0.00	0.00	0.00	0.11	0.15	97.67
90N002j	47	in altered plag	??bad an	30.17	0.18	22.43	16.36	0.27	17.90	0.86	1.19	0.08	0.01	0.01	0.00	0.00	0.00	0.00	0.15	0.00	89.60
90N002j	48	ss light rim	amphibole	42.41	0.47	15.14	15.11	0.23	9.52	12.32	1.37	0.46	0.15	0.12	0.00	0.02	0.00	0.00	0.00	0.00	97.31
90N002j	49	ss dark core	amphibole	53.59	0.07	2.75	10.04	0.14	17.47	12.97	0.45	0.03	0.13	0.10	0.00	0.02	0.00	0.00	0.00	0.00	97.74
90N002j	50	ss core	epidote	37.67	0.23	26.27	7.72	0.26	0.00	24.18	0.00	0.00	0.06	0.00	0.00	0.01	0.00	0.00	0.00	0.00	96.41
90N002j	51	ss rim	epidote	37.69	0.04	25.75	8.85	0.00	0.15	24.43	0.14	0.00	0.09	0.00	0.00	0.00	0.00	0.00	0.00	0.00	97.14
90N002j	52	ss	chlorite	25.95	0.04	21.06	18.39	0.26	19.78	0.16	0.04	0.04	0.01	0.12	0.05	0.00	0.00	0.03	0.00	0.00	85.95
90N002j	53	ss	epidote	38.33	0.22	26.58	7.75	0.11	0.06	24.43	0.00	0.00	0.07	0.00	0.00	0.00	0.00	0.11	0.00	0.00	97.66
90N002j	54	ss	amphibole	48.80	0.22	7.67	13.31	0.27	13.87	12.05	0.97	0.14	0.01	0.00	0.00	0.05	0.00	0.08	0.06	0.18	97.67
90N002j	55	ss dark core	epidote	36.68	0.00	27.13	7.37	0.14	2.31	21.61	0.00	0.00	0.04	0.00	0.00	0.03	0.00	0.00	0.00	0.00	95.30
90N002j	56	ss light rim	epidote	37.99	0.00	26.71	7.83	0.22	0.04	24.56	0.16	0.00	0.00	0.00	0.00	0.02	0.00	0.01	0.18	0.08	97.78
90N002j	57	ss core	epidote	37.50	0.17	24.42	10.36	0.15	0.16	23.95	0.04	0.00	0.11	0.00	0.06	0.04	0.00	0.00	0.09	0.00	97.04
90N002j	58	ss rim	epidote	38.26	0.14	26.87	8.17	0.15	0.06	24.58	0.05	0.00	0.04	0.00	0.04	0.04	0.00	0.00	0.12	0.00	98.53
90N002j	59	ss light core	amphibole	42.32	0.35	15.80	15.37	0.20	9.46	12.08	1.63	0.44	0.01	0.01	0.00	0.00	0.00	0.06	0.04	0.00	97.78
90N002j	60	ss dark rim?	amphibole	43.96	0.42	12.90	14.43	0.26	10.82	12.19	1.40	0.37	0.05	0.04	0.00	0.00	0.00	0.00	0.12	0.08	97.04
90N002j	61	ss	apatite	0.08	0.00	0.05	0.35	0.00	0.11	57.40	0.10	0.01	0.04	0.00	42.55	0.24	0.00	0.10	0.05	0.02	101.09
90N002j	62	ss	apatite	0.13	0.04	0.19	0.77	0.00	0.10	56.86	0.05	0.04	0.07	0.00	42.77	0.07	0.00	0.00	0.00	0.00	101.11
90N002j	63	ss	chlorite	26.26	0.22	21.50	18.04	0.29	20.23	0.06	0.05	0.06	0.00	0.06	0.00	0.00	0.00	0.00	0.11	0.00	86.87
90N002j	64	ss core	chlorite	25.29	0.09	21.84	18.49	0.33	19.76	0.03	0.06	0.00	0.00	0.01	0.00	0.00	0.00	0.00	0.00	0.00	85.90
90N002j	65	ss	chlorite	25.67	0.11	21.53	18.73	0.16	19.74	0.06	0.08	0.00	0.04	0.00	0.00	0.02	0.00	0.07	0.00	0.00	86.22
90N002j	66	ss	epidote	37.31	0.00	24.56	10.76	0.42	0.12	22.81	0.02	0.02	0.00	0.14	0.04	0.00	0.00	0.00	0.00	0.06	96.27
90N002j	67	ss core	chlorite	26.17	0.07	21.75	18.22	0.23	20.47	0.08	0.16	0.04	0.10	0.23	0.00	0.03	0.00	0.00	0.21	0.11	87.88
90N002j	68	ss	plag	60.57	0.00	24.20	0.18	0.01	0.07	5.89	7.74	0.10	0.00	0.16	0.00	0.00	0.00	0.01	0.00	0.02	98.95
90N002j	69	ss	plag	61.68	0.09	23.47	0.32	0.00	0.00	5.11	8.55	0.08	0.04	0.06	0.00	0.00	0.00	0.01	0.00	0.00	99.41
90N002j	70	ss	plag	60.08	0.00	24.86	0.31	0.00	0.03	6.55	8.24	0.00	0.00	0.03	0.00	0.04	0.00	0.00	0.11	0.05	100.30
90N002f	2f1	dark core	amphibole	50.11	0.20	5.68	13.63	0.45	14.55	12.08	0.98	0.08	0.13	0.11	0.00	0.03	0.00	0.07	0.00	0.00	98.09
90N002f	2f2	light rim	amphibole	44.28	0.31	11.24	16.07	0.34	10.77	11.64	1.63	0.28	0.00	0.12	0.00	0.00	0.00	0.05	0.19	0.21	97.13
90N002f	2f3	dark core	amphibole	52.66	0.06	3.24	12.03	0.47	16.46	12.07	0.75	0.05	0.22	0.00	0.00	0.00	0.00	0.11	0.00	0.00	98.12
90N002f	2f4	light rim	amphibole	42.96	0.40	12.73	16.88	0.31	10.12	11.53	1.87	0.29	0.05	0.00	0.00	0.00	0.00	0.00	0.00	0.00	97.15
90N002f	2f5	c in p/b	plag	61.38	0.05	24.39	0.16	0.02	0.09	5.65	8.59	0.10	0.00	0.00	0.00	0.02	0.00	0.00	0.10	0.03	100.58
90N002f	2f6	c in p/b	plag	62.60	0.00	22.24	0.19	0.05	0.00	3.83	8.93	0.06	0.00	0.00	0.00	0.01	0.00	0.11	0.09	0.24	98.33
90N002f	2f7	edge of p/b	chlorite	25.87	0.09	20.53	21.45	0.27	18.48	0.00	0.11	0.00	0.00	0.17	0.00	0.00	0.00	0.22	0.05	0.00	87.24
90N002f	2f8	ss	ilmenite	2.82	48.99	0.27	41.29	3.22	1.36	0.38	0.00	0.00	0.01	0.01	0.00	0.00	0.01	0.11	0.64	1.19	100.30
90N002f	2f9	ss	ilmenite	1.30	49.89	0.23	42.02	2.88	0.60	0.30	0.01	0.00	0.00	0.06	0.00	0.00	0.00	0.16	0.78	1.97	100.21
90N002f	2f10	ss core	amphibole	41.80	0.28	14.03	17.12	0.31	9.18	11.26	1.89	0.28	0.05	0.00	0.00	0.03	0.00	0.07	0.00	0.00	96.31
90N002f	2f11	ss core	amphibole	43.15	0.32	12.39	16.83	0.28	10.33	11.57	1.79	0.29	0.01	0.00	0.00	0.00	0.00	0.00	0.05	0.00	97.00
90N002f	2f12	ss	amphibole	44.84	0.28	11.29	15.87	0.28	10.92	11.42	1.70	0.27	0.09	0.08	0.00	0.03	0.00	0.00	0.16	0.20	97.42
90N002f	2f13	ss	chlorite	25.22	0.07	20.59	21.85	0.25	17.79	0.03	0.03	0.03	0.00	0.04	0.00	0.02	0.00	0.03	0.13	0.13	86.19
90N002f	2f14	ss	chlorite	25.48	0.09	20.67	21.55	0.24	17.87	0.04	0.03	0.00	0.00	0.17	0.00	0.00	0.00	0.00	0.16	0.11	86.41
90N002f	2f15	ss	kspar??	65.16	0.09	18.28	0.28	0.00	0.06	0.00	0.18	14.78	0.01	0.04	0.00	0.00	0.00	0.00	0.00	0.00	98.89
90N002f	2f16	ss	plag	62.71	0.00	22.82	0.26	0.00	0.03	4.27	8.53	0.08	0.06	0.11	0.00	0.00	0.00	0.00	0.07	0.07	99.00
90N002f	2f17	ss	plag	62.43	0.00	22.75	0.29	0.00	0.00	4.44	8.62	0.00	0.04	0.00	0.00	0.00	0.00	0.00	0.01	0.17	98.76
90N002f	2f18	ss	plag	63.40	0.00	23.01	0.35	0.12	0.00	4.55	8.82	0.03	0.01	0.13	0.00	0.00	0.00	0.00	0.20	0.22	100.83
90N002f	2f19	ss	chlorite	25.48	0.21	21.03	21.56	0.27	17.90	0.11	0.01	0.00	0.07	0.15	0.00	0.00	0.00	0.00	0.10	0.03	86.92

22

Sample	Analysis	Location	Mineral	SiO2	TiO2	Al2O3	FeO	MnO	MgO	CaO	Na2O	K2O	Cr2O3	NiO	P2O5	Cl	SrO	ZrO2	La2O3	BaO	Total
90N013a	13a1	light r	amphibole	42.67	0.39	15.50	15.64	0.24	9.12	12.00	1.75	0.19	0.00	0.15	0.00	0.00	0.00	0.01	0.17	0.20	98.03
90N013a	13a2	dark core	amphibole	50.93	0.21	4.95	12.04	0.12	15.36	12.39	0.72	0.12	0.31	0.00	0.00	0.00	0.00	0.05	0.14	0.11	97.47
90N013a	13a3	light rim	amphibole	45.05	0.31	13.00	14.88	0.24	10.81	12.09	1.53	0.15	0.00	0.02	0.00	0.00	0.00	0.00	0.11	0.08	98.28
90N013a	13a4	dark core	amphibole	51.97	0.15	4.81	12.35	0.17	15.54	12.68	0.68	0.23	0.34	0.02	0.00	0.02	0.00	0.00	0.00	0.00	98.96
90N013a	13a5	light edge	amphibole	42.74	0.29	15.22	15.11	0.26	9.51	11.74	1.71	0.19	0.12	0.07	0.00	0.00	0.00	0.00	0.00	0.00	96.95
90N013a	13a6	in p/b	plag	60.23	0.00	24.22	0.20	0.03	0.00	6.29	8.47	0.02	0.05	0.00	0.00	0.00	0.00	0.00	0.10	0.20	99.82
90N013a	13a7	in p/b	quartz	97.60	0.00	0.01	0.13	0.00	0.01	0.00	0.00	0.00	0.00	0.06	0.00	0.00	0.00	0.00	0.00	0.00	97.82
90N013a	13a8	in p/b	plag	60.16	0.00	25.78	0.41	0.04	0.13	7.19	7.93	0.07	0.00	0.03	0.00	0.00	0.00	0.07	0.08	0.07	101.97
90N013a	13a9	in p/b	chlorite	25.39	0.10	20.83	23.41	0.30	16.46	0.13	0.19	0.00	0.00	0.01	0.00	0.00	0.00	0.00	0.10	0.01	86.96
90N013a	13a10	in p/b	apatite	0.04	0.00	0.00	0.69	0.00	0.08	56.82	0.00	0.01	0.00	0.26	42.36	0.03	0.00	0.00	0.04	0.07	100.41
90N013a	13a11	edge of p/b	amphibole	42.42	0.38	15.67	15.85	0.27	8.97	11.83	1.66	0.25	0.04	0.00	0.00	0.01	0.00	0.00	0.00	0.00	97.35
90N013a	13a12	ss	plag	60.60	0.00	24.18	0.36	0.06	0.03	5.93	8.49	0.09	0.00	0.00	0.00	0.00	0.00	0.04	0.00	0.00	99.76
90N013a	13a13	ss	chlorite	25.20	0.03	20.83	23.00	0.25	16.48	0.09	0.16	0.06	0.03	0.02	0.00	0.02	0.00	0.16	0.27	0.27	86.87
90N013a	13a14	ss	?	0.59	0.05	0.00	39.90	0.11	0.54	0.32	0.00	0.00	0.00	0.00	10.74	0.00	2.92	0.00	0.30	0.24	55.71
90N013a	13a15	ss	apatite	0.15	0.07	0.10	0.78	0.03	0.03	57.05	0.11	0.00	0.00	0.00	41.44	0.02	0.00	0.29	0.00	0.00	100.07
90N013a	13a16	ss	amphibole	50.25	0.29	13.01	13.85	0.29	8.68	10.41	1.58	0.20	0.12	0.00	0.00	0.00	0.00	0.00	0.04	0.03	98.74
90N013a	13a17	ss	epidote	37.63	0.06	25.80	8.73	0.08	0.11	24.25	0.11	0.02	0.07	0.06	0.00	0.00	0.00	0.00	0.00	0.04	96.96
90N013a	13a18	ss	ilmenite	0.45	52.44	0.10	42.18	2.97	0.22	0.48	0.00	0.01	0.16	0.00	0.00	0.00	0.10	0.14	0.24	0.62	100.12
90N013a	13a19	in p/b	titanite	30.47	39.18	0.88	0.66	0.01	0.03	28.95	0.07	0.00	0.08	0.00	0.00	0.01	0.00	0.00	0.09	0.44	100.86
90N013a	13a20	ss	amphibole	43.01	0.42	14.72	15.63	0.35	9.43	11.94	1.24	0.14	0.00	0.05	0.00	0.00	0.00	0.03	0.08	0.05	97.08
90N013a	13a21	ss	amphibole	47.81	0.31	8.76	13.68	0.24	12.54	12.65	0.84	0.17	0.00	0.07	0.00	0.04	0.00	0.00	0.04	0.00	97.14
90N013a	13a22	ss	epidote	38.30	0.16	27.04	7.46	0.13	0.03	24.74	0.03	0.00	0.08	0.00	0.00	0.01	0.00	0.00	0.00	0.00	97.99
90N013a	13a23	ss	plag	60.35	0.00	25.33	0.19	0.00	0.00	7.22	7.82	0.03	0.04	0.12	0.00	0.06	0.00	0.00	0.19	0.39	101.73
90N013a	13a24	edge of p/b	amphibole	42.02	0.44	16.27	15.32	0.30	8.85	11.91	1.76	0.27	0.02	0.00	0.00	0.00	0.00	0.00	0.00	0.00	97.16
90N013a	13a25	dark edge	chlorite	25.03	0.17	20.88	22.95	0.18	16.72	0.16	0.19	0.00	0.09	0.00	0.00	0.02	0.00	0.00	0.00	0.00	86.41
90N013a	13a26	dark edge	amphibole	47.15	0.22	10.24	14.31	0.16	12.27	12.52	1.27	0.15	0.22	0.00	0.00	0.00	0.00	0.00	0.01	0.06	98.59
90N013a	13a27	m	ilmenite	0.25	52.72	0.04	42.29	3.51	0.17	0.30	0.05	0.00	0.00	0.00	0.00	0.04	0.00	0.00	0.18	0.69	100.27
90N013a	13a28	m	epidote	38.12	0.17	25.26	9.52	0.09	0.07	24.62	0.06	0.00	0.14	0.02	0.00	0.01	0.00	0.11	0.03	0.18	98.40
90N013a	13a29	m	plag	60.00	0.07	25.24	0.11	0.00	0.00	7.15	7.56	0.12	0.05	0.12	0.00	0.00	0.00	0.06	0.01	0.04	100.53
90N013a	13a30	m	amphibole	42.00	0.45	15.45	14.87	0.28	9.25	12.00	1.53	0.32	0.02	0.00	0.00	0.01	0.00	0.00	0.00	0.00	96.19
90N013a	13a31	m	amphibole	42.25	0.32	15.72	14.77	0.33	9.02	11.88	1.58	0.28	0.08	0.11	0.00	0.02	0.00	0.00	0.00	0.00	96.35
90N013a	13a32	m	plag	60.61	0.00	24.74	0.24	0.05	0.03	6.57	7.27	0.06	0.01	0.00	0.00	0.00	0.00	0.00	0.00	0.07	99.64
90N013a	13a33	m	amphibole	42.19	0.39	15.50	15.45	0.32	9.02	12.04	1.70	0.25	0.11	0.00	0.04	0.00	0.00	0.00	0.00	0.00	97.02
90N013a	13a34	dark core	amphibole	49.65	0.26	6.10	12.62	0.32	14.42	12.54	1.02	0.14	0.31	0.02	0.00	0.03	0.00	0.00	0.18	0.07	97.69
90N013a	13a35	light rim	amphibole	42.97	0.25	15.25	15.68	0.25	9.51	12.16	1.60	0.18	0.00	0.00	0.00	0.00	0.00	0.00	0.09	0.14	98.08
90N015c	15c1	dark core	amphibole	52.90	0.15	3.83	11.47	0.22	16.35	12.87	0.64	0.09	0.48	0.00	0.00	0.00	0.00	0.00	0.00	0.00	99.01
90N015c	15c2	light rim	amphibole	42.57	0.34	14.62	15.94	0.25	9.54	11.90	1.59	0.34	0.05	0.00	0.00	0.00	0.00	0.07	0.16	0.35	97.73
90N015c	15c3	broken r	amphibole	43.25	0.42	14.04	14.75	0.29	10.00	11.94	1.53	0.24	0.04	0.01	0.00	0.00	0.00	0.02	0.02	0.00	96.56
90N015c	15c4	in p/b	ilmenite	0.28	52.35	0.06	43.09	2.89	0.22	0.21	0.04	0.03	0.05	0.00	0.00	0.00	0.01	0.10	0.00	0.56	99.90
90N015c	15c5	broken r	amphibole	43.87	0.12	9.85	18.34	0.32	13.10	9.23	0.54	0.19	0.00	0.17	0.00	0.05	0.00	0.00	0.00	0.08	95.84
90N015c	15c6	m	??	2.46	0.07	0.33	57.02	0.06	0.01	0.21	0.26	0.08	0.00	0.12	15.01	0.00	4.25	0.00	0.14	0.00	80.01
90N015c	15c7	ss	amphibole	42.48	0.52	14.40	15.83	0.19	9.02	12.00	1.56	0.33	0.09	0.00	0.00	0.00	0.00	0.06	0.00	0.01	96.49
90N015c	15c9	m	chlorite	24.87	0.12	21.18	21.65	0.23	17.03	0.07	0.16	0.00	0.03	0.09	0.00	0.00	0.00	0.07	0.00	0.00	85.50
90N015c	15c10	m	amphibole	41.91	0.41	15.81	15.67	0.40	8.86	11.91	1.58	0.33	0.00	0.00	0.00	0.00	0.00	0.00	0.00	0.00	96.90
90N015c	15c11	m	plag	62.02	0.00	23.72	0.14	0.00	0.16	5.36	8.80	0.00	0.03	0.09	0.00	0.00	0.00	0.00	0.00	0.00	100.32
90N015c	15c12	fresh ss	amphibole	42.08	0.42	15.82	15.82	0.48	9.17	11.93	1.54	0.33	0.00	0.03	0.00	0.00	0.00	0.10	0.00	0.00	97.75
90N015c	15c13	dark core s	amphibole	51.02	0.12	4.44	12.36	0.21	14.87	12.85	0.57	0.16	0.15	0.00	0.00	0.00	0.00	0.02	0.02	0.00	96.80
90N015c	15c14	light r ss	amphibole	42.87	0.30	13.43	15.76	0.15	9.50	12.01	1.49	0.27	0.19	0.10	0.00	0.05	0.00	0.05	0.00	0.11	96.27
90N015c	15c15	ss	chlorite	24.73	0.07	20.97	21.69	0.24	16.98	0.04	0.17	0.00	0.00	0.00	0.00	0.02	0.00	0.25	0.00	0.00	85.18
90N015c	15c16	ss	epidote	37.50	0.10	25.81	8.59	0.05	0.01	24.41	0.02	0.01	0.01	0.00	0.00	0.00	0.00	0.00	0.00	0.00	96.52
90N015c	15c17	ss	epidote	37.73	0.19	26.26	8.42	0.00	0.00	24.24	0.09	0.02	0.08	0.00	0.00	0.00	0.00	0.03	0.07	0.00	97.15
90N015c	15c18	ss	amphibole	46.92	0.41	9.73	14.10	0.18	12.17	12.23	1.21	0.23	0.06	0.08	0.00	0.03	0.00	0.00	0.00	0.00	97.35
90N015c	15c19	ss	Bad	23.21	0.07	7.23	8.40	0.26	3.61	4.80	1.00	0.34	0.00	0.33	2.78	0.00	3.13	0.00	0.00	0.05	55.21
90N015c	15c20	ss	ilmenite	0.21	52.12	0.10	42.82	3.05	0.32	0.38	0.03	0.00	0.00	0.00	0.00	0.03	0.06	0.05	0.00	0.38	99.54
90N015c	15c21	ss	chlorite	25.85	0.20	21.81	20.65	0.29	18.32	0.08	0.10	0.00	0.03	0.00	0.00	0.00	0.00	0.13	0.06	0.00	87.53
90N015c	15c22	ss	plag	51.93	0.00	30.05	0.47	0.00	0.14	12.99	4.43	0.05	0.00	0.03	0.01	0.03	0.00	0.00	0.02	0.15	100.30
90N015c	15c23	ss	plag	60.24	0.00	24.62	0.26	0.00	0.00	6.56	7.55	0.08	0.03	0.00	0.00	0.01	0.00	0.00	0.00	0.00	99.33
90N015c	15c24	ss	plag	59.35	0.04	25.01	0.21	0.01	0.14	6.93	7.89	0.05	0.00	0.03	0.00	0.00	0.00	0.00	0.00	0.00	99.65
90N015c	15c25	fresh core	amphibole	42.74	0.32	15.63	15.45	0.42	9.54	12.12	1.74	0.26	0.00	0.00	0.00	0.01	0.00	0.00	0.17	0.10	98.50
90N015c	15c26	dark core	amphibole	51.19	0.13	5.13	12.18	0.41	15.21	12.57	0.70	0.12	0.11	0.00	0.00	0.03	0.00	0.03	0.01	0.01	97.83
90N015c	15c27	light rim	amphibole	42.24	0.37	14.49	14.94	0.20	9.69	11.92	1.57	0.32	0.03	0.12	0.00	0.01	0.00	0.09	0.00	0.13	96.12
90N015c	15c28	fresh m	amphibole	41.76	0.53	14.62	15.91	0.28	8.86	11.67	1.34	0.22	0.15	0.05	0.00	0.05	0.00	0.07	0.02	0.00	95.53
90N015c	15c29	m	plag	59.45	0.00	24.52	0.45	0.07	0.03	6.55	7.91	0.03	0.15	0.03	0.00	0.01	0.00	0.00	0.00	0.01	99.19
90N015c	15c30	m	kspar??	64.53	0.00	18.68	0.24	0.00	0.09	0.04	0.44	16.18	0.00	0.00	0.00	0.00	0.00	0.00	0.04	0.24	100.47
90N015c	15c31	m	amphibole	48.05	0.14	7.03	13.90	0.35	12.84	12.33	0.83	0.13	0.00	0.09	0.00	0.00	0.00	0.00	0.06	0.09	95.85
90N015c	15c32	m	ilmenite	0.31	52.45	0.00	42.67	2.96	0.29	0.31	0.00	0.02	0.00	0.03	0.00	0.00	0.16	0.19	0.41	0.52	100.30
90N015c	15c33	m	amphibole	42.73	0.11	9.64	15.33	0.30	15.75	9.49	0.41	0.04	0.00	0.00	0.00	0.00	0.00	0.20	0.01	0.03	94.05
90N015c	15c34	m	chlorite	25.62	0.21	20.51	20.89	0.29	17.49	0.17	0.24	0.03	0.02	0.08	0.00	0.05	0.00	0.08	0.00	0.00	85.67
90N015c	15c35	m	plag	60.00	0.04	24.82	0.25	0.00	0.09	6.75	7.28	0.05	0.12	0.06	0.00	0.01	0.00	0.06	0.00	0.06	99.58
90N015d	15d1	in p/b	chlorite	25.55	0.08	21.10	20.50	0.39	18.91	0.05	0.19	0.00	0.26	0.06	0.00	0.00	0.00	0.00	0.00	0.07	87.16
90N015d	15d2	dark core	amphibole	52.19	0.15	3.65	10.70	0.20	16.64	12.67	0.54	0.09	0.31	0.06	0.00	0.03	0.00	0.00	0.13	0.05	97.39
90N015d	15d3	light rim	amphibole	44.07	0.36	14.11	14.30	0.34	10.71	12.35	1.37	0.30	0.00	0.00	0.00	0.00	0.00	0.09	0.00	0.00	97.99
90N015d	15d4	ss	kspar??	64.76	0.00	18.34	0.02	0.00	0.00	0.01	0.15	16.58	0.00	0.07	0.00	0.02	0.00	0.11	0.22	0.23	100.52
90N015d	15d5	edge of p/b	chlorite	26.10	0.03	19.97	21.33	0.30	18.31	0.04	0.11	0.03	0.00	0.01	0.00	0.02	0.00	0.03	0.19	0.05	86.52
90N015d	15d6	m	amphibole	44.60	0.38	13.41	13.81	0.35	10.97	12.14	1.17	0.30	0.05	0.00	0.00	0.01	0.00	0.00	0.00	0.00	97.20
90N015d	15d7	m	plag	60.09	0.00	25.32	0.19	0.00	0.15	7.02	8.13	0.03	0.01	0.00	0.00	0.00	0.00	0.09	0.00	0.00	101.02
90N015d	15d8	m	titanite	30.17	39.24	0.98	0.26	0.11	0.03	29.67	0.14	0.00	0.17	0.05	0.00	0.02	0.00	0.00	0.21	0.31	101.36
90N015d	15d9	in p/b	titanite	30.16	38.06	1.50	0.85	0.07	0.04	29.21	0.08	0.00	0.05	0.07	0.00	0.00	0.00	0.00	0.23	0.35	100.66
90N015d	15d10	m	titanite	30.26	40.06	0.95	0.36	0.00	0.01	29.74	0.08	0.00	0.04	0.01	0.00	0.02	0.00	0.00	0.00	0.00	101.53
90N015d	15d11	m	amphibole	51.35	0.00	5.05	11.47	0.18	15.48	13.07	0.51	0.11	0.01	0.00	0.00	0.00	0.00	0.00	0.04	0.19	97.45
90N015d	15d12	m	kspar??	50.42	0.00	31.96	2.72	0.04	1.33	0.11	0.08	8.64	0.04	0.00	0.00	0.00	0.00	0.00	0.01	0.15	95.50
90N015d	15d13	m	chlorite	26.28	0.05	21.02	20.39	0.38	19.19	0.07	0.18	0.00	0.11	0.04	0.00	0.00	0.00	0.00	0.13	0.15	88.00
90N015d	15d14	m	amphibole	44.69	0.51	13.40	13.57	0.30	11.27	12.16	1.35	0.23	0.00	0.14	0.00	0.00	0.00	0.00	0.07	0.00	97.68
90N015d	15d15	m	amphibole	31.74	0.21	9.77	5.10	0.12	8.14	6.80	1.05	0.17	0.00	0.00	0.04	0.00	0.02	0.00	0.02	0.07	63.25

22

Sample	Analysis	Location	Mineral	SiO2	TiO2	Al2O3	FeO	MnO	MgO	CaO	Na2O	K2O	Cr2O3	NiO	P2O5	Cl	SrO	ZrO2	La2O3	BaO	Total
90N015I	1.00		kk control	39.17	4.89	13.81	10.43	0.00	12.64	10.26	2.62	2.09	0.00	0.00	0.00	0.00	0.00	0.11	0.00	0.00	96.03
90N015I	2.00		gnt 12442	38.52	0.08	21.78	22.28	0.53	11.28	4.63	0.15	0.00	0.04	0.00	0.00	0.02	0.00	0.08	0.18	0.13	99.71
90N015I	15I2	rim	garnet	36.30	0.02	20.50	31.32	6.83	0.37	4.41	0.00	0.00	0.04	0.00	0.00	0.05	0.00	0.00	0.04	0.00	99.87
90N015I	15I3	rim	garnet	36.73	0.10	20.64	31.14	7.01	0.56	4.74	0.03	0.00	0.00	0.02	0.10	0.00	0.00	0.00	0.00	0.00	101.08
90N015I	15I4	core	garnet	36.25	0.27	20.18	25.21	11.48	0.33	6.33	0.02	0.00	0.00	0.00	0.00	0.01	0.00	0.13	0.08	0.15	100.43
90N015I	15I5	core	garnet	36.67	0.03	20.16	27.28	8.41	0.33	6.94	0.06	0.00	0.01	0.00	0.00	0.01	0.00	0.12	0.07	0.15	100.24
90N015I	15I6	rim	garnet	36.66	0.19	20.42	26.40	11.32	0.44	5.97	0.02	0.00	0.03	0.00	0.00	0.02	0.00	0.02	0.00	0.00	101.50
90N015I	15I9	matrix	biotite	46.19	0.18	33.69	3.02	0.04	0.44	0.15	0.43	8.95	0.00	0.00	0.00	0.00	0.00	0.00	0.00	0.43	93.51
90N015I	15I10	matrix	biotite	46.89	0.09	34.52	3.04	0.07	0.60	0.05	0.52	9.29	0.04	0.26	0.00	0.00	0.00	0.00	0.14	0.64	96.16
90N015I	15I11	edge	biotite	45.63	0.00	32.75	4.68	0.05	0.71	0.15	0.33	8.91	0.00	0.21	0.00	0.00	0.00	0.03	0.00	0.35	93.82
90N015I	15I12	matrix	biotite	46.83	0.02	34.02	3.14	0.00	0.61	0.00	0.29	9.22	0.07	0.08	0.00	0.00	0.00	0.00	0.09	0.67	95.04
90N015I	15I13	matrix	biotite	46.41	0.13	33.40	3.41	0.05	0.76	0.02	0.26	9.18	0.00	0.00	0.00	0.01	0.00	0.04	0.14	0.46	94.29
90N015I	15I14	matrix	biotite	46.80	0.12	34.18	2.89	0.04	0.64	0.05	0.45	8.95	0.00	0.11	0.00	0.02	0.00	0.00	0.03	0.37	94.65
90N015I	15I15	core	plag	67.74	0.01	19.77	0.12	0.00	0.05	0.54	10.31	0.01	0.00	0.00	0.00	0.00	0.00	0.18	0.00	0.00	98.72
90N015I	15I16	rim	plag	68.46	0.12	20.13	0.00	0.03	0.08	0.68	10.38	0.00	0.00	0.13	0.00	0.02	0.00	0.02	0.02	0.00	100.08
90N015I	15I18	matrix	plag	63.50	0.00	22.78	0.00	0.00	0.03	3.74	9.34	0.06	0.08	0.28	0.00	0.02	0.00	0.00	0.00	0.02	99.86
90N015I	15I19	matrix	plag	63.40	0.04	22.26	0.11	0.03	0.01	3.58	10.06	0.09	0.04	0.22	0.00	0.02	0.00	0.00	0.00	0.01	99.88
90N015I	15I20	matrix	plag	63.29	0.00	22.24	0.08	0.00	0.01	3.60	9.68	0.07	0.00	0.01	0.00	0.00	0.00	0.00	0.12	0.19	99.29
90N015I	15I21		?	32.57	1.87	17.12	27.92	0.12	3.16	0.00	0.07	9.19	0.04	0.00	0.00	0.03	0.00	0.00	0.00	0.00	92.09
90N015I	15I22	matrix	chlorite	22.49	0.04	20.00	37.33	0.36	4.50	0.05	0.21	0.10	0.05	0.00	0.01	0.03	0.00	0.00	0.03	0.03	85.22
90N015I	15I23	matrix	?	30.87	1.34	16.73	28.29	0.17	3.36	0.14	0.20	7.65	0.00	0.16	0.00	0.03	0.00	0.00	0.02	0.14	89.10
90N015I	15I24	matrix	?	28.68	1.85	17.56	32.85	0.15	3.89	0.08	0.11	5.22	0.07	0.00	0.00	0.05	0.00	0.07	0.00	0.02	90.60
90N015I	15I25	matrix	?	22.68	0.18	20.25	37.91	0.37	4.64	0.02	0.12	0.01	0.00	0.00	0.00	0.01	0.00	0.10	0.12	0.05	86.46
90N015I	15I26	matrix	?	46.70	0.10	34.20	3.26	0.01	0.55	0.00	0.41	8.91	0.02	0.18	0.00	0.00	0.00	0.00	0.02	0.49	94.84

22

Sample	Analysis	Location	Mineral	SiO2	TiO2	Al2O3	FeO	MnO	MgO	CaO	Na2O	K2O	Cr2O3	NiO	P2O5	Cl	SrO	ZrO2	La2O3	BaO	Total
			kkcontrol	39.58	4.81	13.59	10.42	0.00	12.61	10.37	2.60	2.08	0.15	0.03	0.00	0.00	0.00	0.00	0.00	0.00	96.23
15-43	1		calcite	0.18	0.00	0.00	0.00	0.05	0.08	55.19	0.08	0.00	0.07	0.00	0.04	0.02	0.00	0.00	0.08	0.09	55.88
15-43	2		calcite	0.18	0.00	0.00	0.64	0.57	0.45	56.27	0.01	0.01	0.01	0.10	0.02	0.02	0.00	0.00	0.11	0.16	58.56
15-43	3	matrix	amphibole	42.78	0.39	14.81	16.60	0.11	8.97	11.73	1.55	0.33	0.06	0.05	0.00	0.00	0.00	0.02	0.02	0.06	97.48
15-43	4		amphibole	47.64	0.36	8.27	13.82	0.31	12.72	12.41	0.95	0.23	0.13	0.05	0.00	0.00	0.00	0.00	0.00	0.00	96.90
15-43	5		amphibole	43.86	0.30	12.87	14.81	0.50	10.76	12.24	1.35	0.45	0.00	0.00	0.00	0.00	0.00	0.02	0.00	0.00	97.17
15-43	6		epidote	38.48	0.32	27.07	6.92	0.17	0.12	24.43	0.00	0.01	0.24	0.00	0.00	0.01	0.00	0.00	0.00	0.00	97.75
15-43	8		chlorite	25.44	0.13	19.99	22.91	0.24	15.96	0.27	0.03	0.01	0.11	0.00	0.00	0.00	0.00	0.10	0.05	0.02	85.26
15-43	9		titanite	30.34	37.77	1.33	0.70	0.12	0.02	29.44	0.00	0.01	0.08	0.06	0.00	0.00	0.00	0.00	0.35	1.42	101.65
15-43	10		titanite	30.24	37.37	1.52	0.18	0.03	0.05	29.23	0.00	0.00	0.11	0.00	0.00	0.00	0.00	0.17	0.21	0.78	99.90
15-43	11		calcite	0.17	0.02	0.00	0.95	0.44	0.47	58.17	0.01	0.01	0.00	0.25	0.05	0.00	0.04	0.00	0.08	0.00	60.66
15-43	12		plag	60.58	0.00	24.44	0.34	0.00	0.06	6.23	8.16	0.02	0.14	0.00	0.00	0.00	0.00	0.00	0.00	0.00	99.97
15-43	13		plag	59.82	0.00	24.66	0.28	0.03	0.05	6.66	7.24	0.04	0.08	0.04	0.00	0.00	0.00	0.02	0.00	0.22	99.13
15-43	14		plag	60.29	0.00	23.99	0.14	0.00	0.00	5.87	7.91	0.08	0.00	0.08	0.00	0.02	0.00	0.11	0.18	0.43	99.09
15-43	15		chlorite	26.41	0.08	19.04	22.89	0.41	17.28	0.01	0.12	0.00	0.08	0.00	0.00	0.00	0.00	0.00	0.00	0.00	86.31
15-43	16		ilmenite	0.17	51.70	0.00	41.75	3.16	0.34	0.39	0.21	0.00	0.00	0.04	0.00	0.01	0.07	0.22	0.13	0.89	99.07
15-51b	51b-1		calcite	0.15	0.00	0.00	0.12	0.39	0.21	58.59	0.16	0.00	0.05	0.05	0.04	0.03	0.04	0.00	0.02	0.14	59.99
15-51b	51b-2		chlorite	25.24	0.11	20.14	22.99	0.29	16.40	0.01	0.03	0.00	0.00	0.00	0.00	0.03	0.00	0.00	0.11	0.07	85.41
15-51b	18.00		kkcontrol	39.53	4.86	13.55	10.22	0.00	12.86	10.24	2.68	2.03	0.00	0.00	0.00	0.00	0.00	0.10	0.14	0.21	96.42
15-51b	51b-3		epidote	37.54	0.11	23.97	10.48	0.03	0.09	24.19	0.02	0.00	0.02	0.00	0.00	0.01	0.00	0.03	0.00	0.04	96.52
15-51b	51b-4		calcite	0.11	0.00	0.00	0.17	0.01	0.00	57.10	0.06	0.00	0.00	0.10	0.03	0.00	0.03	0.00	0.09	0.25	57.94
15-51b	51b-5		plag	67.46	0.00	20.50	0.29	0.00	0.06	1.43	9.56	0.09	0.08	0.00	0.00	0.00	0.00	0.02	0.00	0.24	99.74
15-51b	51b-6		ilmenite	0.25	51.34	0.03	41.98	2.93	0.24	0.37	0.02	0.00	0.00	0.00	0.01	0.00	0.10	0.06	0.57	1.82	99.73
15-51b	51b-7		amphibole	40.73	0.33	12.84	18.65	0.14	10.92	9.46	1.20	0.25	0.16	0.00	0.00	0.00	0.00	0.00	0.00	0.00	94.69
15-51b	51b-8	dark core	amphibole	53.97	0.04	1.95	11.80	0.17	16.77	12.66	0.36	0.04	0.07	0.00	0.00	0.00	0.00	0.00	0.17	0.18	98.18
15-51b	51b-9	light rim	amphibole	43.04	0.38	13.04	16.16	0.23	9.39	11.86	1.58	0.39	0.14	0.00	0.00	0.00	0.00	0.03	0.00	0.13	96.37
15-51b	51b-10	dark core	amphibole	52.41	0.19	4.31	13.27	0.11	15.55	12.60	0.52	0.11	0.12	0.02	0.00	0.00	0.00	0.00	0.15	0.07	99.43
15-51b	51b-11	light rim	amphibole	42.33	0.35	13.57	16.68	0.23	9.21	11.70	1.76	0.41	0.00	0.10	0.00	0.00	0.00	0.13	0.00	0.04	96.52
15-51b	51b-12	light rim	amphibole	42.24	0.55	13.69	16.62	0.16	8.98	11.84	1.59	0.48	0.09	0.10	0.00	0.07	0.00	0.01	0.00	0.00	96.39
15-51b	51b-13		plag	62.21	0.05	23.79	0.36	0.00	0.09	5.40	8.48	0.01	0.02	0.22	0.00	0.01	0.00	0.00	0.07	0.09	100.80
15-51b	51b-14		?mica	30.45	0.14	16.94	31.79	0.27	8.86	0.25	0.72	0.00	0.00	0.21	0.00	0.04	0.00	0.19	0.04	0.00	89.92
15-51b	51b-15		ilmenite	0.26	51.95	0.01	43.03	2.35	0.16	0.35	0.00	0.01	0.00	0.10	0.10	0.00	0.09	0.07	0.42	0.45	99.36
15-51b	51b-16		plag	62.17	0.06	23.72	0.35	0.00	0.02	5.05	8.42	0.04	0.00	0.06	0.00	0.00	0.00	0.05	0.07	0.00	100.01
15-51b	51b-17		chlorite	25.91	0.00	19.80	22.85	0.26	16.72	0.03	0.00	0.01	0.00	0.00	0.00	0.00	0.00	0.06	0.04	0.14	85.82
15-51b	51b-18		chlorite	25.55	0.01	20.20	23.81	0.33	16.33	0.00	0.10	0.05	0.04	0.00	0.00	0.02	0.00	0.00	0.03	0.09	86.56
15-51b	51b-19	small	amphibole	46.06	0.28	9.77	15.46	0.24	11.08	12.51	1.13	0.30	0.10	0.09	0.39	0.00	0.00	0.00	0.00	0.00	97.40
15-51a	51a-1	dark	amphibole	52.58	0.20	5.24	8.22	0.27	18.22	12.61	0.85	0.10	0.15	0.00	0.00	0.02	0.00	0.00	0.00	0.00	98.45
15-51a	51a-2		plag	62.58	0.00	22.81	0.20	0.00	0.00	4.52	9.25	0.10	0.02	0.03	0.00	0.02	0.00	0.02	0.00	0.10	99.65
15-51a	51a-3	dark core	amphibole	55.72	0.11	1.86	6.68	0.18	20.35	13.03	0.22	0.08	0.40	0.27	0.00	0.00	0.00	0.00	0.23	0.14	99.28
15-51a	51a-4	light	amphibole	43.91	1.48	12.46	10.33	0.28	14.22	12.01	1.68	0.84	0.03	0.05	0.00	0.00	0.00	0.06	0.00	0.00	97.35
15-51a	51a-5		plag	63.47	0.00	23.11	0.14	0.01	0.00	4.60	8.31	0.08	0.06	0.03	0.00	0.01	0.00	0.00	0.00	0.14	99.94
15-51a	51a-6		?	27.70	0.00	13.06	6.26	0.44	0.13	18.81	0.40	0.93	0.00	0.03	7.75	0.06	0.09	0.01	0.00	0.06	75.74
15-51a	51a-7	in p/b	plag	65.16	0.07	21.98	0.14	0.01	0.10	3.14	10.09	0.03	0.00	0.00	0.00	0.00	0.00	0.00	0.00	0.00	100.72
15-51a	51a-8	dark p/b	amphibole	55.50	0.00	2.37	6.49	0.20	20.28	13.22	0.42	0.10	0.33	0.00	0.00	0.04	0.00	0.07	0.00	0.12	99.16
15-51a	51a-9	light p/b	amphibole	42.92	0.89	12.85	12.41	0.12	13.88	12.35	2.19	0.94	0.05	0.00	0.00	0.01	0.00	0.04	0.03	0.01	98.68
15-51a	51a-10		titanite	30.69	38.17	1.24	0.29	0.00	0.09	29.47	0.00	0.06	0.18	0.00	0.00	0.00	0.00	0.00	0.35	1.12	101.65
15-51a	51a-11	light rim p/b	amphibole	43.89	0.76	13.43	11.53	0.14	13.28	12.00	1.66	0.68	0.12	0.00	0.00	0.03	0.00	0.00	0.11	0.01	97.64
15-51a	51a-12	dark rim p/b	amphibole	53.63	0.09	3.05	7.96	0.15	18.73	13.03	0.47	0.11	0.62	0.00	0.00	0.04	0.00	0.01	0.00	0.00	97.89
15-51a	51a-13	dark	amphibole	53.15	0.13	4.20	7.28	0.06	18.86	12.96	0.60	0.05	0.15	0.20	0.00	0.00	0.00	0.00	0.04	0.00	97.68
15-51a	51a-14	light	amphibole	41.98	0.50	16.08	11.68	0.26	11.50	11.67	1.84	1.09	0.15	0.13	0.00	0.01	0.00	0.00	0.04	0.06	96.99
15-51a	51a-15		plag	65.21	0.00	22.23	0.00	0.00	0.03	3.31	9.73	0.02	0.00	0.07	0.00	0.00	0.00	0.01	0.08	0.10	100.79
kk	1-kk		kkcontrol	39.31	4.93	13.74	10.16	0.00	12.97	10.34	2.71	2.08	0.00	0.17	0.03	0.00	0.00	0.00	0.00	0.00	96.44
01N037	37-1	core	amphibole	55.07	0.11	0.81	8.93	0.30	18.86	12.85	0.28	0.03	0.00	0.00	0.00	0.02	0.00	0.00	0.00	0.00	97.26
01N037	37-2	rim	amphibole	53.87	0.10	1.60	12.73	0.34	16.22	12.16	0.29	0.00	0.04	0.00	0.00	0.00	0.00	0.10	0.06	0.05	97.56
01N037	37-3		plag??	53.08	0.00	28.96	0.47	0.00	0.02	12.31	4.74	0.08	0.00	0.02	0.00	0.00	0.00	0.00	0.16	0.11	99.95
01N037	37-4		epidote??	37.78	0.04	25.53	8.62	0.00	0.06	24.29	0.11	0.00	0.05	0.00	0.00	0.00	0.00	0.00	0.00	0.00	96.48
01N037	37-5		epidote??	36.91	0.27	23.34	10.90	0.16	0.00	24.07	0.17	0.05	0.01	0.05	0.00	0.00	0.00	0.00	0.00	0.00	95.92
01N037	37-6		epidote??	38.14	0.01	28.11	5.29	0.06	0.00	24.73	0.03	0.02	0.00	0.13	0.00	0.00	0.00	0.03	0.00	0.07	96.62
01N037	37-7		epidote??	38.51	0.18	30.00	3.40	0.03	0.04	24.76	0.00	0.00	0.00	0.00	0.00	0.02	0.00	0.00	0.01	0.00	96.96
01N037	37-8		biotite	49.94	0.00	35.20	0.44	0.01	0.30	0.15	1.41	8.77	0.00	0.03	0.00	0.00	0.00	0.08	0.00	0.34	96.67
01N037	37-9		plag	66.68	0.00	21.09	0.16	0.03	0.00	1.81	9.37	0.10	0.03	0.00	0.00	0.06	0.00	0.16	0.11	0.09	99.71
01N037	37-10		ilmenite	1.98	47.96	0.62	38.49	2.23	0.59	0.46	0.04	0.04	0.09	0.00	0.03	0.00	0.10	0.08	0.15	0.64	93.52
01N037	37-11		epidote??	37.77	0.09	23.91	10.94	0.16	0.05	24.31	0.11	0.00	0.03	0.00	0.00	0.00	0.00	0.00	0.00	0.00	97.36
01N037	37-12	core	amphibole	53.38	0.32	2.32	13.32	0.30	15.53	13.04	0.48	0.01	0.00	0.00	0.00	0.01	0.00	0.04	0.00	0.00	98.74
01N037	37-13	rim	amphibole	53.31	0.11	1.88	13.44	0.27	15.27	12.75	0.32	0.01	0.01	0.14	0.00	0.00	0.00	0.14	0.04	0.05	97.74
01N037	37-14	center	epidote??	39.55	0.00	33.09	0.65	0.04	0.04	25.34	0.04	0.04	0.00	0.00	0.00	0.03	0.00	0.00	0.00	0.07	98.91
01N037	37-15		epidote??	38.03	0.00	27.17	6.90	0.10	0.06	24.27	0.02	0.00	0.05	0.23	0.00	0.00	0.00	0.12	0.00	0.14	97.10
01N037	37-16	core	amphibole	55.20	0.12	1.22	9.49	0.46	19.45	12.14	0.39	0.01	0.03	0.00	0.00	0.02	0.00	0.00	0.00	0.00	98.52
01N037	37-17	rim	amphibole	54.22	0.17	1.74	12.06	0.38	17.20	12.12	0.47	0.02	0.00	0.08	0.00	0.00	0.00	0.06	0.09	0.04	98.64
01N037	37-18	core	amphibole	54.43	0.11	1.70	11.73	0.29	17.80	11.89	0.52	0.06	0.01	0.13	0.00	0.00	0.00	0.00	0.13	0.05	98.84
01N037	37-19	rim	chlorite	25.68	0.00	19.83	24.36	0.17	15.39	0.05	0.04	0.00	0.00	0.13	0.00	0.00	0.00	0.00	0.00	0.00	85.65
01N037	37-20		ilmenite	0.15	51.65	0.00	43.20	2.48	0.05	0.29	0.07	0.00	0.00	0.16	0.00	0.02	0.11	0.16	0.34	0.94	99.61
01N037	37-21		epidote??	37.16	0.17	22.43	11.77	0.03	0.00	23.85	0.00	0.03	0.36	0.01	0.00	0.00	0.00	0.00	0.00	0.00	95.81
01N030d	30d-1	core	amphibole	44.13	0.64	11.50	13.89	0.35	11.48	11.41	1.47	0.28	0.14	0.00	0.00	0.01	0.00	0.00	0.08	0.07	95.44
01N030d	30d-2	rim	amphibole	42.93	0.62	13.45	14.28	0.27	10.88	11.75	1.77	0.40	0.11	0.00	0.00	0.00	0.00	0.00	0.00	0.00	96.46
01N030d	30d-3	core	amphibole	42.63	0.47	13.63	14.49	0.29	10.61	11.65	1.63	0.29	0.22	0.13	0.00	0.00	0.00	0.00	0.07	0.26	96.37
01N030d	30d-4	rim	amphibole	42.81	0.33	13.60	14.53	0.21	10.47	11.95	1.74	0.36	0.09	0.05	0.00	0.00	0.00	0.00	0.02	0.15	96.30
01N030d	30d-5	core	amphibole	43.01	0.56	13.35	14.83	0.28	10.76	11.82	1.61	0.34	0.14	0.15	0.00	0.02	0.00	0.00	0.09	0.07	97.02
01N030d	30d-6	rim	amphibole	43.01	0.58	13.01	15.03	0.25	10.93	11.61	1.54	0.33	0.12	0.00	0.00	0.00	0.00	0.00	0.16	0.17	96.74
01N030d	30d-7	rim	plag	60.14	0.00	25.08	0.10	0.00	0.07	7.23	7.52	0.05	0.03	0.00	0.00	0.00	0.00	0.03	0.00	0.15	100.40
01N030d	30d-8	core	plag	57.64	0.09	26.56	0.27	0.02	0.00	9.25	6.66	0.05	0.00	0.07	0.00	0.02	0.00	0.00	0.00	0.00	100.63
01N030d	30d-9		??	39.03	0.00	32.83	0.16	0.00	0.00	25.26	0.07	0.02	0.01	0.00	0.00	0.04	0.00	0.00	0.00	0.04	97.46
01N030d	30d-10		kspar	65.26	0.02	18.30	0.08	0.09	0.00	0.06	0.50	15.30	0.03	0.14	0.00	0.08	0.00	0.00	0.00	0.00	99.87
01N030d	30d-11		kspar	65.24	0.11	18.46	0.00	0.01	0.04	0.07	0.48	14.77	0.15	0.13	0.00	0.04	0.00	0.00	0.11	0.17	99.78
01N030d	30d-12		bt	49.43	0.03	30.44	3.56	0.00	2.16	0.07	0.25	8.06	0.00	0.00	0.00	0.05	0.00	0.00	0.02	0.09	94.15
01N030d	30d-13		plag	57.87	0.00	25.63	0.06	0.03	0.01	8.32	6.74	0.03	0.04	0.11	0.00	0.00	0.00	0.00	0.00	0.00	98.86
01N030d	30d-14		apatite	0.02	0.07	0.08	0.26	0.00	0.14	57.32	0.04	0.00	0.04	0.12	41.97	0.06	0.00	0.00	0.07	0.00	100.19
01N030d	30d-15		rutile	0.24	97.42	0.00	0.79	0.06	0.00	0.49	0.08	0.01	0.00	0.15	0.00	0.01	0.03	0.16	0.91	2.38	102.74
01N030d	30d-16	core	plag	60.92	0.00	24.78	0.16	0.01	0.04	6.40	7.56	0.09	0.00	0.06	0.00	0.00	0.00	0.00	0.00	0.10	100.11
01N030d	30d-17	rim	plag	60.44	0.00	24.27	0.35	0.00	0.04	6.33	7.38	0.04	0.09	0.00	0.00	0.00	0.00	0.00	0.01	0.07	99.03
01N030d	30d-18	core	plag	57.79	0.09	26.55	0.19	0.00	0.11	9.02	6.99	0.08	0.06	0.00	0.00	0.00	0.00	0.00	0.05	0.04	100.97
01N030d	30d-19	rim	plag	60.82	0.00	24.49	0.10	0.00	0.00	6.32	7.95	0.06	0.00	0.00	0.00	0.00	0.00	0.00	0.01	0.12	99.87
01N030d	30d-20		quartz	98.34	0.00	0.00	0.14	0.00	0.06	0.00	0.05	0.00	0.07	0.00	0.00	0.00	0.00	0.00	0.00	0.00	98.66
15-44	44-1	core light	amphibole	42.90	0.30	13.98	15.68	0.19	8.79	11.95	2.21	1.03	0.64	0.08	0.00	0.00	0.00	0.00	0.00	0.00	97.74
15-44	44-2	rim light	amphibole	42.28	0.47	15.04	15.95	0.24	8.68	12.08	1.51	0.30	0.05	0.00	0.00	0.01	0.00	0.09	0.00	0.00	96.71
15-44	44-3	dark	amphibole	50.01	0.18	7.01	13.04	0.25	13.94	12.48	0.81	0.27	0.55	0.05	0.00	0.02	0.00	0.00	0.00	0.00	98.62
15-44	44-4		chlorite	25.61	0.16	20.67	22.03	0.28	17.43	0.04	0.15	0.02	0.03	0.11	0.00	0.00	0.00	0.11	0.00	0.00	86.64
15-44	44-5		chlorite	25.54	0.03	21.12	23.74	0.33	16.30	0.06	0.16	0.05	0.00	0.09	0.00	0.00	0.00	0.02	0.00	0.00	87.42
15-44	44-6		chlorite	25.97	0.11	20.71	23.09	0.32	16.82	0.06	0.14	0.04	0.00	0.13	0.00	0.05	0.00	0.00	0.02	0.00	87.45
15-44	44-7	ss matrix	amphibole	44.13	0.47	14.13	16.11	0.30	9.55	12.37	1.45	0.26	0.04	0.04	0.00	0.00	0.00	0.10	0.00	0.04	99.00
15-44	44-8	ss	amphibole	53.09	0.04	4.01	12.08	0.37	16.02	12.77	0.50	0.13	0.00	0.00	0.00	0.00	0.00	0.00	0.00	0.00	99.01
15-44	44-9	rim	amphibole	42.58	0.49	15.68	15.97	0.26	8.88	12.01	1.68	0.25	0.03	0.00	0.00	0.02	0.00	0.00	0.00	0.00	97.84
15-44	44-10	matrix	amphibole	43.36	0.29	15.03	17.11	0.29	8.65	12.03	1.26	0.19	0.00	0.00	0.00	0.00	0.00	0.14	0.02	0.00	98.37
15-44	44-11	matrix	plag	60.08	0.04	25.41	0.12	0.00	0.10	7.24	7.55	0.05	0.06	0.00	0.00	0.00	0.00	0.00	0.00	0.00	100.66
15-44	44-12		ilmenite	0.25	53.39	0.05	43.21	2.86	0.28	0.16	0.09	0.01	0.00	0.00	0.00	0.02	0.06	0.03	0.30	0.83	101.56
15-44	44-13		ilmenite	1.52	52.33	0.04	42.19	2.86	0.22	1.48	0.07	0.00	0.02	0.08	0.04	0.00	0.10	0.18	0.22	0.93	102.27
15-44	44-14	ss	plag	59.99	0.00	24.72	0.09	0.00	0.06	6.99	7.55	0.08	0.10	0.08	0.00	0.00	0.00	0.10	0.10	0.11	99.97
15-44	44-15	matrix	plag	60.23	0.00	24.83	0.06	0.09	0.00	6.83	7.26	0.24	0.00	0.11	0.00	0.01	0.00	0.00	0.00	0.15	99.80
15-44	44-16	in p/b	plag	58.35	0.01	25.70	0.21	0.04	0.06	7.92	7.60	0.05	0.12	0.00	0.00	0.01	0.00	0.00	0.00	0.00	100.06
15-44	44-17		epidote	39.04	0.11	27.91	6.78	0.12	0.06	24.85	0.16	0.00	0.01	0.00	0.00	0.00	0.00	0.08	0.35	0.19	99.67
15-44	44-18		chlorite	25.49	0.04	21.23	21.92	0.36	17.04	0.25	0.09	0.00	0.02	0.12	0.00	0.01	0.00	0.03	0.00	0.09	86.69
15-44	44-19		plag	58.31	0.00	25.63	0.27	0.07	0.00	7.91	7.26	0.05	0.00	0.08	0.00	0.00	0.00	0.00	0.00	0.00	99.58
15-44	44-20		epidote	37.89	0.00	28.04	0.95	0.12	0.29	22.80	0.28	0.19	0.08	0.01	0.00	0.02	0.00	0.04	0.00	0.07	90.79
01N043	43-1		chlorite	25.66	0.07	19.82	23.06	0.43	16.86	0.02	0.12	0.04	0.01	0.02	0.00	0.02	0.00	0.00	0.00	0.01	86.15
01N043	43-2		epidote	37.39	0.17	22.45	11.38	0.00	0.05	23.94	0.11	0.00	0.03	0.00	0.00	0.01	0.00	0.00	0.12	0.11	95.76
01N043	43-3	matrix	titantie	29.64	36.62	1.14	1.10	0.00	0.00	28.50	0.01	0.00	0.15	0.07	0.00	0.00	0.00	0.00	0.18	0.94	98.33
01N043	43-4		biotite	47.28	0.02	35.67	1.81	0.00	0.67	0.00	0.28	8.76	0.00	0.00	0.00	0.03	0.00	0.04	0.02	0.31	94.90
01N043	43-5		plag	67.91	0.00	19.98	0.07	0.00	0.02	0.92	10.00	0.04	0.00	0.08	0.00	0.01	0.00	0.12	0.20	0.35	99.71
01N043	43-6		apatite	0.08	0.00	0.04	0.09	0.06	0.00	57.24	0.02	0.07	0.02	0.09	42.13	0.12	0.00	0.00	0.00	0.11	100.05
01N043	43-7		chlorite	25.18	0.07	19.20	22.87	0.43	17.04	0.01	0.11	0.00	1.32	0.03	0.00	0.02	0.00	0.05	0.00	0.00	86.32
01N043	43-8		epidote	37.90	0.28	22.38	12.59	0.09	0.00	24.22	0.00	0.01	0.00	0.14	0.00	0.00	0.00	0.00	0.03	0.00	97.63
01N043	43-9		mica	35.88	1.61	15.70	18.51	0.27	11.31	0.00	0.02	9.58	0.11	0.00	0.00	0.07	0.00	0.11	0.00	0.25	93.41
01N043	43-10		mica	37.46	1.64	15.98	18.53	0.20	12.20	0.00	0.19	9.69	0.08	0.12	0.00	0.02	0.00	0.06	0.03	0.02	96.23
01N043	43-11		mica	36.07	1.32	16.06	19.39	0.24	11.84	0.06	0.19	9.28	0.02	0.00	0.00	0.07	0.00	0.00	0.13	0.31	94.98
01N043	43-12		mica	36.77	1.40	16.53	18.80	0.15	11.78	0.03	0.06	9.87	0.01	0.06	0.00	0.01	0.00	0.00	0.00	0.00	95.49
01N043	43-13		muscovite	47.35	0.21	32.79	2.44	0.10	1.63	0.03	0.20	8.17	0.00	0.13	0.00	0.01	0.00	0.00	0.00	0.74	93.81
01N043	43-14		plag	68.25	0.03	20.24	0.02	0.11	0.00	1.02	8.99	0.04	0.00	0.00	0.00	0.00	0.00	0.00	0.00	0.00	98.70
01N043	43-15		chlorite	25.16	0.00	19.72	22.59	0.37	16.43	0.01	0.19	0.00	0.00	0.00	0.00	0.00	0.00	0.00	0.07	0.10	84.65
01N043	43-16		titanite	30.88	37.77	1.64	0.67	0.00	0.00	29.93	0.04	0.04	0.04	0.00	0.00	0.02	0.00	0.06	0.18	0.84	102.11
01N040	40-1	core	amphibole	53.41	0.00	2.94	10.56	0.19	16.68	13.35	0.40	0.10	0.74	0.00	0.00	0.00	0.00	0.05	0.11	0.09	98.61
01N040	40-2	rim	amphibole	49.97	0.51	5.84	13.69	0.27	14.63	11.74	1.27	0.05	0.16	0.00	0.00	0.06	0.00	0.07	0.00	0.11	98.38
01N040	40-3		amphibole	53.50	0.04	2.81	10.65	0.13	16.67	13.28	0.27	0.07	0.28	0.06	0.00	0.00	0.00	0.00	0.00	0.00	97.76
01N040	40-4		amphibole	48.95	0.33	5.95	14.15	0.53	15.31	10.78	1.35	0.06	0.02	0.08	0.00	0.15	0.00	0.08	0.01	0.00	97.74
01N040	40-5		titanite	30.44	38.94	0.87	0.40	0.00	0.06	28.94	0.00	0.00	0.05	0.03	0.00	0.02	0.00	0.06	0.00	0.51	100.32
01N040	40-6		chlorite	26.76	0.02	19.39	17.77	0.26	20.31	0.03	0.11	0.01	0.69	0.15	0.00	0.00	0.00	0.26	0.00	0.00	85.76
01N040	40-7		amphibole	43.27	3.12	9.70	12.82	0.10	14.05	11.44	2.77	0.42	0.00	0.12	0.00	0.32	0.00	0.00	0.14	0.00	98.28
01N040	40-8		epidote	38.51	0.07	25.92	8.56	0.04	0.00	24.89	0.06	0.01	0.18	0.00	0.00	0.02	0.00	0.00	0.11	0.03	98.39
01N040	40-9		epidote	39.16	0.01	31.57	1.93	0.00	0.08	25.45	0.00	0.01	0.08	0.10	0.00	0.01	0.00	0.00	0.03	0.06	98.51
01N040	40-10		chlorite	27.68	0.05	19.82	18.47	0.21	20.20	0.31	0.11	0.01	0.00	0.07	0.00	0.00	0.00	0.00	0.03	0.00	86.95
01N040	40-11		plag	66.49	0.09	21.37	0.20	0.09	0.06	2.43	8.92	0.02	0.00	0.12	0.00	0.00	0.00	0.02	0.14	0.08	100.03
01N040	40-12		epidote	39.61	0.00	31.25	2.95	0.20	0.00	24.99	0.14	0.00	0.03	0.07	0.00	0.02	0.00	0.00	0.00	0.21	99.47
01N040	40-13		amphibole	53.48	0.01	2.22	13.40	0.28	15.46	13.11	0.25	0.04	0.08	0.00	0.00	0.00	0.00	0.04	0.00	0.00	98.38
01N040	40-14		kspar	52.71	0.07	29.32	2.17	0.06	3.13	0.00	0.11	8.27	0.00	0.17	0.00	0.00	0.00	0.00	0.07	0.08	96.16